K. Shimoji
W.D. Willis, Jr.
(Eds.)

Evoked Spinal Cord Potentials

An Illustrated Guide to Physiology, Pharmacology, and Recording Techniques

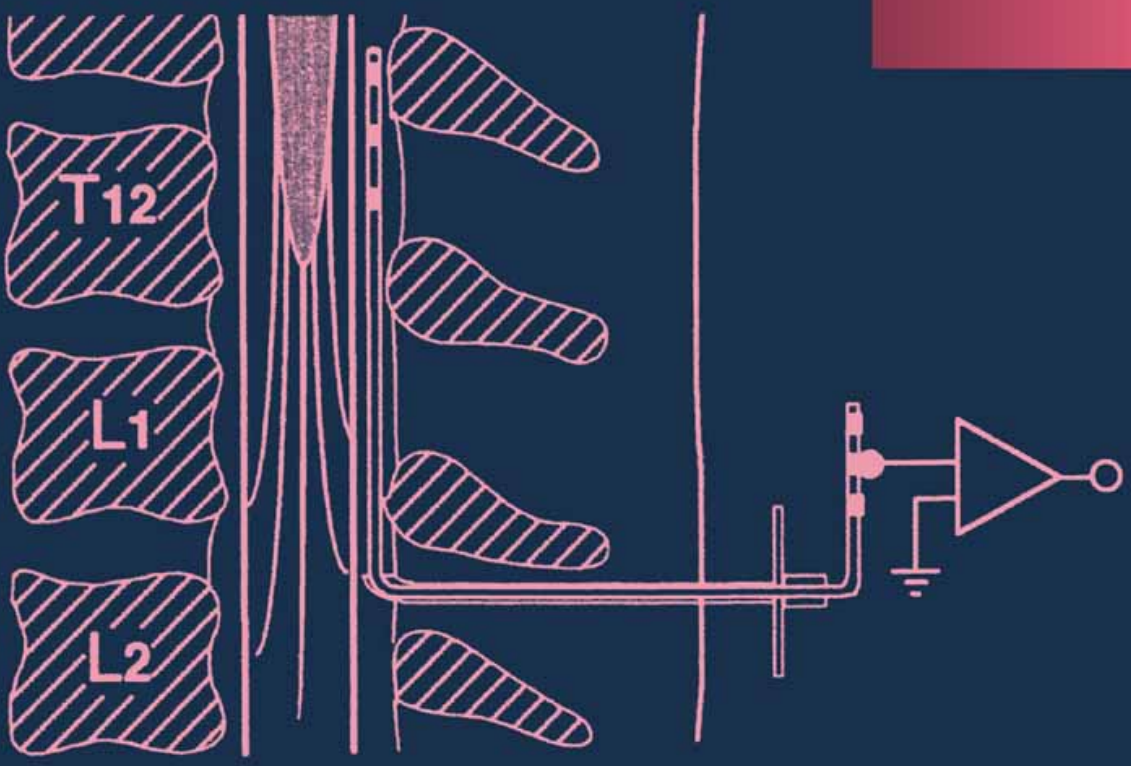

Springer

K. Shimoji, W.D. Willis, Jr. (Eds.)
Evoked Spinal Cord Potentials
An Illustrated Guide to Physiology, Pharmacology, and Recording Techniques

K. Shimoji, W.D. Willis, Jr. (Eds.)

Evoked Spinal Cord Potentials

An Illustrated Guide to Physiology, Pharmacology, and Recording Techniques

With 130 Figures

Springer

Editors:

Koki Shimoji, M.D., Ph.D., FRCA
Professor, Frontier University Ube Graduate School of Human Sciences
2-1-1 Bunkyodai, Ube, Yamaguchi 755-0805, Japan
Professor Emeritus, Niigata University
Visiting Professor, Saitama Medical College

William D. Willis, Jr., M.D., Ph.D.
Professor of Neuroscience and Cell Biology
University of Texas Medical Branch
301 University Blvd., Galveston, TX 77555-1069, USA

Authors:

Tatsuhiko Kano, M.D., Ph.D.
Professor and Chairman
Department of Anesthesiology
Kurume University School of Medicine

Yoichi Katayama, M.D., Ph.D.
Professor and Chairman
Department of Neurosurgery
Nihon University School of Medicine

Satoru Fukuda, M.D., Ph.D.
Professor and Chairman
Department of Anesthesiology and Reanimation
Fukui University School of Medicine

Library of Congress Control Number: 2005935847

ISBN-10 4-431-24026-8 Springer-Verlag Tokyo Berlin Heidelberg New York
ISBN-13 978-4-431-24026-6 Springer-Verlag Tokyo Berlin Heidelberg New York

This work is subject to copyright. All rights are reserved, whether the whole or part of the material is concerned, specifically the rights of translation, reprinting, reuse of illustrations, recitation, broadcasting, reproduction on microfilms or in other ways, and storage in data banks.
The use of registered names, trademarks, etc. in this publication does not imply, even in the absence of a specific statement, that such names are exempt from the relevant protective laws and regulations and therefore free for general use.
Product liability: The publisher can give no guarantee for information about drug dosage and application thereof contained in this book. In every individual case the respective user must check its accuracy by consulting other pharmaceutical literature.

Springer is a part of Springer Science+Business Media
springeronline.com
© Springer-Verlag Tokyo 2006
Printed in Japan

Typesetting: SNP Best-set Typesetter Ltd., Hong Kong
Printing and binding: Hicom, Japan

Printed on acid-free paper

Dedicated to Our Parents
and Teachers

Preface

The technique of using evoked spinal cord potentials (SCPs) has become an important clinical tool for monitoring spinal cord surgery and diagnosing spinal cord diseases. The technique is a result both of the technical development of recording evoked SCPs from the epidural space without perforation of the dura mater and of the development of medical electronics. Its use as a monitoring tool is based on continuous epidural analgesia with an epidural catheter. Since the first development of epidural recording of evoked SCPs in 1971, the technique has been applied in various institutes, particularly for monitoring during spine or spinal cord surgery and cardiovascular surgery, and recently for diagnosis of spinal cord diseases.

Although the results of studies on monitoring during surgery have proved useful, more detailed neurophysiological mechanisms in the origin of each component of evoked SCPs remain to be explained in the area of diagnosis of spinal or central nervous system diseases. Further neurophysiological and neuropharmacological studies of the human spinal cord may contribute to the clinical application of recording evoked SCPs for diagnosis of spinal cord diseases.

The aim of this book is to furnish a survey of the neurophysiological and neuropharmacological bases of evoked SCPs with reference to animal studies and the techniques of recording the potentials mainly from the spinal epidural space. The authors have been involved in the field from the beginning of the 1970s. Many illustrations are presented for better understanding the neurophysiological and neuropharmacological backgrounds of monitoring spinal cord functions. Case studies also are presented and discussed to provide more insight into the monitoring and diagnosis of spinal cord dysfunctions and spinal cord diseases.

This book is thus appropriate even for students or those new to the fields of clinical neurophysiology, neurosurgery, neurology, orthopedics, and neuroanesthesia who are interested in monitoring spinal cord function during surgery or diagnosing spinal cord diseases. A diverse range of terminology has been used in the literature to date, sometimes leading to misinterpretation of each component in the field of evoked SCPs. To avoid such misinterpretation and to provide readers with an accurate understanding, terminology referring to basic animal studies is used, and lucid explanations are included in this volume.

K. Shimoji and W.D. Willis, Jr.
Editors

Acknowledgments

The editors wish to thank the late Dr. P.D. Wall, who gave us valuable criticism and encouragement throughout our studies. Special thanks are also directed to the Section of Research Promotion of Kurume University and to the Aderans Co., Ltd. for their financial support. The authors also thank Mr. Yukio Sato for his skillful assistance to prepare the illustrations.

Contents

Section A
Bases of Understanding the Spinal Cord

Chapter 1
Neuroanatomical Considerations

William D. Willis, Jr.

1.1 Gross Anatomy of the Human Spinal Cord

The central nervous system includes the spinal cord and the brain. The spinal cord is an elongated, roughly cylindrical structure that is found within the vertebral canal (Fig. 1.1A,C). It joins the medulla oblongata at the level of the foramen magnum of the skull (Fig. 1.1A), and in adults it terminates caudally at the interspace between the first and second lumbar vertebrae (Fig. 1.1C). The spinal cord of the adult human is about 42–45 cm long and 1 cm in diameter at its widest extent, and it weighs about 35 g (Nolte, 2002).

The spinal cord develops in relation to the body segments (somites) that it innervates. This gives the spinal cord a segmented structure. The segments are best recognized by reference to pairs of dorsal and ventral roots[1] that enter or emerge from the spinal cord at each segmental level (Figs. 1.1C, 1.2, 1.3). Each dorsal and ventral root breaks up into a series of rootlets that extend the length of the corresponding spinal cord segment; the number of rootlets varies with the segment (see Fig. 1.2). Therefore, a segment of spinal cord can be demarcated by locating the entry or exit points of the most rostral and most caudal of the rootlets of the appropriate root.

The dorsal roots contain axons from sensory neurons whose cell bodies are in the dorsal root ganglia (Figs. 1.2 and 1.3), which form swellings located at the intervertebral foramina. Sensory axons passing to the periphery from the dorsal root ganglion cells intermingle with ventral root axons in the spinal nerves, which are just distal to the dorsal root ganglia (Fig. 1.3A). The ventral roots are composed of axons from alpha and gamma motor neurons and, at the appropriate segmental levels (T1–L2; S1–S3), of autonomic preganglionic neurons. Sympathetic white and gray communicating rami contain axons that connect the spinal nerves with sympathetic paravertebral ganglia (Fig. 1.3A). Sacral parasympathetic preganglionic axons distribute through the pelvic nerves and terminate on parasympathetic postganglionic neurons in ganglia close to or in the walls of the pelvic viscera.

[1]Dorsal and ventral are terms that apply best to quadrupeds. Posterior and anterior are more appropriate for humans. However, common usage equates dorsal with posterior and ventral with anterior with respect to human spinal cord structures.

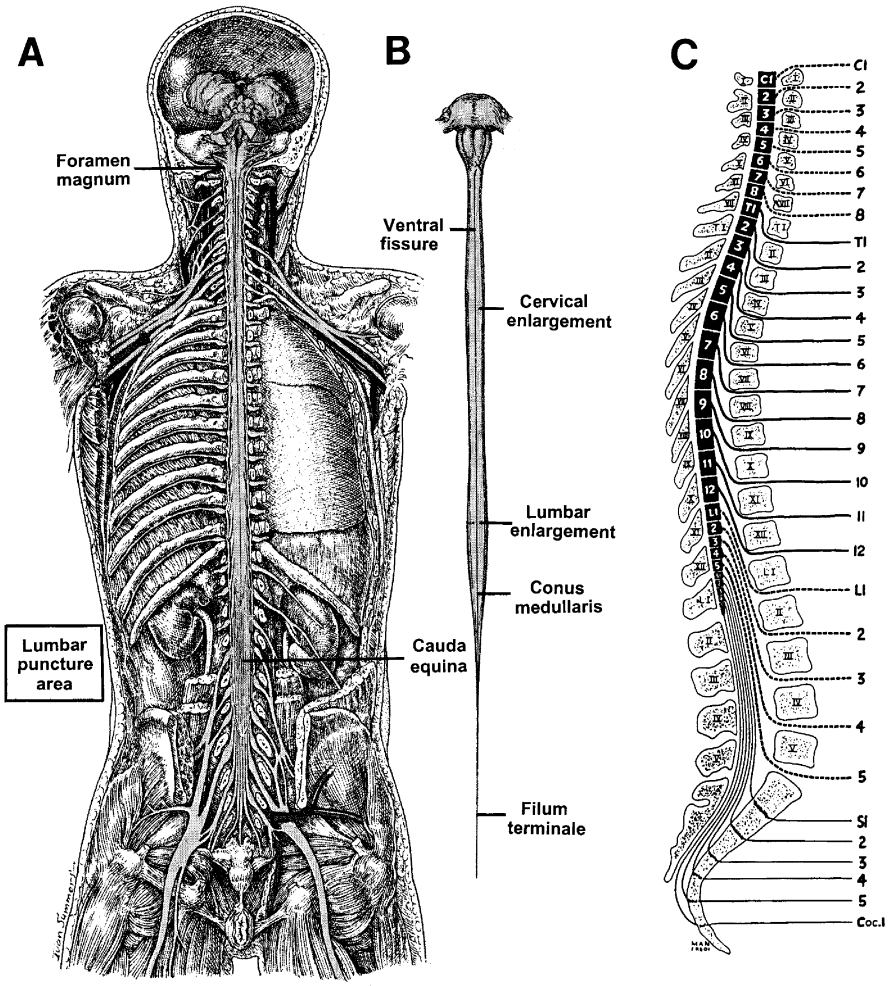

Fig. 1.1A–C. The shape of the spinal cord and its relationship to the vertebral column. **A** Gross dissection of the back in a human cadaver. A complete laminectomy was done and the dura opened, exposing the dorsal aspect of the spinal cord. The brachial and the lumbosacral plexuses are also shown. The spinal cord terminates at the L1–L2 interspace. The remainder of the dural sac contains the cauda equina. The filum terminale penetrates the dura and is attached to the coccyx. **B** Ventral view of the isolated spinal cord. The ventral fissure separates the two halves of the cord (**A** and **B** from Mettler, 1948). **C** Relationship of the spinal cord segments and spinal nerves to the vertebral column (from Crosby et al., 1962)

There are a total of 31 segments (8 cervical, 12 thoracic, 5 lumbar, 5 sacral, and 1 coccygeal) in the human spinal cord (Figs. 1.1 and 1.2). Other mammals may have slightly different numbers of segments. There are seven cervical vertebrae, and so there is one more cervical spinal cord segment than cervical vertebrae. The ventral roots of the first cervical segment emerge rostral to the first cervical vertebra (there are generally no first cervical dorsal roots; Fig. 1.2), and the eighth cervical dorsal and

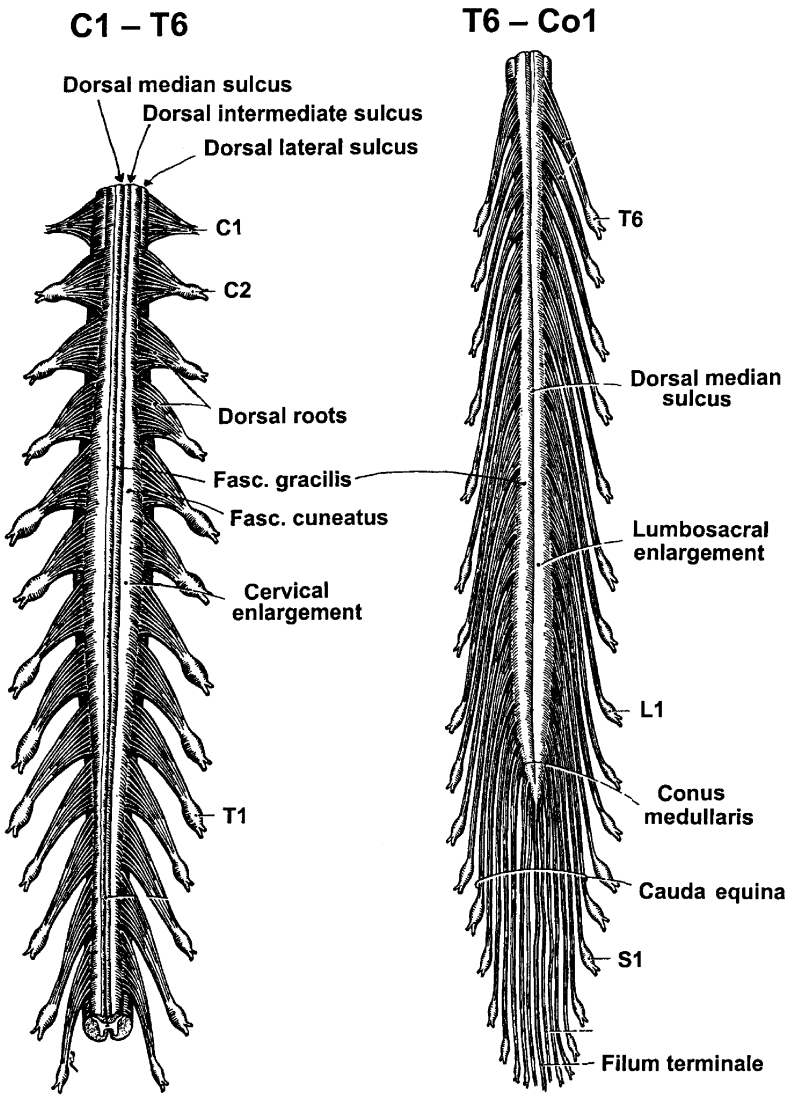

Fig. 1.2. Drawing of the dorsal surface of the spinal cord, dorsal roots and dorsal root ganglia. The spinal cord was transected between the T5 and T6 segments. The cervical and upper thoracic cord are shown at the *left* (including the cervical enlargement) and the lower thoracic and lumbosacral cord are shown at the *right* (including the lumbosacral enlargement). Note that at C1, only the ventral roots are seen because of the absence of C1 dorsal roots. The dorsal median sulcus is present throughout the length of the spinal cord, as is the dorsal lateral sulcus, which is the groove through which the dorsal roots pass to enter the spinal cord. However, there is a dorsal intermediate sulcus at T6 and more rostrally. This separates the fasciculus gracilis from the more laterally situated fasciculus cuneatus. Below T6, only the fasciculus gracilis is found. Caudal to the termination of the conus medullaris are seen the cauda equina and the filum terminale (from Crosby et al., 1962)

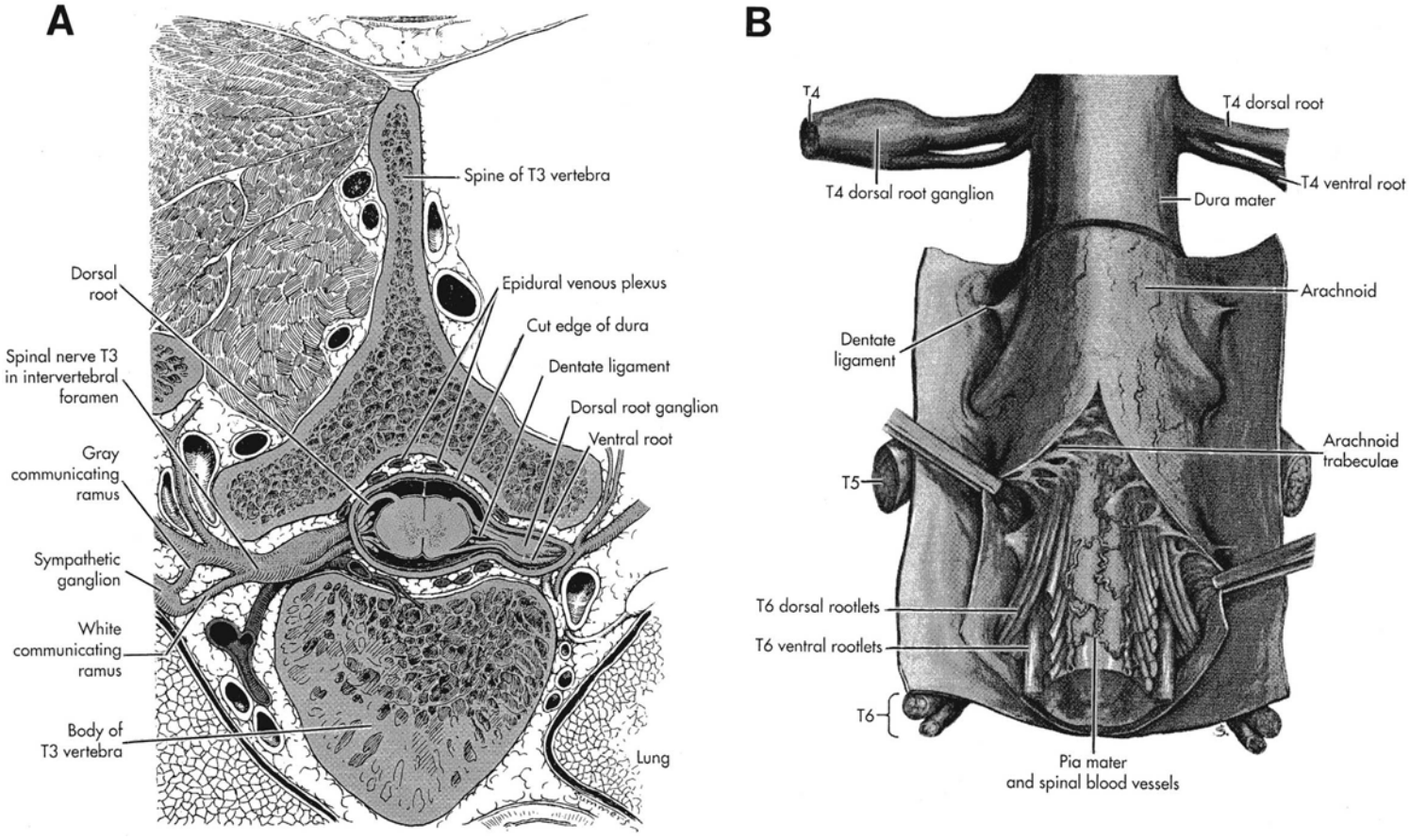

FIG. 1.3A,B. Spinal cord, associated components of the peripheral nervous system, and supportive bony and connective tissue structures. **A** Transverse section of the third thoracic vertebra, the spinal cord, T3 spinal roots, T3 dorsal root ganglia, T3 spinal nerves and meninges. Note the connections of the white and gray communicating rami with the T3 prevertebral sympathetic ganglion. Also note the epidural fat and venous plexus. **B** Dorsal view of the T4–6 levels of the spinal cord, showing the meningeal coverings, including the dura mater, arachnoid, and pia mater. Note the attachment points between the dentate ligament and the dura, as well as the arachnoid trabeculae (from Mettler, 1948)

ventral roots leave the vertebral canal just caudal to the seventh cervical vertebra (Fig. 1.1C). The roots of the remaining spinal segments exit from the vertebral canal below the vertebra of the same number.

The reason that the first cervical segment lacks dorsal roots is that it participates in trigeminal rather than in spinal cord sensory functions. Correlated with this lack of C1 dorsal roots is the absence of a C1 dermatome (see standard dermatome maps used for neurological examinations). The C1 segment receives input from descending branches of primary afferents belonging to the trigeminal nerve. Nociceptive, thermoreceptive, and tactile afferents with cell bodies in the trigeminal ganglion enter the brain stem at the level of the mid-pons through the trigeminal nerve and give off collaterals that project caudally through the spinal tract of the trigeminal nerve, which terminates in the spinal nucleus of the trigeminal nerve. This nucleus extends from the level of the pons to the upper cervical spinal cord. The subnucleus caudalis of the trigeminal complex, which is in the lower medulla and upper cervical spinal cord, resembles the dorsal horn of the spinal cord and is often referred to as the "medullary dorsal horn." Neurons in this nucleus give rise to a part of the trigeminothalamic tract that has equivalent sensory functions for the head to the spinothalamic tract for the extremities and trunk (pain, temperature and crude touch).

In the upper cervical spinal cord, the spinal roots leave the spinal cord and pass directly laterally to the appropriate intervertebral foramen. However, since the adult spinal cord does not extend beyond the L1–2 intervertebral space, roots below L2 must travel progressively more caudally to reach the appropriate intervertebral foramen (Fig. 1.1C). The collection of spinal roots below L2 is called the cauda equina from its fancied resemblance to a horse's tail (Figs. 1.1A and 1.2). At levels between the upper cervical spinal cord and L2, the roots angle progressively more. This leads to a discrepancy between vertebral level and spinal cord segmental level that can amount to a difference of 2 or more segments, depending on the level (Fig. 1.1C).

The diameter of the spinal cord is larger at the levels of the brachial (C5–T1) and lumbosacral (L2–S3) plexuses than at other levels (Figs. 1.1A,B and 1.2). The cervical and lumbosacral enlargements are produced by increases in the numbers of neurons and their connections at these levels, as required for the sensory and motor innervation of the upper and lower extremities.

The surface of the spinal cord is indented longitudinally by several sulci (shallow grooves) and a fissure (deep groove). These grooves define the boundaries between areas of the spinal cord white matter called funiculi (large bundles of axons) and between two fasciculi (smaller bundles of axons). At the dorsal midline is the dorsal median sulcus. This separates the left and right sides of the spinal cord (Fig. 1.2). The dorsal lateral sulcus is a groove that corresponds to the dorsal root entry zone. The dorsal funiculus extends from the dorsal median sulcus to the dorsal lateral sulcus. At some segmental levels (C1–T6), there is a dorsal intermediate sulcus, which separates the fasciculus gracilis from the more laterally placed fasciculus cuneatus (Fig. 1.2, left). Caudal to T6, there is no dorsal intermediate sulcus and there is only a fasciculus gracilis (Fig. 1.2, right). The ventral lateral sulcus is not well defined but marks the ventral root exit zone. The lateral funiculus extends from the dorsal lateral to the ventral lateral sulcus. At the midline ventrally is the ventral median fissure (Fig. 1.1B). The ventral funiculus lies between the ventral lateral sulcus and the ventral median fissure. Contained within the ventral median fissure is the ventral spinal artery.

1.2 Spinal Meninges

The spinal cord, like the brain, is enclosed within and protected by connective tissue sheaths called the meninges (Fig. 1.3A,B). The meninges include the dura mater, the arachnoid, and the pia mater. The dura mater is a thick connective tissue membrane that is continuous rostrally to the foramen magnum with the inner layer of the cranial dura mater. There is an epidural space between the spinal dura mater and the periosteum of the vertebral canal. This space contains epidural fat and a venous plexus (Fig. 1.3A). The dura mater extends caudally as far as the level of the S2 vertebra.

Beneath the dura mater is a thinner membrane, the arachnoid (Fig. 1.3B). The arachnoid bridges over surface features of the spinal cord, such as the sulci and the anterior median fissure. Tight junctions between cells of the arachnoid give this membrane a barrier function. The subarachnoid space contains cerebrospinal fluid, which is confined to this space by the barrier properties of the arachnoid. The cerebrospinal fluid originates largely from the choroid plexuses in the cerebral ventricles. The lumbar cistern, which is the subarachnoid space around the cauda equina, serves as a convenient reservoir from which to remove cerebrospinal fluid by lumbar puncture (Fig. 1.1A).

The innermost of the meninges is the pia mater (Fig. 1.3B). This thin membrane adheres tightly to the surface of the spinal cord and thus follows its contours closely. It fuses with astrocytic end-feet, forming a pia-glial membrane. Arachnoid trabeculi are connective tissue attachments between the arachnoid and pia. A thickening of the pia mater on each side of the spinal cord is called the dentate (or denticulate) ligament (Fig. 1.3B). Passing through the arachnoid, the dentate ligament makes a series of 20–22 firm attachments to the dura along the length of the spinal cord (Fig. 1.3B). The caudal end of the spinal cord is connected to the coccyx by the filum terminale (Fig. 1.1A,B). This is another thickening of the pia mater that penetrates the arachnoid and fuses with the dura. The dentate ligaments and filum terminale permit some movement of the dura without allowing much movement of the spinal cord (Romanes, 1981).

(Standard references that describe the anatomy of the spinal cord include Mettler, 1948; Crosby et al., 1962; Carpenter and Sutin, 1983; Nolte, 2002; Paxinos and Mai, 2004).

1.3 Cross-Sectional Anatomy of the Spinal Cord

A transverse section of the spinal cord reveals the basic arrangement of the spinal cord white and gray matter. The white matter is located around the periphery of the spinal cord, and the gray matter forms a butterfly-shaped region deep to the white matter (Fig. 1.4). The grooves at the surface of the spinal cord allow the subdivision of the white matter into dorsal, lateral and ventral funiculi, and, in the cervical and upper thoracic spinal cord, the further subdivision of the dorsal funiculus into the fasciculi gracilis and cuneatus (Fig. 1.4A,B). At lower thoracic levels and caudally, the dorsal fasciculus consists of just the fasciculus gracilis (Fig. 1.4C). Just deep to

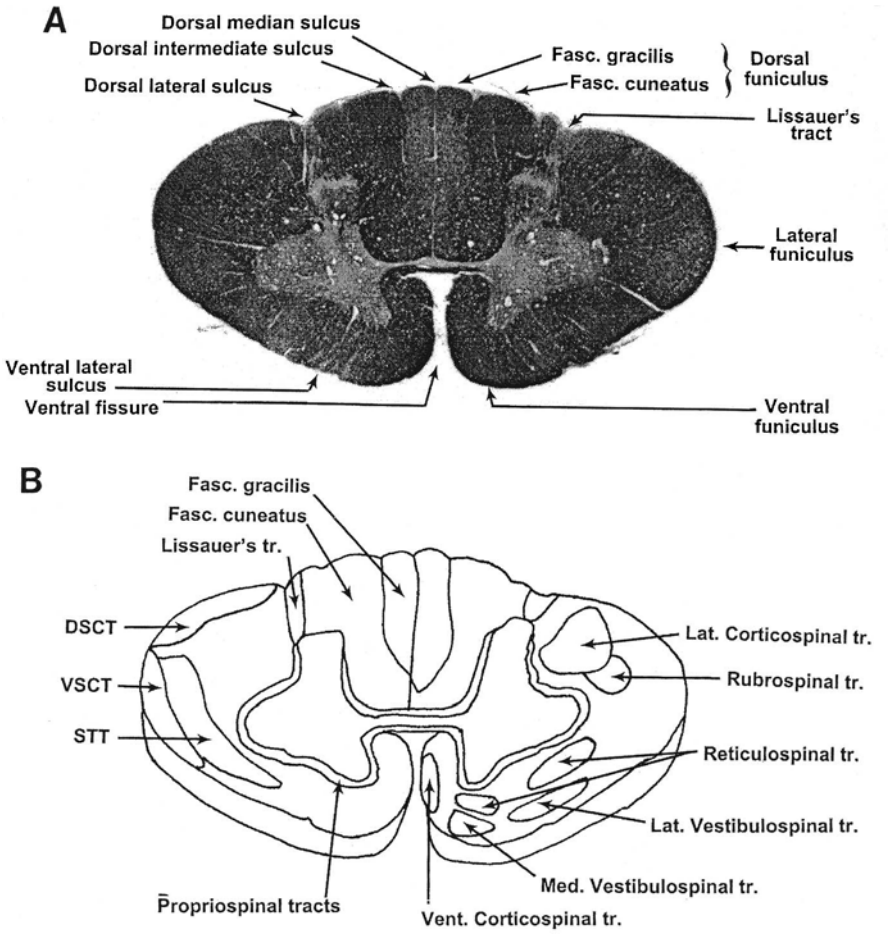

Fig. 1.4A–C. Transverse sections of the spinal cord. **A** Myelin-stained section of cervical enlargement of human spinal cord, emphasizing the different parts of the white matter. The dorsal median and dorsal lateral sulci demarcate the dorsal funiculus. Within the dorsal funiculus, the fasciculus gracilis is separated from the fasciculus cuneatus by the dorsal intermediate sulcus. Lissauer's tract is shown deep to the dorsal lateral sulcus. Between the dorsal lateral and the ventral lateral sulci is the lateral funiculus. The ventral lateral sulcus and the ventral median fissure are the boundaries of the ventral funiculus. **B** Drawing of a section through the cervical enlargement and showing the approximate locations of ascending (*left side of section*) and descending (*right side of section*) tracts. Propriospinal tracts surrounding the gray matter are also indicated. **C** Lumbar enlargement, emphasizing the main parts of the gray matter, including the dorsal horn, intermediate region, ventral horn and central gray. The dorsal funiculus includes only the fasciculus gracilis. The substantia gelatinosa is a special part of the gray matter that is lightly stained because of the relative lack of myelin in this region. These different parts of the gray matter are present throughout the length of the spinal cord

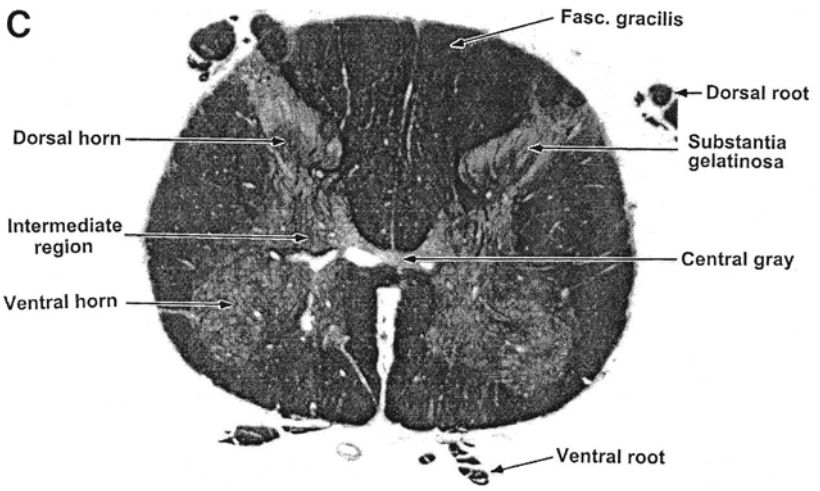

Fig. 1.4A–C. *Continued*

the dorsal root entry zone is a bundle of lightly myelinated and unmyelinated axons called Lissauer's tract (Fig. 1.4A,B; Lissauer, 1886).

The dorsal funiculus includes important ascending sensory pathways, the dorsal column pathway, and the postsynaptic dorsal column pathway (see below), and the lateral and ventral funiculi contain several ascending and descending tracts. These long pathways transmit information from the spinal cord to the brain or from the brain to the spinal cord (Fig. 1.4B). The names of these tracts often indicate the origin and destination of these pathways. For example, the dorsal and ventral spinocerebellar tracts (DSCT and VSCT) originate from neurons in the spinal cord and project to the cerebellum, and the lateral and ventral corticospinal tracts originate in the cerebral cortex and project to the spinal cord. Another ascending pathway is the spinothalamic tract (STT), and additional descending tracts include the pontine and medullary reticulospinal tracts, the lateral and medial vestibulospinal tracts, and the rubrospinal tract. The spinal cord white matter also contains propriospinal tracts, some of which are located just outside the gray matter and which interconnect different segmental levels of the spinal cord.

The gray matter of the spinal cord can be subdivided into the dorsal horn, intermediate region, ventral horn, and central gray (Fig. 1.4C). These extend longitudinally throughout the length of the spinal cord. A part of the dorsal horn called the substantia gelatinosa is prominent in myelin-stained sections because of the relative lack of myelin in this region (Fig. 1.4C; also Fig. 1.5A,B, left side of the sections). The substantia gelatinosa also extends the length of the spinal cord.

The cellular composition of the spinal cord gray matter is best revealed when the sections are stained by the Nissl method. In Nissl-stained sections, the substantia gelatinosa is seen to contain many small, densely packed neurons (Fig. 1.5A,B, right side of the sections). In the ventral horn are the motor nuclei, which contain numerous large alpha motor neurons, as well as smaller gamma motor neurons. An indi-

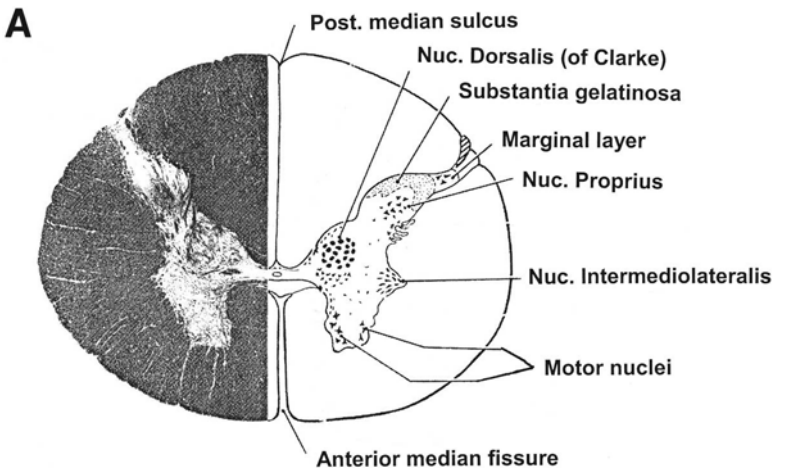

Fig. 1.5A–C. Transverse sections of the human thoracic and sacral spinal cord. The *left sides* of the sections in **A** and **B** are stained for myelin. The *right sides* of these sections are drawings of the locations of neuronal cell bodies stained with the Nissl technique. **A** Section through spinal cord segment T12 showing the locations of neurons in the marginal layer, substantia gelatinosa, nucleus proprius, Clarke's column (or nucleus dorsalis), the intermediolateral cell column, and motor nuclei. **B** Section through the S3 segment showing the locations of neurons in the marginal layer, substantia gelatinosa, nucleus proprius, sacral parasympathetic nucleus and motor nuclei (modified from Carpenter and Sutin, 1983). **C** Section through the lumbar enlargement showing the cell body, dendrites, and axon of an alpha motor neuron that had been injected intracellularly with horseradish peroxidase (from Nolte, 2002)

vidual alpha motor neuron labeled intracellularly with horseradish peroxidase is shown in Fig. 1.5C to have dendrites that are widely distributed throughout much of the ventral horn. In the enlargements, the gray matter of the spinal cord is expanded compared with that in the thoracic, upper lumbar and sacral levels (cf. sections through enlargements in Fig. 1.4 with sections through the thoracic and sacral spinal cord in Fig. 1.5A,B). This is especially evident for the ventral horn, which contains several columns of motor neurons. A given motor neuron column innervates a particular muscle and may extend longitudinally for several segments. The motor nuclei have a somatotopic arrangement. Motor neurons that supply distal muscles are located dorsolaterally, those that supply proximal muscles are placed more ventromedially, and motor neurons that innervate axial muscles are located medially in the ventral horn (Figs. 1.5B and 1.6).

At certain levels of the spinal cord, there are additional components of the gray matter. In the thoracic and upper lumbar spinal cord, there is a lateral horn, which contains a column of sympathetic preganglionic neurons called the intermediolateral cell column (Fig. 1.5A). At the same segmental levels, the intermediate region also contains the nucleus dorsalis (or Clarke's column); this nucleus projects to the cerebellum through the dorsal spinocerebellar tract (Fig. 1.5A). In the sacral spinal cord, the sacral parasympathetic nucleus (Fig. 1.5B) is located in a position similar to that of the sympathetic intermediolateral cell column and is composed of parasympathetic

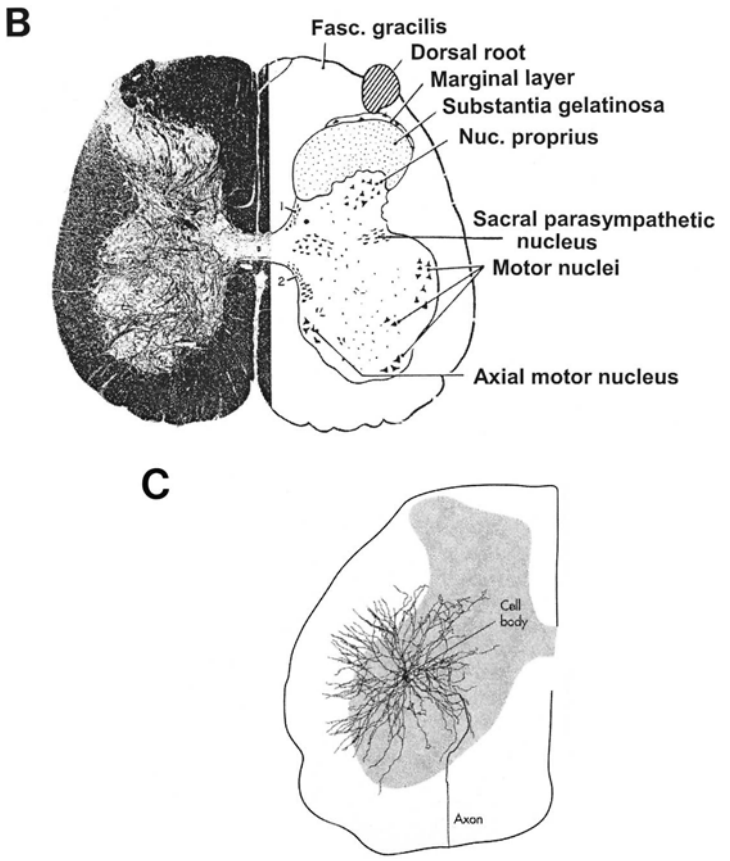

Fig. 1.5A–C. *Continued*

preganglionic neurons (Nadelhaft et al., 1983). The sacral parasympathetic nucleus extends through segments S1–S3. Visceral afferents reaching the spinal cord through the pelvic nerve enter Lissauer's tract and synapse on interneurons in the vicinity of the sacral parasympathetic nucleus. The neural circuits that are formed contribute to visceral reflexes.

A Swedish neuroanatomist named Rexed was able to show in Nissl-stained material that the spinal cord gray matter of cats is layered (Fig. 1.6A; Rexed, 1952, 1954). He subdivided the gray matter into 10 layers (Rexed's laminae). In the enlargements, the dorsal horn includes laminae I–VI (the substantia gelatinosa is equivalent to lamina II). The intermediate region is the dorsal part of lamina VII. The medial ventral horn is lamina VIII, and the motor nuclei collectively form lamina IX (which includes several separate motor neuron columns). The gray matter around the central canal (central gray) is lamina X. In the thoracic and upper lumbar cord, the intermediolat-

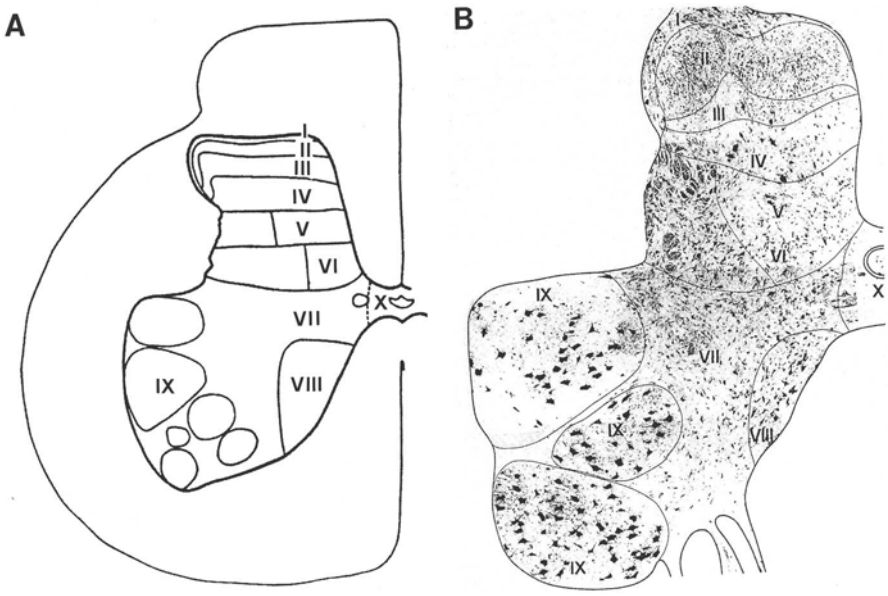

Fig. 1.6. A Diagram of Rexed's laminae in the cat lumbosacral enlargement, based on Nissl-stained material. The dorsal horn is subdivided into laminae *I–VI*, the intermediate region is the dorsal part of lamina *VII*, the medial ventral horn is lamina *VIII*, the various motor nuclei are included within lamina *IX*, and the central gray matter is lamina *X* (from Rexed, 1954). **B** Rexed's laminae are shown in a section of the human L5 spinal cord stained by the Nissl method (from Schoenen and Faull, 2004)

eral cell column and Clarke's column are within lamina VII (Fig. 1.5A,B). The human spinal cord gray matter can be subdivided into Rexed's laminae in a similar fashion (Fig. 1.6B).

Figure 1.7 shows some of the types of neurons that can be found in the dorsal horn of the human spinal cord (Schoenen and Faull, 2004). The dendrites of many neurons in laminae I and II are oriented longitudinally, although some have transversely oriented dendrites. Neurons in laminae IV and V often have dorsally directed dendrites ("antenna neurons"), some of which reach lamina II or even lamina I.

An example of an "antenna neuron," in this case a primate spinothalamic tract neuron, is shown in Fig. 1.8C. The spinothalamic tract cell was labeled intracellularly with horseradish peroxidase, reconstructed histologically and then sectioned for electron microscopy (see Willis, 2005). The electron micrographs in Fig. 1.8A and B show synaptic terminals ending on dendrites of this neuron within lamina III. Immunostaining showed that the synaptic ending in Fig. 1.8A contained substance P (see Carlton illustration in Willis, 2002) and that the one in Fig. 1.8B contained calcitonin gene-related peptide (Carlton et al., 1990). Other immunohistochemical experiments have demonstrated that synaptic endings containing glutamate (Westlund et al., 1992) or GABA (Carlton et al., 1992) contact the cell bodies and dendrites of spinothalamic

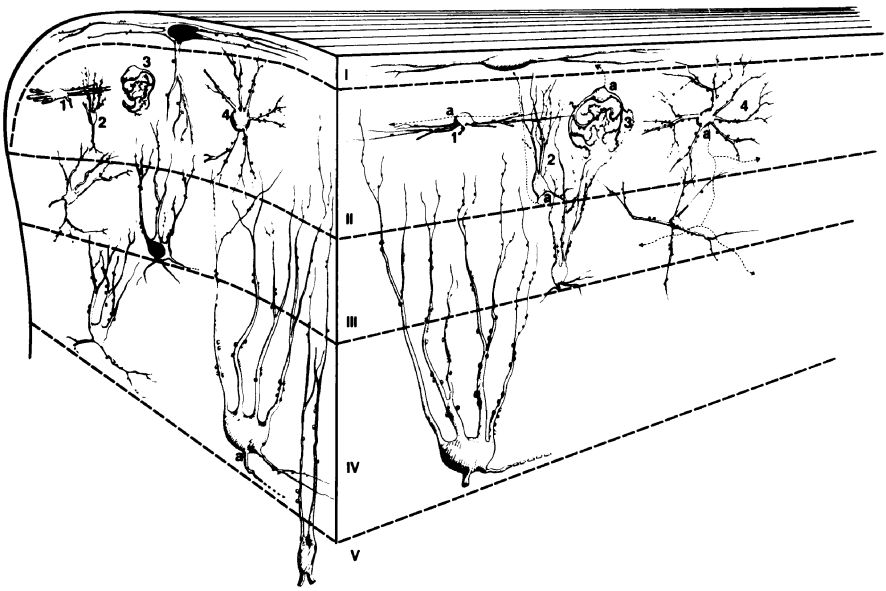

Fig. 1.7. Morphological types of neurons found in the dorsal horn of the human spinal cord. Laminae *I–V* of the dorsal horn are shown in a three-dimensional representation. Note that many neurons in laminae *I* and *II* have dendrites that are oriented longitudinally, whereas neurons in deep layers have dendrites that are oriented transversely. Some of the deeper neurons have dorsally projecting dendrites that may reach lamina *II* or even lamina *I*. Such neurons are sometimes called "antenna cells" (from Schoenen and Faull, 2004)

tract neurons. Some implications of these synaptic arrangements are that receptors for peptides (NK1 receptors, CGRP1 receptors) are present on the dorsal dendrites of STT cells and other neurons within the superficial dorsal horn, whereas receptors for glutamate and for inhibitory amino acids, like GABA, are present on the cell bodies, as well as the dendrites, of these neurons (see Ye and Westlund, 1996; Ye et al., 1999; Todd, 2002; Nagy et al., 2004).

1.4 Afferent Input to the Spinal Cord

As already mentioned, the cell bodies of primary afferent sensory neurons that project to the spinal cord are located in dorsal root ganglia (Fig. 1.9A). These neurons have roughly spherical cell bodies that give off a single neurite, which then bifurcates into a peripherally directed and a centrally directed axon. The peripheral process is distributed through a spinal nerve and the peripheral nervous system and terminates in sensory receptors in skin, muscle, joint, or visceral tissue. The central process enters the spinal cord through a dorsal root. If the axon is large, it passes through the medial part of the dorsal root (Fig. 1.9B), and then it bifurcates to send processes rostrally

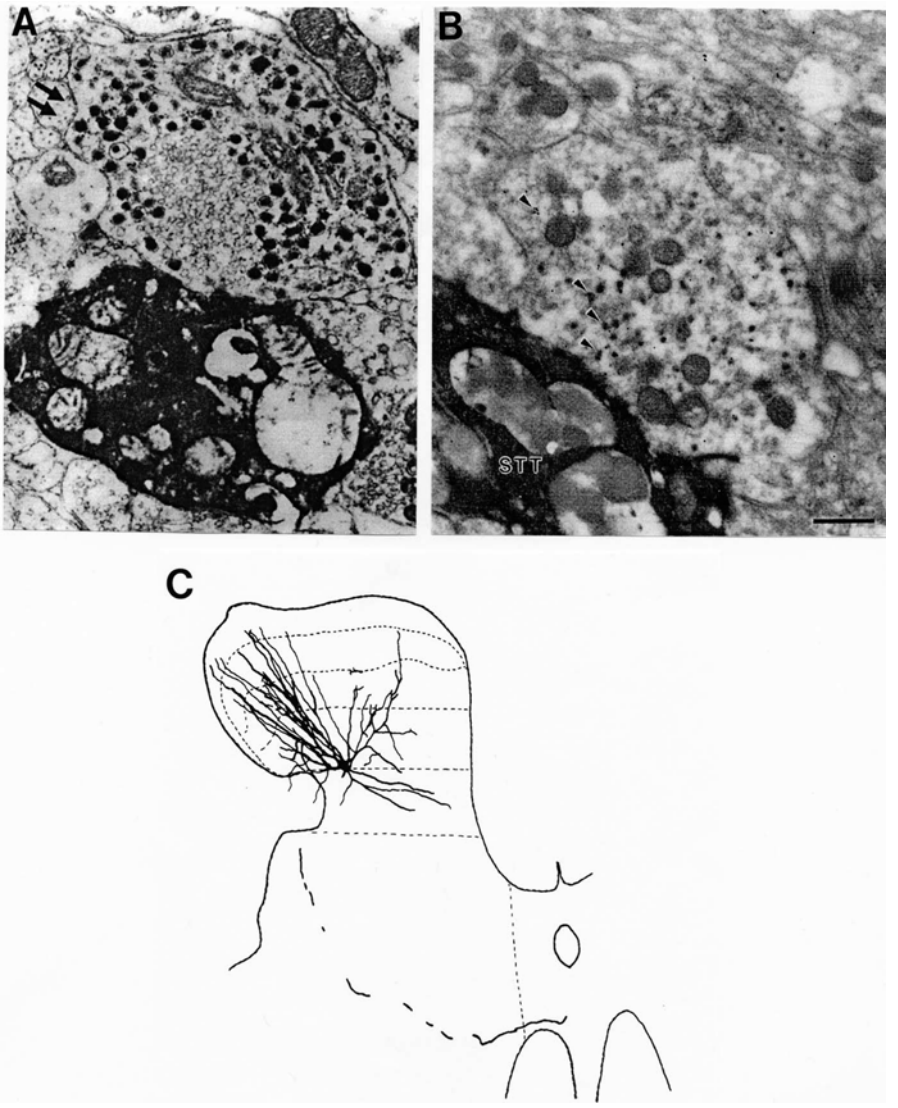

FIG. 1.8A–C. Example of an "antenna cell" belonging to the spinothalamic tract. Synapses containing substance P or calcitonin gene-related peptide are shown to contact dendrites of an STT cell identified by antidromic activation from the contralateral VPL nucleus and then labeled intracellularly with horseradish peroxidase. **A** A terminal containing numerous dense core vesicles immunostained for substance P is seen to synapse on a dendrite stained for horseradish peroxidase belonging to the STT cell shown in **C**. **B** A similar ending immunostained for calcitonin gene-related peptide synapsing with another dendrite of the STT cell in **C**. The reconstructed STT cell in **C** had its cell body at the border of laminae IV and V and dendrites that extended dorsally as far as lamina I. The synapses in **A** and **B** were on dendrites in lamina III (from Carlton et al., 1990; Willis, 2002, 2005)

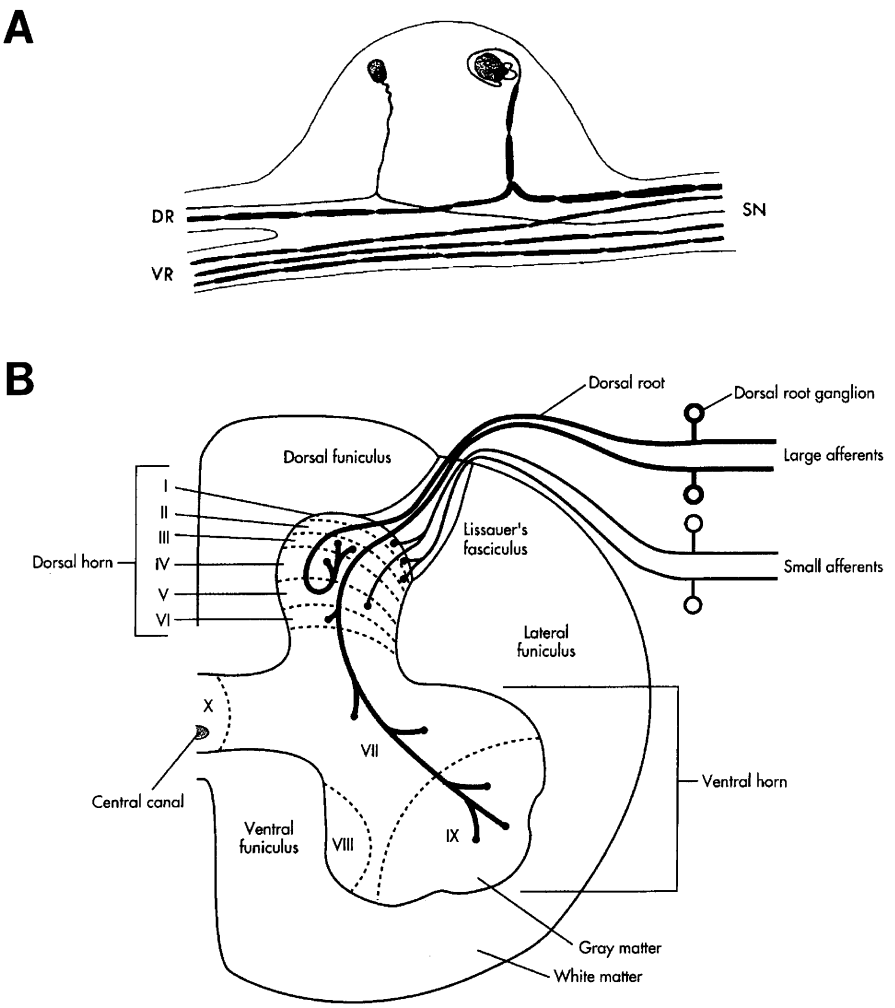

FIG. 1.9A–B. Dorsal root ganglion cells giving rise to small and large primary afferent fibers and the terminations of these afferent fibers in the spinal cord. **A** The cell bodies of a small (*left*) and of a large (*right*) dorsal root ganglion (DRG) cell are shown. The small DRG cell on the left gave off a neurite that divided into a centrally directed unmyelinated axon that entered the spinal cord through a dorsal root (*DR*) and a peripherally directed unmyelinated axon that projected to the periphery through the spinal nerve (*SN*). A large DRG neuron is shown on the right. This cell gave off a longer neurite, and the centrally and peripherally directed axons were myelinated. *VR*, ventral root (from Willis and Grossman, 1981). **B** The peripheral and central processes of large and small afferents are shown to originate from DRG cells at the *right*. The central processes of the large cutaneous afferents that supply hair follicles form "flame-shaped" arbors in the dorsal horn, whereas the central processes of muscle spindle afferents synapse on interneurons in laminae *VI* and *VII* and on alpha motor neurons in lamina *IX*. Small afferents from nociceptors and thermoreceptors terminate in laminae *I*, *II*, and *V* (from Berne and Levy, 2000)

and caudally in the dorsal funiculus (Fig. 1.10). These processes give off collaterals that terminate within the spinal cord gray matter. The exact region of termination depends on the type of sensory receptor that is innervated by the sensory neuron. For example, large myelinated cutaneous afferents that supply hair follicle receptors often swing through the deep part of the dorsal horn and then recurve to end in laminae III and IV (Fig. 1.9B). These endings have been described by Scheibel and Scheibel (1968) as "flame-shaped arbors." By contrast, large myelinated muscle afferents that supply muscle spindles continue into the deep dorsal horn, intermediate region, and ventral horn, forming terminals on interneurons in laminae VI and VII and on alpha motor neurons in lamina IX (Fig. 1.9B; Brown, 1981).

Fine primary afferent fibers include small myelinated and unmyelinated axons that supply nociceptors and thermoreceptors, as well as certain types of mechanoreceptors (see Willis and Coggeshall, 2004). The dorsal root ganglion cells of the fine afferents are smaller than are those having large myelinated axons (Fig. 1.9A). After entering the spinal cord through the lateral part of a dorsal root, these small fibers enter Lissauer's tract (Fig. 1.9B). They bifurcate and send branches rostrally and caudally in Lissauer's tract for one to several segments (a greater distance for visceral afferents, up to six segments, than for cutaneous afferents; Sugiura et al., 1986, 1989), and these branches give off collaterals that end in the gray matter of the spinal cord. Finely myelinated (Aδ) fibers terminate in laminae I and V and sometimes also in lamina X (Light and Perl, 1979). Unmyelinated (C) fibers synapse in laminae I and II (Sugiura et al., 1986).

There is a somatotopic relationship between the locations of the receptive fields of neurons in the dorsal horn that respond to mechanical stimulation of the skin and the locations of the neurons within the dorsal horn (Brown and Fuchs, 1975). In general, the receptive fields of neurons in the lateral part of the dorsal horn within the enlargements are located proximally and the receptive fields of more medially located dorsal horn neurons are located distally.

1.5 Somatosensory and Other Ascending Tracts

A number of ascending tracts originate in the spinal cord and terminate in the brain (see Willis and Coggeshall, 2004). The dorsal column pathway and the spinothalamic tract are the most important ones that convey information leading to somatic sensations. However, other pathways that may also contribute to somatosensory experience are the postsynaptic dorsal column path and the spinocervical, spinoreticular, and spinomesencephalic tracts. There are also several ascending pathways whose function is related to limbic system function, including the spinohypothalamic tract, the spinoparabrachial tract, and several paths that project directly to the amygdala and other telencephalic limbic structures. The spinocervical tract will not be discussed because it is unclear if this tract is important or even exists in humans.

1.5.1 Dorsal Column System

The dorsal column pathway includes axons that are branches of primary afferent neurons whose cell bodies are located in dorsal root ganglia (Willis and Coggeshall, 2004). Each afferent bifurcates as it enters the spinal cord, and one branch may ascend

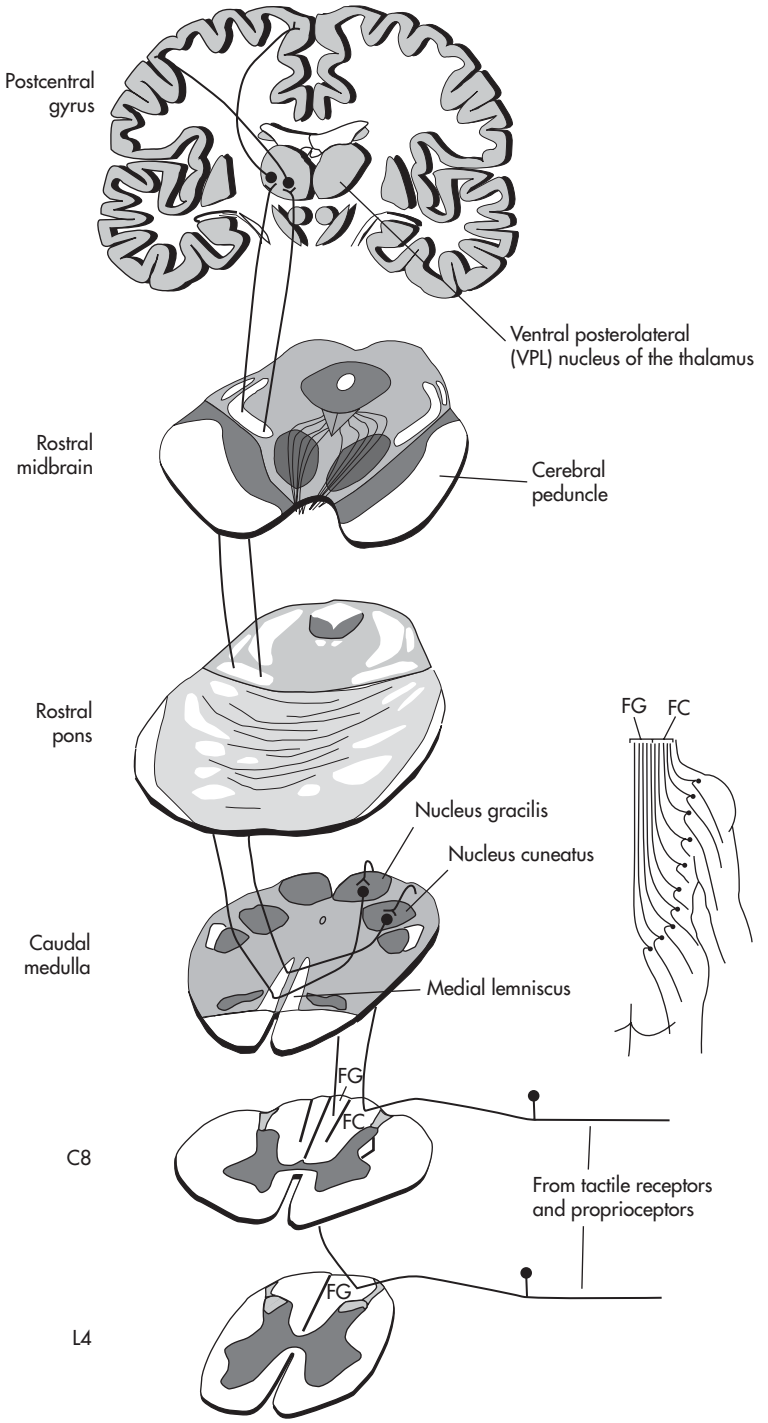
Postcentral gyrus
Ventral posterolateral (VPL) nucleus of the thalamus
Rostral midbrain
Cerebral peduncle
Rostral pons
FG
FC
Nucleus gracilis
Nucleus cuneatus
Caudal medulla
Medial lemniscus
FG
FC
C8
From tactile receptors and proprioceptors
FG
L4

in the dorsal column all the way to the caudal medulla (Fig. 1.10), where it terminates in one of the dorsal column nuclei. If the primary afferent fiber enters the spinal cord through a dorsal root caudal to T6, the ascending branch travels in the fasciculus gracilis and terminates synaptically in the nucleus gracilis. If the primary afferent fiber enters the spinal cord through a dorsal root rostrally to T6, the branch ascends in the fasciculus cuneatus and ends in the nucleus cuneatus. Second-order neurons in the dorsal column nuclei project their axons across the midline to join the medial lemniscus. The axons then ascend to the level of the thalamus, where they synapse in the ventral posterior lateral (VPL) nucleus. Third order neurons in the VPL nucleus project their axons through the posterior limb of the internal capsule to the primary and secondary areas of the somatosensory cortex. The thalamocortical axons terminate in the somatotopically appropriate cortical zones. The postsynaptic dorsal column pathway also ascends in the dorsal column to end in the dorsal column nuclei. However, the cell bodies of neurons belonging to this pathway are located in the dorsal horn, rather than in dorsal root ganglia. Postsynaptic dorsal column neurons receive afferent synaptic input from dorsal root ganglion neurons and then transmit information by way of the dorsal column nuclei and VPL thalamic nucleus to the somatosensory cortex.

The dorsal column system is generally regarded as a mechanoreceptive pathway, responsible for touch, vibratory sensation, and proprioception. Many of the axons that ascend directly from dorsal root ganglion cells to the dorsal column nuclei supply cutaneous mechanoreceptors, such as hair follicle, Meissner corpuscle, and Pacinian corpuscle afferents (Brown, 1968; Petit and Burgess, 1968; see Willis and Coggeshall, 2004). The dorsal column also contains afferents from slowly adapting receptors in the skin, such as Merkel cell and Ruffini endings. However, proprioceptive afferents that originate from muscle spindles and Golgi tendon organs of the cat hindlimb terminate in Clarke's column, rather than projecting all the way to the nucleus gracilis (Burgess and Clark, 1969). Clarke's column sends its output to the cerebellum but also to nucleus z, which is located just rostral to the nucleus gracilis (Pompeiano and Brodal, 1957). Nucleus z projects to the contralateral thalamus. Thus, proprioceptive input from the lower extremity depends on afferents that ascend in the fasciculus gracilis only to Clarke's column and then upon the axons of second order neurons of Clarke's column that ascend to the medulla along with the dorsal spinocerebellar tract (Grant et al., 1973). It is presumed that this pathway also exists in humans, since a nucleus z has been described in the human medulla (Sadjapour and Brodal, 1968). By contrast, proprioceptive afferents from the forelimb ascend in the fasciculus cuneatus (Whitsel et al., 1969) and terminate in the nucleus cuneatus and in the lateral cuneate

Fig. 1.10. The dorsal column–medial lemniscus pathway. Branches of primary afferent fibers from the lower part of the body (T6 and below) ascend in the fasciculus gracilis (*FG*) to synapse in the nucleus gracilis. Branches of afferents from the upper part of the body (T6 and above) ascend in the fasciculus cuneatus (*FC*) to synapse in the nucleus cuneatus. The *inset* shows the systematic addition of ascending afferent collaterals to the lateral aspect of the dorsal funiculus at progressively more rostral levels. Neurons of the dorsal column nuclei project their axons contralaterally and through the medial lemniscus to synapse in the ventral posterior lateral (*VPL*) nucleus of the thalamus. Neurons in the VPL nucleus project to the somatotopically appropriate parts of the somatosensory cortex (from Nolte, 2002)

nucleus. In primates, both of these nuclei project to the contralateral thalamus to provide proprioceptive information to thalamocortical neurons (see Willis and Coggeshall, 2004). In addition, the lateral cuneate nucleus projects to the cerebellum through the cuneocerebellar tract.

The dorsal column is not regarded as important for pain or thermal sensations, although it does contain unmyelinated axons that ascend from dorsal root ganglion cells to the dorsal column nuclei (Patterson et al., 1989). Some of the terminals of these axons contain peptides, such as substance P and calcitonin gene-related peptide (Patterson et al., 1990). However, the function of these afferents is unknown. In addition, some postsynaptic dorsal column neurons and neurons in the gracile nucleus respond to noxious stimuli (Uddenberg, 1968; Angaut-Petit, 1975; Ferrington et al., 1988; Cliffer et al., 1992). Recently, Al-Chaer et al., (1996a,b, 1997, 1999) have shown that postsynaptic dorsal column neurons may respond to noxious stimulation of viscera, as well as to mechanical stimulation of the skin. These investigators suggested that interruption of the axons of these viscerosensitive postsynaptic dorsal column neurons accounts for the successful alleviation of pelvic cancer pain that follows interruption of the gracile fasciculi at a thoracic level (Hirshberg et al., 1996; Nauta et al., 2000).

1.5.2 Spinothalamic and Associated Tracts of the Anterolateral Quadrant

There are several somatosensory pathways that ascend in the anterolateral white matter of the spinal cord (Willis and Westlund, 1997; Willis and Coggeshall, 2004). One of these is the spinothalamic tract (STT; Fig. 1.11A,B). This pathway originates in part from neurons whose cell bodies are located in the dorsal horn (Fig. 1.11A) and in part from the intermediate region and ventral horn (Fig. 1.11B). The input to the STT cells is from nociceptors, thermoreceptors, and some mechanoreceptors. The axons of STT cells cross the midline of the spinal cord in the ventral white commissure, and the axons then ascend all the way to the thalamus, where they end in several nuclei, including the ventral posterior lateral (VPL), ventral posterior inferior (VPI), posterior (Po), and central lateral (CL) nuclei (Mehler et al., 1960; Mehler, 1962; Boivie, 1979; Apkarian and Hodge, 1989; Gingold et al., 1991; Apkarian and Shi, 1994). The VPL nucleus projects to the primary and secondary somatosensory areas of the cerebral cortex (Jones, 1985). However, nociceptive information is also distributed by other thalamic nuclei to the anterior cingulate gyrus and to the insula (reviewed in Willis, 2003).

There are also collateral projections from STT cells and independent projections of pathways that accompany the STT in the anterolateral quadrant of the spinal cord (Fig. 1.12A–D). These pathways terminate in the pontomedullary and midbrain reticular formation (spinoreticular and spinomesencephalic tracts; Mehler et al., 1960; Mehler, 1962; Kevetter and Willis, 1982; Wiberg et al., 1987; Spike et al., 2003) and in several limbic system structures (spinoparabrachial, spinohypothalamic, and other spinolimbic pathways; Hylden et al., 1985; Wiberg et al., 1987; Burstein et al., 1987, 1990; Burstein and Giesler, 1989; Bernard and Besson, 1990; Cliffer et al., 1991; Burstein and Potrebic, 1993; Spike et al., 2003).

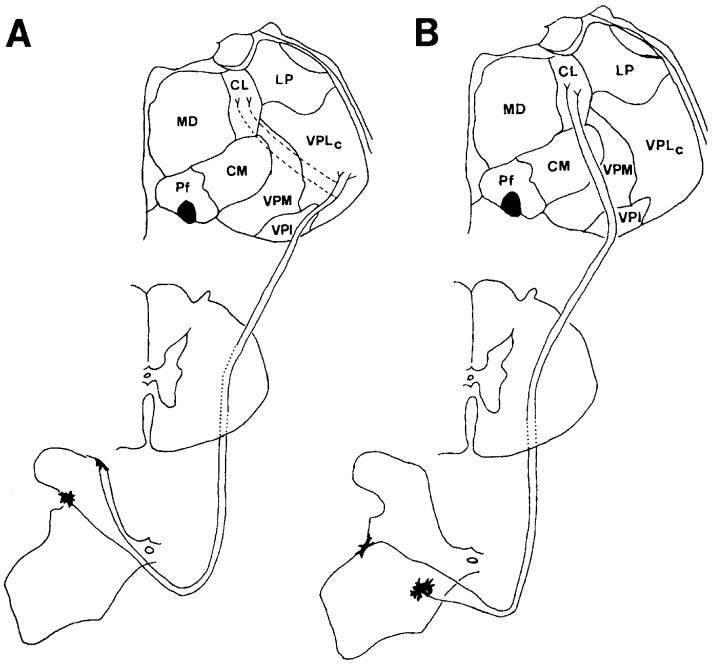

FIG. 1.11A,B. The axons of spinothalamic neurons cross to the contralateral side near the cell body of origin and then ascend to the thalamus through the anterolateral quadrant of the spinal cord white matter. **A** Course of axons belonging to one component of the spinothalamic tract. Primate spinothalamic neurons in the marginal zone and neck of the dorsal horn project to the caudal part of the ventral posterior lateral (*VPL*) nucleus (and also to the ventral posterior inferior nucleus and the posterior nuclear complex). Many of the axons also send collaterals to the central lateral (*CL*) nucleus of the intralaminar complex. **B** Course of another component of the spinothalamic tract that arises from neurons in the deep dorsal horn and the ventral horn and that projects just to the CL nucleus. *MD*, mediodorsal nucleus; *CL*, central lateral nucleus; *LP*, lateral posterior nucleus; *VPLc*, ventral posterior lateral complex; *VPM*, ventral posterior medial nucleus; *VPI*, ventral posterior inferior nucleus; *Pf*, parafascicular nucleus; *CM*, central medial nucleus (from Willis and Westlund, 1997)

1.6 Input to the Spinal Cord from Pathways Descending from the Brain

Several pathways originate in the brain and project directly to the spinal cord. The approximate locations of the lateral and ventral corticospinal tracts, the pontine and medullary reticulospinal tracts, the lateral and medial vestibulospinal tracts, and the rubrospinal tract are shown in Fig. 1.4B. Not shown are other descending pathways, including the tectospinal, hypothalamospinal, coeruleospinal, and raphespinal tracts.

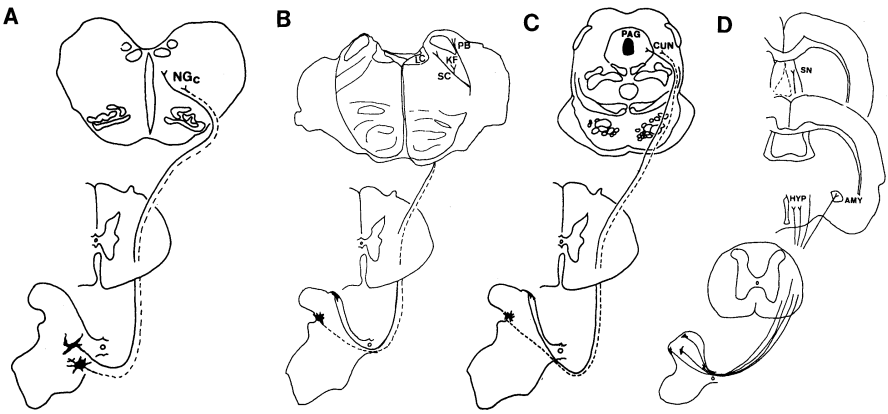

FIG. 1.12A–D. Projections of nociceptive tracts that accompany the axons of spinothalamic neurons in the anterolateral quadrant. **A** Spinoreticular tract neurons are in the intermediate region and ventral horn, and project to the medullary and pontine reticular formation, including the nucleus gigantocellularis (*NGc*). **B** Spinoparabrachial neurons are in the marginal zone and deep dorsal horn, and terminate in several nuclei, including the locus coeruleus (*LC*) and subcoeruleus (*SC*), Kölliker–Fuse nucleus (*KF*), and parabrachial nuclei (*PB*). **C** The spinomesencephalic tract originates from neurons of the marginal zone and deep dorsal horn, and projects to the midbrain reticular formation (cuneiform nucleus, *CUN*) and periaqueductal gray (*PAG*). **D** Spinolimbic tracts project from the marginal zone and deep dorsal horn to the hypothalamus (*HYP*), amygdala (*AMY*), and septal nucleus (*SN*) (from Willis and Westlund, 1997)

In primates, including humans, the lateral corticospinal tract makes monosynaptic excitatory synapses directly on alpha motor neurons (Fig. 1.13), especially on motor neurons to distal muscles, such as those that move the digits (Phillips and Porter, 1977). This provides the primary motor cortex with a mechanism to exert fine control over such motor tasks as writing or picking up objects between the thumb and index finger. The reticulo- and vestibulospinal projections are helpful for postural control (Wilson and Melville Jones, 1979). Some of the descending pathways function not so much in motor control but more in regulating afferent input. For example, the raphespinal and coeruleospinal tracts project to the dorsal horn and can inhibit nociceptive transmission (Willis and Coggeshall, 2004).

1.6.1 Corticospinal Tract

The corticospinal tract originates from pyramidal cells in layer 5 of several different cortical areas, including the primary motor cortex, the premotor and supplementary motor cortex, and the primary somatosensory cortex (Coulter and Jones, 1977; reviewed by Creutzfeldt, 1995). The corticospinal axons pass caudally through the internal capsule, cerebral peduncle, base of the pons and medullary pyramid (Fig. 1.13). Most corticospinal axons cross the midline in the pyramidal decussation and

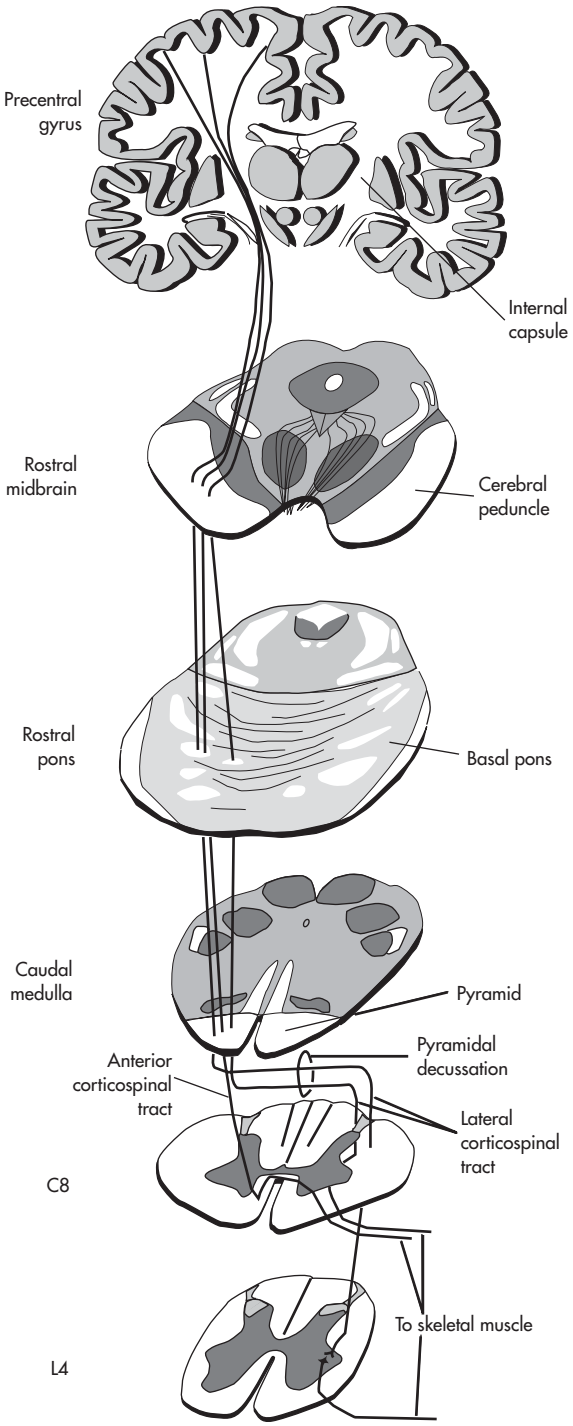

FIG. 1.13. The course of the lateral and ventral corticospinal tracts. The cells of origin are in cortical layer 5 in the primary motor, premotor, supplementary motor, and somatosensory regions of the cerebral cortex. The axons descend through the posterior limb of the internal capsule, cerebral peduncle, base of the pons, and medullary pyramid. Most of the axons cross to the opposite side in the pyramidal decussation and descend into the spinal cord in the dorsal part of the lateral funiculus as the lateral corticospinal tract. In primates, including humans, this pathway has monosynaptic terminations on motor neurons, especially on those motor neurons that innervate distal muscles. There are also synapses on interneurons. Some corticospinal axons do not cross in the decussation of the pyramid but instead continue into the ipsilateral ventral funiculus as the ventral corticospinal tract. These axons synapse on motor neurons to axial muscles of both sides of the body (from Nolte, 2002)

continue caudally in the lateral corticospinal tract, which is located in the dorsal part of the lateral funiculus (Figs. 1.4B and 1.13). Some corticospinal axons do not cross but rather descend in the ventral funiculus as the ventral corticospinal tract (Figs. 1.4B and 1.13).

Monosynaptic excitatory projections are made by the motor cortex on motor neurons, but there are also synapses on interneurons, so that many cortical actions involve modulation of reflex circuits in the spinal cord. The corticospinal projections from the somatosensory cortex are to the dorsal horn (Coulter and Jones, 1977) and function to modulate the effects of sensory input to the spinal cord (Yezierski et al., 1983).

1.6.2 Other Descending Pathways from the Brain

As mentioned, in addition to the lateral and ventral corticospinal tracts, there are a number of other pathways that originate in the brain and that descend into the spinal cord and modulate motor and/or sensory responses. These include the pontine and medullary reticulospinal tracts, the lateral and medial vestibulospinal tracts, the tectospinal tract, the coeruleospinal and raphespinal tracts, and the rubrospinal tract. The locations of most these tracts within a transverse section of the spinal cord are shown in Fig. 1.4B. In general, each pathway that projects from the brain to the spinal cord receives input from one or more pathways that ascend from the spinal cord to the brain.

The descending pathways can be divided into lateral and medial systems (Kuypers, 1981; Holstege, 1996). The lateral pathways include the lateral corticospinal tract and in animals the rubrospinal tract (which is not prominent or perhaps is nonexistent in humans). The main target of the lateral corticospinal tract is motor neurons and/or interneurons that control muscles of the distal limb (there are monosynaptic excitatory projections from the cerebral cortex to alpha motor neurons in primates, but not in cats or rats). The rubrospinal tract, when present, controls somewhat more proximal muscles. The medial system, by contrast, activates interneurons and motor neurons that control the girdle and axial muscles.

1.6.3 Spino-Bulbospinal and Other Spinal Cord–Brain Loops

Pathways that ascend from the spinal cord to end in the brain may affect sensory processing, leading to perception or alterations in perception. For example, noxious stimuli can activate not only the spinothalamic tract, leading to the perception of pain, but such stimuli can also activate brainstem pathways that produce analgesia (Schaible et al., 1991; Wei et al., 1999; Guan et al., 2003; see Willis and Coggeshall, 2004) or conversely allodynia or hyperalgesia (Haber et al., 1978; Wei et al., 1999; Sun et al., 2001).

Ascending spinal pathways may instead affect motor control by modulating the activity in descending motor pathways. A well-known example of a "spino-bulbospinal reflex" is the mechanism used by normal adults for emptying the urinary bladder. The reflex component of micturition depends on discharges in mechanoreceptive afferents supplying the wall of the urinary bladder, an ascending spinoreticular pathway

to the micturition center (Barrington's nucleus) in the rostral pons, and a descending reticulospinal pathway that activates detruser motor neurons and inhibits sympathetic and somatic motor outflow to the sphincters of the urethra (De Groat, 1998). There are also spinobulbospinal reflexes that produce somatic motor responses (Oguro et al., 1997). These depend on input to the reticular formation that then evokes a discharge in reticulospinal neurons, resulting in the activation of spinal cord motor neurons.

Acknowledgment

This work was supported in part by grants NS09743 and NS11255 from the National Institutes of Health. The author would like to thank Griselda Gonzales for her help with illustrations.

Chapter 2
Physiology of the Spinal Cord

William D. Willis, Jr.

2.1 Electrophysiological Recordings from the Spinal Cord

2.1.1 Single Unit Recordings

Using a microelectrode, it is a straightforward procedure to record the responses of single neurons within the spinal cord gray matter to stimulation of primary afferents (Willis and Coggeshall, 2004). Interneurons in the dorsal horn can be distinguished from afferent axons by their response properties and by the configuration of their action potentials. For example, interneurons can generally be activated by a number of different types of sensory receptors, whereas a primary afferent fiber would belong to just a single kind of sense organ. The extracellular action potentials of interneurons are predominantly negative (Fig. 2.1A), whereas those of afferent axons are chiefly positive in sign (because they are usually recorded just outside an internode and only rarely outside a node of Ranvier). Intracellular recordings from dorsal horn interneurons reveal postsynaptic potentials in response to stimulation of primary afferent fibers (Fig. 2.1B, upper trace). In the ventral horn, a motor neuron can be identified by antidromic activation following stimulation of its motor axon.

2.1.2 Population Recordings

Population responses evoked by stimulation of primary afferent fibers can also be recorded from large numbers of dorsal horn interneurons as "negative cord dorsum potentials" by means of a gross electrode placed in contact with the dorsal surface of the spinal cord (Fig. 2.1B, lower trace, and Fig. 2.2A; Beall et al., 1977; Willis, 1984) or as a "negative field potential" by a microelectrode inserted into the dorsal horn (Fig. 2.3; Beall et al., 1977; Willis, 1984). In monkeys, the negative cord dorsum potentials include the N1, N2 and N3 waves (Fig. 2.2B). The N1 wave is evoked by stimulation of Aβ afferent fibers, for example in a peripheral cutaneous nerve such as the sural nerve or, as in Fig. 2.2B, in a mixed nerve, the common peroneal nerve. The N2 wave is evoked by stimulation of the slowest Aβ and the largest Aδ fibers, and the N3 wave by stimulation of smaller Aδ fibers (Beall et al., 1977). Corresponding excitatory potentials can be recorded intracellularly from dorsal horn interneurons (Fig. 2.1B, upper trace; Beall et al., 1977).

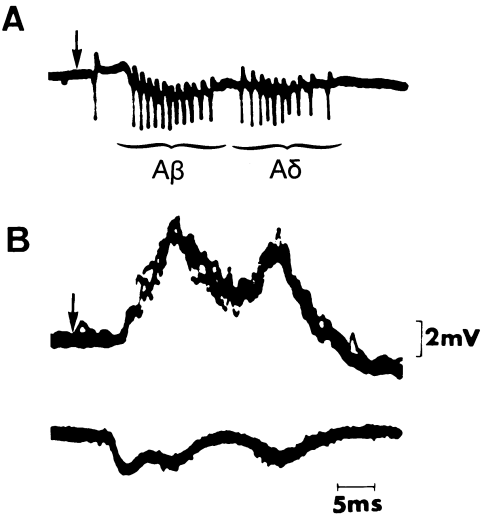

FIG. 2.1A,B. Extracellular and intracellular recordings of responses of a primate spinothalamic tract cell to electrical stimulation of the sural nerve. **A** Extracellular recording showing two bursts of action potentials that could be attributed to sequential volleys in Aβ and then Aδ fibers. Negativity is downward. **B** The upper trace is an intracellular recording of excitatory postsynaptic potentials underlying the action potential responses shown in **A**. The lower trace is the simultaneously recorded cord dorsum potential (from Beall et al., 1977)

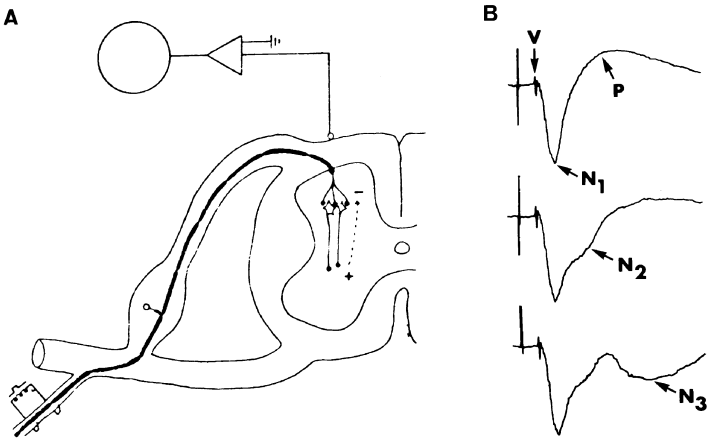

FIG. 2.2A,B. Cord dorsum potentials. **A** Method used for recording cord dorsum potentials. A gross recording electrode is placed in contact with the dorsal surface of the spinal cord. A pair of stimulating electrodes is used to activate afferent fibers in a peripheral nerve. The afferent volley excites interneurons in the dorsal horn. The region of neuropil around the cell bodies and dendrites of the interneurons becomes negative relative to ground because of the net influx of cations into the activated interneurons (that is, the region becomes a current "sink"). Current then flows extracellularly in a dorsal direction from the more ventral "source" region around the axons of the interneurons and their terminals. The dipole that is formed results in a potential that can be recorded from the cord dorsum as a negative (N) wave (from Willis, 1984). **B** Cord dorsum potentials recorded in a monkey in response to stimulation of the common peroneal nerve. The initial deflection is the stimulus artifact. This is followed by the afferent volley (*V*), one or more N waves (*N1*, *N2*, and *N3*) and a P wave (*P*) (from Beall et al., 1977)

The diagram in Fig. 2.2A provides an explanation of the cord dorsum N waves. In extracellular recordings from the cord dorsum, the gross recording electrode samples the potential in the "sink" area near the cell bodies of excited dorsal horn interneurons. The potential is negative because of the influx of cations across the postsynaptic membranes and into the cytoplasm of the nearby interneurons. This ion shift leaves behind a net negative charge in the extracellular fluid. Because of this ion shift, current will flow from the extracellular region around the axons of the interneurons, which in general project ventrally, establishing a dorsally to ventrally oriented dipole, with the positive pole in the source region around the axons and the negative pole in the sink region near the interneuronal cell bodies and dendrites. A microelectrode inserted into the "sink" area in the dorsal horn will record negative potentials, in this case termed "negative field potentials" in response to comparable stimuli. Contour maps of the field potentials equivalent to the N1, N2 and N3 cord dorsum potentials can be plotted by systematically moving the recording microelectrode across the spinal cord, as shown in Fig. 2.3A–C (Beall et al., 1977).

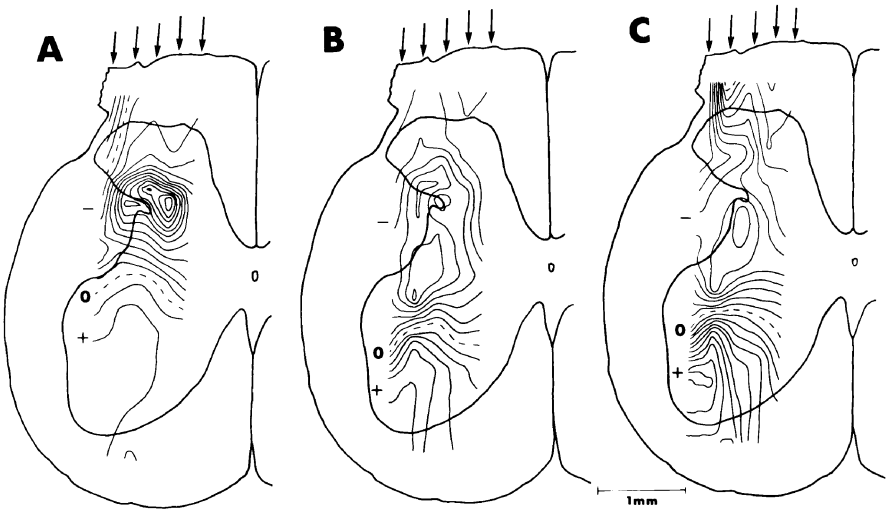

Fig. 2.3A–C. Isopotential contour plots are shown of the field potentials recorded within the spinal cord corresponding to the cord dorsum N waves evoked by electrical stimulation of the sural nerve in a monkey. **A** Distribution of the field potential that was produced by activity in response to stimulation at a strength that activated Aβ fibers and evoked the maximal N1 cord dorsum potential. The negativity peaks in the lateral part of the neck of the dorsal horn. There is a zero potential line near the border between the dorsal and ventral horns, and much of the ventral horn develops a positive potential. **B** The negative field potential evoked by the slowest Aβ fibers and the fastest Aδ fibers and the N2 cord dorsum potential. The negative region extends from the dorsal horn well into the ventral horn; the zero line and the positive region are deep in the ventral horn. **C** There are two areas of peak negativity when the stimulus activated the slowest Aδ fibers, one area along the dorsal border of the dorsal horn and the other in the neck of the dorsal horn. The stimulus was appropriate for activating the N3 wave. The zero line and positivity were deep in the ventral horn. The *arrows* at the surface of the spinal cord show where the microelectrode entered the spinal cord when the recordings were made (from Beall et al., 1977)

Following the N waves in recordings from the cord dorsum, there is a positive or P wave (Fig. 2.2B). The P wave reflects primary afferent depolarization (Fig. 2.4). Primary afferent depolarization (PAD) is thought to be produced by an action of GABA on $GABA_A$ receptors located on the terminals of primary afferent fibers in the spinal cord gray matter (Eccles et al., 1963a; see Eccles, 1964). GABA is released from GABAergic interneurons in response to volleys in the appropriate primary afferent fibers. For example, in Fig. 2.4C a series of primary afferent volleys were initiated by electrical shocks applied to group I afferents in the nerves to different sets of hindlimb flexor muscles (PBST, posterior biceps-semitendinosus, or PDP, peroneal-deep peronei; Eccles et al., 1963b). The afferent volleys presumably excited interneurons that released GABA, which then activated $GABA_A$ receptors, allowing the efflux of chloride ions. Chloride ions are concentrated in the primary afferent neurons by a special co-transporter (Alvaraez-Leefmans et al., 2001), and thus the opening of chloride channels by activation of $GABA_A$ receptors results in a depolarization of the afferent terminals in the gray matter (see Willis, 1999). The primary afferent depolarization was recorded from a population of muscle afferents in a filament of dorsal root as a negative dorsal root potential and from the cord dorsum as a P wave (Fig. 2.4C). The methods for recording these events are shown in Fig. 2.4A. The sink and source areas are shown in Fig. 2.4B.

2.2 Responses of Nociceptive Dorsal Horn Neurons to Peripheral Input

The response properties of spinothalamic tract (STT) and other spinal nociceptive neurons are often described in reference to the activity elicited by mechanical stimulation of the skin (Fig. 2.5; Mendell, 1966; Chung et al., 1979; Owens et al., 1992). Occasional STT cells respond best to weak mechanical stimuli. These are termed "low threshold" (LT) cells (referred to as cluster 1 type neurons in Fig. 2.5). Other STT cells respond to innocuous as well as noxious mechanical stimuli, although best to noxious intensities. They receive afferent input not only from nociceptors, but also from hair follicle afferents, Meissner corpuscles, and slowly adapting mechanoreceptors (but not from Pacinian corpuscles). These STT neurons are called "wide dynamic range" (WDR) cells (termed cluster 2 neurons in Fig. 2.5). Some STT cells respond only or best to intense mechanical stimuli applied to the skin. Therefore, the cutaneous mechanical input to these STT cells is restricted to nociceptors. Such neurons are often referred to as "high threshold" (HT) cells (cluster 3 neurons in Fig. 2.5).

In monkeys, over half of the STT cells in lamina I are of the WDR (cluster 2) type (Ferrington et al., 1987; Owens et al., 1992). The others are HT (cluster 3) cells. Similarly, more than half of the STT cells in laminae IV–VI of monkeys are WDR (cluster 2) cells (Owens et al., 1992). Most of the remaining STT cells are of the HT (cluster 3) type, although there are a few LT (cluster 1) STT cells in these layers of the dorsal horn. The STT cells in lamina VII are generally HT cells (Giesler et al., 1981). Some lamina I STT cells respond to innocuous thermal stimuli and thus appear to contribute to warm or cool thermal sensations (Dostrovsky and Craig, 1996; Andrew and Craig, 2001; Craig et al., 2001).

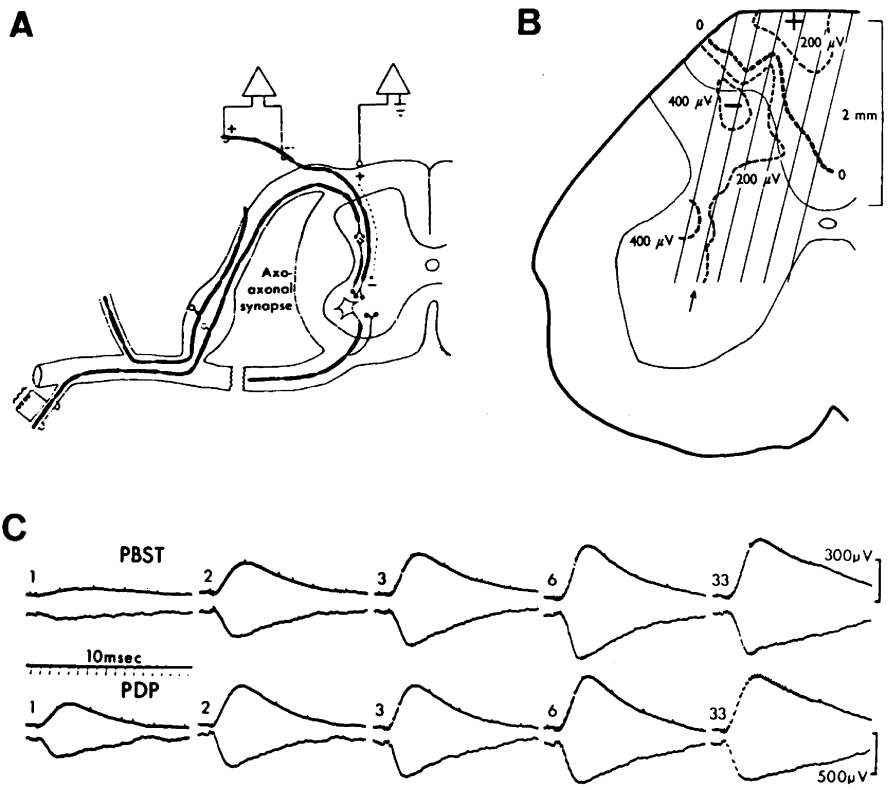

FIG. 2.4A–C. Primary afferent depolarization. **A** Methods for recording primary afferent depolarization (PAD). At the *right* is shown a gross recording electrode placed on the dorsal surface of the spinal cord. Such an electrode can be used to record the cord dorsum P wave, which reflects PAD, when primary afferent fibers are activated by a pair of stimulating electrodes in contact with a peripheral nerve. At the *upper left*, a pair of recording electrodes is placed along a filament of dorsal root. During PAD, there is a potential difference between the electrodes because of the electrotonic spread of PAD from the synaptic endings, where PAD is generated, distally along the axons. Since the length constant of the largest afferents is in the order of millimeters, it is possible to record PAD in dorsal rootlets. The electrode nearest the spinal cord becomes negative to that placed more distally, resulting in a negative dorsal root potential (from Willis, 1984). **B** Distribution of potential in the spinal cord during PAD. The extracellular fluid near primary afferent fibers entering the dorsal part of the spinal cord serves as the area of current sources and the region around their terminals as the area of current sinks, since the afferents that develop PAD act as dipoles, with the negativity located ventrally and the positivity in the dorsal part of the cord (from Eccles et al., 1962). **C** Temporal summation of the PAD produced by 1, 2, 3, 6, or 33 volleys in nerves to groups of flexor muscles (posterior biceps-semitendinosus [*PBST*] and peroneal-deep peronei [*PDP*] nerves). The *upper rows* of records are dorsal root potentials, and the *lower rows* are cord dorsum P waves (from Eccles et al., 1963b)

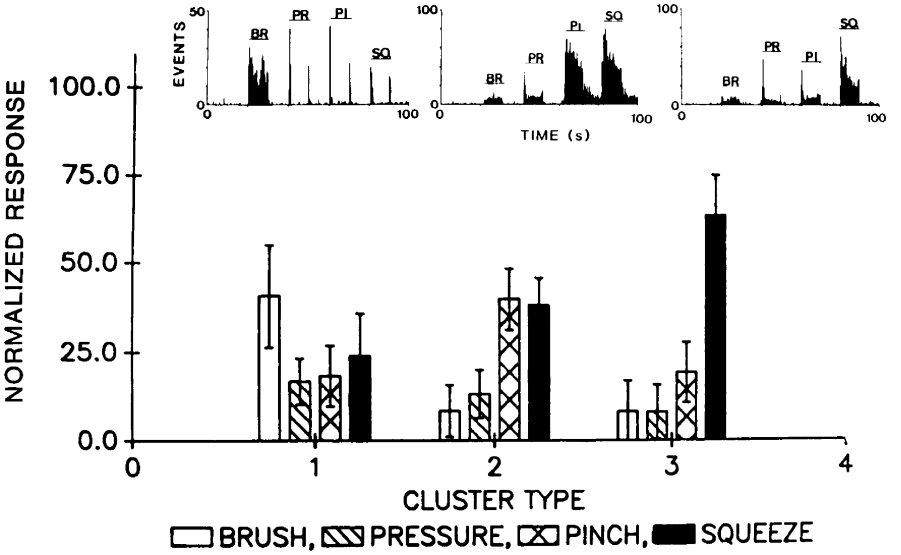

FIG. 2.5. Responses typical of different types of primate spinothalamic tract cells. The skin was stimulated using four graded intensities of mechanical stimuli. The weakest stimulus was repeated brushing (*BR*) of the skin. A strong, maintained pressure (*PR*) stimulus was produced by application of a large arterial clip to a fold of skin. The same stimulus applied to the skin of the investigators was near threshold for pain. A distinctly painful pinch (*PI*) stimulus that did not produce overt damage was produced by a small arterial clip. The strongest stimulus was squeezing (*SQ*) the skin with serrated forceps, a damaging stimulus. The peristimulus time histograms show responses of typical low threshold (LT) (cluster 1), wide-dynamic range (WDR) (cluster 2), and high threshold (HT) (cluster 3) spinothalamic tract (STT) cells. The bar graphs represent the averaged responses to the four stimuli of populations of LT, WDR, and HT STT cells. Cluster analysis was used to provide an objective basis for distinguishing the different types of STT cells (from Owens et al., 1992)

Other sensory inputs to STT cells arise from sensory receptors in muscle, joints and viscera (Foreman et al., 1979, 1984; Milne et al., 1981; Dougherty et al., 1992). The afferents include mechanoreceptors and nociceptors. Widespread convergence of afferents that supply several different target organs, including the skin, is common. Convergent input from skin and from viscera and/or muscle may help account for pain referral.

The spinothalamic tract in primates originates from neurons whose cell bodies are distributed widely in the spinal cord gray matter (Willis and Coggeshall, 2004). There are at least three main groups of STT cells. One group has its cell bodies in lamina I, the second group in laminae IV–VI, and the third in lamina VII (see Fig. 1.11; Willis et al., 1979, 2001; Giesler et al., 1981; Ferrington et al., 1987; Apkarian and Hodge, 1989). Spinothalamic tract cells in lamina I tend to have small receptive fields (Willis, 1989), and they are somatotopically organized (Willis et al., 1974). These features suggest that the lamina I STT cells provide sensory information about the location of a stimulus. Spinothalamic tract cells in laminae IV–VI generally have larger receptive fields (Willis, 1989), and so they would not be as helpful for stimulus localization. However, wide dynamic range STT cells have steeper stimulus—response functions

than do high threshold STT cells, whether the cells are in lamina I or deep layers of the dorsal horn, and so they are better able to discriminate stimulus intensity (Surmeier et al., 1986; cf. Maixner et al., 1986). Lamina I STT cells project to the VPL nucleus, as well as to the posterior (Po) complex of thalamic nuclei. Spinothalamic tract cells in laminae IV–VI also project to VPL and Po, and in addition many send collaterals to the central lateral (CL) nucleus of the intralaminar complex (Giesler et al., 1981). Spinothalamic tract cells in lamina VII tend to have very large, bilateral receptive fields (often covering the entire body and face), and so they could not convey reliable information about stimulus location. They project just to the CL nucleus and are high threshold neurons (Giesler et al., 1981). They may contribute to arousal, attention and other motivational-affective responses to painful stimuli.

2.3 Responses of Spinal Cord Neurons to Corticospinal Volleys

Single unit or population responses of spinal cord neurons can also be recorded following the activation of corticospinal neurons (e.g., Zhang et al., 1991). In Fig. 2.6A, the responses of an STT neuron are shown following stimulation of the cerebral

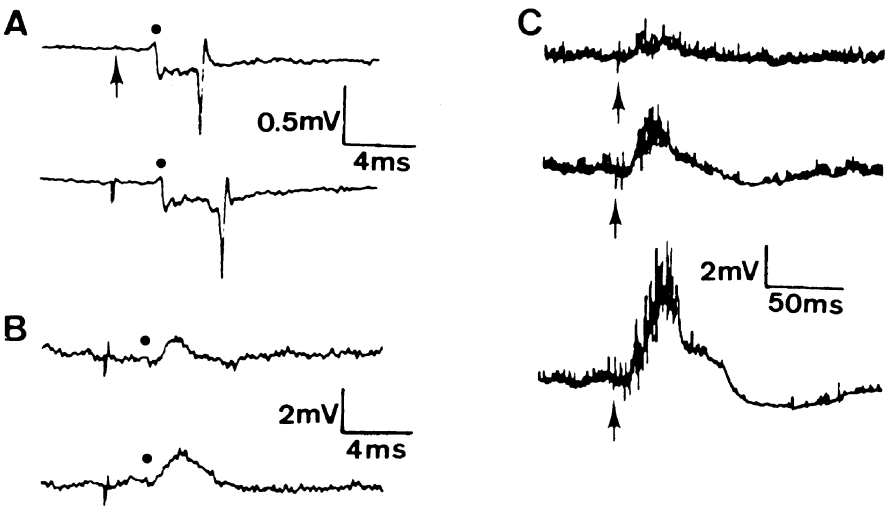

Fig. 2.6A–C. Excitation of primate spinothalamic tract (STT) neurons by corticospinal tract volleys. **A** Extracellular recordings of field potential in the dorsal horn and an action potential generated by an STT cell in response to a volley in corticospinal neurons evoked by stimulation of the cerebral peduncle (*upper trace*) or of the motor cortex (*bottom trace*). The *dots* indicate the corticospinal tract volleys. **B** Intracellular recordings of excitatory postsynaptic potentials (EPSPs) produced by stimulation of the cerebral peduncle at two different strengths. **C** Temporal summation of EPSPs evoked by one, two, and four stimuli applied to the cerebral peduncle. Each trace represents 50 signal-averaged responses. The first stimulus artifact in each trace is indicated by an *arrow*. The EPSPs evoked action potentials at various latencies (from Zhang et al., 1991)

peduncle (upper trace) or of the primary motor cortex (lower trace). The responses were recorded extracellularly and included a negative field potential, followed by a single action potential generated by the STT cell. In Fig. 2.6B, intracellular recordings from another STT cell show the excitatory postsynaptic potentials (EPSPs) evoked by activation of the corticospinal tract in the cerebral peduncle by two different stimulus strengths. The sizes of the EPSPs recorded from another STT cell showed considerable temporal summation (Fig. 2.6C).

Acknowledgment

This work was supported in part by grants NS09743 and NS11255 from the National Institutes of Health. The author would like to thank Griselda Gonzales for her help with illustrations.

Chapter 3
Pharmacology of the Spinal Cord

William D. Willis, Jr.

As in the brain, the presynaptic terminals of most excitatory synapses in the spinal cord release glutamate as a fast excitatory neurotransmitter (Curtis et al., 1959; reviewed in Willis and Coggeshall, 2004). In addition to glutamate, primary afferent terminals of nociceptors can also contain excitatory neuropeptides, such as substance P (SP; De Biasi and Rustioni, 1988) and calcitonin gene-related peptide (CGRP; Wiesenfeld-Hallin et al., 1984). Aspartate does not appear to be a transmitter in primary afferent terminals, since it is not stored in synaptic vesicles in such endings (Broman and Adahl, 1994). However, aspartate is released from dorsal horn interneurons and may well serve as a fast excitatory transmitter of interneurons, in addition to glutamate.

A number of synthetic excitatory amino acids have been used to explore the responses of different excitatory amino acid receptors. Synthetic excitatory amino acids include DL-α-amino-3-hydroxy-5-methylisoxazolepropionic acid (AMPA), kainic acid, and *N*-methyl-D-aspartic acid (NMDA). These selectively activate, respectively, AMPA, kainate, and NMDA receptors, the three types of ionotropic glutamate receptors (Hollman and Heinemann, 1994; Dingledine et al., 1999). The term "ionotropic" refers to the opening of ligand-gated ion channels when such receptors are activated. Antagonists of these receptors are also available. 6-Cyano-7-nitroquinoxaline-2,3-dione (CNQX) blocks both AMPA and kainate receptors, which are often grouped together as non-NMDA receptors. More selective antagonists are now available for AMPA and for kainate receptors. Selective NMDA receptor antagonists include 2-amino-5-phosphonovaleric acid (AP5) and 2-amino-7-phosphonoheptanoic acid (AP7).

Other glutamate receptors that are known as metabotropic glutamate receptors activate signal transduction cascades, rather than directly opening ion channels. Metabotropic glutamate receptors are divided into groups I, II and III (see Conn and Pin, 1997; Schoepp, 2001). The actions of group I metabotropic glutamate receptors tend to oppose those of groups II and III. A number of agonists and antagonists are now available for studies designed to assess the functional role of these receptors.

Intracellular recordings have been made of monosynaptic excitatory postsynaptic potentials or of excitatory postsynaptic currents during whole-cell patch-clamp experiments in spinal cord slices from dorsal horn interneurons following stimula-

tion of a dorsal root. The earliest component of the excitatory responses is largely blocked by CNQX (antagonist of non-NMDA glutamate receptors), whereas the late components, as well as polysynaptic EPSPs, are reduced by AP5 (antagonist of NMDA receptors; Yoshimura and Jessell, 1990; Näsström et al., 1994; Miller and Woolf, 1996).

An example of the responses of a primate spinothalamic tract (STT) neuron to excitatory amino acids released in the vicinity of the cell by microiontophoresis and of the blocking of the responses to several excitatory amino acids by administration of the NMDA receptor antagonist AP7 by microdialysis is shown in Fig. 3.1 (Dougherty et al., 1992). The results of this experiment suggest that the responses of STT cells to AMPA and glutamate are largely mediated by AMPA receptors and those to NMDA and to aspartate by NMDA receptors.

Another putative fast excitatory transmitter in the dorsal horn is adenosine triphosphate (ATP) (Sawynok and Sweeney, 1989; Salter et al., 1993), which acts on purinergic receptors, including ionotropic P2X receptors and metabotropic P2Y receptors (see Willis and Coggeshall, 2004).

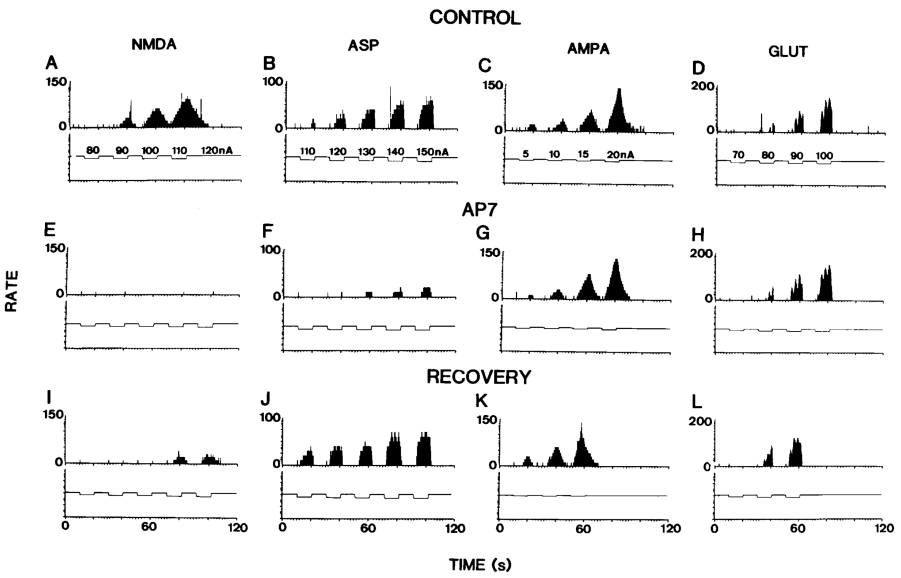

Fig. 3.1A–L. Excitation of a primate spinothalamic tract neuron by iontophoretic release of excitatory amino acids. **A–D** show the effects of graded current doses of iontophoretically released *N*-methyl-D-aspartic acid (*NMDA*), aspartate (*ASP*), DL-α-amino-3-hydroxy-5-methylisoxazolepropionic acid (*AMPA*), and glutamate (*GLUT*) near an antidromically identified spinothalamic tract (STT) cell. The monitor traces show the current strengths used. 2-Amino-7-phosphonoheptanoic acid (*AP7*) (antagonist of NMDA receptors) was then administered through a nearby microdialysis fiber, and then the traces in **E–H** were recorded. The AP7 completely blocked the effects of NMDA and greatly reduced those of ASP, without affecting those of AMPA or GLUT. **I–L** show partial recovery of the responses 2 h after termination of AP7 administration (from Dougherty et al., 1992)

As already mentioned, a number of neuropeptides are thought to serve as slow neurotransmitters or as "modulators" in the dorsal horn. These include substance P (Nicoll et al., 1980) and other neurokinins, calcitonin gene-related peptide (Chung et al., 1988), vasoactive intestinal polypeptide, neurotensin, and cholecystokinin (see Willis and Coggeshall, 2004). Each peptide acts on one or more receptors, which are generally G-protein coupled receptors. Examples include NK1, NK2, and NK3 neurokinin receptors, and CGRP1 receptors. Substances that activate metabotropic receptors are considered neuromodulators because they generally do not directly elicit action potentials, in contrast to excitatory ligand-gated ion channels or "ionotropic" receptors (Kandel et al., 2000). Figure 3.2 shows the modulatory effect of SP on the responses of a primate spinothalamic tract cell to iontophoretically applied NMDA (Dougherty and Willis, 1991). Initially, a current dose of 20 nA of NMDA had no effect on the neuron. However, after iontophoretic release of SP (20 nA) for 30 s, the same current dose of 20 nA of NMDA was able to excite the neuron, and this excitation grew progressively more powerful over a period of 15 min. The response continued to be enhanced for hours. It is evident from the recordings that NMDA, acting on the ionotropic NMDA receptor, had a powerful action in evoking action potentials in this neuron. By contrast, SP did not itself elicit action potentials (not illustrated), but

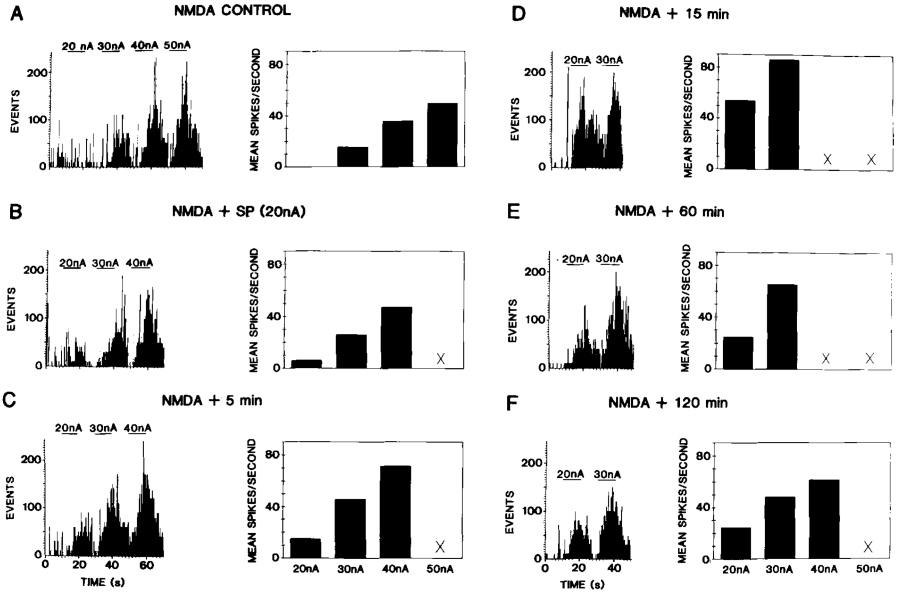

FIG. 3.2A–F. Modulatory effect of substance P (*SP*) on the responses of an STT cell to iontophoretically released NMDA. **A** Peristimulus time histogram and a bar graph show the responses of the STT cell to graded current doses of NMDA (20, 30, 40, and 50 nA). The 20 nA dose had no effect. **B–D** After iontophoretic application of SP (20 nA), the 20 nA dose of NMDA became progressively more effective over a period of 15 min. **E, F** The response then declined but was still present after 120 min (from Dougherty and Willis, 1991)

instead enhanced the ability of NMDA to do so. Thus, SP in this case could be described as a modulator.

Inhibitory neurotransmitters in the spinal cord include inhibitory amino acids and peptides. γ-Aminobutyric acid (GABA) and glycine are prominent inhibitory amino acid transmitters in the dorsal horn, and glycine is preferentially concentrated in the ventral horn (Willis and Coggeshall, 2004). GABA receptors include GABAA and GABAB receptors. GABAA receptors are ionotropic and are associated with chloride channels, whereas GABAB receptors are metabotropic G-protein coupled receptors. Muscimol is an agonist and bicuculline a selective antagonist of GABAA receptors. Baclofen is a selective agonist and phaclofen a selective antagonist of GABAB receptors. Glycine receptors are ionotropic and, like GABAA receptors, they activate chloride channels. Strychnine is a selective antagonist of glycine receptors. Figure 3.3 shows the inhibitory effects of GABA, glycine, and baclofen on primate STT cells, as well as the antagonistic action of baclofen on GABAB receptors (Willcockson et al., 1984; Lin et al., 1996).

GABAA receptors are found both on presynaptic terminals and on postsynaptic neurons. However, the action of GABA on presynaptic endings is to produce primary afferent depolarization (PAD), whereas the postsynaptic action is a hyperpolarization. The reason for these opposite actions is that primary afferent neurons contain a chloride cotransporter that concentrates chloride ions within these neurons, and so opening the chloride channels results in an efflux of chloride ions and a depolarization (Alvarez-Leefmans et al., 1988; see Willis, 1999). By contrast, the chloride transporter in dorsal horn interneurons concentrates chloride extracellularly, and so the action of GABA or glycine on these neurons results in an influx of chloride ions and a hyperpolarization. In all of these cases, however, the actions are inhibitory, since PAD causes presynaptic inhibition, whereas the postsynaptic hyperpolarization causes postsynaptic inhibition (see Eccles, 1964; Willis, 1999; Willis and Coggeshall, 2004). Activation of GABAB receptors on primary afferent terminals results in a type of presynaptic inhibition that does not depend on PAD. Instead, the GABAB receptors block the influx of calcium through presynaptic calcium channels associated with transmitter release. $GABA_B$ receptors are also found postsynaptically.

Inhibitory peptides in the spinal cord include the opioids, somatostatin, galanin, and others (Willis and Coggeshall, 2004). Several different opioid peptides are found in the dorsal horn, including endomorphin 1 and 2 (Zadina et al., 1997; Wu et al., 1999), enkephalin (Hunt et al., 1980), and dynorphin (Ruda et al., 1988). These act, respectively, at μ-, δ-, and κ-opiate receptors (see Willis and Coggeshall, 2004). Opiate receptors are found at both pre- and postsynaptic sites. Figure 3.4 shows the inhibition of an STT cell when morphine was released iontophoretically near the cell (Willcockson et al., 1986). In the same study, some STT cells were excited by iontophoretic release of morphine.

Low doses of barbiturates, such as sodium pentobarbital, can have an excitatory effect of the responses of STT cells to C-fiber volleys, although higher doses reduce the responses to C fibers (Hori et al., 1984). The responses to A-fiber volleys are just reduced.

In addition to the neurotransmitters released by primary afferent terminals and propriospinal neurons, several additional neurotransmitters are used by brainstem

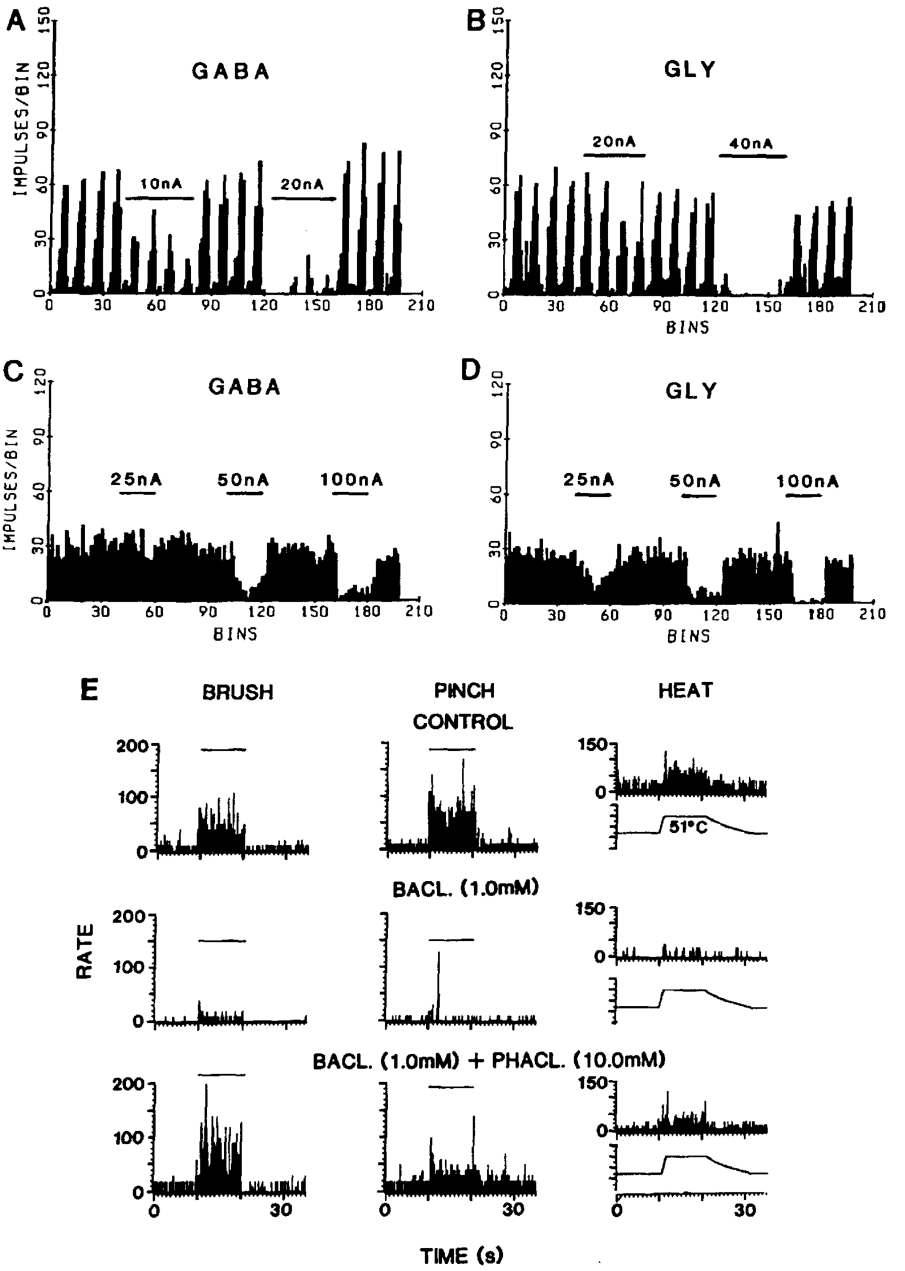

FIG. 3.3A–E. Actions of inhibitory amino acids and baclofen on γ-aminobutyric acid (*GABA*) and glycine (*GLY*) receptors on primate STT cells. **A, B** Inhibition of the responses of a primate spinothalamic tract cell to iontophoretically applied pulses of glutamate by GABA and glycine also released iontophoretically. **C, D** Inhibition of the responses of an STT cell to noxious pinch by iontophoretically released GABA and glycine (from Willcockson et al., 1984). **E** Inhibition of the responses of an STT cell to brush, pinch, and heat by microdialysis administration of baclofen (*BACL*), and reversal of this action by phaclofen (*PHACL*) (from Lin et al., 1996)

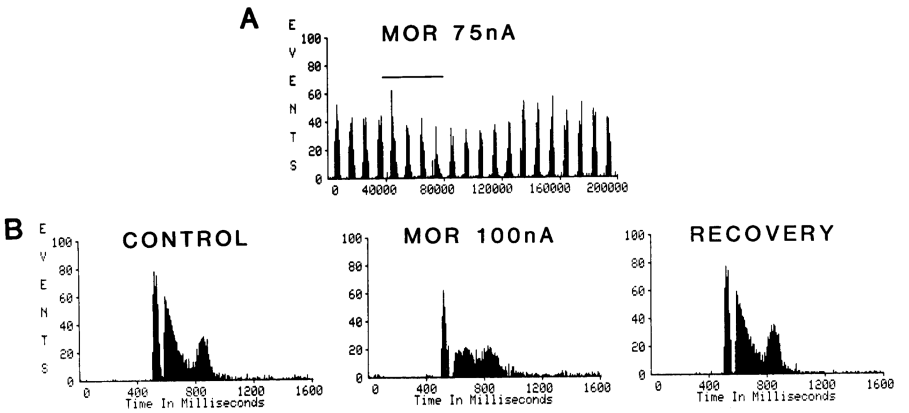

Fig. 3.4A,B. Effect of morphine (*MOR*) on the responses of an STT cell. **A** Morphine released iontophoretically near a primate STT neuron inhibited the responses of the cell to pulsed release of glutamate. **B** The STT cell was activated by volleys in A and C fibers of the tibial nerve evoked by electrical stimulation. Iontophoretically applied morphine reduced the responses, although the effect of morphine was more powerful for the later components of the responses than for the early component (from Willcockson et al., 1986)

neurons whose axons descend to the spinal cord from the brain. These include serotonin, which is contained in raphe-spinal axons, norepinephrine and epinephrine in catecholaminergic neurons of the locus coeruleus and other nuclei in the parabrachial region and in the medulla, as well as peptides contained in some of the descending projections (see Willis, 1982, 1988; Besson and Chaouch, 1987; Willis and Coggeshall, 2004).

Acknowledgment

This work was supported in part by grants NS09743 and NS11255 from the National Institutes of Health. The author would like to thank Griselda Gonzales for her help with illustrations.

Chapter 4
Overviews of Human (Evoked) Spinal Cord Potentials (SCPs): Recording Methods and Terminology

Koki Shimoji

4.1 Animal SCPs and Human SCPs

Since Gasser and Graham (1933) first recorded the segmental spinal cord potential (SCP) from the dorsal surface of the cord in response to stimulation of the dorsal roots, its origin has been investigated by many neurophysiologists (Armett et al., 1961; Austin and McCouch, 1955; Barron and Matthews, 1938; Beall et al., 1977; Bernhard, 1953; Campbell, 1945; Carpenter and Rudomín, 1973; Fitzgerald and Wall, 1980; Howland et al., 1955; Lindblom and Ottoson, 1953a,b; Lupa and Niechaj, 1977). The fundamental pattern of the segmental SCP consists of an initially positive spike and subsequent slow negative (N) and positive (P) waves (refer to basic physiology, Chapter 2). It is generally agreed that the initially positive spike and N- and P-waves reflect the incoming afferent volleys along the root, the activities of interneurons in the dorsal horn, and the generation of primary afferent depolarization (PAD), respectively (Anders-Trelles, 1976; Barron and Matthews, 1938; Bernhard, 1953; Eccles and Malcolm, 1946; Eccles et al., 1963a; Fernandez de Molina and Gray, 1957; Fitzgerald and Wall, 1980; Hughes and Gasser, 1934a,b; Koketsu, 1956a,b; Mendell, 1972; Wall, 1958) (Fig. 4.1). The N-wave has been subdivided into two (Austin and McCouch, 1955; Bernhard, 1953) or three components (Beall et al., 1977; Christensen and Perl, 1970), the origins of which are variously interpreted.

Although the basic pattern of the segmental SCP is similar in the frog, cat, and monkey, the time course of the slow waves has been found to be somewhat different across the species (Austin and McCouch, 1955; Eccles and Malcolm, 1946; Rudomín et al., 1978; Schmidt, 1971; Shimoji et al., 1975, 1977; Yates et al., 1982), leading to the suggestion that their origins may differ in part among the species (Eccles and Malcolm, 1946; Shimoji et al., 1976).

In humans, Magladery (Magladery et al., 1951) first attempted to record the SCP with electrodes inserted into the lumbar arachnoidal space in volunteers. He noted the slow "intermediary potentials," but did not characterize the origin of the potentials further, because the risk of recording by his technique was high. A safe method of recording the human SCP was developed by Shimoji et al. (1971) using epidural catheter electrodes, based on the anesthetic technique of continuous epidural block (Figs. 4.2 and 4.3). It has been shown that the basic pattern of the human SCP evoked

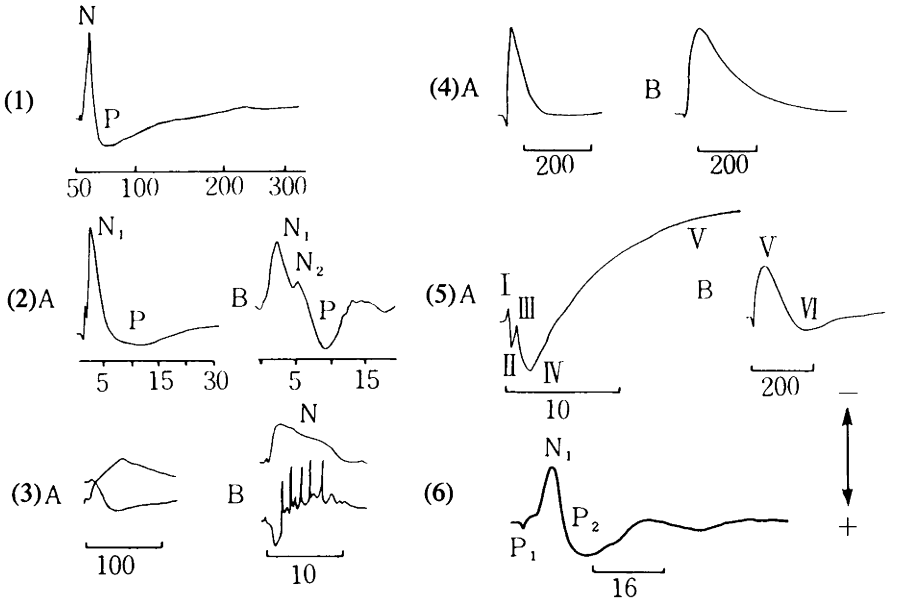

Fig. 4.1. Spinal cord potentials (SCPs) and dorsal root potentials (DRPs) evoked by segmental roots or nerves in animals. **1** SCP recorded from the dorsal surface of the lumbar spinal cord in a spinalized cat in response to electrical stimulation of the 7th lumbar dorsal root reported first by Gasser and Graham in 1933. **2** SCPs also in the intact cat during resting (*A*) and alert (*B*) states. Note that negative and positive waves now have secondary components (Bernhard, 1953). **3A** Dorsal root potential (a slow negative potential recorded from the dorsal root in the vicinity of the dorsal root entry through the DC amplifier, DRP5 by Lloyd's terminology, which reflects primary afferent depolarization, PAD) (*upper trace*) and SCP recorded from the dorsal surface of the cord (*lower trace*) in response to gastrocnemius-soleus nerve stimulation in pentobarbital-anesthetized cat. Note that both the DRP5 and slow positive wave of the cord share a similar time course with opposite polarity, which suggests the same origin of the two potentials. **3B** The SCP recorded from the dorsal surface of the cord (upper trace) and extracellularly recorded spike potentials of a single cell (D-type interneuron) from the dorsal horn by stimulation of the gastrocnemius-soleus nerve in the cat (Eccles et al., 1962a,b,c). **4A** The DRPV in the cat. **4B** The DRPV in the frog. Note the differences in the time courses between the two potentials. **5A** The components of the DRP in an expanded timescale and increased amplitude, showing its five components, advocated by Lloyd (1952). The initial three components, *I–III*, may reflect the incoming volleys along the root. The following positive wave may reflect activity of dorsal horn neurons **5B** The same potential as that in **5A** with a contracted timescale, showing DRPV and DRPVI. The origin of the DRPVI is variously interpreted as a reversal potential of the preceding potential or a primary afferent hyperpolarization. **6** The SCP in a human recorded from the dorsal epidural space at the L1 level in response to tibial nerve stimulation (Shimoji et al., 1971, 1977). Upward deflection represents negativity in all records in this figure. Timescales are shown in milliseconds

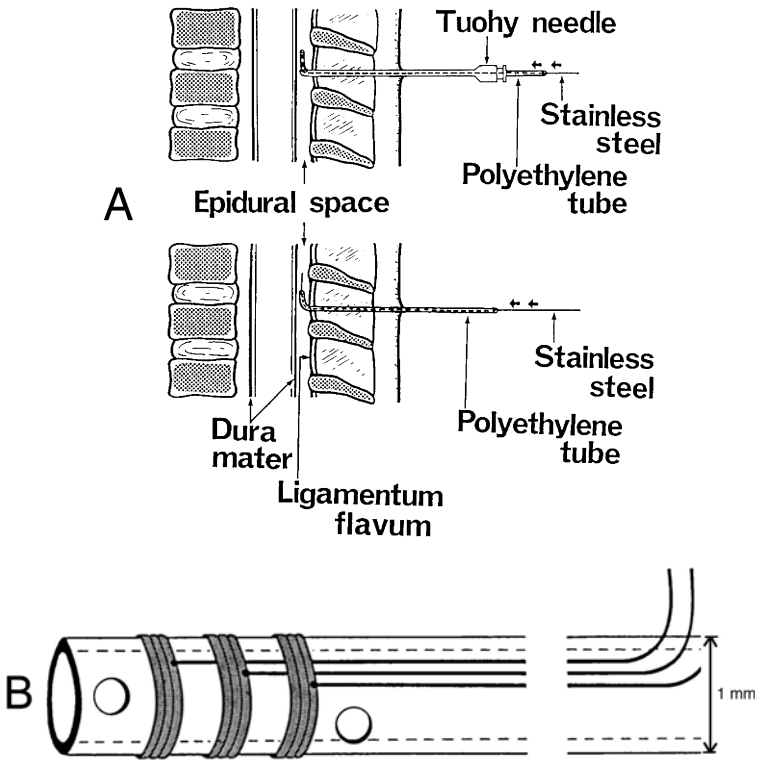

Fig. 4.2A–D. Techniques for recording human SCPs from the epidural space. **A** The original methods of placing the catheter electrodes into the epidural space, shown schematically. After making a skin wheal and injecting local anesthetics over the selected interspaces aseptically, an 18-gauge Tuohy needle is inserted into the epidural space by a paramedian approach, which makes it possible to reach any level of the epidural space without interfering with spinal processes. Placement of the tip of the Tuohy needle in the epidural space can be confirmed by a loss of resistance or a negative pressure in the syringe (loss of resistance method). After ascertaining that neither blood nor spinal fluid is aspirated, a polyethylene tube (epidural catheter) 200–400 mm in length is inserted through the Tuohy needle to approximately 50 mm beyond the tip of the needle to prepare a smooth canal for the stainless-steel wire. One stainless wire is advanced through the catheter up to 5 mm from the tip of the catheter. Then the Tuohy needle is removed by sliding through the catheter (Shimoji et al., 1971). **B** Commercially available epidural catheter electrodes, which can also be used for epidural stimulation of the spinal cord for management of pain (Hayatsu et al., 2001).

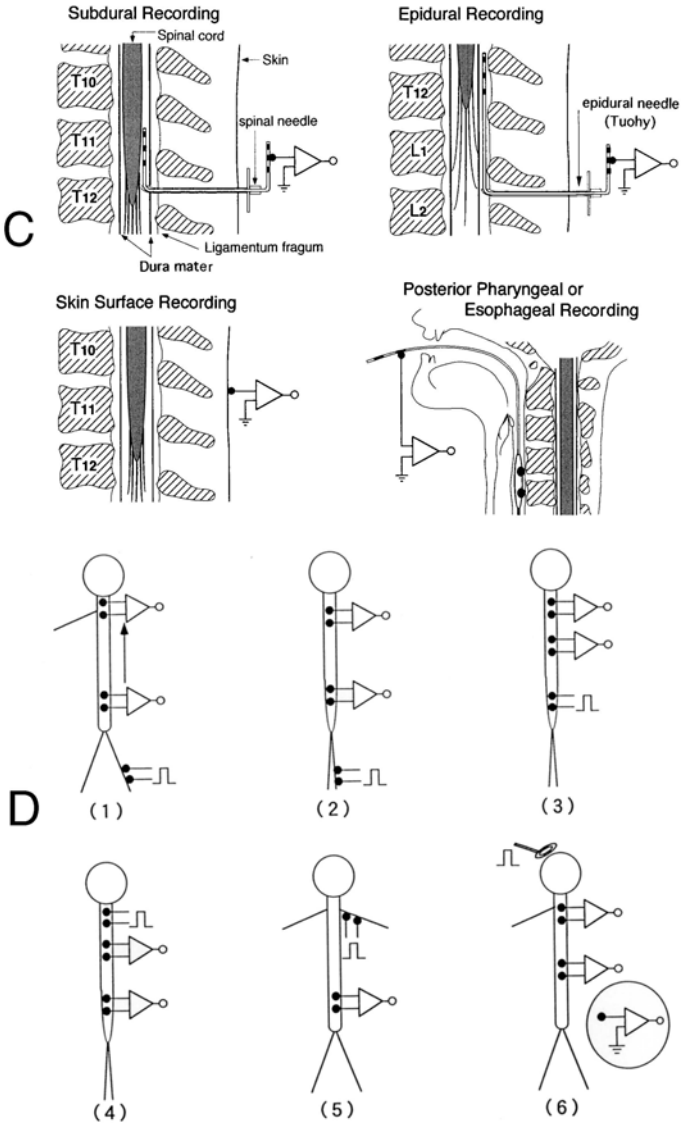

FIG. 4.2A–D. *Continued*. **C** Schematic drawing of various electrode placements for recording the SCPs. *Upper left*, subdural placement; *upper right*, epidural placement; *lower left*, skin surface placement; *lower right*, posterior pharyngeal (or esophageal) placement. **D** Some examples of stimulating and recording electrode placements (bipolarly placed): *1*, tibial nerve stimulation at the popliteal fossa, and recording from the posterior epidural space at cervical enlargement (ascending SCP) and at lumbar enlargement (segmental SCP); *2*, cauda equina stimulation from the posterior epidural space at the L3/4 vertebral level and recording from the posterior epidural space at cervical (ascending SCP) and lumbar (segmental SCP) enlargements; *3*, spinal cord stimulation from the posterior epidural space at the lumbar region and recording the ascending SCPs from the posterior epidural space at the thoracic and cervical levels; *4*, cervical spinal cord stimulation from the posterior epidural space and recording the descending SCPs from the posterior epidural space at the thoracic and lumbar regions; *5*, brachial plexus stimulation at Erb's point and recording the heterosegmental SCP from the posterior space at the level of lumbar enlargement; *6*, transcranial electric or magnetic simulation of the motor area through the scalp and recording the motor evoked SCPs from the posterior epidural space at cervical and lumbar regions. Recordings of the SCPs bipolarly or monopolarly (shown inside the circle) may vary depending on the purpose of the test

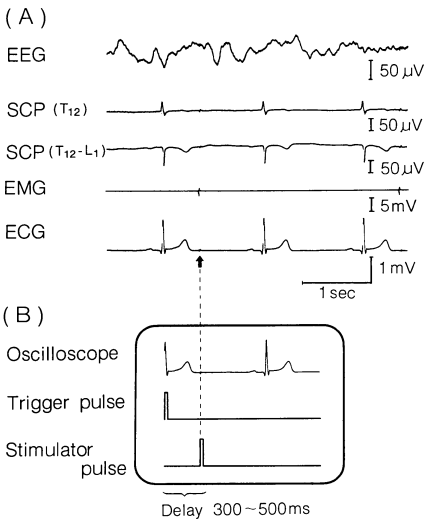

FIG. 4.3A,B. Arrangements for timing of delivery of electrical stimuli to the peripheral nerves to eliminate electrocardiogram contamination in the SCP recording. **A** Upper traces (polygraphic recordings). From the top: EEG (left F-P), monopolar recording of the SCP from the posterior epidural space at T12 (the reference electrode, skin surface at the same segment), bipolar recording between T12 and L1 from the posterior epidural space, and ECG (lead two). Note large artifacts of ECG even in the recordings from the epidural space. **B** Lower oscilloscope traces. *Top trace*, ECG display triggered by the QRS complexes; *second trace*, a pulse triggered by QRS complexes of ECG; *third trace*, stimulating pulse triggered by the above pulse at a certain delay during silent period of the ECG (Shimoji et al., 1984)

by a segmental volley is the same as that of animals, but somewhat more complex (Shimoji et al., 1972, 1975, 1977) (see Figs. 4.4–4.6).

Although there are several terminologies used in the literature regarding the human SCP in terms of the sites or methods of stimulation and recording, some suggestions follow in the next chapter.

4.2 Recording Methods of Human SCPs from the Posterior Epidural Space

The human spinal cord potential (SCP) can be safely and reliably recorded from the epidural space. It can also be recorded from the skin, but interpretation of its components is difficult because the spinal cord is deeply situated in the spinal canal far from the skin, surrounded by spines, muscles, and other organs such as the heart, aorta, and diaphragm. Although these organs may interfere with the electrical activities of the human SCPs, other methods of recording the human SCPs are valuable in a situation when recording from the epidural space is difficult (see Fig. 4.3).

Procedures to introduce the electrodes into the posterior epidural space are basically the same as those of continuous epidural analgesia. Subjects are asked to lie on

the table in the lateral position and to be well flexed in order to open the interspaces of the vertebral column. The skin in the segmental area of the electrode placement is sterilized, and a local anesthetic is injected. A Tuohy needle of 16–18 gauge is inserted into the posterior epidural space by a paramedian approach, which makes it possible to reach any level of the epidural space without interfering with spinal processes (Fig. 4.2). Recording of the human SCPs should be carried out in a quiet, soundproof room or operating room with shielded wall.

For delivering electrical stimulation to the peripheral nerves at the appropriate interval, it is best to do so by eliminating interference of the electromyogram (EMG), electrocardiogram (ECG), and other sources of electrical activity in the body. To eliminate the EMG artifacts, the patients must be relaxed during recording. To eliminate ECG artifacts, it might be more reliable to record the SCPs during the silent interval of the ECG. Figure 4.3A represents a specimen polygraphic record of the SCPs recorded from the posterior epidural space at the T12 vertebral level monopolarly and at the T12–L1 bipolarly (the second and third traces, respectively), and an evoked electromyogram from the calf muscle (the fourth trace) simultaneously with an electroencephalogram (the first trace) and ECG (the fifth trace). The stimuli are delivered to the posterior tibial nerve in the right popliteal fossa. As demonstrated in Fig. 4.3A, the polygraphic records of the SCPs are contaminated by large ECG artifacts that may interfere with the evoked SCPs. To eliminate these ECG artifacts, the evoked potentials are obtained at intervals between the T and P waves of the ECG (Shimoji et al., 1976, 1982). This is accomplished by the following arrangement as demonstrated schematically in Fig. 4.3B. The ECGs are displayed on an oscilloscope with the sweep triggered by every (or every other) QRS complex. A pulse is generated at the start of each sweep and is fed into the stimulator as the trigger. Thus the stimulus is delivered with a variable delay after every (or every other) complex of the ECG. The SCPs, which are monitored on other channels of the oscilloscope and continuously recorded on the polygraph, are fed into a computer for averaging. The computer is triggered by the stimulus pulses. The time constant or frequency band of analysis of the SCPs must be set at a longer duration (0.3–2.0 s) or a lower band for the accurate recording of the slow component of the SCPs.

The position of the tip of the catheter electrode (Fig. 4.2) can be verified by three methods: first, by X-ray photography or imaging; second, stimulation of the spinal cord by the catheter electrodes epidurally and observation of the segmental muscle twitches; third, judgment based on the waveform of the segmental SCPs. When the catheter electrodes are situated in the posterior epidural space on the midline, stimulation through the catheter electrodes produces bilateral twitches of the segmental muscles, while stimulation lateral to the midline produces unilateral muscle twitches in the same spinal segment. By this stimulation test, one can verify the spinal segment and laterality of the catheter electrode in the posterior epidural space (Fig. 4.5). When the catheter electrodes are situated in the anterior epidural space, the polarity of the segmental SCPs is reversed. Laterality of the catheter electrodes in the posterior epidural space can also be judged by the waveform characteristics of the SCPs. When the catheter electrodes are situated ipsilateral to the stimulated peripheral nerves and close to the roots, the initial positive spikes recorded are larger than those recorded contralateral to the nerves (see Fig. 4.5).

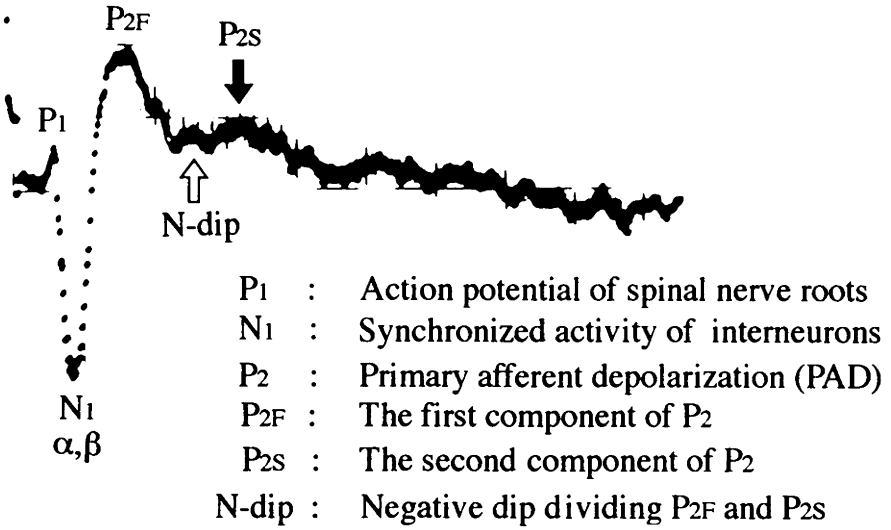

FIG. 4.4. A typical example of the segmental SCP recorded from the PES at the C5 vertebral level in response to radial nerve stimulation in a wakeful subject. The spike potential, *P1*, the sharp negative potential, *N1*, and the slow positive potential, *P2*, are clearly demonstrated. Note that another slow potential, *P2s* (*arrow*) is present, preceded by a negative dip (refer to Figs. 2.3 and 2.5 in Section B)

4.3 Six Different Kinds of Human SCPs Recorded from the Epidural Space

4.3.1 Segmental SCPs (Segmentally Evoked SCPs)

Human SCPs recorded from the same or nearby segments in response to the peripheral nerve or roots. For instance, the human SCPs recorded from the posterior epidural space at the 6th cervical segment in response to median nerve stimulation (Fig. 4.6-1) or the SCPs recorded from the posterior epidural space at the 12th thoracic segment in response to tibial nerve stimulation (Fig. 4.6-1) (Kano and Shimoji, 1995).

4.3.2 Conducting or Conducted SCPs

Spike potentials (summated action potentials) along the spinal cord in response to spinal cord stimulation from the epidural space of upper or lower spinal segments, cauda equina, or peripheral nerve stimulation. For instance, human SCPs recorded from the epidural space at the 7th cervical segment in response to cauda equina stimulation at the L3–4 vertebral level (Fig. 4.6-2) or spinal cord stimulation by an electrode situated in the epidural space at the 12th thoracic segment or vice versa (Fig. 4.6-2).

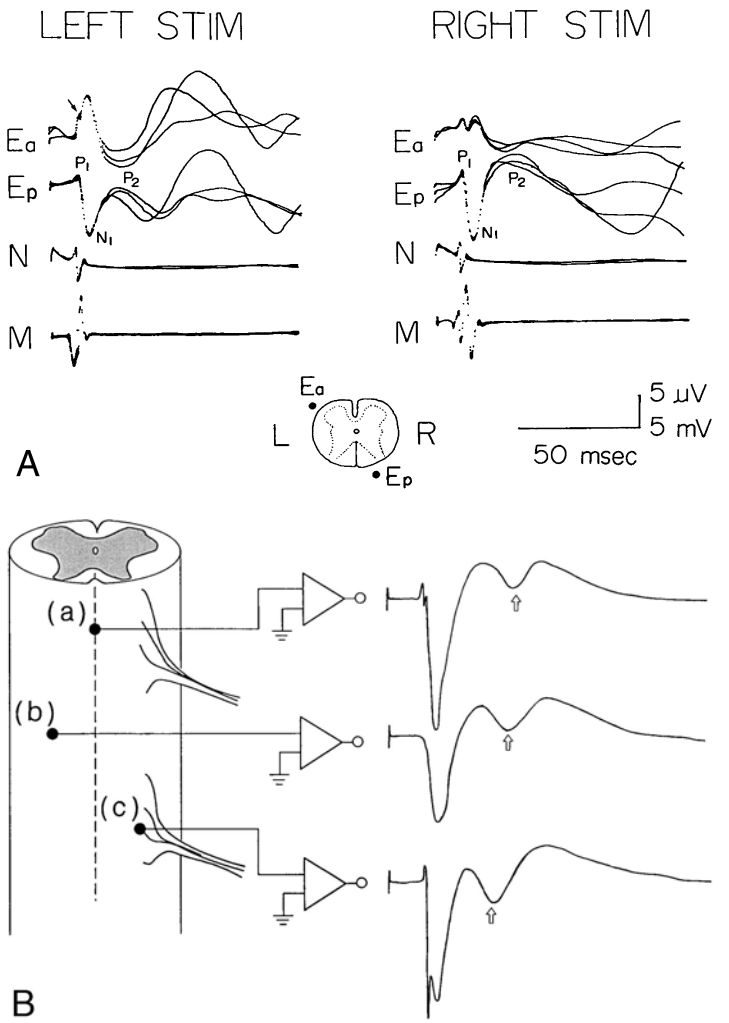

FIG. 4.5. **A** The segmental SCPs recorded from the anterior (*Ea*) and posterior (*Ep*) epidural spaces at the T12 vertebral level in response to left (*left traces*) and right (*right traces*) tibial nerve stimulations (*STIM*) at the popliteal space in a human. Three averaged responses are superimposed. A schematic presentation of the position of the epidural electrodes in the epidural space is shown at the *bottom*. The Ea electrode is situated in the left anterior epidural space, while the Ep electrode is situated in the right posterior epidural space. *N*, nerve action potential recorded from the posterior epidural space at the L4 vertebral level. *M*, the evoked electromyogram recorded from the calf muscle, showing the supramaximal response for the M wave (Shimoji et al., 1977). **B** Schematic drawings of waveform characteristics of segmental SCPs recorded from the posterior epidural space at midline (*a*), contralateral (*b*), and close to roots (*c*). Note that the typical waveform can be obtained at the midline recording (*a*), while the initial spikes can be unrecordable and the subsequent slow waves become small (*b*). When the recording electrode is situated close to the roots, the initial spikes become large (*c*)

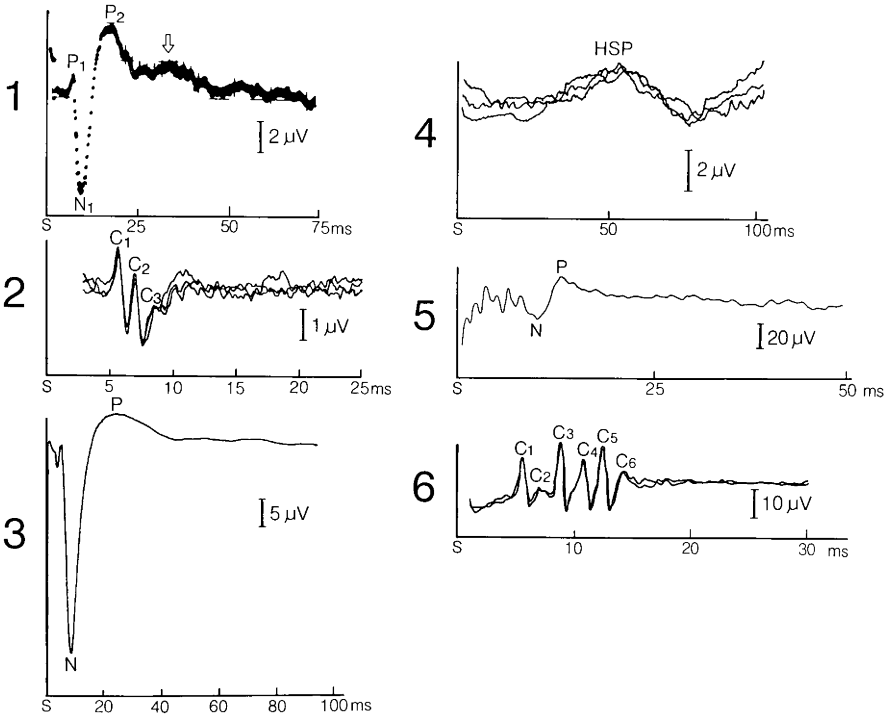

Fig. 4.6. Six different kinds of SCP recorded from the posterior epidural space (PES). **1** The segmental SCP (C5 vertebral level) in response to the segmental nerve (radial nerve) stimulation (photograph of the oscilloscope trace). **2** The conducting (ascending) SCPs recorded from the PES at the C7 vertebral level in response to cauda equina stimulation at the L3–4 vertebral level. **3** The SCP recorded from the PES at the T12 vertebral level in response to the (antidromic) volleys in the spinal cord from the PES at the C7 vertebral level. **4** The heterosegmental SCPs recorded from the PES at the T12 vertebral level in response to stimulation of the brachial plexus. **5** The motor evoked SCP, recorded from the PES at the T12 vertebral level, produced by transcranial magnetic stimulation of the motor area in a wakeful subject. **6** The motor evoked SCP, recorded from the PES at the T11 vertebral level, produced by transcranial electric stimulation of motor area during neuroleptanalgesia in a patient who underwent scoliosis surgery

4.3.3 Slow SCPs Produced by Antidromic Stimulation of the Spinal Cord (Descending SCP)

Slow SCPs recorded from a lower segment in response to stimulation of an upper spinal segment. For instance, slow SCPs recorded from the posterior epidural space at the 12th thoracic segment in response to spinal cord stimulation from the epidural space at the 7th cervical segment (Fig. 4.6-3).

4.3.4 Heterosegmental SCP, Heterosegmentally Evoked SCP

Slow (positive) SCPs recorded from a certain spinal segment in response to a large heterosegmental peripheral nerve in the vicinity of the spinal cord. For instance, SCPs

recorded from the posterior epidural space at the 12th thoracic segment in response to stimulation of the brachial plexus (Fig. 4.6-4).

4.3.5 Motor Evoked Human SCPs: TCM-Evoked SCPs

Potentials recorded from the spinal cord (from the epidural space) in response to transcranial magnetic stimulation of the motor area (TCM-evoked SCPs) (Fig. 4.6-5).

4.3.6 Motor Evoked Human SCPs: TCE-Evoked SCPs

Potentials recorded from the spinal cord (from the epidural space) in response to transcranial electrical stimulation of the motor area (TCE-evoked SCPs) (Fig. 4.6-6).

4.3.7 Polarity of Recording Spinal Cord Potential

There is no rule for polarity of recording spinal cord potentials (SCPs). However, it might be practical to record SCPs upward negative if EEG or evoked potentials from the scalp are simultaneously recorded. On the other hand, it might be more comprehensive to record the SCPs upward positive, particularly when these are recorded from the epidural space, since there have been many previous data in animals that have been recorded directly from the cord surface upward positive. Thus, it might be easier to compare human SCPs produced in the epidural space with animal SCPs recorded directly from cord surface in waveform characteristics.

Section B
Somatosensory Evoked Spinal Cord Potentials (Segmental SCPs)

Chapter 1
Segmental SCPs

Sumihisa Aida and Koki Shimoji

1.1 Waveform Characteristics

Figure 4.6 in Section A shows a typical example of the spinal cord potentials (SCPs) recorded from the posterior epidural space (PES) and evoked by segmental volleys in a healthy subject during wakefulness. The segmental SCP waveform characteristics, spatial distributions, and changes induced by several drugs have been reported elsewhere (Ferner et al., 1963; Shimoji et al., 1972, 1976, 1977). The segmental SCPs consist of an initially positive spike (P1) wave followed by a sharp (sometimes called slow) negative (N1) wave and a slow positive (P2) wave, which are very similar to the wave patterns of the SCPs recorded directly from the dorsal surface of the spinal cord in spinalized animals (Bernhard, 1953; Gasser and Graham, 1933). Differences in segmental SCP in intact humans from those of spinalized animals include the existence of a second component (Fig. 4.6 in Section A, arrows) in the slow P2 wave preceded by a negative dip.

The P1 wave typically consists of an initially positive spike potential. This configuration of the P1 wave is more clearly demonstrated in the segmental SCP recorded from the lumbar enlargement in response to cauda equina stimulation than in that produced by the peripheral nerve stimulation (Maruyama et al., 1982). Although the initially positive component of the P1 wave is sometimes hardly noticed, the negative-going component is sometimes demonstrated as a notch on the sharp negative-going phase of the N1 wave (Maruyama et al., 1982).

The N1 wave is sometimes composed of one to three peaks. Even in a record with an N1 having one peak, the two components (N1a and N1b) can be clearly demonstrated by a stronger stimulation or by applying a tourniquet, which produces ischemia in the arm. These N1a and N1b components may correspond to the N1 wave and N2 wave, respectively, of the SCP in the monkey, as described by Beall et al. (1977).

The P2 wave is usually separated by a negative dip to give a secondary component (P2s), depending on the level of anxiety of the subject and the stimulus intensity during wakefulness (Shimoji et al., 1975, 1977).

The waveforms of the segmental SCPs recorded in the cervical and lumbosacral enlargements are very similar to each other.

Beall et al. (1977) recorded the negative waves of the SCP in anesthetized monkeys (see Section A, Chapter 2). They observed three peaks in the negative wave when stim-

ulus strengths were intense enough and proposed that the third peak (the N3 wave according to their terminology) is produced by Aδ fibers. However, such a peak in the N1-wave of intact human subjects has not been observed even when stimulus strength is increased to a very high intensity during anesthesia (Shimoji et al., 1976, 1977). Differences in stimulus strength or sites of stimulation rather than those of species must be considered in this regard. However, different response patterns of both the N1 wave and P2 wave have been found between single shocks and brief trains of repetitive pulses (Shimoji et al., 1976) (Fig. 1.4, p. 61). The observation of Fitzgerald and Wall (1980) revealed that some superficial units in cat dorsal horn often do not respond to C-fiber stimulation unless a train of two or more stimuli (10 ms apart) are applied, while deep units tend to need only one strong stimulus for excitation. Thus, the response patterns of spinal interneurons (and therefore, the patterns of the N1 and P2-waves) also seem to be affected by the stimulus strength and pattern.

1.2 Comparison with Skin Surface Recordings

Figure 1.1A represents the simultaneous recordings of the SCPs from the posterior epidural apace at the level of C7 and the somatosensory evoked potentials from the cervical skin surface at the same segmental level with various reference electrode placements, in response to ulnar nerve stimulation at the wrist in a healthy, non-obese subject. The initial spike-like potential can be recorded in all skin surface recordings with variable polarities depending on the sites of reference electrode. It is demonstrated that the peak latency of the initial spike in all skin surface recordings coincides with the P1 potential in the epidural recording (Shimoji et al., 1978). Subsequent small negative dips in the surface recordings share the same peak latency with the N1 in the epidural recording. However, the slow wave corresponding to the P2 potential is not clearly demonstrated in the surface recordings. The initial spike like potential and subsequent negative potential have been recorded in all and in about one third of the subjects tested, respectively, while the slow positive potential was not recorded in any of the subjects. Thus it could be assumed from the anatomical position of the spinal cord, deep from the skin surface, and surrounding tissues, such as muscles and vessels (Fig. 1.1B). Another problem that should be kept in mind is the possible potential reversal or modification of the original potential field when an obstacle lies between the potential source and skin recording electrode (Fig. 1.1C).

1.3 Comparison with Posterior Pharyngeal Recordings

Figure 1.2A shows the somatosensory evoked potentials (SEP) from the posterior wall of the pharynx (Es), compared with segmental spinal cord potentials that were recorded simultaneously from the posterior (Ep) and anterior (Ea) epidural space, in response to stimulation of the median nerve at the wrist in the patients who underwent spinal surgery under general anesthesia. The SEP is recorded using disc electrodes attached to the endotracheal tube (Fig. 1.2B). The SEP recorded from the posterior pharynx consists of the initially positive spike (P1), which corresponds to P9, followed by a slow positive (P13) or reversed N1, which corresponds to N1 in the epidural recording, and slow negative (N22) waves, which correspond to the P2

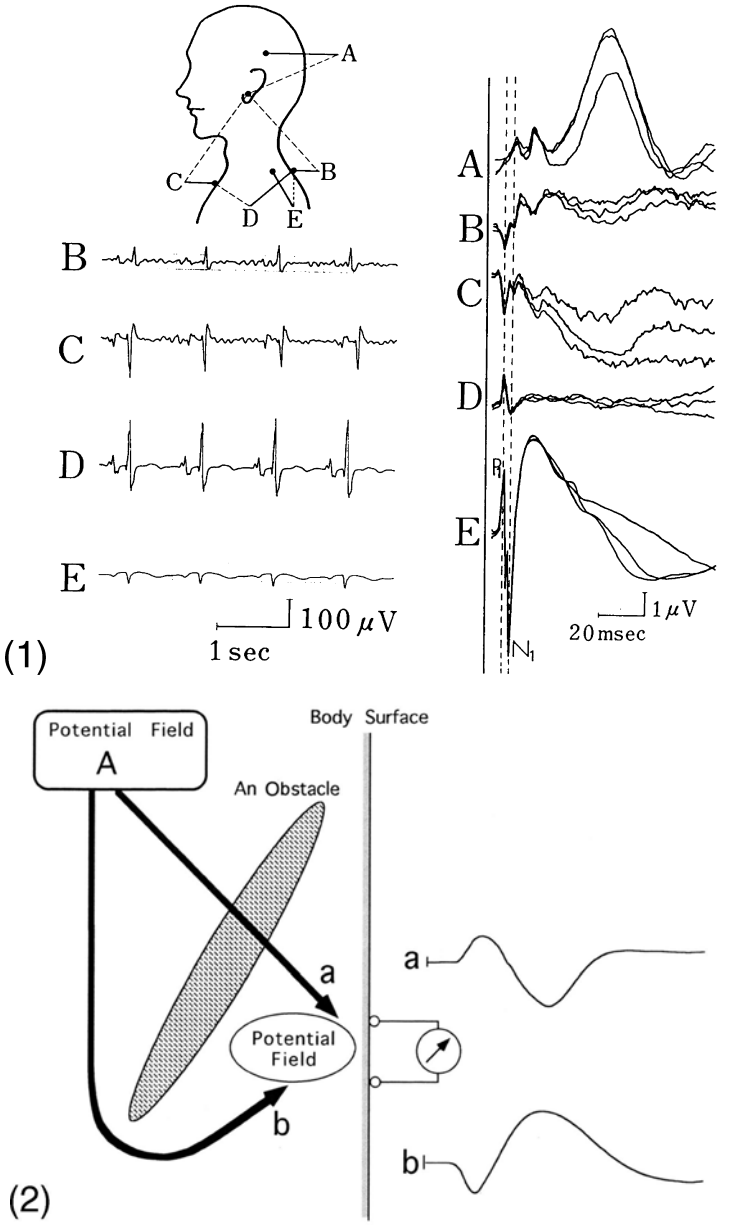

FIG. 1.1. (1) Comparison of spinal cord potentials (SCPs) recorded from the posterior epidural space (*E*) with somatosensory evoked potentials from the cervical skin surface (*B, C, D*) and the scalp. Electrode placements are shown schematically at the *top left*. *Solid lines* represent active electrodes; *broken lines* denote reference electrodes. Polygraphic records are also shown on the *left*.(From Shimoji et al., 1985). (2) Theoretical presentation of a reversed potential due to an electrically resistant obstacle lying between the source of potential and recording electrode placed on the skin. *a*, the potential without any electrical obstacle; *b*, the reversed potential due to an obstacle that changes the current flow

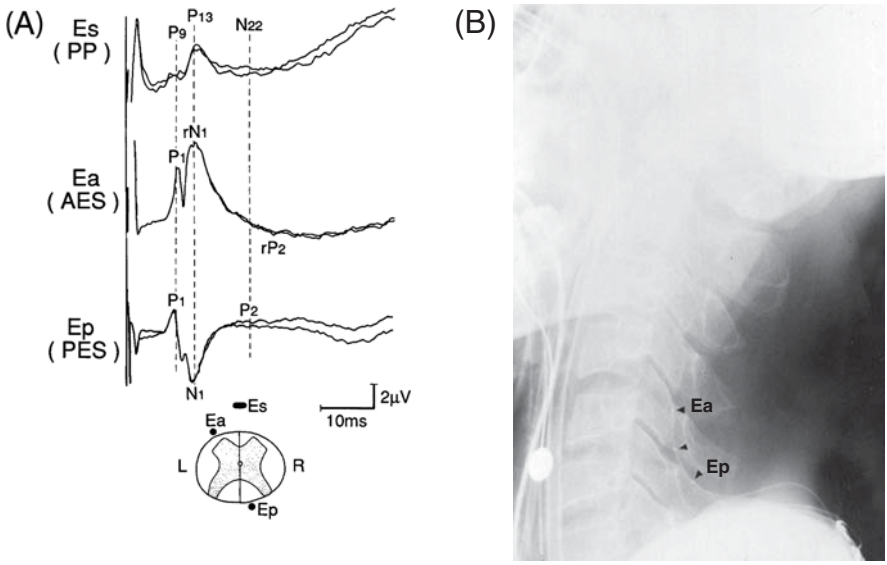

FIG. 1.2. **A** Comparison of the SCP recorded from the posterior (*Ep*) and anterior (*Ea*) epidural space with the evoked potential from the posterior pharyngeal wall (*Es*) in response to median nerve stimulation at the wrist in a patient during nitrous oxide halothane anesthesia. Note that polarities and peak latencies of the initially positive-going spike are the same in all records and polarities of the following positive-going potentials are reversed in the records from posterior pharynx wall (*Es*) and anterior epidural space (*Ea*) with the same peaks. The initially positive spike is large in the record from the posterior epidural space (*Ep*) due to ipsilateral placement of the catheter electrode. Note also that the *P2* potential can be identified with reversed polarity in the record from the posterior pharynx. Electrode positions are schematically shown in the *transverse plane* at the *bottom.* **B** An X-ray photograph in this case. A surface electrode attached to the endotracheal tube is placed on the posterior pharyngeal wall. *Arrowheads* indicate positions of epidural catheter electrodes. *Ea*, rostral electrode; *Ep*, caudal electrode. (From Takada et al., 1996)

potential in the epidural recording. The polarity of the esophageal or posterior pharynx recording is the same as that of anterior epidural recording, while the amplitudes of the potentials are smaller than those in epidural recording, as expected. However, it might be more reliable to monitor the cervical cord function during surgery than to record from the skin surface. The SEPs from the posterior pharynx or esophagus are recorded more clearly with a reference electrode on the dorsal surface of the neck than with the reference electrode at the earlobe or back of the hand. The threshold and maximal stimulus intensities were also similar between the esophageal SEPs and segmental SCPs. Thus, the P9, P13, and N22 components of esophageal SEPs are thought to have the same origin as the P1, N1, and P2 of the segmental SCPs, respectively. Therefore, the P9, P13, and N22 of esophageal SEPs may reflect incoming volleys through the root, synchronized activities of the interneurons, and primary afferent depolarizations (PAD), respectively. Esophageal SEPs in response to cauda equina stimulation show that the latencies of the two initial components (4.6 $\pm$ 0.4 and 6.4 $\pm$ 0.6 ms) correspond to those of the SCPs recorded from the posterior epidural space (4.6 $\pm$ 0.3 and 6.3 $\pm$ 0.5 ms), suggesting that these potentials reflect

impulses conducting through the spinal cord, similar to epidurally recorded SCPs (Takada et al., 1996).

1.4 Origins of the Segmental SCP

1.4.1 The Initially Positive Spike (Triphasic Spike) (P1)

It was shown by Gasser and Graham (1933) in their earliest work in animals that at body temperature the average duration of the initially positive spike (triphasic spike) produced by dorsal root stimulation is 0.5 ms in the anesthetized cat. This component corresponds to the P1 potential (wave) in human segmental SCPs recorded from the PES. They also noted that the spike is maximal when the recording electrode is placed on the dorsal root entry zone (see Section A, Fig. 4.4). Gasser and Graham were able to record the same component at least 3–4 cm rostral and caudal to the stimulated rootlet and observed that it had an average conduction velocity of 80 m/s over this distance. An Aα fiber conducts action potentials at a similar velocity. It is well known that dorsal root fibers divide at cord entry (dorsal root entry zone; DREZ) and form ascending and descending branches that travel in the dorsal columns. These branches give off collaterals to the gray matter, the greatest number arising over the distance in which the spike can be recorded (Willis and Coggeshall, 2004). These data are consistent with the interpretation that the initially positive spike (triphasic spike) (P1) is the extracellular manifestation of a compound action potential propagating through the large primary afferent fibers (Fig. 1.3). Thus, the P1 potentials appear to be different in amplitude depending on the electrode positions. When an active electrode is close to the dorsal root entry zone, a large negative deflection of the P1 tends to be misinterpreted as the N1 potential (see Fig. 4.4B in Section A).

The conclusion that the P1 represents action potentials in the large afferent fibers was substantiated by further experiments by Bernhard (1953) and Fernandez de Molina and Gray (1957). Eccles and Sherrington (1930) concluded, based on comparisons of dorsal root action potentials and ventral root action potentials, that the potentials generated by primary afferents have a much shorter "relative refractory period" than those generated by spinal neurons of the second order or more.

The interpretation of the initially positive spike as a manifestation of action potentials in the afferent fibers was unconditionally verified by Campbell (1945), using a technique that he developed. He impaled the spinal cord with recording electrodes and recorded the potentials elicited by nerve stimulation. Several electrode tracts were made across the spinal cord at the same cord segment. The amplitudes of the potentials elicited at a particular time after nerve stimulation were recorded on a master drawing of the spinal cord in the appropriate places. Isopotential contours were then drawn according to cartographic technique to reveal that the potential fields associated with the triphasic spike are confined to the area of the primary afferent fibers (see Fig. 2.3 in Section A).

1.4.2 The Sharp (or Slow) Negative Wave (N1)

The following sharp or slow negative wave (N1) has properties different from those of the initially positive spike (P1). The duration of the negative wave (N1 wave) (5–

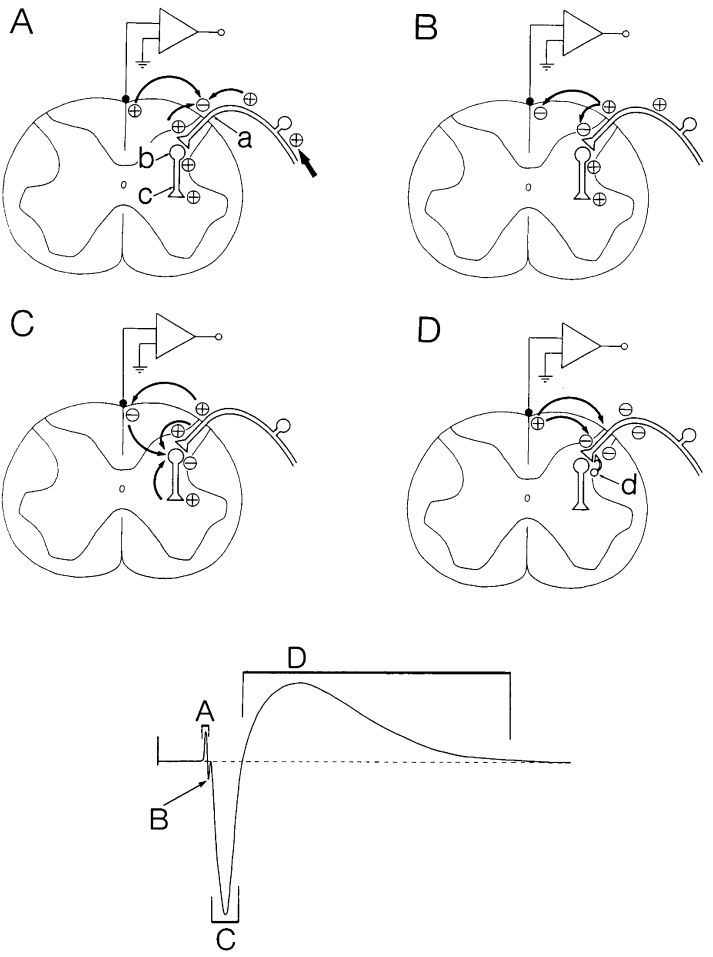

FIG. 1.3A–D. Schematic representation of the mechanisms by which components of somatosensory evoked SCPs (bottom) are generated in recordings from the posterior epidural space in humans.

The letters of the waveforms refer to the diagram, which explains how the components are generated. **A** Afferent volleys approaching the epidural electrode. **B** Afferent volleys passing through the epidural electrode to make the initial spike reversed. **C** Afferent volleys transmitting to the second-order neurons or interneurons to make the negative potential. **D** Afferent volleys also relaying themselves to the inhibitory interneurons, which transmit these volleys to the afferent terminals to produce the slow positive wave

11 ms) is more or less 10 times that of the P1 potential (0.5–1.0 ms), and it consistently has a longer onset latency and longer latency to its peak (Andres-Trelles et al., 1976; Beall et al., 1977; Bernhard, 1953; Coombs et al., 1956; Fernandez de Molina and Gray, 1957). More importantly, the amplitude of the N1 wave, in contrast to that of the P1 wave, is reduced by high frequency repetitive stimulation, indicating that it is pro-

duced by spinal neurons of the second-order or more (Eccles and Sherrington, 1930). Both the N1 wave and the P1 wave are always maximal in the same cord segment—the cord segment of entry of the afferent fibers stimulated—and also have similar thresholds (Bernhard, 1953).

It has been found in the cat (Gasser and Graham, 1933; Bernhard, 1953) that the N1 wave is not produced by antidromic stimulation of the ventral roots, indicating that it is not generated by motoneurons. This observation was confirmed by others (Lindblom and Ottoson, 1953). The relatively long duration of the wave was proposed to result from repetitive firing of the interneurons or extensive relaying (Coombs et al., 1956) with postsynaptic potentials (Willis and Coggeshall, 2004).

Several reports have described the characteristics of the interneurons that generate the N1 wave. Coombs et al. (1956) recorded dorsal root action potentials simultaneously with spinal cord field potentials and found that the firing of the interneurons that produce the N1 wave was correlated with activity in the Aα fibers. Beall et al. (1977) showed that the large Aβ fibers also activate N1 wave interneurons. Isopotential contour maps have provided the most detailed description of the distribution of these neurons (see Fig. 2.3 in Section A). Figure 2.3 shows an isopotential contour map of the distribution of the N1 wave at the time of its maximum. The map indicates that the wave can be recorded as a negative deflection in almost any part of the dorsal gray matter. However, in the ventral gray matter the N1 wave is observed as a positive deflection. The negativity is accounted for by current flow in the extracellular space pools as sinks produced at the somata and dendrites of excited interneurons; the positivity is accounted for by current flow out of sources along the ventrally projecting axons of the interneurons (Willis and Coggeshall, 2004). The negativity is spatially localized, indicating that the neurons contributing to the N1 wave form distinct pools in the dorsal gray matter. Willis et al. (1973) have shown, through stimulation of different hindlimb cutaneous nerves, that N1 wave interneuron pools seem to have a somatotopic organization.

1.4.2.1 The "Intramedullary Spike" or N1α

Bernhard (1953) and Austin and McCouch (1955) noted that the earliest portion of the first negative wave of the spinal cord field potential evoked by stimulation of cutaneous afferent fibers had characteristics different from those of the later portion. The early N1 component, called the "intramedullary spike, N1α, or late components of the initially positive spikes (P1)," is sometimes resolved as a component separated from the N1 wave proper by a minimal interval of one synaptic delay. This spike has a duration (0.8–1.0 ms) similar to that of the triphasic spike. This component is also much more resistant to asphyxia and repetitive stimulation than is the late N1 component. Thus, the intramedullary spike resembles the initially positive triphasic spike (P1) more than the N1 wave, suggesting that it is produced by activity in the primary afferent fibers rather than by the dorsal horn interneurons. Austin and McCouch (1955) have suggested that the intramedullary spike is the result of action potentials propagating into the afferent terminals. This potential is often observed in the segmental SCP recorded from the PES in humans, particularly when the epidural electrode is situated ipsilaterally (see Section A, Fig. 4.4).

1.4.2.2 "The Second Negative Wave (N2)" (N1β)

The fact that dorsal root stimulation sometimes elicits a second negative wave (N2) (or N1β) in cats was already noted by Gasser and Graham (1933). This wave shares several characteristics in common with the N1 wave: it is approximately the same duration (Beall et al., 1977; Coombs et al., 1956; Fernandez de Molina and Gray, 1957; Hughes and Gasser, 1934a); it has a similar sensitivity to repetitive stimulation (Fernandez de Molina and Gray, 1957); and it has a constant negativity in the dorsal gray matter (Beall et al., 1977; Coombs et al., 1956; Fernandez de Molina and Gray, 1957; Willis et al., 1973), which is spatially localized (Beall et al., 1977; Willis et al., 1973). However, the N1β (or N2) wave is more sensitive to anesthesia than the N1α wave (Hughes and Gasser, 1934a) and it has a somewhat higher threshold (Beall et al., 1977; Coombs et al., 1956; Fernandez de Molina and Gray, 1957), suggesting that the neurons generating the wave are activated by smaller fibers than those activating the N1 or N1α wave. Recordings from afferent fibers have shown that the N1β (N2) threshold is equal to that of the small Aβ or the large Aδ afferents (Beall et al., 1977). Thus, it seems that the N1β (or N2) is produced by a pool of interneurons that is different from that which produces the N1α. The conclusion that the N1α (or N1) and N1β (or N2) interneuron pools are spatially separated was verified by isopotential contour mapping studies, as shown in Fig. 1.13 in Section A. This map suggests that both the maximal negative isopotential contour and the zero isopotential contours are more ventral for the N1β potential than for the N1α potential (Beall et al., 1977; Willis et al., 1973). No somatotopic organization has been observed for the N1β potential (Willis et al., 1973).

Potential peaks similar to these N1α and N1β potentials have been observed in the segmental SCP recorded from the PES in humans, particularly when intense stimulation or repetitive stimulation is applied to the peripheral nerve, although it is not clear whether the origins are the same as those observed in the anesthetized monkeys (Shimoji et al., 1976; Maruyama et al., 1982) (Fig. 1.4).

1.4.2.3 "The Third Negative Wave (N3)"

Christensen and Perl (1970), in lampreys, and Beall et al. (1977), in monkeys, noted that spinal cord field potentials produced by intense stimulation of cutaneous afferents sometimes have a third negative component (Fig. 1.12 in Section A). This wave can be recorded only when Aδ afferent fibers are activated (Beall et al., 1977; Christensen and Perl, 1970). Isopotential contour maps such as Fig. 2.3 in Section A show that the N3 potential (wave) differs from the N1 potential (or N1 wave) and the N2 potential in that it is focused in two different regions of the dorsal horn—the dorsalmost dorsal gray matter and the base of the dorsal gray matter. Both of these pools have a location different from that of either the N1 or the N2 potential pools (Beall et al., 1977). Thus, it appears that the N3 wave is produced by interneurons different from those that produce the N1 wave and the N2 wave. However, such negative peaks as the N2 wave and N3 wave have not clearly been demonstrated in human SCPs recorded from the epidural spaces in response to even an intense stimulation of a peripheral nerve (see Fig. 1.4).

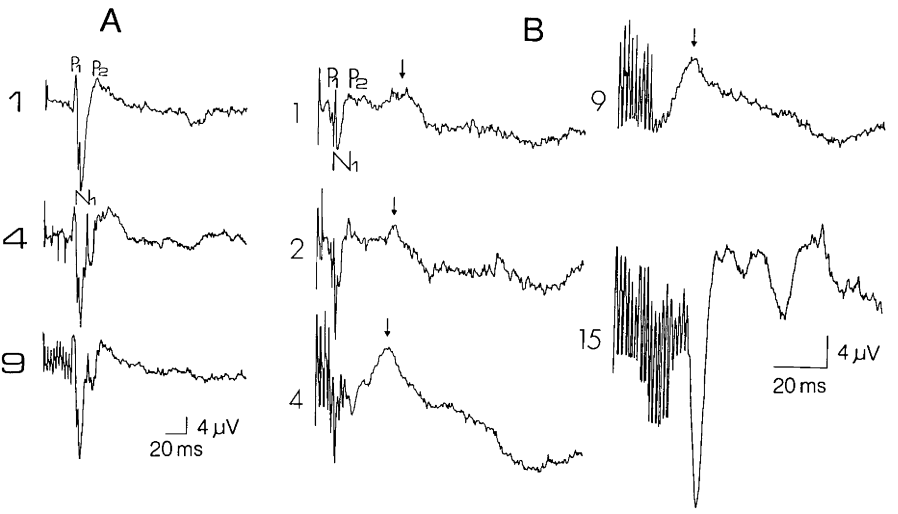

Fig. 1.4. **A** Somatosensory evoked SCPs recorded from the posterior epidural space at the T12 vertebral level in response to single volleys (1.5 threshold strength) and repetitive stimulations of the common peroneal nerve (CPN) at the popliteal space in a wakeful subject. *1*, single volleys; *4*, 4 pulses at 300 Hz; *9*, 9 pulses at 800 Hz. Note that another peak of N1 potential appears at the same time period and is present in both 4 and 8 repetitive pulses. **B** SCPs recorded from the posterior epidural space at the T12 vertebral level in response to single volleys at 3 times threshold strength and trains of repetitive volleys (350 Hz) to the CPN at the popliteal space in another wakeful subject. Number at left side of each trace represents number of stimulating pulses. Note that by 15 pulse trains the N1 potential is suddenly augmented and followed by increased P2 potential having several peaks. *Arrows* indicate the second components of P2 (P2s). Calibration: 4 μV, 20 ms. (From Shimoji et al., 1976)

1.4.3 The Slow Positive Wave (P Wave; P2 Wave)

Stimulation of a peripheral nerve characteristically evokes a slow P wave, corresponding to the P2 wave in humans, recorded from the cord dorsum in animals. Bernhard (1953) noted that the threshold for the slow P wave is the same as that for the N wave corresponding to the N1 wave in humans, and that both waves are maximal in the same cord segment. However, the duration of the P wave (60–80 ms) is more than six times the duration of the N wave (Coombs et al., 1956), and the P wave and the negative waves react differently to asphyxia; the P wave is more vulnerable than the negative waves (Bernhard and Koll, 1953). Also, the P wave, unlike the negative waves, can still be recorded after the dorsal columns have been severed between the recording point and the input segment of the stimulated cutaneous nerve (Bernhard and Widen, 1953; Hallstrom et al., 1989). It is therefore clear that, although the structures that generate the P wave interact functionally with those that generate the negative waves, they are different in origin.

An understanding of the nature of the P wave awaited the unraveling of the process of primary afferent depolarization (PAD), the causative agent of presynaptic inhibition, by Koketsu (1956a,b) and Eccles et al. (1962a,b,c, 1963a,b; Eccles and Krnjevic,

1959) and by Wall (1958, 1962) in the late 1950s and early 1960s. Koketsu (1956a,b) and Eccles et al. (1963a,b) recorded intracellularly within primary afferent fibers and found that the time course of PAD corresponded exactly with the time course of the P wave. Thus, it seems that the P wave is correlated closely with PAD. The mechanism by which the P wave is generated is also summarized in Fig. 1.5 (see also Fig. 1.3). It is suggested that PAD reflects a selective inhibitory mechanism to sharpen the effectiveness of novel stimuli (Benoist et al., 1972, 1974; Carpenter and Rudomin, 1973; Schmidt, 1973).

Stimulation of low-threshold cutaneous fibers in intact preparations sometimes elicits a secondary maximum in the P wave, corresponding to the secondary component of the P2 wave in humans (P2s). The secondary P wave component has a latency of 40–50 ms from the initially positive triphasic spike, corresponding to the P1 wave in humans, and has a much wider longitudinal distribution than the primary P wave component (corresponding to the P2f in humans). The secondary component is abolished by spinal cord transection and by the administration of pentobarbital (Shimoji et al., 1975; Tang, 1969). Thus, the generation of the secondary P-wave component seems to involve supraspinal mechanisms. It is known that PAD is also evoked in the spinal cord by stimulation of certain areas of the somatosensory cortex (Andersen et al., 1962, 1964; Carpenter et al., 1963) and brainstem (Carpenter et al., 1962). These areas are probably the relay structures in producing the secondary P-wave component (see Fig. 1.3).

Several different accounts of the location of the interneurons inducing PAD and the P wave have been given in the literature. Wall (1962) suggested that small interneurons located in the substantia gelatinosa make the axo-axonal synapses with the primary afferent fibers. This proposal was modified by Réthelyi and Szentágothai (1969), who conducted electron microscopic studies on the spinal cord. They proposed that primary afferent fibers excite substantia gelatinosa interneurons either directly or secondarily through other interneurons. The substantia gelatinosa interneurons in turn activate large pyramidal cells that lie slightly deeper in the spinal cord. The pyramidal cells make the axo-axonal synapses with the primary afferent fibers. Eccles et al. (1962b) reported intracellular recording from interneurons near the base of the dorsal horn with firing properties like those expected for cells initiating presynaptic inhibition. Thus, no definite conclusion can yet be made as to the peripheral nerve groups (Gregor and Zimmermann, 1973) and the location of the neurons inducing PAD and the P wave. It is also assumed that slow inhibitory postsynaptic potentials (IPSPs) of the interneurons in the substantia gelatinosa recently found (Baba et al., 1993; Yoshimura et al., 1990) are also involved for generation of the P wave or dorsal root potential (DRPv, by Lloyd's terminology).

In summary, the initially positive spike, P1, is a reflection of the extracellular events associated with the propagation of action potentials through the roots into the spinal cord. The generation of an action potential at a node of Ranvier creates a positive capacitative current, which is conducted electrotonically down the axon. This current is responsible for the initial positivity of the triphasic spike (Figs. 1.3 and 1.5). The capacitative current is also responsible for depolarizing the cell membrane at the next node to threshold, thereby initiating the production of an action potential here. The rising phase of the action potential is generated by an influx of Na^+ into the axon from the extracellular space. The loss of Na^+ causes the extracellular space to become neg-

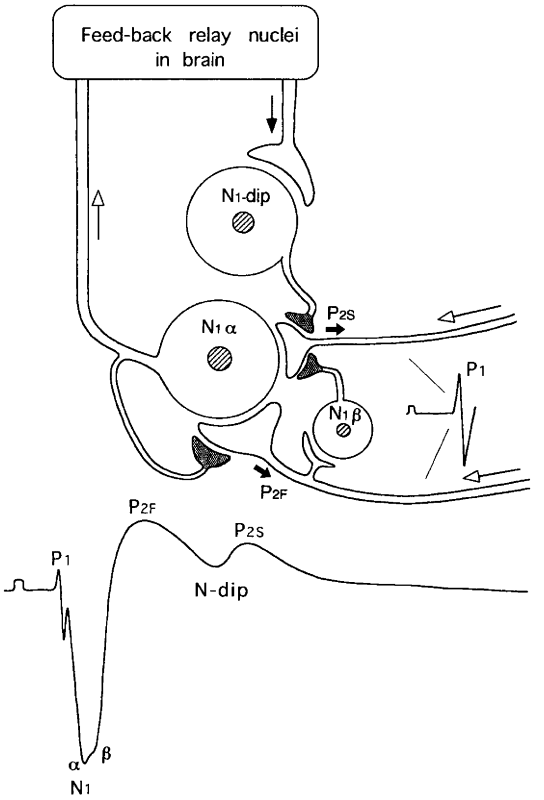

FIG. 1.5. Hypothetical and schematic representation of the origin of each component in the SCP recorded from the posterior epidural space in humans. The initial spike is produced by large incoming afferent volleys through the root. *N1α*, activity (postsynaptic potentials with spikes) of the second-order neurons (*N1α*) in the posterior horn activated by the large afferents; N1β activity produced by the second-order neurons and/or interneurons are activated by smaller afferent fibers. An inhibitory interneuron (*N1β*) that generates primary afferent depolarization (PAD), recorded as P2 potential, is shown in *black*. The second-order neurons send the impulses to the supraspinal relay nuclei, which send back the impulses to the interneurons (*N1-dip*) to produce the N-dip potential. The interneurons, N1-dip, then transmit the feedback impulses to the afferent terminals to produce the P2s potential. *White arrows and terminals* indicate excitatory impulses and excitatory transmissions, respectively. *Black arrows and terminals* indicate inhibitory impulses and inhibitory transmissions, respectively. Refer also to Fig. 1.3

atively charged; this event is recorded as the negative component of the triphasic spike (Figs. 1.3 and 1.5). The falling phase of an action potential is due to a K^+ efflux from the axon into the extracellular space. The additional positivity in the extracellular space is recorded from the cord dorsum as the second positive component of the triphasic spike.

The slow (or sharp) negative waves, N1, of spinal cord potentials (Figs. 1.3 and 1.5) are reflections of changes in the extracellular environment produced by activity of dorsal horn interneurons. When the interneurons are synaptically activated, positive

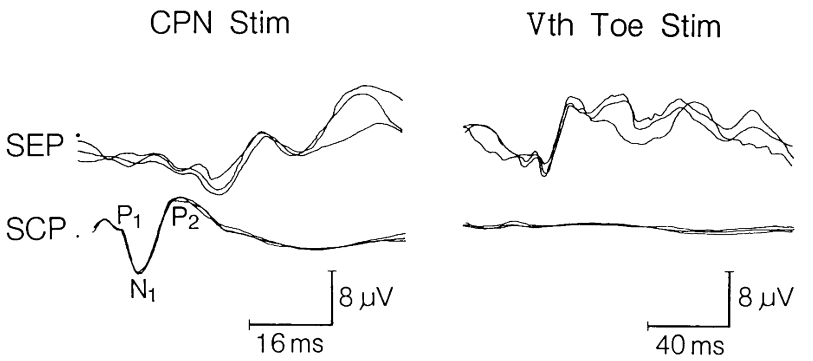

FIG. 1.6. The SCPs (*lower traces*) recorded from the posterior epidural space at the T12 vertebral level and the simultaneously recorded somatosensory evoked potentials from the scalp at the contralateral somatosensory area (*upper traces*) in response to common peroneal nerve stimulation (*CPN Stim; left*) and fifth toe stimulation (*Vth Toe Stim; right*).
Three averaged responses are superimposed. Brief trains of repetitive pulses (four at 300 Hz) are applied at 2 V (2 T, not painful) on the common peroneal nerve (*left*) and at 5 V (painful) on the fifth toe. Note absence of the SCPs in spite of clear configuration of the somatosensory potentials from the scalp (*right*). (From Shimoji et al., 1977)

ionic current leaves the extracellular space at the synapses (sinks) and reappears along the ventrally projecting axons of the cells (sources). Thus, the dorsal horn takes on a negative charge and the ventral horn takes on a positive charge.

The slow positive wave, P2, of the cord dorsum potential (Fig. 1.5) is the extracellular manifestation of the process of primary afferent depolarization (PAD). Positive ionic current leaves the extracellular space at excited axo-axonal synapses (sinks) and reappears along the primary afferents (sources). Thus, the dorsalmost portion of the spinal cord becomes positively charged.

Another important aspect that should be noted in recording SCPs in humans is shown in Fig. 1.6. When a nerve trunk is stimulated, the segmental SCPs can be recorded at the same segmental level of the spinal epidural space. However, when the stimulation site is moved to a more peripheral area, the SCPs can no longer be recorded, whereas the somatosensory evoked potentials from the scalp are clearly demonstrated. This seems to indicate that a certain level of the synchronization of the afferent volleys recorded as P1 potentials are needed for recording the SCPs in humans.

Chapter 2
Spinal Cord Potentials Evoked by Ascending Volleys

Yoichi Maruyama and Koki Shimoji

2.1 Waveform Characteristics of SCPs Evoked by Ascending Volleys

Segmentally evoked SCPs are recordable over several segments in cats (Bernhard, 1953; Lupa and Niechaj, 1977), monkeys (Barron and Matthews, 1938), and humans (Shimoji et al., 1971, 1972). Recording electrodes situated more rostrally, however, do not detect the slow negative (N1) and positive (P2) waves, but only small spike-like potentials (Fig. 2.1). These spike-like potentials seem to reflect compound action potentials in ascending tracts within the cord and are more consistently evoked by epidural stimulation of the cauda equina or lumbosacral enlargement than by peripheral nerve stimulation. Figure 2.1 shows specimen records of SCPs simultaneously led from the cervical and lumbosacral enlargements in response to stimuli applied from the posterior epidural space (PES) to the cauda equina at the L3–4 vertebral level (Maruyama et al., 1982).

For instance, epidural stimulation of the cauda equina at 2 times threshold strength (2T) for the initial spike produced only a single small spike in the anesthetized human, as shown in Fig. 2.2. With increasing stimulus strength, a second and then a third spike appeared. Strong stimulation often produced a slow negative wave of 20–25 ms duration after the polyphasic spikes. With a moderate degree of stimulus intensity (4–6 T), components later than the third component (C3) and the slow negative wave could not be reliably evoked. Components 1 (C1) and 3 (C3) reached maximum amplitudes at 4–6 and 12–14 times threshold strength, respectively, while component 2 (C2) was not maximal at 30 times threshold. Epidural stimulation of the posterior surface of the lumbosacral enlargement in humans also produced similar spike-like potentials at the cervical enlargement and, in some instances, several spike-like components following the third component could be obtained with intense stimulation. On the other hand, peripheral stimulation of nerves, such as the common peroneal or tibial nerves, can sometimes produce a small monophasic spike-like potential in the cervical PES (Shimoji et al., 1972).

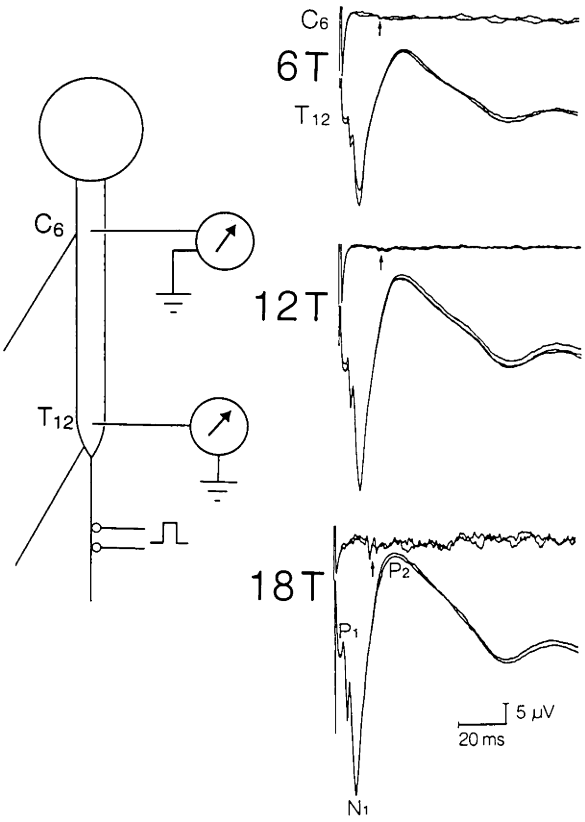

Fig. 2.1. Specimen records of spinal cord potentials (SCPs) simultaneously led from the cervical (*upper traces*) and lumbosacral (*lower traces*) enlargements in response to stimuli applied to the cauda equina at the level of L3–4 from the posterior epidural space (PES) ($n = 50$) in humans anesthetized with neuroleptanesthesia. Note that the potential (ascending SCP) at the cervical enlargement (*arrow*) is small compared with that at the lumbosacral enlargement (segmental SCP). Stimuli were delivered at 6, 12, and 18 times threshold strength. The stimulating and recording electrode positions are schematically shown on the *left*. (From Maruyama et al., 1982)

2.2 SCPs Evoked by Two Ascending Volleys from the Cauda Equina

To test whether postsynaptic components are involved in the ascending SCPs, double shocks at various intervals are applied to the cauda equina from the PES (Maruyama et al., 1982). It is expected that postsynaptic components might show facilitation or inhibition when paired stimuli are used.

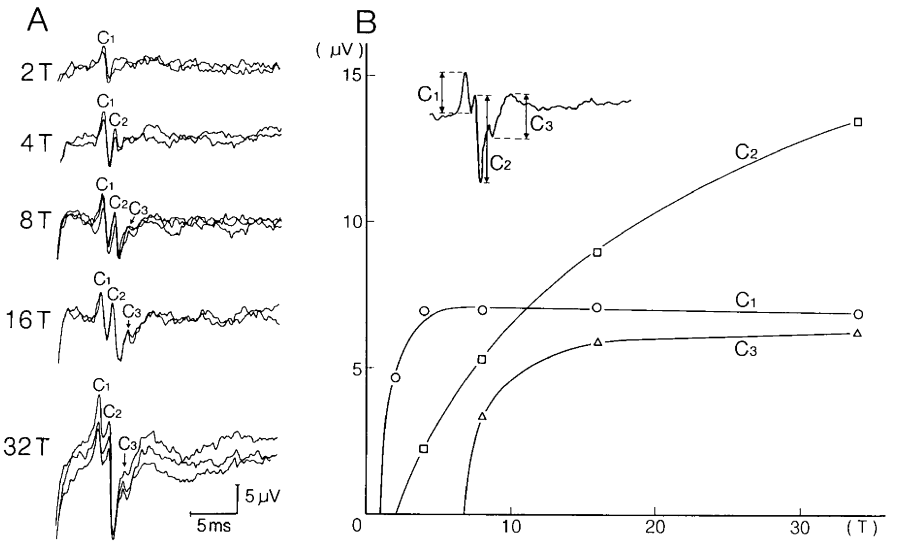

Fig. 2.2A,B. Effects of stimulus strength on ascending SCPs recorded at the C7 vertebral level elicited by cauda equina stimulation from the epidural space at the L3–4 vertebral level in humans anesthetized with neuroleptanesthesia. **A** Only the first component is seen at 2 times threshold strength (*2T*). The second and third components appear at 4 (*4T*) and 8 (*8T*) times threshold strength, respectively. Each sweep represents the summation of 25 responses. **B** Changes in amplitudes of three components (*C1*, *C2*, *C3*) of the ascending SCP (*ordinate*) as a function of stimulus intensity (*abscissa*). (From Maruyama et al., 1982)

When double shocks are applied within 5-ms intervals, the first and second components evoked by the test stimuli show facilitation (Fig. 2.3). On the other hand, the third component has a different pattern and is reduced for more than 20 ms (Fig. 2.3C). Since the intensity of each of the double shocks is maximal for components 1 and 3, the facilitation of component 1 must represent an increase in firing of transynaptically excited neurons whose axons form ascending tracts. Furthermore, the facilitation of C2 is unlikely to be due to a peripheral mechanism. Therefore, both the first and second components probably reflect action potentials conducted through certain tracts within the spinal cord with at least one synapse in their pathways. The third component appears to be an action potential of a different spinal tract also having at least one synapse in its course with different characteristics (Maruyama et al., 1982).

2.3 Conduction Velocities of Ascending Volleys Along the Cord

The mean maximum conduction velocity of ascending volleys along the spinal cord is 82.0 ± 5.4 (SE) m/s with a range of 55.0–119.0 m/s. This was calculated by measuring the distances between the cervical and lumbosacral electrodes and the latencies

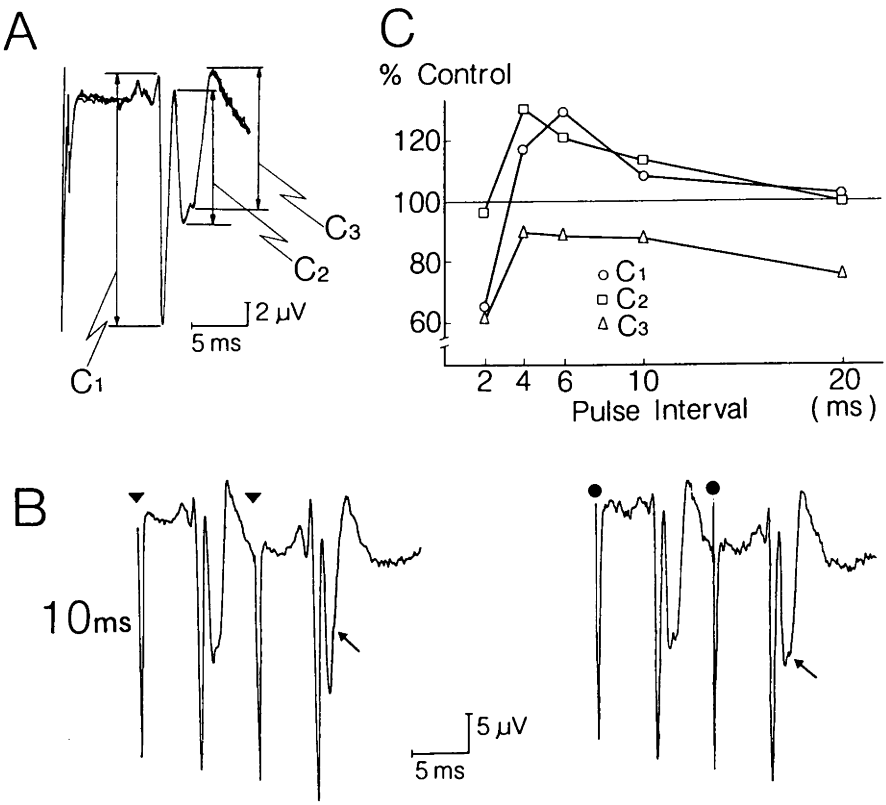

FIG. 2.3A–C. Effect of double shocks to the cauda equina (L3–4 vertebral level) on the SCP recorded from the cervical enlargement in a subject anesthetized with neuroleptanesthesia. **A** Measurement of amplitudes of three components. **B** Specimen records of SCPs evoked by double ascending volleys (*left*) and those produced by summation of the two single volleys (*right*) at the interval indicated. When the conditioning and testing stimuli were delivered at very short intervals, measurement of the amplitude of each component became difficult due to the complex wave shapes (*left*) and often led to false estimates. Thus, the simple summation of potentials with the two stimuli was also made for comparison (*right*). This procedure provided an accurate measurement of the amplitude of each component in reference to the simple summation of the two potentials. Each sweep represents the summation of 25 responses. The stimulus intensity was at 20 times threshold strength and supramaximal for components 1 and 3, respectively. *Arrows* indicate the third component (C3). **C** Recovery curves of C1, C2, and C3 components constructed by double ascending volleys. (From Maruyama et al., 1982)

of the initial dip of the first spike of the ascending SCPs (Maruyama et al., 1982). There was a great deal of individual variation in conduction velocities along the cord evoked by the ascending volley among the subjects tested (Table 2.1). Sex and age differences seemed to have a minimal effect on the conduction velocities. In addition, no obvious correlation between the conduction velocities and electrode positions in the epidural space could be observed. The great variability of maximum conduction velocities among the subjects (Table 2.1) is thought to be caused mainly by differences in the

Table 2.1. Maximum conduction velocities of ascending volleys along the cord, calculated by the initial spike potentials recorded from the posterior epidural space

Case no.	Age (years)	Sex	MCV (m/s)
1	21	F	70.5
2	22	F	100.0
3	52	F	72.0
4	47	F	109.0
5	51	F	57.0
6	15	M	112.0
7	62	F	66.0
8	30	F	78.6
9	23	F	119.0
10	10	M	59.5
11	18	F	55.0
12	55	F	89.7
13	58	M	85.7
14	14	F	91.8
15	13	M	63.5
Mean ± SE			82.0 ± 5.4

current distributions of the submaximal stimulating pulses in the epidural space due to a combination of differences in electrode positions and anatomy of the epidural space, which might, in turn, result in stimulation of different spinal tracts.

Dorfman (1977) described a method for deriving an indirect estimate of the velocity of ascending impulse propagation in the spinal cord of the intact human. The estimate was computed from measurements of motor and sensory nerve conduction velocity in the limbs, the F-wave (the electromyogram produced by recurrent orthodromic activation of motoneurons) latencies, and the latencies of somatosensory evoked potentials(SEPs) recorded from the scalp. The mean estimated spinal cord conduction velocity in normal subjects was found to be 55.1 m/s, with a standard deviation of 9.9 and a range of 35–90 m/s. Direct measurement of afferent impulses through the spinal cord was made by Ertekin (1978), who recorded the SCPs with electrodes located intrathecally. He found that conduction velocity along the spinal cord was 23 m/s on average (range, 16–28 m/s) in five multiple sclerosis patients and more than 30 m/s in normal subjects.

With skin-surface electrodes placed over the lumbar, thoracic, and cervical spine, Cracco (1973) also recorded the summation of evoked responses to median and peroneal nerve stimulation and found that conduction velocity measured by the latency of the surface response to peroneal nerve stimulation was about 65 m/s from lumbar to cervical recording locations.

Abnormally slow spinal cord conduction velocity recorded with skin electrodes was defined by Dorfman et al. (1978) as 33.5 ± 18.5 (SE) m/s in multiple sclerosis patients, which was more than 2 SD below the mean of the normal population (55.8 ± 11 m/s). Gross estimates of approximately 60 m/s for the conduction velocity between the T12 spinous process and contralateral somatosensory cortex in several healthy subjects were also made by Delbeke et al. (1978).

Thus, conduction velocities along the spinal cord estimated by the above authors vary considerably, ranging from 35 to 90 m/s, and are slower than our results (Maruyama et al., 1982) obtained with moderately strong epidural stimulation of the cauda equina. Since the peak of the compound action potential represents only a part of the population of conducting fibers, its latency may be varied depending on occurrence of synchronization of the population spikes. In other words, the most likely explanation for this variability is that different tracts are being stimulated.

In the cat, Lloyd and McIntyre (1950) found that impulses in the dorsolateral tract conducted at a uniform and slower velocity (less than two thirds to one quarter the initial value) compared with the initial velocity of impulses (110 m/s) in the presynaptic afferent fibers from muscle. Sarnowski et al. (1975) stimulated the sciatic nerve and recorded the summation of evoked potentials using surface electrodes placed over the cat spine. They found that the conduction velocity of the response was about 90 m/s from the rostral sacral to the cervical region. Happel et al. (1975) suggested that conducted responses recorded from the cat spine surface had at least one synapse along the ascending spinal pathway. This suggestion was substantiated by Glees and Soler (1951) and Rustioni (1972), who showed that only 20% of first-order afferent fibers in the fasciculus gracilis reached the dorsal column nuclei. Similarly, Trevino et al. (1972) have shown that the lateral spinothalamic tract does not contain first-order fibers. Thus, the majority of long-tract ascending fibers are considered to be nonprimary and involve at least one synapse. The recovery curves of the spike-like components (C1, C2, and C3) (Fig. 2.3), the ascending potentials elicited by cauda equina stimulation in our human study, coincide with these animal experiments. Prolonged recovery of the C3 component, as compared to those of C1 and C2, may indicate a polysynaptic pathway for its origin.

Chapter 3
Spinal Cord Potentials Evoked by Descending Volleys

Hiroyuki Shimizu and Koki Shimoji

3.1 Waveform Characteristics of SCPs Evoked by Descending Volleys to the Spinal Cord

When the dorsal surface of the human spinal cord is stimulated through a pair of electrodes situated in the cervical posterior epidural space (PES), a series of potentials can be recorded from the PES of the lumbosacral enlargement. The potentials begin with mono- or polyphasic spikes associated with the arrival of the volleys at the lumbar enlargement. Following these spikes, a series of slow potentials occur. These include a slow and sharp negative wave followed by a slow positive wave (Fig. 3.1). These slow negative (descending N) and positive (descending P) complexes resemble the segmentally evoked N1 and P2 waves (segmental N1 and P2), respectively. The similarity between the negative-positive complex evoked by descending volleys and the N1–P2 wave complex elicited by segmental nerve stimulation suggests that the origins of these slow descending N and P waves of SCPs are similar to those of the N1 and P2 waves of segmentally evoked SCPs (Shimizu et al., 1979a) (Table 3.1). The segmental N1 and P2 waves in humans show approximately the same characteristics as the slow negative and positive waves of the cord dorsum potential in animals (Shimoji et al., 1975, 1977), which are believed to be produced by the excitation of interneurons and primary afferent depolarization (PAD), respectively (Bernhard and Widen, 1953; Schmidt, 1971).

The descending N and P waves, however, reach their peaks 0.8–1.0 ms faster than the N1 and P2 waves after the arrival of the afferent volleys (measured from the positive peak of the initial spike potential. This may indicate that the descending volley is more synchronous than that in the peripheral nerve. In addition, the descending N wave always has one peak, while the segmentally evoked N1 wave is sometimes subdivided into two peaks, as reported in the cat (Austin and McCouch, 1955), the monkey (Beall et al., 1977), and also in humans (Maruyama et al., 1982). This suggests that the dorsal column, which may have no A-delta-fibers, conveys more homogenous volleys than the peripheral nerve.

Sometimes the descending P wave is followed by a slow and shallow negative wave (Fig. 3.2, at 15.0 T), which has also been demonstrated as DRPVI in the cat (Lloyd, 1952). However, in humans this late negative potential has not been analyzed due to

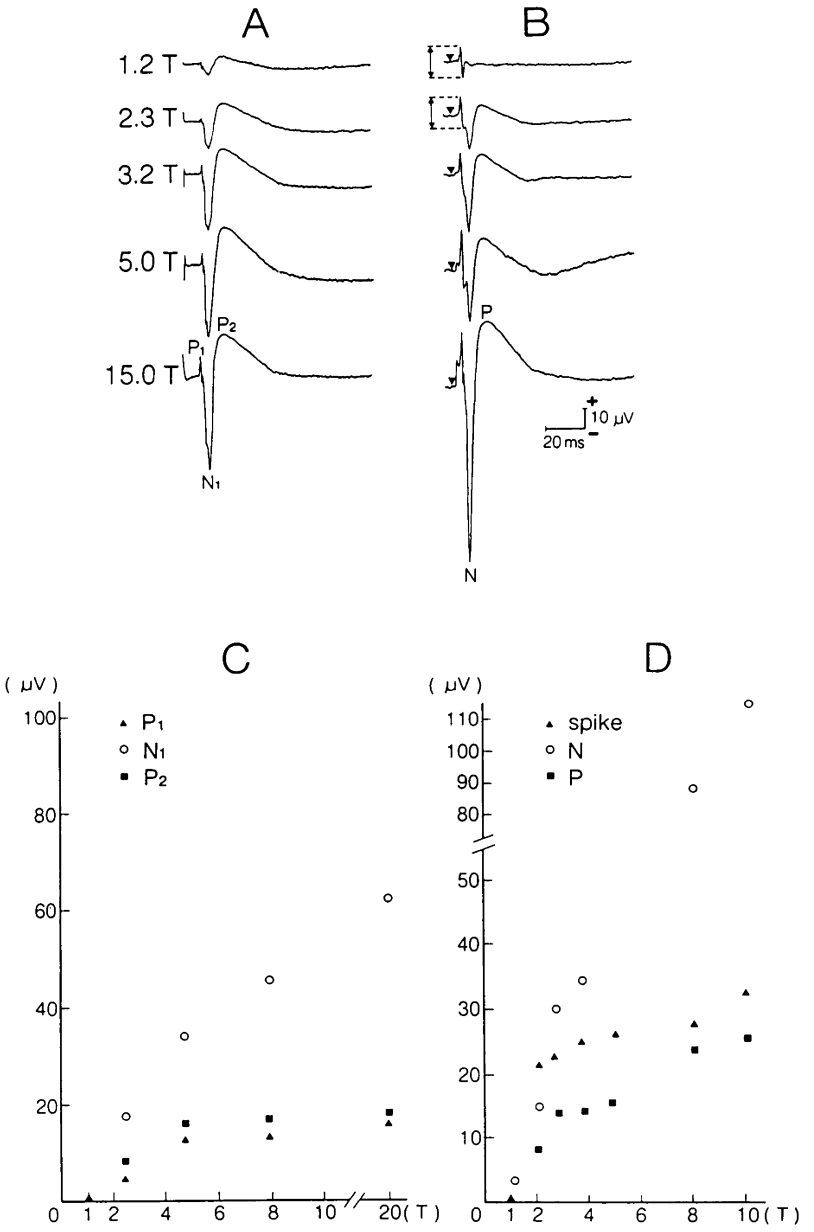

FIG. 3.1. Effects of graded stimulation on each component of the SCP produced by a segmental volley (**A**) and on that evoked by a descending volley (**B**). Spinal cord potentials were recorded at the T12 vertebral level in a subject anesthetized with neuroleptanesthesia. The *numbers at the left* indicate the stimulus intensity expressed as times threshold strength (*T*). Note that the amplitude of the biphasic spike potentials evoked by 1.2 T stimuli coincides with that evoked by 2.3 T stimuli, as demonstrated by *broken lines* in **B**. *Triangles* indicate time of stimulus onset. The relationship between the stimulus and size of each component was plotted for the SCP elicited by the segmental volley (**C**) and that evoked by the descending volley (**D**). The stimuli evoking segmental and descending volleys were applied to the tibial nerve at the popliteal space and to the cervical enlargement from the posterior epidural space at the C7 vertebral level, respectively. (From Shimizu et al., 1982)

Table 3.1. Central latencies of descending N and P waves

	Central latency (ms)		Central latency (ms)
des N	2.8 ± 0.2	des P	9.4 ± 0.3
N1[a]	3.6 ± 0.1	P2	10.4 ± 0.2
Significance	$P < 0.05$		$P < 0.05$

Values are means ± SD calculated from the initial positive peak of the spike compared to those of segmental N1 and P2 waves. $n = 8$.
[a] The latency to the first peak (N1a) was calculated in the records that displayed the two peaks. (From Shimizu et al., 1982).

its variability and poor reproducibility (refer to the interacted slow negative wave in Fig. 3.3).

When the stimulating electrodes are shifted laterally in the PES, the descending N and P waves can barely be recorded, although the initial spike potentials can still be seen (Shimizu et al., 1982; Tomita et al., 1996).

3.2 Effects of Graded Stimulation to Determine the Population of Spinal Tract Fibers that Produce "Descending SCPs"

When stimulating electrodes are situated within 5 mm from midline in the PES, descending N and P waves are invariably elicited in the lumbosacral enlargement, and the amplitude of the response grows with an increase in intensity of the stimulus-eliciting descending volleys (Shimoji et al., 1982; Tomita et al., 1996). At near threshold strength for the initial spike potential, both the descending P and segmental P2 waves are hardly noticeable but increase in height with the amplitude of the descending volley (Fig. 3.1B). In Fig. 3.1B, at 1.2 times threshold strength (1.2 T), only a biphasic spike potential is produced by the descending volley without accompanying slow waves. At 2.3 times threshold strength (2.3 T), however, the descending N and P waves appear without a significant increase in the initial spike-potential amplitude. This indicates that the initial spike at these stimulating strengths is not responsible for producing the subsequent slow waves and that an additional tract produces the descending N and P waves. The spike potential of the responsible tract may be masked by other potentials. Another shorter latency spike appeared at 3.2 T and then increased with concomitant augmentation of the slow waves by higher stimulus strength (Shimizu et al., 1982).

Similar behavior in response to graded stimulation was also observed in the segmentally evoked SCP (Shimoji et al., 1976). For instance, in Fig. 3.1A the peak-to-peak size of the initial biphasic spike was just the same between 1.2 and 2.3 T and between 3.2 and 5.0 T. This fact also reveals that smaller fibers rather than the largest primary afferents are more responsible for producing both the segmental N1 and P2 waves.

The amplitude of the descending P wave grows quickly and remains much the same even with intense stimulation (Fig. 3.1D). This is comparable to the characteristics of

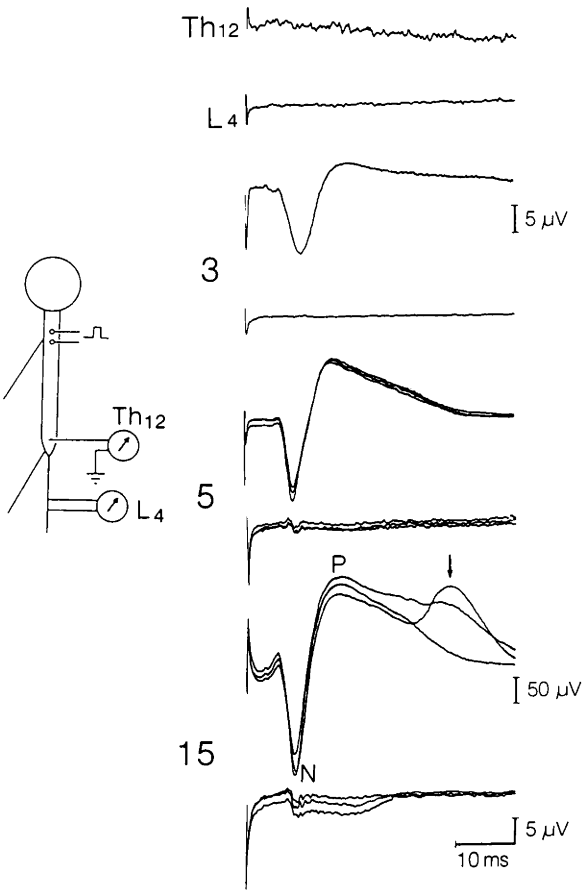

Fig. 3.2. Effects of graded stimulation applied to the cervical posterior epidural space (PES) on the SCP produced in the lumbosacral enlargement and on the cauda equina potential during surgery in a neuroleptanesthetized subject. The SCP (*upper sweep*) and the cauda equina potential were recorded from the PES at the T12 and L4 vertebral levels, respectively. The number at the left of each pair of sweeps indicates the intensity of stimulus (times threshold strength, T). Top records were made just below the threshold strength. The spike potential is still not seen in the cauda equina potential at 3 T. The descending volley was first clearly demonstrated in the cauda equina potential at 5 T. Note the variability of the superimposed descending SCPs, and the appearance of a slow and shallow negative wave in the cauda equina at 15 T. The slow negative waves recorded from the posterior epidural space at the cauda equina level seem to be the dorsal root potentials (DRP by Lloyd's terminology). The *arrow* indicates the secondary component of the descending P-wave. (From Shimizu et al., 1982)

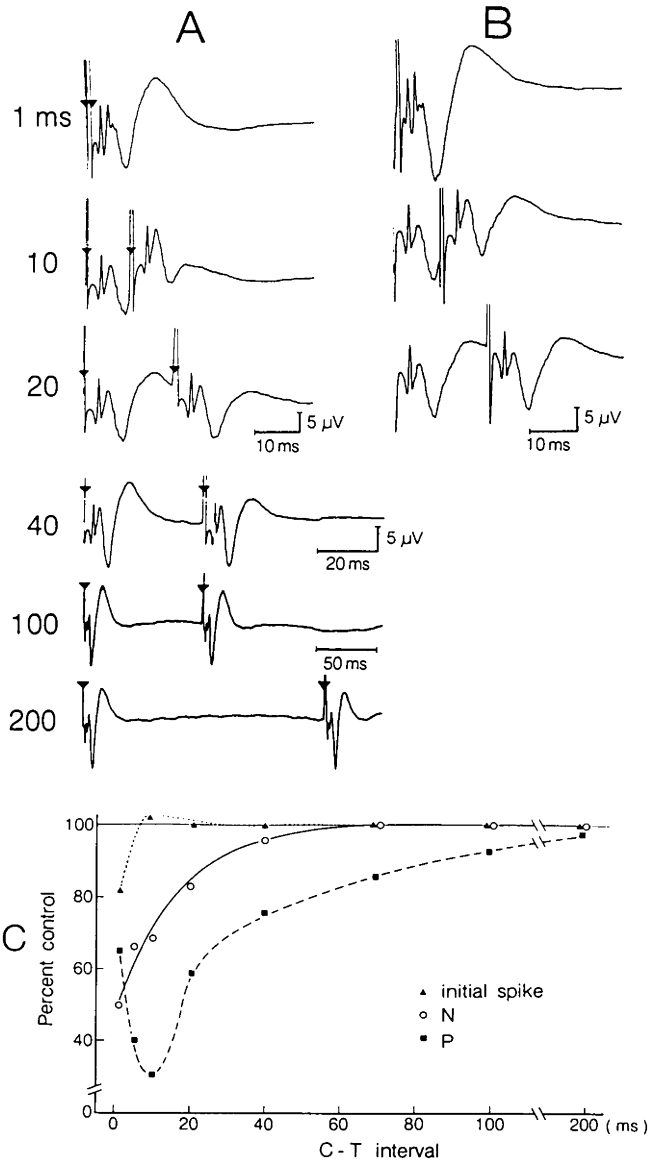

Fig. 3.3A–C. Effects of double shocks to the cervical cord from the PES on the descending N and P waves. **A** Specimen records of the descending SCPs evoked in the lumbosacral enlargement by double shocks. **B** Simple summation of two descending SCPs evoked separately at intervals shown on the left side. This simple summation of two responses was made for easier calculation of the degree of reduction of the test responses, particularly at the shorter intervals between two volleys. **C** Time course of the conditioned changes in the initial spike and in the descending N and P waves. The test was carried out during neuroleptanesthesia in a subject without neurological abnormality. (From Shimizu et al., 1982)

the segmental P2 wave elicited by graded stimulation of the segmental nerve (Fig. 3.1C). This may indicate that PAD evoked by descending volleys to the human spinal cord from the posterior epidural space is produced by a certain restricted population of fibers, as in the case of PAD evoked by the segmental volleys (Eccles, 1964; Shimoji and Kano, 1975; Shimoji et al., 1976). In contrast, the increase in amplitude of the descending N wave has a much wider range and did not attain its maximum even at 10 times threshold strength. This nature of the descending N wave is similar to that of the N1 wave evoked segmentally (Fig. 3.1C). However, the ratio of increase in amplitude by graded stimulation is more prominent in the descending N wave than in the segmental N1 wave (Fig. 3.1C,D). The ratio of amplitude of the N1 at 10 T to that at 2.5 T is 2.6–3.2, while the same calculation for the descending N wave results in values ranging from 5.5 to 6.3. This reveals that the populations of fibers, as well as numbers of interneurons activated by the descending volleys, are larger than those activated by segmental nerve stimulation, as might be expected.

The discrete fiber spike potential evoked by the descending volley below the intensity of 3 T is sometimes barely noticeable in the lumbosacral enlargement or in the region of the cauda equina (Fig. 3.2), presumably because the range of conduction velocities in the spinal tract results in multiple low-amplitude fiber potentials occurring throughout the slow waves. Then the fiber spike potential becomes clearly recordable in the PES at the level of the cauda equina with an increase in the stimulus strength (5 T). When intense stimulation (15 T) is applied epidurally, the constancy of the configuration of the descending N and P waves is lost (Fig. 3.2, bottom traces). In addition, another component (arrow in Fig. 3.2), the "secondary component," appears on the decaying phase of the descending P wave even during neuroleptanesthesia (NLA anesthesia). The secondary component of the P2 wave has also been observed in the SCP elicited by segmental nerve stimulation when the stimulus strength is increased or subjects are excited (Shimoji et al., 1977). Thus, the secondary component of the descending P wave evoked by a strong volley might also be produced by a feedback loop via supraspinal structures. Variability of the descending N and P waves with intense stimuli may also be due to additional effects mediated by supraspinal structures. Such strong stimulation also produces a slow and shallow negative wave following the spike potential at the level of the cauda equina (Fig. 3.2). This slow potential at the level of the cauda equina is thought to reflect the electrotonic spread of the potential to the dorsal root (the dorsal root potential, DRP) evoked in the lumbosacral enlargement. However, the time course of this slow negative wave in the cauda equina region does not coincide with that of the descending P wave, which might be due to the time constant (about 0.3 s) applied in the recording. The slow negative wave produced in the PES at the cauda equina region by descending volleys may reflect the dorsal root potential (DRPv by Lloyd's terminology) (Lloyd, 1952) in human spinal cord (Shimizu et al., 1982).

3.3 Effects of Double Shocks on "Descending SCPs"

When double shocks are applied to the cervical enlargement from the PES, the SCP produced in the lumbosacral enlargement by the second volley should be affected by the preceding volley when the SCP contains postsynaptic components. To test this, the

amplitude of each component of the SCP produced by the second stimuli (Fig. 3.3A) is calculated in comparison with that produced by a simple summation (Fig. 3.3B). When the two stimulating volleys are separated by more than 200 ms (the lowest record in Fig. 1.3A, Section B), both the descending N and P waves produced by the testing volley are minimally affected by the preceding (conditioning) volley. However, when the intervals between two volleys are reduced, the amplitude of the slow P wave produced by the second volley is inhibited. The maximum inhibition of the descending P wave elicited by the testing volley is obtained at interstimulus intervals of 8–12 ms (Fig. 3.3C) in four NLA-anesthetized subjects tested.

The N wave produced by the second volley decreases when the conditioning-testing interval is shortened to less than 70 ms. The initial spike potential is barely affected when the two stimuli are separated by more than 5 ms. The recovery curves of these potentials constructed from conditioning-testing experiments (Fig. 3.3C) also indicate that the initial spike potential of the SCP produced by the descending volley is a compound action potential of a certain spinal tract without interposing synapses along the tract. The recovery curves of the subsequent N and P waves indicate that both these potentials are transynaptic in origin, but they possess different characteristics.

3.4 Origins of Descending N and P Waves in Human SCPs

Our study (Shimizu et al., 1982) has demonstrated that descending volleys delivered from the PES at the cervical level produce slow negative and positive waves in the lumbosacral enlargement recorded from the PES in normal humans, and also that waveform characteristics of these descending N and P waves are very similar to those of the segmental N1 and P2 waves, the origins of which are believed to be the synchronized activity of interneurons and PAD, respectively (Shimoji et al., 1975, 1977). Therefore, the descending N and P waves are thought to reflect the interneuronal activities and PAD, respectively, activated by descending impulses along the cord. Further, the results obtained in the conditioning-test experiment (Fig. 3.4) may indicate that descending inhibitory systems originating supraspinally exist in the human spinal cord, as manifested in the characteristics of these descending N and P waves. The slow P wave also contains one or two peaks separated by the negative dip during its decay as found in the segmental SCPs, which is hardly observed during general anesthesia (see Figs. 3.1–3.4).

Animal experiments have shown that dorsal root potentials (DRPs) or cord dorsum positive waves (P-waves) can be produced by stimulation of a variety of supraspinal structures (Abdelmoumene et al., 1970, Andersen et al., 1962; Chan, 1980; Chan and Barnes, 1972; Lundberg, 1964; Motamedi and York, 1980; Proudfit and Anderson, 1974; Schmidt, 1971). Direct stimulation of the dorsal surface of the spinal cord also evoked cord dorsum negative (N)-positive (P) complexes over the lumbosacral enlargement (Foreman et al., 1976; Handwerker et al., 1975). Foreman et al. (1976) clearly demonstrated that direct dorsal column stimulation produced negative (N) and positive (P) cord dorsum potentials in the lumbosacral enlargement with concomitant depression

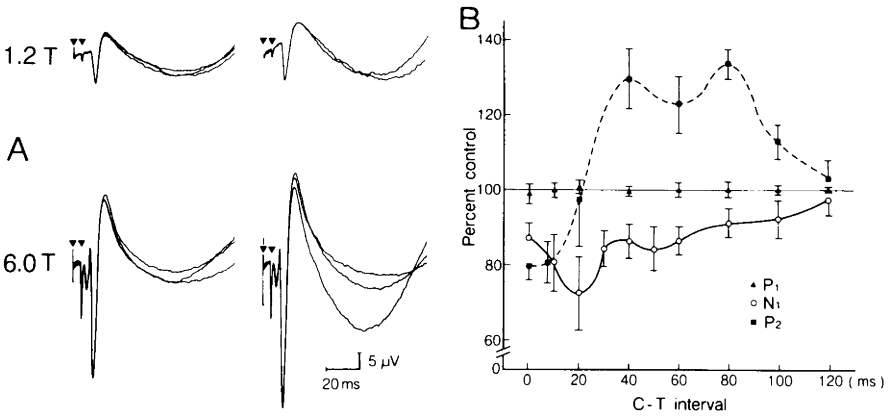

FIG. 3.4A,B. Inhibition of segmentally evoked SCPs by conditioning stimulation applied to the cervical enlargement from the PES. **A** Specimen records of the interaction of two SCPs produced at the same time period by adjusting the interval between the segmental and descending volleys (*left*) and simple summation of the two (segmental and descending) SCPs (*right*) in a subject. The *numbers at the left* denote the multiple of the threshold strength. The deflection at the start of each sweep and the subsequent downward (negative) deflection indicate the stimulus artifacts of the segmental and descending volleys, respectively. Note that the degree of occlusion is greater at 6.0 T than at 1.2 T. **B** Time courses of changes in sizes of the N1 and P2 waves as a function of conditioning (descending volley)–testing (segmental volley) (C-T) intervals. Means ± SE (vertical bars) were calculated in five subjects tested during neuroleptanesthesia. The conditioning stimuli were delivered at 6.0 T. (From Shimizu et al., 1982)

of the responses of the spinothalamic tract cells to the peripheral stimuli in anesthetized monkeys.

The shorter central latencies of the descending N and P waves (calculated by the interval between the onset of the initially positive spike, the arrival of the impulse, and that of the N and P wave) as compared with those of the segmental N1 and P2 waves demonstrated in our study (Shimizu et al., 1982) may indicate synchronous arrival of the descending volley or the dominance of paucisynaptic connections of descending fibers to the interneurons in the lumbosacral enlargement as compared with the connections of the segmental fibers to the interneurons. The differences in the central latencies of the descending N and P waves from those of the segmental N1 and P2 waves are reminiscent of the animal studies (Besson and Rivot, 1973; Eccles et al., 1962; Hongo et al., 1966; Menétrey et al., 1980; Rudomín et al., 1978; Skinner and Willis, 1970). Experiments with cats have shown that interneuronal populations are activated monosynaptically from different descending pathways. There is some spatial separation of the interneuronal groups activated by various descending tracts (Eccles et al., 1962; Kostyuk and Vasilenko, 1979). In addition, a wide convergence of segmental and descending effects has also been found on many interneurons (Hongo et al., 1966; Kostyuk and Vasilenko, 1979; Rudomín et al., 1978; Skinner and Willis, 1970; Willis and Coggeshall, 2004). For instance, the interneurons connected monosynaptically to the reticulo- and vestibulospinal pathways are located predominantly in the medial parts of laminae VII and VIII, while low-threshold cutaneous afferents acti-

vate the interneurons in laminae IV and V monosynaptically and polysynaptically, respectively. High-threshold afferents excite interneurons in laminae I and II and also those in laminae IV and V polysynaptically and monosynaptically, respectively (Kostyuk and Vasilenko, 1979). The validity of extrapolating these animal experiments to the interneurons in the human spinal cord is also supported by our observations that there is partial occlusion between the slow waves activated by the descending volleys and those activated segmentally (Fig. 3.4).

Thus, the interneurons producing the descending N wave may differ for the most part from those producing the segmental N1 wave, but some interneurons show convergence of the descending and segmental volleys (Besson and Rivot, 1973; Kostyuk and Vasilenko, 1979; Tobita et al., 2003). The degree of convergence of the descending and segmental volleys on the primary afferent terminals might be increased, since the descending P and segmental P2 waves interact more than the descending N and segmental N1 waves (Fig. 3.4).

3.5 Spinal Tracts Producing N and P Waves

The question of the extent of effective current spread from the epidural stimulating electrodes must arise. Although the cathodal electrode was placed as close as possible to the midline in the PES, the spread of stimulating current might not be localized within the dorsal column. The effect of graded stimulation on the descending N and P waves (refer to Fig. 3.1) reveals that several types of fibers or tracts rather than a single type of fiber within the cord are stimulated from the PES. Other tracts including some in the dorsolateral funiculus could be also activated by the current intensity employed in the human study (Tomita et al., 1996).

Our previous studies (Shimizu et al., 1979a,b; Shimoji et al., 1974) have shown that a single electrical pulse applied from the PES produces a tingling or a vibratory sensation, but no unpleasantness, in the wakeful subject. When the stimulus strength is increased, a muscle twitch is provoked in the segmental area but not beyond, even by an intense stimulation (15 T). Therefore, it is more likely that the effective stimulating pulses from the PES spread to superficial tracts of the dorsolateral funiculus but not to the corticospinal pathway under the human experimental conditions. Nevertheless, some effects on motoneuron pools in the lumbosacral enlargement cannot be entirely ruled out. Thus, the dorsal column and/or the dorsolateral funiculus might be the main tracts contributing to the provocation of the descending N and P waves in the lumbosacral enlargement. This thesis is also supported by the fact that if the stimulating electrodes in the cervical PES were shifted from midline to the lateral sides, the descending N and P waves could not be produced in the lumbosacral enlargement (Shimoji et al., 1982; Tomita et al., 1996) (Fig. 3.5A,B).

A number of spinal pathways descending from the brain have been shown to influence the activity of spinal cord interneurons in animals (Hodge et al., 1981; Kostyuk and Vasilenko, 1979; Lindblom and Ottoson, 1953; Lundberg et al., 1962; Tang, 1969). Even the pyramidal tract inhibits many cells in laminae IV and V and excites many cells in laminae V and VI (Dubuisson and Wall, 1980; Wall, 1967; Willis and Coggeshall, 2004). A pathway originating in the nucleus raphe magnus and descending in the dorsolateral funiculi was shown to inhibit many spinal interneurons,

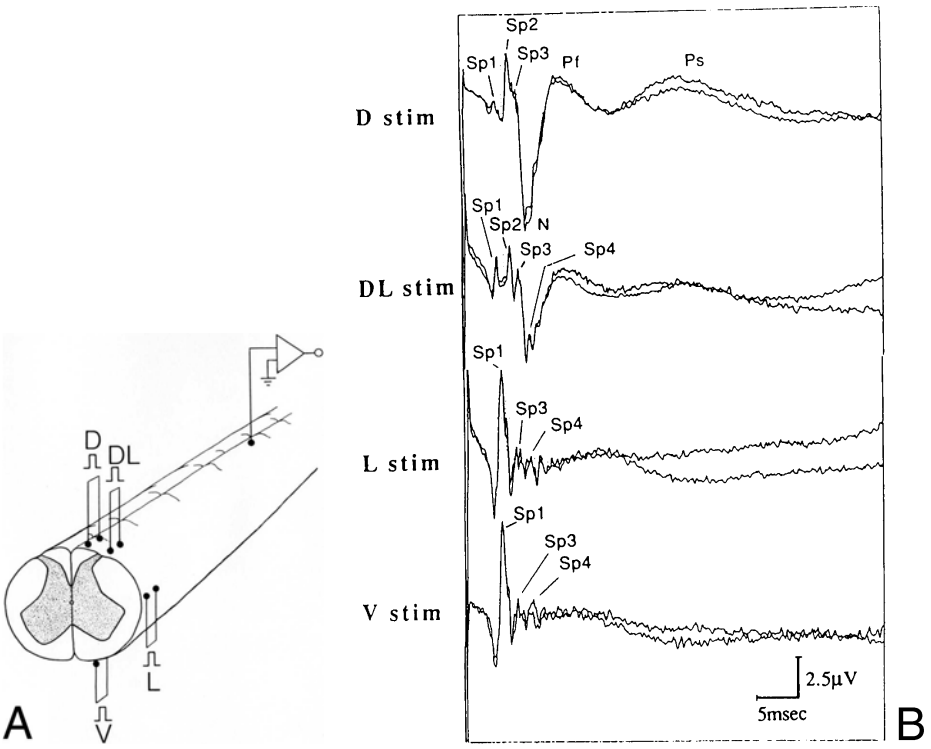

FIG. 3.5A,B. Effects of stimulating electrode positions in the cervical epidural space on the descending SCP recorded from the lumbar epidural space in humans anesthetized with neuroleptanesthesia. **A** Arrangements of stimulating electrodes at various points placed in the cervical epidural space and a recording electrode near the midline in the lumbar epidural space. **B** Spinal cord potentials recorded in the posterior epidural space of the lumbar enlargement (T11/12 level) in response to cervical spinal cord stimulation (C5/6 vertebral level) of four different columns at 2 times threshold strength during spinal cord monitoring for scoliosis surgery under general anesthesia (nitrous oxide–fentanyl anesthesia). Spike potentials (*Sp*) are numbered sequentially. Note that the slow negative (descending *N*) and slow positive (descending *P*) potentials are elicited by dorsal (*D*) and dorsolateral (*DL*) column stimulation, but not by lateral (*L*) or ventral (*V*) column stimulation (*stim*). Note also that the second spike appears only with dorsal and dorsolateral stimulation, suggesting that the second spike represents dorsal column volleys. Note also that the slow P potential is divided into two components (*Pf* and *Ps*) by a negative dip. (From Tomita et al., 1996)

especially those that respond to noxious peripheral stimuli (Basbaum et al., 1976; Fields and Basbaum, 1978; Fields et al., 1977; Kuypers and Maisky, 1975; Martin et al., 1979; Willis and Coggeshall, 2004). Therefore, stimulation of the nucleus raphe magnus produces inhibition of many dorsal horn interneurons through the dorsolateral funiculi, eliciting PAD at the same time (Proudfit and Anderson, 1974). In addition to this raphe spinal pathway, the dorsolateral funiculi also contain descending projections originating in several other brain stem nuclei (Barnes et al., 1979; Cervero et al., 1980; Fields and Basbaum, 1978; Kneisley et al., 1978; Willis and Coggeshall, 2004), the "dorsal reticulospinal system" of Lundberg's group (Engberg et al., 1968a,b).

In summary, then, the descending N and P waves in the lumbosacral enlargement activated by volleys from the cervical PES are thought to be produced mainly via the dorsal column and/or the dorsolateral funiculi at a moderate strength of stimulation (3–6 times threshold) in humans.

Chapter 4
Heterosegmental SCPs (HSPs)

Misao Tomita and Koki Shimoji

4.1 The HSP in Humans

The bottom traces of Fig. 4.1A show the specimen records from the posterior epidural space (PES) of the lumbar enlargement in response to median nerve stimulation at the wrist in a wakeful subject. Any potentials were hardly noticeable in the lumbar enlargement. Thus, peripheral nerve stimulation at a distal site in the upper extremity can hardly evoke any potential change in the caudal segments of the spinal cord in a normal human. This, however, does not mean that peripheral nerve stimulation at a distal site in the upper extremity can hardly evoke any potential change in the caudal segments of the upper extremity or has no influence on spinal function in the lumbar enlargement. It is rather more likely that the electrical activity does exist but is barely demonstrated due to the temporal and spatial dispersion of the potential when the distal site of a peripheral nerve is stimulated. Therefore, it is predicted that when a more rostral site on the peripheral nerve is stimulated, a potential deflection could be more clearly demonstrated in the lumbosacral enlargement in humans, similar to that observed in the rat (Shimoji et al., 1986a,b,c).

The relevance of this thesis is demonstrated as follows. When the stimulation electrodes are placed at a more rostral site, i.e., Erb's point, a slow potential change is clearly demonstrated in the wakeful subject, as shown in the top traces in Fig. 4.1A. The waveform of this slow potential is very similar to that of the heterosegmental slow potential (HSP) produced in the lumbar cord of the rat by stimulation of the forepaw (Shimoji et al., 1992a,b). Therefore, the HSP is thought not to be specific to the rat. The results might indicate that a large amount of synchronized afferent volleys are needed to evoke the HSP. In the rat, paw stimulation alone might be enough to provoke sufficient synchronized volleys in the cord, since the distance between the forepaw and the cord is very much smaller than that in humans. Our recent findings (Shimoji et al., 1992a) indicate that there are two components in HSPs, the early (HSP1) and late (HSP2) components, also suggesting that there are at least two nuclei which send back the feed-back volleys to the spinal cord in response to peripheral nerve stimulation (see Fig. 4.6). Principal nuclei, however, which send back the impulses producing the HSP, are believed to be located in the upper and lower parts of the medulla oblongata (Denda et al., 1996).

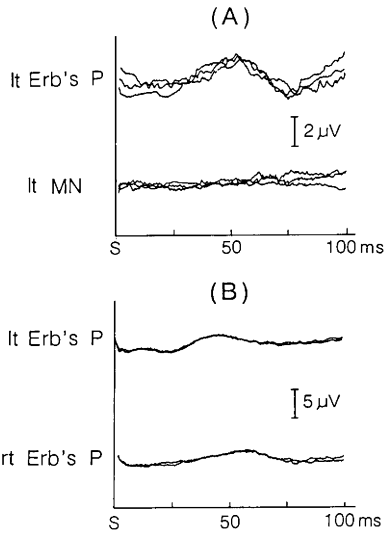

FIG. 4.1. **A** The SCP produced in the lumbar enlargement in response to stimulation at Erb's point. Erb's point was stimulated with two subcutaneous Ag–AgCl needle electrodes (200 μm in diameter and 10 mm in length), inserted 10 mm apart, and SCPs were recorded from the epidural space at the T1 level. Three averaged responses ($n = 50$) are superimposed in **A**. Note that a slow positive wave with long latency is clearly demonstrated by stimulation of the left Erb's point (*lt Erb's P*) but not by stimulation of the left median nerve at the wrist (*lt MN*). **B** The SCPs produced by stimulation of both sides in the same patient with herpes zoster in the right upper arm (T1 segment). Right Erb's point stimulation also produced a slow positive wave but its peak latency was prolonged in comparison to that by left stimulation, seemingly due to the partial nerve degeneration caused by herpes zoster. (From Shimoji et al., 1986a,b,c)

The HSPs could be recorded from the posterior epidural space (PES) at the cervical and lumbrosacral enlargements in response to electrical stimulation of the brachial plexus at Erb's point in 13 of 17 chronic pain patients. Erb's point stimulation produced slow positive potentials (heterosegmental slow positive potentials, HSPs) in the PES at the lumbosacral enlargement in all 13 subjects without spinal cord lesions but not in four subjects with spinal cord lesions. The HSP1 with a central peak latency of 21 ± 2 ms (mean ± SE) was recorded at stimulus intensities up to two to three times the threshold strength (T) of the initially positive spike (P1) of the segmental SCP, which was simultaneously recorded from the PES at the cervical enlargement (Fig. 4.2) (Shimoji et al., 1994). At the stimulus intensity of more than 3 T, another slow positive potential (HSP2) with central peak latency of 71 ± 6 ms was recorded. These slow positive potentials (HSP1 and HSP2) might be produced by a feedback loop via supraspinal structures, presumably primary afferent depolarizations, in comparison to the HSPs of our previous studies in the rat (Fig. 4.3) (Shimoji et al., 1990, 1992a,b). Slow negative potentials were sometimes noted before (5 of 13) and/or after (2 of 13) the HSP1. These slow negative potentials probably reflect the activities of dorsal horn neurons producing the HSP1 and HSP2.

4.2 Fundamental Patterns of the HSP

Figure 4.3 shows an example of the spinal cord potentials recorded from the cord dorsum in the cervical and lumbar enlargements in response to intense (25 times threshold) forepaw and hindpaw stimulation in a ketamine-anesthetized rat (Shimoji et al., 1992a,b). Forepaw stimulation produces a segmental spinal cord potential at the cervical enlargement and also a characteristic slow positive wave, or heterosegmental slow positive potential (HSP), at the lumbosacral enlargement (lumbar HSP) (Fig. 4.3A). The HSP sometimes has a negative dip in its course (in 18 of 21 lumbar HSPs

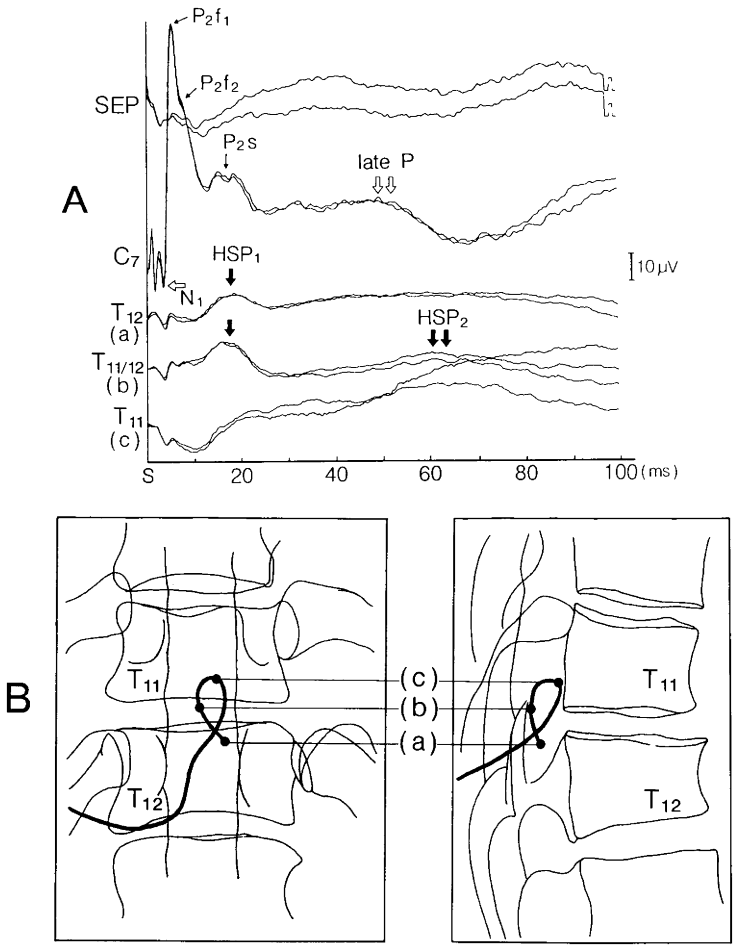

FIG. 4.2. An example of the relationship between the waveforms of the heterosegmentally evoked slow positive waves (HSPs) (**A**) and the positions of epidural electrodes at the lumbosacral enlargement (**B**) in response to strong stimulation at Erb's point (10 T) in a wakeful subject (53 years). Note that the second prolonged HSP2 (*two closed arrows*) following HSP1 are demonstrated in the recording from the electrode (*b*) located centrally in the PES but not in any recording from the other electrodes located laterally (*a*) and anteriorly (*c*). Note also that another late positive potential (*late P*) (*two open arrows*) is present following the P2s in the segmental SCP. *SEP*, somatosensory evoked potential from the scalp (C3′); *C7*, the segmental SCP recorded from the PES at the C7 vertebral level; *T11*, *T11/12*, *T12*, heterosegmentally produced slow positive potentials (HSPs) at three different sites in the coronary and sagittal planes. Two sequentially averaged ($n = 50$) responses are superimposed. A-P (*left*) and lateral (*right*) views of X-ray photographs were pencil-traced to make the electrodes' positions clear. (From Shimoji et al., 1992a,b)

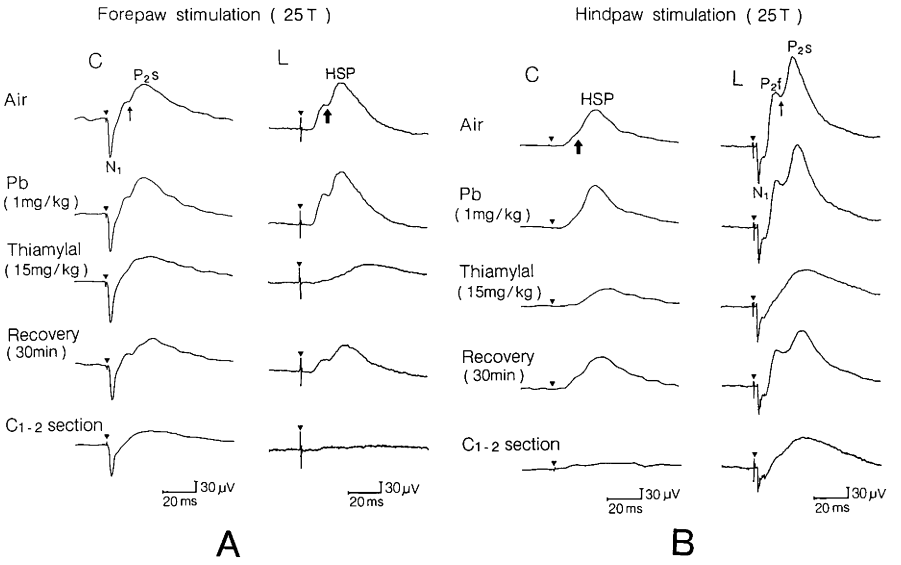

FIG. 4.3. Heterosegmentally evoked slow positive cord dorsum potentials (*HSP*s) in lumbar (*L*) and cervical (*C*) cord in response to forepaw (**A**) and hindpaw (**B**) stimulation, respectively, recorded simultaneously with the segmental spinal cord potentials in a ketamine-anesthetized rat. *Small* and *large arrows* indicate the negative dips in the segmental spinal cord potential and HSP, respectively. *Pb*, pancuronium bromide. *Reversed triangles* denote stimulus artifacts. (From Shimoji et al., 1992a,b)

and in 6 of 15 cervical HSPs). The HSP is not changed in waveform by injection of a muscle relaxant, pancuronium bromide, but is profoundly suppressed by thiamylal sodium (Fig. 4.3A,B). The HSP completely disappears after transection of the spinal cord at the C1–2 level without a fundamental change in the waveform of the segmental spinal cord potential. The secondary component of the slow positive (P2s) wave in the segmental spinal cord potential, however, is also eliminated by transection of the spinal cord (Fig. 4.4). Thus, the P2 wave of the segmental SCP is thought to consist of the first, segmentally activated, positive wave (P2f) and suprasegmentally activated secondary component (P2s) as demonstrated in humans (Shimoji et al., 1975, 1976, 1977; Shimizu et al., 1982). Hindpaw stimulation also evokes an HSP at the cervical enlargement (cervical HSP) in 15 out of 22 animals and segmental spinal cord potentials in all animals at the lumbosacral enlargement, respectively (see Fig. 4.3). The physiological characteristics of the cervical HSP are the same as those of the lumbar HSP (Fig. 4.3A,B). Peak latencies of cervical and lumbar HSPs (30 ± 1 ms and 31 ± 2 ms; means ± SE) are not significantly different from those of cervical and lumbar P2s (32 ± 2 ms and 29 ± 1 ms), respectively.

4.3 Central Nuclei of the HSP

It is evident that the origin of the HSP comes from supraspinal structures through a feedback loop, since high spinal transection completely eliminates the potential (Shimoji et al., 1992a,b).

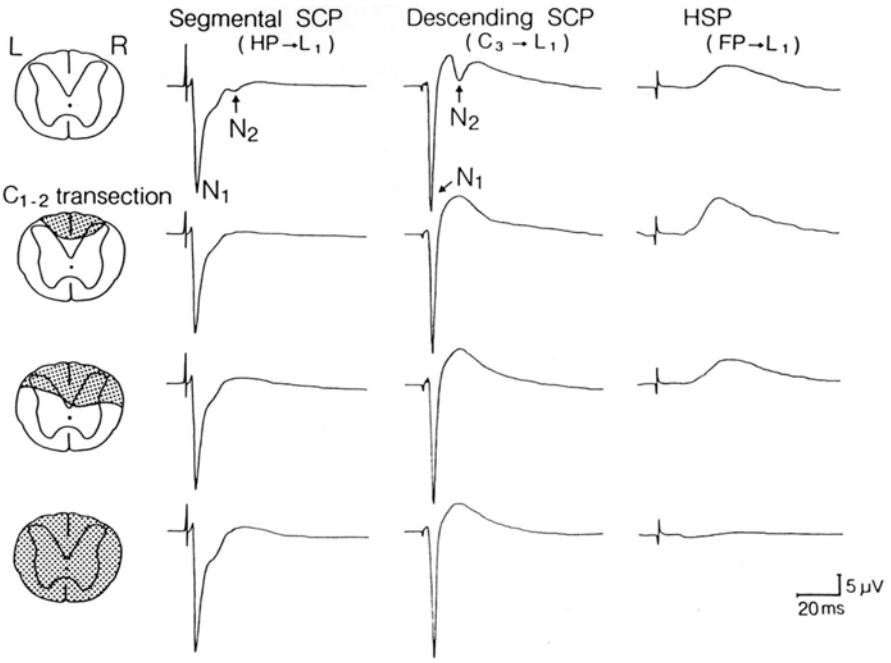

FIG. 4.4. The SCPs produced in the L5 level of the spinal cord in response to stimulation of the hindpaw (*segmental SCP*), dorsal column at the C3 level (*descending SCP*), and forepaw (heterosegmental slow potential; *HSP*) in the rat during ketamine anesthesia. Note the disappearance of the HSP without fundamental changes in segmental and descending SCPs following spinal transaction. Note also that secondary components of the slow positive potentials with preceding negative dip (*N2*, termed only in this figure) in both segmental and descending SCPs become silent after partial spinal transection but the HSP is still present. The HSP disappears following complete spinal transection. (From Shimoji et al., 1994)

Electrophysiological and anatomical studies have also demonstrated the existence of a considerable number of neurons present in several nuclei of the brainstem that give rise to branching axons that project to widely separate levels of the spinal cord such as the cervical and lumbar enlargements (Basbaum et al., 1986; Mokha et al., 1986; Wolters et al., 1986; Sirkin and Feng, 1987). A high variability of onset and peak latencies of both the cervical and lumbar HSPs as demonstrated in our study (Shimoji et al., 1992a,b) might be brought about by the existence of several nuclei in the brainstem which constitute the feedback loops sending descending impulses to the spinal cord (Fung and Barnes, 1984; Willis, 1984).

Although latencies of the HSP and P2s are variable among the rats, they remain consistent throughout the experiment in a single rat. Some set point mechanisms, which may vary among the individual rats, could exist for selection of a certain nucleus in the central structures to send back the inhibitory control over the spinal cord. Such an assumption may be allowed from the fact that stimulation of cerebral cortex as well as brainstem nuclei evoke the dorsal root potential, a reflection of presynaptic inhibition (Andersen et al., 1962; Carpenter et al., 1966). Exact mechanisms,

however, to explain such variability of response latencies of the HSP and P2s remain to be investigated in animals and even in humans.

Judging from their waveform characteristics and also from a close time course relationship with the inhibition of WDR neurons (Shimoji et al., 1992a,b), the HSPs probably reflect primary afferent depolarization (PAD) activated by a feedback loop via supraspinal structures (Besson and Rivot, 1972; Besson et al., 1975; Villanueva et al., 1986; Morton et al., 1987). High vulnerability of the HSPs to an anesthetic, thiamylal, also support the above thesis. However, other inhibitory potentials, such as inhibitory postsynaptic potentials, might also contribute to production of the HSPs, as suggested by Rudomín et al. (1987) in their segmental dorsal root potentials.

It was suggested that dorsal column and even peripheral nerve stimulation inhibits pain through a feedback loop via brainstem nuclei (Saadé et al., 1985; Gebhart, 2004). Thus, the HSP may represent such a feedback inhibitory activity activated by peripheral nerve stimulation, which is used clinically as transcutaneous electric nerve stimulation or as acupuncture.

4.4 The Relationship Between WDR Neuron Activities and HSP

To assess a physiological role of the HSP, we made simultaneous recordings from interneurons and the HSP in the lumbar spinal cord of the rat.

Four types of interneurons were recorded in lamina V (32 units). Eleven units were spontaneously active but did not respond to somatosensory stimuli. Five units responded to touch in the segmental area with rapid adaptation and low threshold hindpaw electrical stimulation, but did not respond to forepaw stimulation. Four units responded only to pinch to the hindpaw, but hardly showed any responsiveness to an intense stimulation (25 times threshold strength of the N1) of the forepaw.

Twelve neurons in lamina V and the boundary zone of V–VI responded to hindpaw touch as well as pinch (segmental stimulation) with increased firing (Fig. 4.5A). These neurons, of wide dynamic range (WDR), also responded to graded electrical stimuli of hindpaw with increases in firings. On the other hand, heterosegmental stimuli, such as tail (Fig. 4.5B) and forepaw (Fig. 4.5C) pinches, or electrical shock (Fig. 4.5D), suppressed the neuronal firing. Pinch stimuli also evoked slow cord dorsum positive waves at both cervical and lumbar spinal cord levels (Fig. 4.5E). Both the HSP and peristimulus time histogram of a WDR neuron firing, simultaneously evoked by forepaw electrical stimulation, are displayed on the same time scale in Fig. 4.5F. The time courses of both the HSP and inhibition of the neuronal activity were found to be similar in these nine WDR neurons. This suggests that the HSP reflects inhibitory activity, probably primary afferent depolarization, activated by a feedback loop via supraspinal structures (Shimoji et al., 1992a). Similar mechanisms may exist in human spinal cord (Shimizu et al., 1982).

Presuming that the origins of the feedback loops which produce the HSP and the secondary component of the slow positive potential (P2s) are the same, it might be expected that the peak latencies of the P2s in cervical segmental spinal cord potentials would be shorter than those of the lumbar HSPs in response to forepaw stimulation. Likewise, the peak latencies of the P2s in lumbar segmental spinal cord

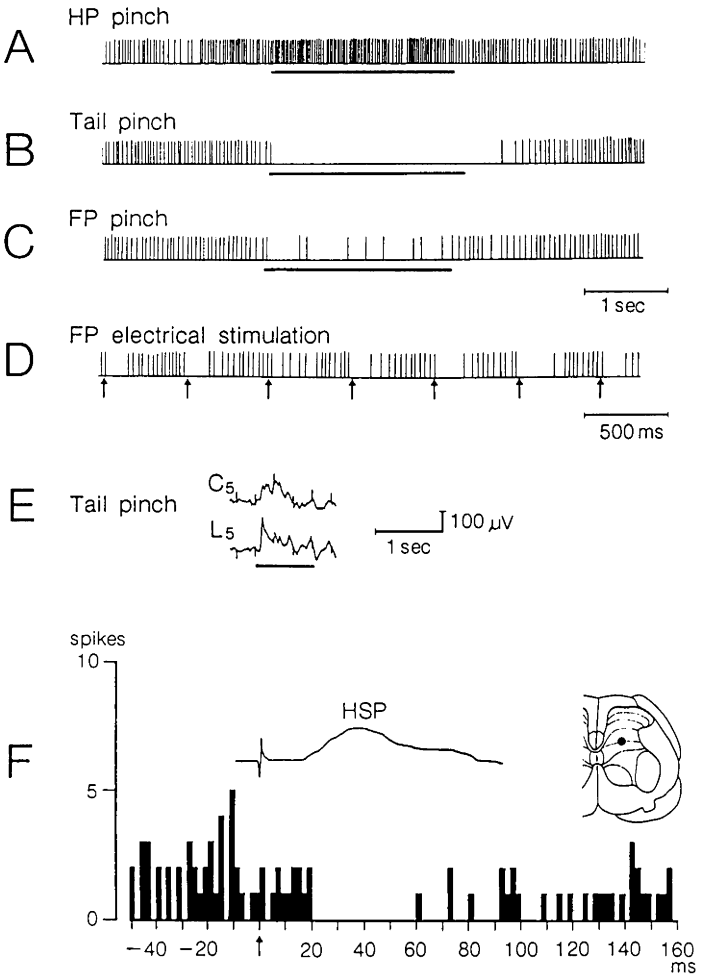

FIG. 4.5A–F. The relationship between the HSP and firings of a wide dynamic range (WDR) neuron recorded from the lumbar cord. **A–D** Polygraphic records of square-wave pulses, triggered by a discriminator, synchronous with the WDR neuron spikes. *Horizontal lines* under the traces indicate the time periods of stimulation. *Arrows* in **D** denote the times of electrical stimuli. **E** Polygraphic traces of cord dorsum potentials recorded from C5 and L5 levels in response to tail pinch are indicated by *bars*. Spike-like potentials overlapping the traces in **E** are ECG artifacts. *HP*, hindpaw; *FP*, forepaw. **F** The HSP and peristimulus time histogram (PSTH) of a WDR neuron firing in response to FP electrical stimulation, displayed on the same timescale. The spike-like artifact in the HSP trace and the arrow under the PSTH represent the time of electrical stimulation. Location of the WDR neuron is illustrated in the *right insert*. (From Shimoji et al., 1992)

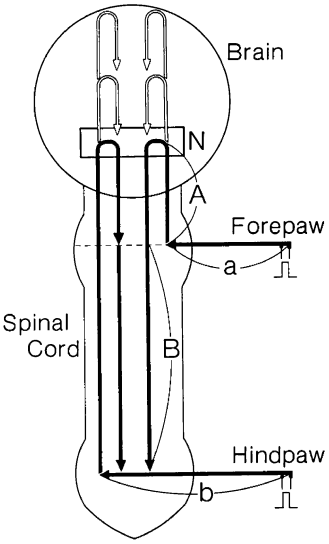

FIG. 4.6. Schematic drawing of hypothetical impulse feedback loops traveling through the spinal cord and brain in response to Erb's point stimulation to produce the HSPs and segmental P2s and late P. *A*, the distance between the cervical epidural electrode (C7 vertebral level) and a feedback nucleus (*N*). *B*, the distance between the cervical and lumbar (T12 vertebral level) electrodes. *N*, a presumed midbrain nucleus which relays the ascending and descending impulses to produce the HSPs, P2s, and late P. *a*, the distance between forepaw (corresponding Erb's point in humans) and cervical spinal cord. *b*, the distance between hindpaw stimulating electrode and lumbar epidural electrode (Shimoji et al., 1992a,b)

potentials should be longer than those of cervical HSPs (Fig. 4.6). However, it was demonstrated that the peak latencies of cervical P2s did not differ from those of lumbar P2s and the cervical or lumbar HSPs. This suggests that the origins of the feedback pathway of the cervical P2s are somewhat different from those of the lumbar P2s and also from those of the HSPs. However, since there exist several similarities between the segmental P2s and HSP, such as high vulnerability to anesthetic, complete disappearance after high cervical transection, and comparable responses to graded stimulus intensities, there must be a close relationship in the feedback nuclei and/or pathways between them (Shimoji et al., 1992a).

Chapter 5
Clinical Pharmacology

Tatsuhiko Kano and Yoshikado Miyagawa

5.1 Introduction

The effects of anesthetic drugs, hypothermia, and ischemia on segmentally evoked spinal cord potentials (segmental SCPs) and/or the longitudinally conducting evoked spinal cord potentials (conducting SCPs) were studied in adult patients undergoing surgery under general anesthesia. The segmental SCP was recorded from the posterior epidural space at the lumbosacral or cervical spinal enlargement in response to electrical stimulation of the posterior tibial nerve at the popliteal fossa or the ulnar/median nerve at the wrist, respectively. The segmental SCP consisted of an initial positive spike wave (P1) followed by a sharp negative wave (N1) and a slow positive wave (P2). It is generally agreed that the P1 wave is related to the arrival at the spinal cord of afferent volleys conducted through the dorsal roots and the N1 wave has its origin in the activity of interneurons in the dorsal horn. The characteristics of the P2 wave closely resemble those of the positive cord dorsum potentials (P wave) in animals, as well as the negative dorsal root potential (DRP-V), which is thought to reflect primary afferent depolarization (PAD) in the spinal dorsal horn (Kano et al., 1971; Shimoji et al., 1972, 1974; Kano and Shimoji, 1974). Following tibial nerve stimulation at the popliteal fossa, the segmental SCP was observed along with the M and H waves of the evoked electromyogram (EMG) recorded simultaneously from the calf muscle. After ulnar/median nerve stimulation at the wrist, the segmental SCP was observed, along with the ulnar/median nerve action potentials (NAP) at the elbow and the somatosensory evoked potentials (SEP) from the contralateral scalp. The NAP of the cauda equina was also simultaneously recorded in some patients through an electrode introduced into the lower lumbar epidural space, when the tibial nerve was stimulated at the popliteal fossa.

The conducting SCP was recorded from the epidural space at the level of the lumbosacral enlargement in response to epidural electrical stimulation of the cervical enlargement, and vice versa. The conducting SCP consisted of two spike-like components: the first wave, which had a low threshold and high amplitude, followed by a second small wave, considered to originate in both the ascending and descending long nonsynaptic tracts in the posterolateral white matter of the spinal cord.

5.2 Effects of Intravenous Anesthetics

5.2.1 Thiamylal Sodium

Clinical doses (2.5–5 mg/kg) of thiamylal affected not only the SEP but the segmental SCP and the H wave of the evoked EMG, without significant effect on the NAP or the M wave of the evoked EMG (Kano et al., 1971; Shimoji et al., 1972). The clinical dose of thiamylal increased the N1 and P2 amplitudes of the segmental SCP and the H wave amplitude, and a comparatively large dose of the drug (7.5 mg/kg) prolonged the N1 and P2 durations and decreased the H wave amplitude. Figure 5.1 shows a typical sequence of changes of the evoked potentials in a patient undergoing surgery under general anesthesia. No significant change was seen in the P1 of the segmental SCP or the conducting SCP after an intravenous injection of a clinical dose of thiamylal.

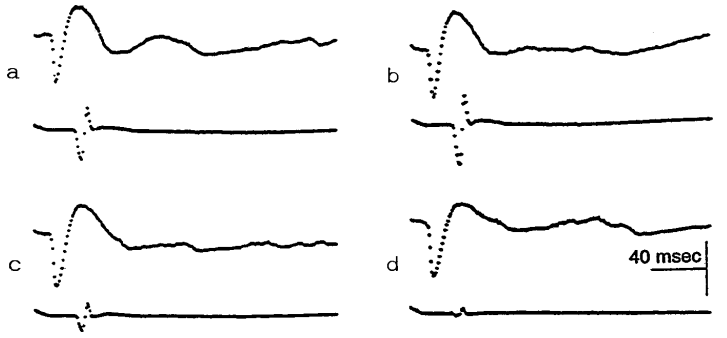

Fig. 5.1a–d. Effects of intravenous thiamylal and inhaled halothane on the segmental spinal cord potential (SCP) (*upper trace*) and the H wave of the evoked electromyogram (EMG) (*lower trace*) in humans. Supramaximal electrical stimulation was applied to the posterior tibial nerve at the popliteal fossa, and the SCP was recorded from the posterior epidural space at the T12 vertebral level and the evoked EMG from the calf muscle simultaneously. (Supramaximal stimulation means the stimulation strength applied for induction of compound nerve action potentials, in which the amplitude of compound nerve action potentials is not increased even if the strength of stimulation is further elevated.) **a** During wakefulness; **b** during the light stage of thiamylal anesthesia (2.5 mg/kg); **c** during the deep stage of thiamylal anesthesia (7.5 mg/kg); **d** during the deep stage of halothane anesthesia (2.0%). Calibration was 10 μV for the SCP and 10 mV for the H wave. Upward deflection indicates positivity in this and the following figures. Note that the small dose of thiamylal increased the N1 and P2 amplitudes of the segmental SCP and the H wave amplitude, and large doses of the drug prolonged the N1 and P2 durations and decreased the H wave amplitude. The effect of halothane at a moderate dose on the N1 wave of the segmental SCP was similar to that of thiamylal. The N1 wave increased in amplitude and in duration with successive deepening of halothane. The P2 wave prolonged its duration during the moderate stage and decreased its amplitude at the deep stage of halothane anesthesia. (From Kano et al., 1971)

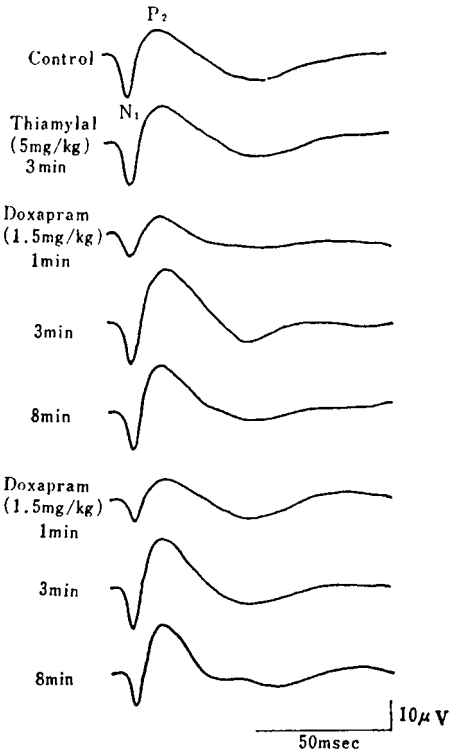

FIG. 5.2. Effects of intravenous thiamylal and subsequent doxapram (nonspecific analeptic) on the segmental SCP in humans. Supramaximal electrical stimulation was applied to the posterior tibial nerve at the popliteal fossa, and the SCP was recorded from the posterior epidural space at the T12 vertebral level. Doxapram (1.5 mg/kg) was intravenously applied twice, 3 and 15 min after the thiamylal (5 mg/kg). Note that the N1 and P2 amplitudes of the segmental SCPs, especially the P2 amplitude, were profoundly increased after the doxapram administrations as compared with the pre-thiamylal level, while those were preceded by transient reduction. The peak latencies remained unchanged even after the doxapram administrations. (From Kano et al., 1984)

Subsequent intravenous administration of doxapram (1.5 mg/kg, nonspecific analeptic) increased the N1 and P2 amplitudes of the segmental SCP, especially the P2 amplitude, exceeding the pre-thiamylal level, while the N1 and P2 amplitude augmentation after doxapram was preceded by a transient reduction of the amplitudes without significant changes in the peak latencies (Kano et al., 1984) (Fig. 5.2).

Discussion. The significant changes in the SEP, the N1 and P2 waves of the segmental SCP, and the H wave of the evoked EMG indicate that thiamylal affects spinal as well as supraspinal nervous structures. Moreover, the insignificant changes in the P1 of the segmental SCP, the NAP, and the conducting SCP, which are thought of as nonsynaptic components, and the M wave of the evoked EMG confirm that thiamylal in clinical doses does not act on nerve conduction and neuromuscular transmission in humans. Thiamylal in clinical doses is supposed to cause synchronized discharges of the interneurons in the dorsal horn, giving rise to an increase in N1 amplitude of the segmental SCP. The increase in amplitude of the P2 wave of the segmental SCP with widening the duration is interesting. This might reflect an enhancement of PAD at the spinal level. Spinal monosynaptic reflexes are known to receive inhibitory and excitatory influences from supraspinal structures. A small dose of thiamylal might preferentially block the supraspinal inhibitory influence on the spinal monosynapse rather than having a direct action, resulting in a temporary increase of the H wave. The reversal effect of doxapram after thiamylal at the spinal level is successfully

demonstrated. The recovery of the N1 and P2 amplitudes exceeding the control after doxapram and the transient amplitude reduction immediately after doxapram indicate that doxapram is not a simple antagonist drug for thiamylal.

5.2.2 Ketamine Hydrochloride

Intravenous administration of a moderate dose of ketamine (2 mg/kg) increased the N1 amplitude of the segmental SCP and the H wave amplitude of the evoked EMG, and markedly decreased the P2 amplitudes of the segmental SCP (Kano and Shimoji, 1974). At 15 min after ketamine administration, both the N1 and P2 waves of the segmental SCP showed a tendency to return to the pre-ketamine level, while the H wave was still greatly affected. No significant change was observed in the P1 wave of the segmental SCP. The typical pattern recorded from a surgical patient without neurological disorders is shown in Fig. 5.3. The conducting SCP was also not affected by an intravenous injection of a clinical dose of ketamine. Ketamine was given intravenously for pain relief and sedation in a patient with quadriplegia due to a cervical spinal cord injury. The segmental SCP in response to tibial nerve stimulation was not affected at all by clinical doses of ketamine in the patient during the acute phase of spinal injury (Shimoji and Kano, 1973).

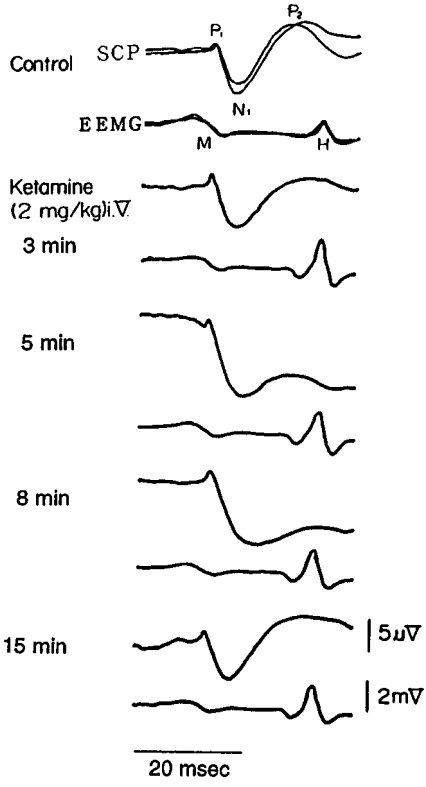

Fig. 5.3. Effects of intravenous ketamine on the P1, N1, and P2 waves of the segmental SCP (*upper tracings*) and the M and H waves of the evoked EMG (*lower tracings*) in humans. Supramaximal electrical stimulation was applied to the posterior tibial nerve at the popliteal fossa, and the SCP was recorded from the posterior epidural space at the T12/L1 level and the evoked EMG from the calf muscle simultaneously. Sequential changes of those potentials after ketamine (2 mg/kg) were observed. Note the increases in the N1 and H amplitudes concomitant with the profound decrease in the P2 amplitude. (After Kano and Shimoji, 1974)

Discussion. Ketamine in clinical doses is thought to cause synchronized discharges of the interneurons in the dorsal horn, giving rise to an increase in N1 amplitude of the segmental SCP, a similar effect to that of thiamylal. Profound depression of the P2 wave of the segmental SCP after ketamine seems to indicate inhibition of PAD, because ketamine induces facilitation of the H wave at the same time. The spinal PAD through segmental afferent pathways might be occluded[1] because of enhancement of the PAD through descending pathways. It is shown in humans (Shimizu et al., 1982; Shimoji et al., 1982) and in spinal animals (Kano and Hashiguchi, 1991) that epidural stimulation of the cervical spinal cord does affect the segmental SCP, including the P2 wave recorded from the lumbar epidural space. The discrepancy of ketamine effects on the segmental SCP between patients with and without supraspinal influences would indicate that the descending influences from supraspinal structures on the segmental spinal function are strong.

5.2.3 Fentanyl Citrate and Droperidol

The P1, N1 and P2 waves of the segmental SCP and the M and H waves of the evoked EMG were all depressed in amplitude by intravenous fentanyl (5–8 μg/kg) given alone or in combination with droperidol, although the amplitude decreases of the P1 wave and the M wave were less than those of the N1, P2 waves, and the H wave (Kano and Shimoji, 1974). The sequential changes of the N1 and P2 waves of the segmental SCP and the H wave of the evoked EMG recorded in a patient at induction of anesthesia are presented in Fig. 5.4. Neither the segmental SCP nor the evoked EMG was affected by clinical doses of droperidol (0.4 mg/kg) alone. The conducting SCP was little affected by intravenous fentanyl (50–100 μg) or by fentanyl (50 μg) injected into the subarachnoid space for postoperative pain relief (Kano et al., 1998).

Discussion. The results indicate that a clinical dose of intravenous fentanyl is likely to suppress all the components of the segmental SCP, including the afferent peripheral nerve and the synaptic transmission in the spinal cord, although the role of descending influences from supraspinal structures are unknown.

5.2.4 Morphine Hydrochloride

Intravenously injected morphine (1 mg/kg) depressed the amplitudes of the P1, N1, and P2 waves of the segmental SCP. The depressant effects of morphine were most pronounced on the P2 wave. The change in the evoked EMG after morphine was not remarkable. Subsequent intravenous injection of naloxone (0.1 mg/kg) reversed the effects of morphine completely or partially. In some cases the amplitudes of the P1, N1, and P2 waves of the segmental SCP even exceeded those before morphine

[1] Occlusion is a physiological failure of impulse transmission at the synapse. There are two types of occlusion. When a postsynaptic neuron is still in the refractory period induced by preceding impulses, the neuron cannot respond to the arrival of new impulses; temporal occlusion. The synapse does not always consist of one to one connections between neurons. When a postsynaptic neuron is still in the refractory period by preceding impulses of a presynaptic neuron, impulses newly arrived from another presynaptic neuron will not be transmitted at the synapse; this is spatial occlusion.

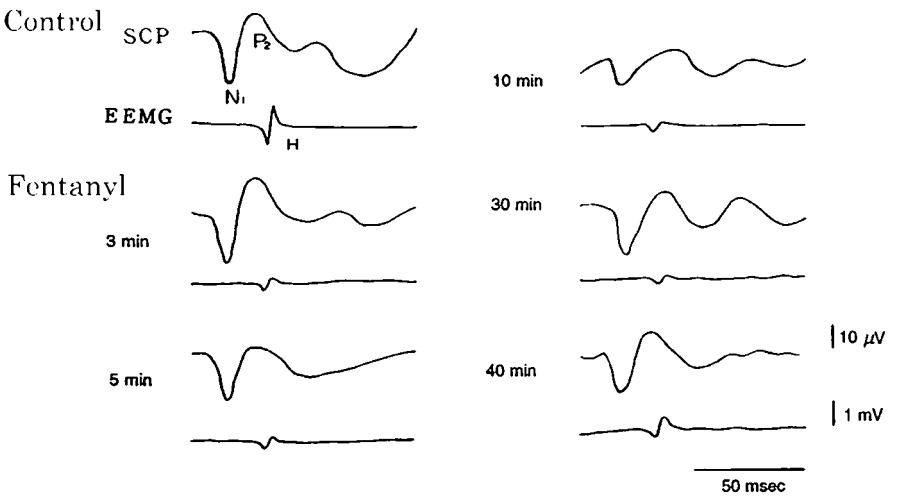

FIG. 5.4. Effects of intravenous fentanyl on the N1 and P2 waves of the segmental SCP (*upper traces*) and the H wave of the evoked EMG (*lower traces*) in humans. Supramaximal electrical stimulation was applied to the posterior tibial nerve at the popliteal fossa, and the SCP was recorded from the posterior epidural space at the T12 vertebral level and the evoked EMG from the calf muscle simultaneously. Sequential changes in the potentials after administration of fentanyl (8 μg/kg) were observed. Note the overall decreases in the N1 and P2 waves of the segmental SCP and the H wave after the intravenous fentanyl. (After Kano and Shimoji, 1974)

(Maruyama et al., 1980) (Fig. 5.5). The depressant effects of morphine on the segmental SCP were minimized under nitrous oxide anesthesia. Morphine (2 mg), applied in the epidural space for postoperative pain relief, did not produce any significant change in the conducting SCP (Tabo et al., 1993).

Discussion. Morphine in a clinical dose affected spinal cord function, especially the function that is thought to correspond to PAD. Afferent volleys along the roots were also depressed by morphine as well as by fentanyl. The findings support evidence that an opiate receptor may be present in the afferent nerve fibers. The depressant effects were minimized under nitrous oxide anesthesia, indicating the existence of an interaction between morphine and nitrous oxide.

5.2.5 Diazepam

The amplitude and duration of the P2 wave of the segmental SCP were increased 10–30 min after intravenous diazepam (0.2 mg/kg), while those of the N1 wave remained without any significant change (Kaieda et al., 1981). The H wave of the evoked EMG decreased in amplitude after the diazepam.

Discussion. Intravenous diazepam in clinical doses affects the function of human spinal cord. The most significant findings were the increase in the P2 wave amplitude and the decrease in the H wave amplitude, which suggest enhancement of presynaptic inhibition.

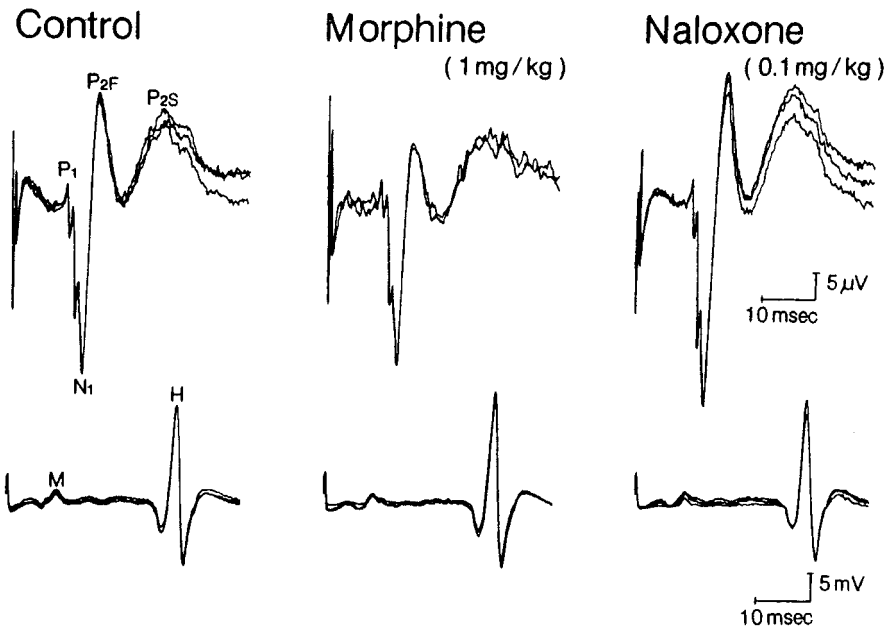

FIG. 5.5. Effects of intravenous morphine and naloxone on the P1, N1, and P2 waves of the segmental SCP (*upper traces*) and the M and H waves of the evoked EMG (*lower traces*) in humans. Supramaximal electrical stimulation was applied to the posterior tibial nerve at the popliteal fossa, and the SCP was recorded from the posterior epidural space at the T12 vertebral level and the evoked EMG from the calf muscle simultaneously. Three tracings are superimposed before (*Control*), 3–8 min after the morphine (1 mg/kg), and 2–6 min (17–21 min after the morphine) after the naloxone (0.1 mg/kg). The P2 wave was divided into two peaks; *P2F* and *P2S*. Note that intravenous morphine depressed the amplitudes of the P1, N1, and P2 waves, especially of the P2 wave, of the segmental SCP. The change in the evoked EMG after morphine was unremarkable. Subsequent intravenous injection of naloxone reversed the effects of morphine completely or partially. (From Maruyama et al., 1980, with permission)

5.2.6 Summary

Intravenous anesthetics, opioids, and sedatives in clinical doses affect the P1, N1, and P2 waves of the segmental SCP in various ways (Table 5.1), while these drugs have little effect on the conducting SCP. It is likely that thiamylal and ketamine cause synchronized discharges of the interneurons in the dorsal horn, giving rise to an increase in N1 amplitude of the segmental SCP. The decrease in the N1 amplitude after fentanyl and morphine indicate a blocking action of the drugs on both nerve conduction and synaptic transmission to spinal interneurons. Depression of the P1 wave after the opioids supports the direct blocking action on the afferent volleys along the dorsal roots, suggesting the existence of opioid receptor on the root or the peripheral nerve in human.

Profound depression of the P2 wave after ketamine seems to indicate inhibition of PAD through supraspinal structures, because ketamine induces facilitation of the H wave at the same time. Supraspinal descending tracts are confirmed to have more

Table 5.1. Effects of clinical doses of anesthetics on each component of the evoked segmental spinal cord potentials recorded from the posterior epidural space in humans

	P1 amplitude	N1 amplitude	N1 duration	P2 amplitude	P2 duration
Thiamylal	→	↑	↑	↑	↑
Diazepam	→	→	→	↑	↑
Ketamine	→	↑	→	↓	↓
Morphine	↓	↓	→	↓	↑
Fentanyl	↓	↓	→	↓	↑
Nitrous oxide	→	↓ – →	→	↓	↑
Halothane	→	↑	↑	↓	↑
Enflurane	→	↑	↑	↓	↑
Sevoflurane	→	↑	↑	↓	↑
Isoflurane	→	↑	↑	↓	↑

P1 reflects the action potential along the spinal root; N1 and P2 are thought to represent the activity of interneurons in the dorsal horn and the primary afferent depolarization, respectively.
→, no change; ↑, increased; ↓, decreased.

influence on the spinal PAD compared with segmental afferent roots, since intravenous ketamine in clinical doses induces significant changes in the P2 wave of the segmental SCP in neurologically healthy patients but not in a quadriplegic patient (Shimoji and Kano, 1973). The P2 depression by morphine and fentanyl suggest that spinal PAD through segmental afferent pathways might be occluded because of enhancement of PAD through descending pathways. The descending effects on the segmental SCP were observed in humans (Shimizu et al., 1982; Shimoji et al., 1982) and in spinal animals (Kano and Hashiguchi, 1991). Shimizu et al. (1982) recorded a SCP similar to the segmental SCP in configuration from the epidural space at the human lumbosacral enlargement following epidural stimulation of the cervical spinal cord and proved the interaction between the descending and segmental SCPs. Shimoji et al. (1982) reported facilitation of the P2 wave of the segmental SCP by descending volleys in humans. Kano et al. (1991) demonstrated that repetitive epidural stimulation of the cervical spinal cord distal to a section suppresses the segmental SCP from the lumbar epidural space in spinal dogs. Diazepam in a clinical dose seems to exert weak effects on the spinal cord through supraspinal descending pathways.

The reversal effects of doxapram after thiamylal and of naloxone after morphine were successfully demonstrated at the spinal level. The recovery of the segmental SCP often exceeds the control level after the reversal, and the transient amplitude reduction or augmentation immediately after doxapram or naloxone indicates that each drug may not indicate a simple reversal for thiamylal or morphine.

The conducting SCP is least affected by clinical doses of intravenously applied opioids and sedatives. The nonsynaptic tracts in the posterolateral white matter of the spinal cord are not likely the site of action of those intravenously applied drugs. The effects of neuroaxial opioids[2] on the segmental SCP are under investigation.

[2] Opioids are often administered into the spinal epidural or subarachnoid space surrounding the spinal cord for intraoperative analgesia or postoperative pain relief. In such a case, the main analgesia would be attained by the direct action of opioids that infiltrate into the dorsal horn and act on opioid receptor, but not by the systemic action of opioids absorbed into the circulation.

5.3 Effects of Inhalation Anesthetics

The effect of a moderate dose of halothane (1%) on the N1 wave of the segmental SCP was similar to that of thiamylal (Kano et al., 1971). The N1 wave increased in amplitude and in duration with successive deepening of halothane (2%). The P2 wave became prolonged its duration during the moderate stage and decreased in amplitude at the deep stage (2%) of halothane anesthesia, as shown in Fig. 5.1. Other halogenated inhalation anesthetics, including enflurane (Shimoji et al., 1984), isoflurane, and sevoflurane showed the similar effects on the segmental SCP. Nitrous oxide (60%) was different from the halogenated inhalation anesthetics in its effects on the N1 wave. Nitrous oxide decreased or did not change the N1 amplitude without significant effect on the peak latency. A clinical dose of those inhalation anesthetics affected least the conducting SCP (Kano et al., 1998).

Discussion and Summary. Halogenated inhalation anesthetics in clinical doses enhanced the N1 wave of the segmental SCP like thiamylal and ketamine but depressed the P2 wave like opioids (Table 5.1). Halogenated inhalation anesthetics are likely to cause synchronized discharges of the interneurons in the dorsal horn, as happens with thiamylal and ketamine. The P2 depression may be based on nonspecific blocking action on the synaptic transmission, while supraspinal influences on spinal PAD could not be ruled out. The nonsynaptic tracts in the posterolateral white matter of the spinal cord are not likely the site of action of halogenated inhalation anesthetics at clinical depth, since the conducting SCP was not affected under clinical inhalation anesthesia.

5.4 Effects of Local Anesthetics

5.4.1 Epidural Lidocaine on Segmental SCPs

The N1 and P2 waves of the segmental SCP at the T12 vertebral level and the M and H waves of the evoked EMG from the calf muscle were suppressed under epidural anesthesia, in which 20 ml of 2% lidocaine (400 mg) was injected into the lumbar epidural space at the L2 vertebral level. The P2 wave of the segmental SCP and the H wave of the evoked EMG were more profoundly affected by the epidural anesthesia as compared with the N1 wave and the M wave, respectively (Shimoji et al., 1987). The cauda equina nerve action potential (NAP) recorded simultaneously from the epidural space at the L5 level was little affected by the epidural injection of lidocaine. A representative case is shown in Fig. 5.6. The plasma lidocaine concentrations determined at 20 min after the epidural injection were within the range of 3–5.5 μg/ml in arterial blood and 1–4 μg/ml in the venous blood.

Discussion. The cauda equina NAP remained unchanged after the epidural injection of lidocaine at the L2 vertebral level. The recording level of cauda equina NAP was at the L5 vertebral level distal to the lidocaine injection level. Some of the lidocaine injected into the epidural space moves in the subarachnoid space through the dura mater. Lidocaine concentration in the cerebrospinal fluid (CSF) at the vertebral L5 level would not reach a level that could block large nerve fibers of the cauda equina.

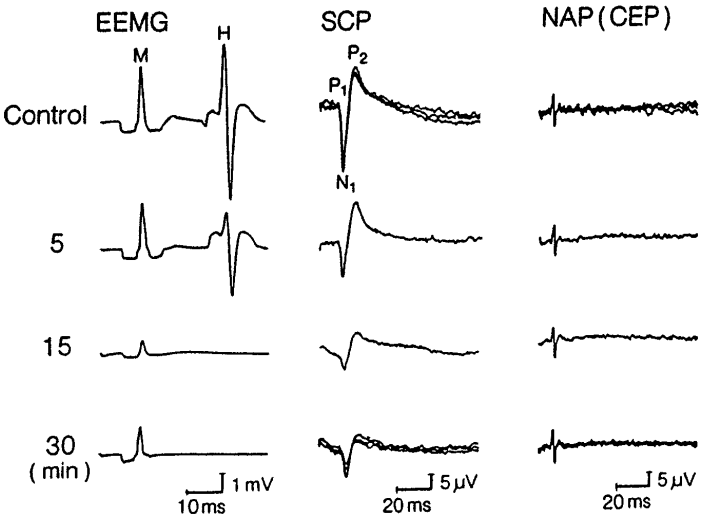

FIG. 5.6. Effects of lidocaine injected into the epidural space on the evoked EMG (*EEMG*), the segmental SCP, and the nerve action potential (*NAP*) of the cauda equina in humans. The M and H waves of the evoked EMG from the calf muscle, the P1, N1, and P2 waves of the segmental SCPs from the epidural space at the T12 vertebral level and the cauda equina NAP from the epidural space at the L5 vertebral level were simultaneously recorded in response to tibial nerve stimulation at the popliteal fossa. Sequential changes of the segmental SCPs after an epidural injection of 20 ml of 2% lidocaine (400 mg) at the L2 vertebral level are shown concomitantly with those of the evoked EMG and the cauda equina NAP. Note that the N1 and P2 waves of segmental SCPs and the M and H waves of the evoked EMG were suppressed by the lumbar epidural anesthesia, while the P1 wave of the SCPs was less affected and the NAP recorded from the cauda equina distal to the injection site remained unchanged. (From Shimoji et al., 1987 with permission)

From another point of view, there is a possibility that the cauda equina NAP presented might be the NAP in the posterior and anterior branches in the epidural space before entering the subarachnoid space. Furthermore, the extension of the lidocaine solution injected in the epidural space was not confirmed in this study. We could not deny the possibility that the lidocaine solution might also extend more cephalad than expected.

The suppressive effect of the lidocaine applied epidurally on the N1 and P2 waves of the segmental SCP and on the H wave of the evoked EMG would be explained by the direct action of lidocaine circulating in the cerebrospinal fluid (CSF) and/or by the systemic action of lidocaine absorbed in the blood. When a comparatively large amount of local anesthetic is given as a bolus for neuroaxial anesthesia,[3] the increased plasma concentration of local anesthetic may systemically affect the synaptic com-

[3] Neuroaxial anesthesia indicates regional anesthesia produced by injecting a local anesthetic into the spinal epidural or subarachnoid space surrounding the spinal cord in a patient undergoing surgery.

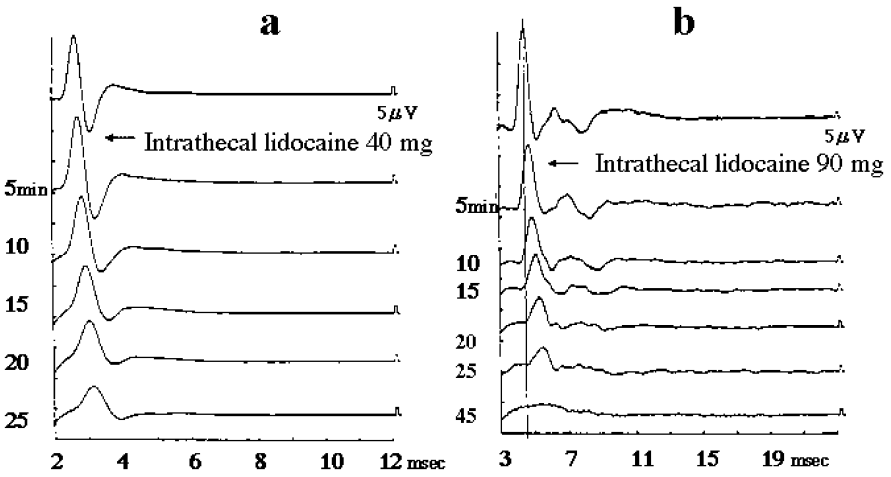

FIG. 5.7a,b. Effects of lidocaine injected into the lumbar subarachnoid space on the conducting SCPs in two typical patients undergoing the repair of thoracic aortic or thoracoabdominal aortic aneurysm. The conducting SCPs were recorded from the epidural space at the T12/L1 vertebral level in response to supramaximal electrical stimulation applied epidurally at the C7/T1 vertebral level. The levels of the epidural electrodes were confirmed preoperatively by X-ray examination. Lidocaine was injected into the lumbar subarachnoid space for postoperative pain relief near the completion of surgery under propofol anesthesia through an indwelling catheter for cerebrospinal fluid drainage. Sequential changes of the conducting SCPs after the intrathecal injection of 40 mg lidocaine (**a**; 61-year-old woman at an esophageal temperature of 36.5°C) or 90 mg lidocaine (**b**; 70-year-old-man at an esophageal temperature of 33.5°C) are shown. Note that the conducting SCP representing the conduction of intraspinal cord tracts was markedly depressed or disappeared completely after the intrathecal injections of lidocaine. (Kano et al., unpublished data)

ponents of the SCPs. Further investigation is needed to differentiate the systemic action from the direct nerve blocking action.

The suppression of the M wave of the evoked EMG after the epidural lidocaine might be due the reduction of continuous efferent impulses to the muscle and/or systemic action of the local anesthetic absorbed into the blood stream.

5.4.2 Epidural Lidocaine on Conducting SCPs

Tabo et al. (1993) reported that both the first and second waves of the conducting SCP decreased in amplitude with the prolongation of the peak latencies when lidocaine (60–120 mg) was injected into the thoracic epidural space at the level between the stimulation and recording sites. The suppressive effects reached a maximum at about 30 min after the lidocaine injection and retuned to the preinjection level within 150 min.

Discussion. The conduction block of spinal tracts taking part in the conducting SCP suggests that the sensorimotor paralysis in clinical epidural anesthesia may be produced by a direct action on the spinal cord, while further studies on the systemic effects of the lidocaine injected epidurally are needed.

5.4.3 Intrathecal Lidocaine on Conducting SCPs

The conducting SCP was markedly depressed or disappeared completely after an intrathecal injection of not only large doses of lidocaine (305–450 mg) for intractable pain treatment, but also of clinical doses of lidocaine (40–90 mg) for postoperative pain relief. No significant decrease in body temperature was observed during that period (Table 5.2). Two typical cases are presented in Fig. 5.7. An intravenous injection of lidocaine (50 mg) given for the treatment of ventricular arrhythmia did not affect the first and second waves of the conducting SCP (Kano et al., 1998).

Discussion. The above finding is proof that the local anesthetic injected into the subarachnoid space results in a nerve blocking action not only on the extraspinal

Table 5.2. Effects of intrathecal local anesthetics on conducting evoked spinal cord potentials

Case	Age (years) /sex	Disease/ surgery	Purpose	Lack of stim. electr.	Level of rec. electr.	Dose of lidocaine (mg)	Body temp. (°C)	Changes in conduct. SCPs (min after inj.)
1	58/F	Neuropathic pain	Total spinal block; pain treatment	T12/L1	T1/T2	450	36.5 (R.T.)	Disappeared (5 min)
2	57/M	Phantom pain	Total spinal block; pain treatment	T11/T12	T6/T7	305	36.6 (R.T.)	Ampli. reduc. (10 min)
3	39/M	Colostomy	Continuous spinal anesth.	T4/T5	T12/L1	4.5[a]	36.2 (R.T.)	Disappeared (10 min)
4	70/M	Repair of TAAA	CSF drainage and postop. analgesia	C7/T1	T12/L1	90	33.5 (E.T.)	Disappeared (15 min)
5	61/F	Repair of TAA	CSF drainage and postop. analgesia	C7/T1	T12/L1	40	36.8 (E.T.)	Ampli. reduc. (20 min)
6	73/F	Repair of TAA	CSF drainage and postop. analgesia	C7/T1	T12/L1	50	35.8 (CSF.T.)	Ampli. reduc. (10 min)

In cases 4, 5, and 6, a catheter was introduced into the lumbar subarachnoid space for CSF drainage before induction of anesthesia, through which lidocaine was injected after completion of surgery.
Stim. electr., stimulation electrode; Rec. electr., recording electrode; Conduct. SCPs, conducting evoked spinal cord potentials; min after inj., minutes after intrathecal injection of local anesthetic; Ampli. reduc., amplitude reduction; R.T., room temperature; E.T., esophageal temperature; CSF.T., cerebrospinal fluid temperature, which was monitored with a thin thermocouple wire probe mounted on the tip of the CSF drainage catheter (From Mishima et al., 1999, with permission); TAAA, thoracoabdominal aortic aneurysm; TAA, thoracic aortic aneurysm (Kano et al., unpublished data).
[a] Dibucaine.

roots/branches but also on the intraspinal tracts. Clinical spinal anesthesia would be attributed to both conduction block of the spinal roots and the spinal cord.

5.4.4 Summary

The direct blocking action of an epidurally or intrathecally applied local anesthetic on the spinal cord contributes at least partly to the development of routine epidural or spinal anesthesia, respectively. When a comparatively large amount of local anesthetic is given as a bolus for neuroaxial anesthesia, the increased plasma concentration of local anesthetic may systemically affect the synaptic components of the SCPs. Further investigation is needed to differentiate the systemic action from the direct nerve blocking action.

Section C
Motor Evoked SCPs

Chapter 1
Transcranial Magnetically Evoked SCPs (TCM-Evoked SCPs)

Toshiyuki Tobita and Koki Shimoji

Spinal cord function monitoring during spine or spinal cord surgery has been carried out mostly with the use of somatosensory evoked potentials (SEPs) induced by peripheral nerve stimulation and recorded from the scalp (Grundy and Villani, 1988; McPherson and Ducker, 1988). The scalp SEPs, however, do not directly reflect the activities of the motor system, and surgical manipulations of the spine or spinal cord often affect the motor systems without producing SEP abnormalities (Ginsburg et al., 1985; Ben-David et al., 1987). Motor-evoked potentials from the peripheral muscles (motor-evoked electromyograms, or EMGs) induced by transcranial magnetic (Barker and Jalinous, 1985) or electrical (Merton and Morton, 1980) stimulation were developed, and might have advantages over SEPs during surgery in which manipulations of the motor tracts are predicted (Kawaguchi and Furuya, 2004).

Evoked EMGs in response to transcranial magnetic stimulation (TCMS) have recently become widely used in clinical studies such as monitoring, diagnosis and even therapy (Huang et al., 2004), since the technique is not painful and is easy to administer. However, evoked EMGs can not be recorded under the use of muscle relaxants during anesthesia and surgery. Evoked SCPs should be recorded in such cases.

1.1 Recording Techniques

A single or repetitive TCMS is usually applied at every 1–30 s to the skull corresponding to the motor cortex on the vertex through a round coil with an external diameter of 140 mm, which is supported by hands or fixed to the head by an acrylic coil holder manufactured in each laboratory, and connected to a magnetic stimulator (Magstim 200; Magstim, Whitland, UK) with a maximal output of 1.5 Tesla (Fig. 1.1). The most effective positioning of the round coil is assessed with a stimulus intensity of 50%–100% of the maximal output, which is not painful for the patients.

The analysis time is usually set at 50–100 ms, and the recording should be repeated at least twice to ensure reproducibility of the responses. Before the start of each test, averaging should be made at an intensity of subthreshold strength to confirm that no artifact, particularly that of the ECG, contaminated the record, and also to take the baseline measurements of the peak latencies and amplitudes of the responses.

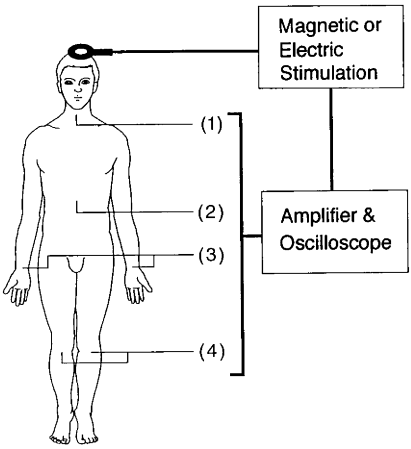

FIG. 1.1. Schematic presentation of arrangement for recording evoked spinal cord potentials (SCPs) from the posterior epidural space (PES) at the cervical (C6–7) and lower thoracic (T11–12) vertebral levels in response to transcranial magnetic stimulation (TCMS) of the cerebral motor area in patients who underwent spine surgery. The catheter electrodes were inserted into the posterior epidural space at the C6–7 and (*1*) T11–12 (*2*) levels. The surface electrodes were placed on the thenar (*3*) and anterior tibial (*4*) muscles of both sides

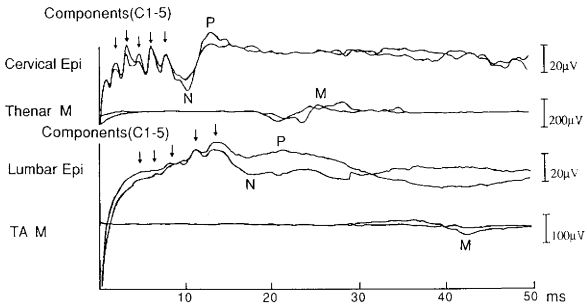

FIG. 1.2. An example of simultaneous recording of TCMS-evoked SCPs from the PES at the C6 and T12 vertebral levels with TCMS-evoked electromyograms (EMGs) from the thenar and tibialis anterior (*TA*) muscles. Note that five distinct spike-like components (*arrows*) followed by a slow negative (*N*) and positive (*P*) wave appeared in the C6 epidural recording in response to TCMS, and also that these five components are less distinct from the background in the lower thoracic recording (T12). Two averaged responses ($n = 10$) were superimposed. Upward deflection indicates positivity. Calibrations: 20 μV for SCPs, 200 μV for thenar EMGs, and 100 μV for TA EMGs. The *vertical axis* at the start of each sweep corresponds to the onset of magnetic stimulation, causing a background deflection. (Tobita, unpublished data)

The TCMS-evoked spinal cord potentials (SCPs) have been recorded from the posterior epidural space (PES) in this laboratory, based on the same method developed by Shimoji et al. for recording the somatosensory SCPs from the spinal epidural space (1971, 1972, 1976).

1.2 Basic Patterns of TCM-Evoked SCPs

Transcranial magnetic stimulation to the vertex produces at least five spike-like components (components C1–6) followed by a slow negative (N) and a subsequent posi-

Table 1.1. Peak latencies (mean ± SE, $n = 17$) of the components of spinal cord potentials (SCPs) in response to TCMS, recorded from the posterior epidural space at the cervical (C6–7) and lumbar (T11–12) enlargements, and the onset latencies of electromyograms recorded at the thenar and anterior tibial muscles in conscious patients

SCP Component	Cervical (C6–7) (ms)	Lumbar (T11–12) (ms)
C1	3.2 ± 0.1	6.9 ± 0.3
C2	4.8 ± 0.1	8.5 ± 0.2
C3	6.3 ± 0.1	9.9 ± 0.3
C4	7.8 ± 0.2	11.7 ± 0.2
C5	9.4 ± 0.3	13.8 ± 0.1
N	11.9 ± 0.9	16.7 ± 1.8
P	15.3 ± 0.3	20.8 ± 2.3
EMG[a]	Thenar (ms)	Anterior tibial (ms)
	19.2 ± 0.8	25.5 ± 1.4

[a] As there were no differences in onset latency of evoked electromyograms (EMGs) in each subject between left and right sides, both values were averaged.

tive (P) wave in recordings from the posterior epidural space (PES), and can evoke EMGs of the thenar and anterior tibial muscles in both sides (Fig. 1.2). Each component of the TCMS-evoked SCP is seen more clearly in the cervical records than in the lumbar records (Fig. 1.2). The five spike-like components of the SCP were delayed in latency and decreased in amplitude in recordings at the T11–12 vertebral level compared to those at the C6–7 vertebral level (Fig. 1.2 and Table 1.1). The mean amplitudes of the components C1–5 recorded at the C6–7 vertebral level are from 7 to 15 μV, and the conduction velocities of these components are between 70 and 78 ms^{-1}. The mean conduction velocities of all the C1–5 components are 74.8 ± 2.9 ms^{-1} (mean ± SE). There were no significant differences in conduction velocity along the cord between these components, as calculated by the latency difference between each component at the cervical and the lower thoracic levels, and the distances between the cervical epidural and the lower thoracic epidural electrodes. The mean amplitudes of N and P waves were 25 ± 3 and 9 ± 2 μV (mean ± SE), respectively.

1.3 Effects of Intravenous Anesthetics

There is little information regarding the mechanisms of the effects of intravenous anesthetics on the motor system at the spinal cord level in humans. Further, during spine or spinal cord surgery, the muscle relaxants routinely used to facilitate the surgery make it difficult to monitor the motor system using the motor-evoked EMG. It is therefore informative to record the activity of the motor system at spinal cord levels during surgery when muscle relaxants are used.

The slow N and P waves were not changed even by complete muscle relaxation following intravenous administration of succinylcholine chloride (1 $mg\,kg^{-1}$).

Fentanyl (5 $\mu g\,kg^{-1}$, i.v.) did not significantly affect the spike-like components but suppressed both the slow negative and positive waves (Fig. 1.3 and Table 1.2).

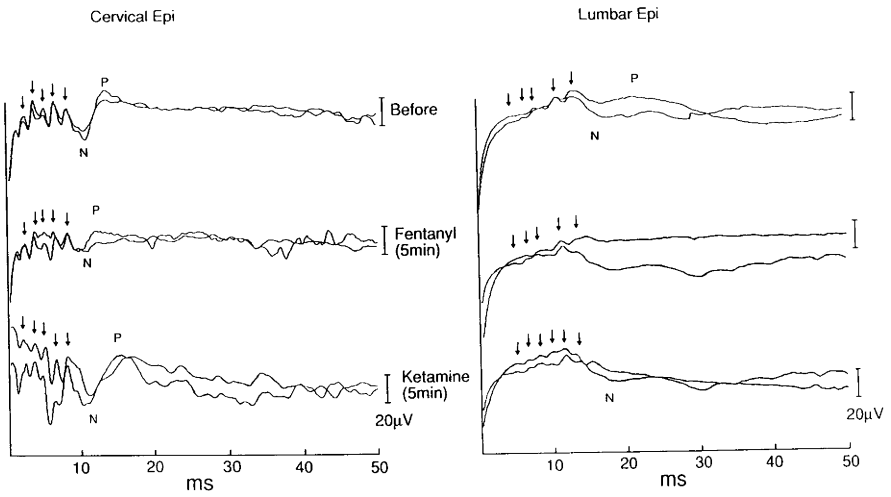

FIG. 1.3. Effects of fentanyl ($6\,\mu g\,kg^{-1}$) and ketamine ($1.5\,mg\,kg^{-1}$) on TCMS-evoked SCPs, recorded from the cervical (C6) and lumbar (L1) posterior epidural space (*Epi*) in a patient who underwent surgical correction. Two averaged ($n = 20$) responses were superimposed. Note that a surgical dose of fentanyl minimally affects motor-evoked SCPs with slight suppression of the slow components (N and P potentials), while subsequent ketamine administration significantly augments the potentials. (Unpublished data, Tobita et al.)

TABLE 1.2. Changes (mean ± SE, $n = 9$) in the amplitude (peak-to-peak) of each component of TCMS-evoked SCP and electromyograms with hemodynamics induced by the sequential administration of three intravenous anesthetics (unpublished data, Tobita et al.)

		Before	Fentanyl (%)	Ketamine (%)	Droperidol (%)
SCP	C1	100.0	116.2 ± 21.0	88.5 ± 15.2	77.7 ± 25.2
	C2	100.0	118.8 ± 22.8	93.7 ± 19.8	74.3 ± 19.7
	C3	100.0	84.7 ± 10.9	125.2 ± 19.6	77.2 ± 15.9
	C4	100.0	81.7 ± 10.4	128.4 ± 36.2	76.0 ± 34.4
	C5	100.0	79.8 ± 16.2	69.0 ± 21.3	40.3 ± 6.6*
	N	100.0	62.9 ± 16.1*	156.8 ± 15.1*†	34.5 ± 9.5*†
	P	100.0	52.9 ± 21.9*	141.3 ± 17.2†	5.2 ± 2.2*††
EMG	Thenar	100.0	87.0 ± 12.4	88.5 ± 14.4	90.9 ± 14.7
	TA	100.0	86.8 ± 12.3	136.0 ± 61.0	68.5 ± 20.9
Hemodynamics	MAP (mmHg)	87.8 ± 6.0	85.4 ± 4.4	92.0 ± 7.2	81.4 ± 4.8
	HR (bpm)	103.4 ± 8.1	99.2 ± 8.9	98.3 ± 7.8	103.3 ± 9.6

C1–C5, spike-like components of motor-evoked SCP; N and P, slow negative and positive waves, respectively, following the spike-like components of motor-evoked SCP; thenar, evoked EMG of the thenar muscle; TA, evoked EMG of the anterior tibial muscle; MAP, mean arterial pressure; HR, heart rate.
* $P < 0.05$ vs before; ** $P < 0.01$ vs before; † $P < 0.05$ vs the previous drug.

The administration of ketamine ($1.5\,mg\,kg^{-1}$) tended to increase the amplitudes of the 3rd (C3) and 4th (C4) components (but not significantly), and significantly increased the slow N and P waves of the SCPs (Fig. 1.3 and Table 1.2). The additional injection of droperidol ($0.15\,mg\,kg^{-1}$) markedly suppressed both the slow N and P waves with the 5th (C5) component of the spike-like potentials, but did not alter significantly the EMGs (Table 1.2).

Even though the magnetic coil was fixed firmly at the same position with the same stimulus intensity throughout the procedures, the amplitudes of each component of the TCMS-evoked SCP and the EMG varied considerably in response to sequential stimuli (Figs. 1.2 and 1.3). Tobita et al. (1998) reported that significant relationship was found only between the amplitude of C4 component of the SCPs and that of the EMG recorded from the thenar muscle during wakefulness and anesthesia. However, there were no significant relationships between other spike-like C1–3 and C5 components or the slow N and P waves of the SCPs and the EMG. The latencies of the SCPs and the EMGs were not significantly affected by these drugs.

The 1st to 3rd (C1–3) spike-like components of the TCMS-evoked SCP may reflect compound action potentials conducted along the spinal tracts, judging from their waveforms (Burke et al., 1990, 1993). The fact that the C1–3 components did not correlate with the thenar EMG even though both were not significantly affected by intravenous anesthetics suggests that the C1–3 components reflect the compound action potentials of certain spinal tracts. Further, the finding that there were no significant differences in conduction velocity between each spike-like component from cervical to lumbosacral enlargements may indicate that these spike-like components reflect impulses conducted along the same spinal tract, and that these latency differences originate in the brain at the site of stimulation rather than in the spinal cord. The conduction velocities of $75–78\,ms^{-1}$ for the C1–3 components are consistent with those for the axons of giant pyramidal (Betz) cells (Ghez, 1981). Thus, it is most likely that the C1–3 components are produced by direct or indirect activation of the large pyramidal neurons in the motor cortex (Iida et al., 1997; Kalkman et al., 1994).

The C4 component was not significantly affected by the intravenous anesthetics but significantly correlated with the thenar EMG (Tobita et al., 1998). The results of Tobita et al. (1998) may indicate that the C4 component is postsynaptic in origin and reflects motoneuron pool activities. By contrast, the C5 component with following slow N-P waves may not directly be involved in the motor activities. The C5 component was significantly suppressed in amplitude by the additional administration of droperidol (Table 1.2), suggesting that this component reflects transynaptically evoked potential along the spinal cord. There have been no reports on the slow N and P waves of the SCPs in response to TCMS.

The present study demonstrated that ketamine ($1.5\,mg\,kg^{-1}$) markedly augmented the amplitude of the slow N and P waves in the TCMS-evoked SCP. In addition, the waveform of the slow N wave in the TCMS-evoked SCP resembles that of the N1 wave of the segmental SCPs. Thus, it is most likely that the slow N wave reflects a synchronized activity of the interneurons located in the dorsal horn close to the recording site. Transcranial electric stimulation of the motor area has been reported to produce "direct" (D) and "indirect" (I) SCPs (Katayama et al., 1988; Edgeley et al., 1990; Thompson et al., 1991; Amassian et al., 1992; Rothwell et al., 1992; Burke et al., 1993; Kitagawa and Møller, 1994; Fujiki et al., 1996). From the present results it is concluded

that the C1–3 components are the "direct" responses, and the C4 and C5 components including the N and P waves are "indirect" SCPs.

The additional administration of droperidol suppressed the slow N and P waves of the SCPs without affecting the EMGs, also suggesting that these slow potentials do not reflect the activities of spinal motor activities. From the clinical standpoint of monitoring motor system activity, these intravenous anesthetics at least each or in combination might be of value since they did not significantly affect the early spike-like potentials of the SCPs and the EMGs.

In summary, the present study suggests that the C1–3 components of the TCMS-evoked SCPs in humans are produced by direct or indirect activation of the corticospinal tract, the C4 component results from the activity of the motoneurons, the C5 component reflects transynaptically evoked potentials of the corticospinal tract, and the slow N and P waves reflect the activities of interneurons rather than those of motoneurons.

1.4 Effects of Inhalation Anesthetics

The motor-evoked electromyogram (EMG) was found to be vulnerable to inhalation anesthetics (Zentner et al., 1989; Haghighi et al., 1990; Calancie et al., 1991; Kalkman et al., 1991; Hicks et al., 1992; Stone et al., 1992; Zentner et al., 1992; Herdmann et al., 1993; Kawaguchi et al., 1996a,b). Thus, intraoperative monitoring of the motor system has been carried out with intravenous anesthetics (Kalkman et al., 1992; Herdmann et al., 1993; Kawaguchi et al., 1993; Taniguchi et al., 1993; Kalkman et al., 1995). However, there has been little information for the effects of inhalation anesthetics on the transcranial magnetically evoked spinal cord potentials (TCMS-evoked SCPs).

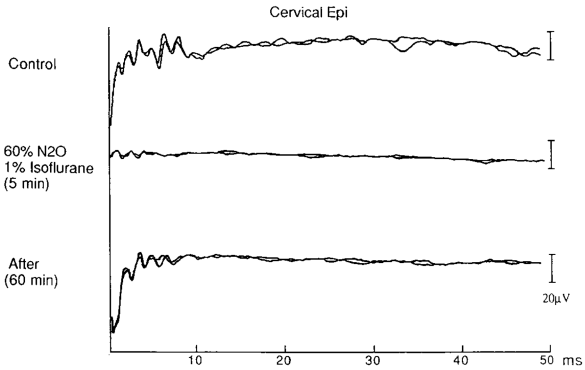

Fig. 1.4. Effect of inhalation anesthetic, isoflurane, on spinal cord potentials produced by transcranial magnetic stimulation (TCMS-evoked SCPs) applied on the motor area. Note that later components of the spike potentials and following slow components are suppressed in 5 min by inhalation of 1% isoflurane/60% nitrous oxide. The TCMS-evoked potential was recorded from the posterior epidural space with the catheter electrode inserted at the C6 level. Note also that the potentials, particularly later components, are still suppressed even 1 h after discontinuation of inhalation anesthesia following approximately 3-h administration of isoflurane for surgical operation. (Tobita et al., unpublished data)

As demonstrated in Fig. 1.4, all components of TCMS-evoked SCPs were profoundly suppressed by isoflurane–nitrous oxide anesthesia. This result indicates that all components of the TCMS-evoked SCPs are postsynaptic in their origins. However, more detailed origins of each component of TCMS-evoked SCP remain to be investigated. Other inhalation anesthetics are also found to suppress the TCMS-evoked SCPs in humans.

Chapter 2
Transcranial Electrically Evoked SCPs (TCE-Evoked SCPs)

2.1 Recording Techniques

Chikashi Fukaya and Yoichi Katayama

2.1.1 Introduction

Even with the use of microsurgical techniques, neurosurgery on the spinal cord involves high risk for serious neurological complications. Over the past five to ten years, neurophysiological monitoring techniques have become increasingly popular, aiming to prevent intraoperative neurological impairment. Several types of evoked spinal cord potential in human subjects have been reported. These have provided hope that spinal cord functions can be assessed objectively by neurophysiological monitoring during surgery.

Transcranial electrically evoked potentials are usually divided into two groups: potentials recorded from muscle, and from epidural spinal cord. Direct motor cortex stimulation has also frequently been used for craniotomy patients in neurosurgery. This chapter, however, focuses on the methodology for transcranial electrical stimulation (TES) and recording from the epidural space of the spinal cord or muscles.

2.1.2 Anesthesia

After endotracheal intubation, patients were anesthetized with a constant intravenous infusion of propofol and fentanyl. Basically inhalation anesthesia does not influence the potentials recorded from epidural spinal cord space, but has generally avoided because of its influence on the response recorded from muscles and other modalities of evoked potential monitoring, which were concomitantly used during the surgery.

Neuromuscular blockade was omitted after intubation, because of its suppressive effect on muscle responses. General anesthesia was maintained by only use of propofol and fentanyl infusion.

2.1.3 Stimulation

Transcranial electrical stimulation was applied by monophasic square wave pulses of 50–100 μsec duration. To activate corticospinal tract (CST) neurons, a pair of small

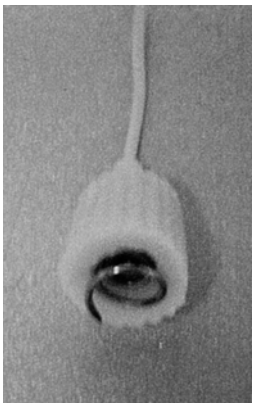

Fig. 2.1. The corkscrew-design electrode is suitable for transcranial electrical stimulation (TES) because of its simple, fast, and secure attachment

electrodes was placed on the scalp over the motor cortex. We used corkscrew-design electrodes because of their simple, fast, and secure attachment (Fig. 2.1). These stimulation electrodes were placed on the scalp over C3 and C4 (International 10–20 system of scalp electrode positions) (Fig. 2.2). The lateral portion was approximately 6–8 cm off the midline. Brief electrical stimuli, up to 1200 V intensity, were delivered over the scalp using a Digitimer D-185 electrical stimulator (D185; Digitimer, Welwyn Garden City, UK). Such short-duration, high-intensity electrical stimuli can overcome the impedance barrier of the skin, bone, and dura mater, and directly activate the fast motoneurons of the corticospinal tract. The intensity required to elicit an adequate response usually did not exceed 960 V for both epidural and muscle recording. During the muscle recording, the Digitimer D-185 stimulator can be used for train stimulation with different numbers of trains and different interstimulus intervals. In our department, transcranial electrical stimulation began with three pulses at 2-ms interstimulus intervals (ISI). Five pulses produced more consistent responses, and so were used for monitoring. The safety of TES has been documented and discussed elsewhere (Agnew and McCreery, 1987; Boyd and De Silva, 1986; Cohen and Hallett, 1988).

2.1.4 Recording

2.1.4.1 From the Spinal Cord

To record transcranial electrically evoked SCPs, flexible platinum catheter-type electrodes (3487A-33; Medtronic, Minneapolis, MN, USA) were inserted into the cervical or thoracic epidural space. This electrode has four platinum iridium recording cylinders separated by 6 mm of insulated length. Each cylinder is 3 mm in length and 1.27 mm in diameter (Fig. 2.3). Each recording surface was numbered according to its position on the electrode, as 0 (distal) to 3 (proximal).

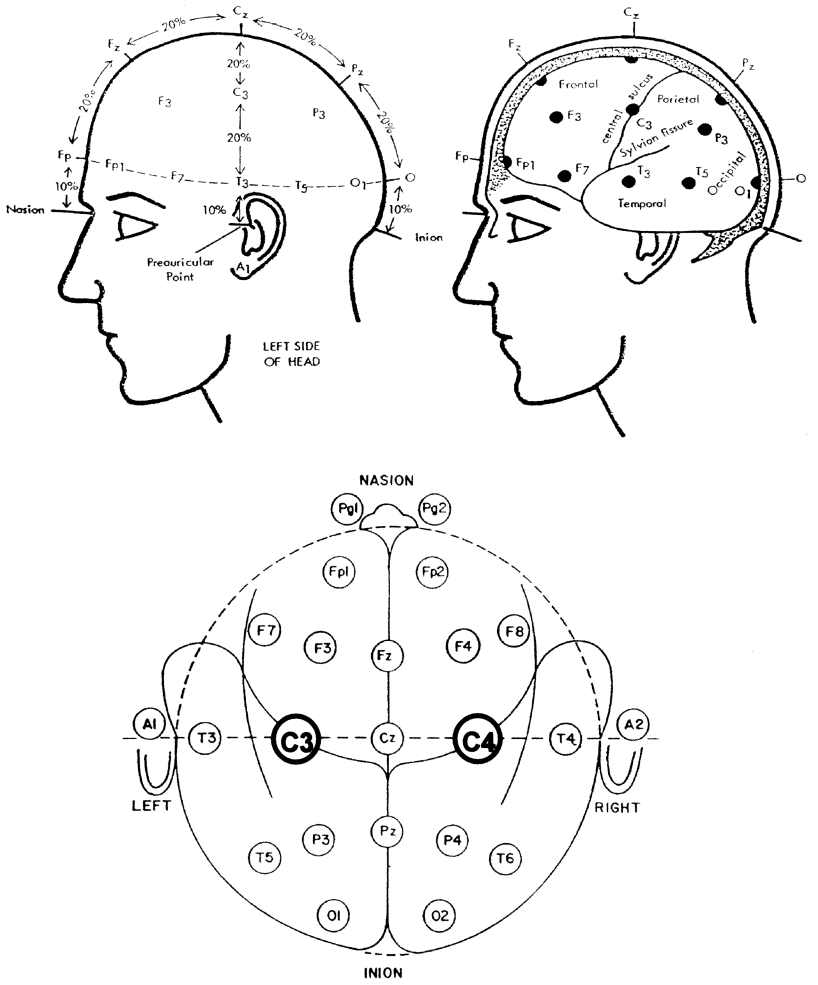

FIG. 2.2. The stimulation electrodes were placed on the scalp over C3 and C4, based on the International 10–20 system of scalp electrode positions. The lateral portion was approximately 6–8 cm off the midline

For monitoring in a case involving an intracranial lesion, this electrode was introduced into the cervical and thoracic epidural space under X-ray control. The subject was placed in the prone position, and 18-gauge epidural needle were inserted at the thoracic epidural space. The electrodes were inserted through the epidural needle and advanced to the appropriate positions. The tip of an electrode was usually placed on the C2 or C3 segment (Fig. 2.4). The epidural needle was then removed, and the electrode was fixed with adhesive tape to the skin.

For spinal cord monitoring, the catheter-type electrodes were inserted in the epidural or subdural space at the upper and lower edges of the laminectomy (rostral

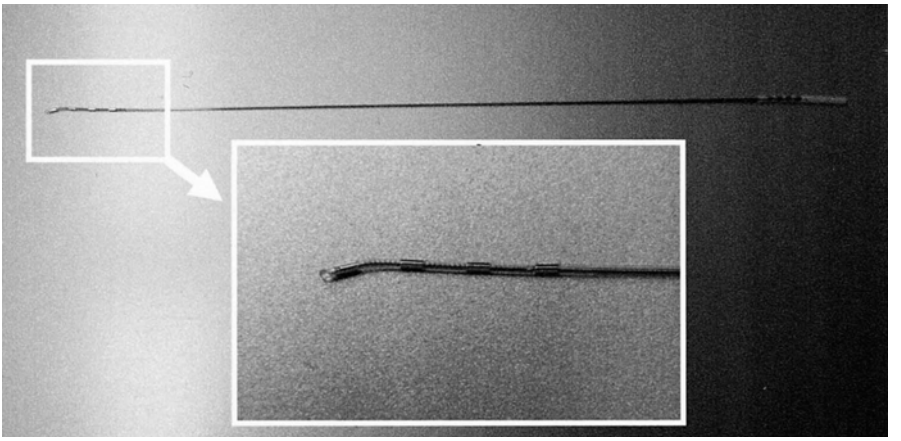

FIG. 2.3. Recordings were obtained using the catheter-type electrode. This electrode has four platinum iridium recording cylinders, separated by 6 mm of insulated length. Each cylinder is 3 mm in length and 1.27 mm in diameter

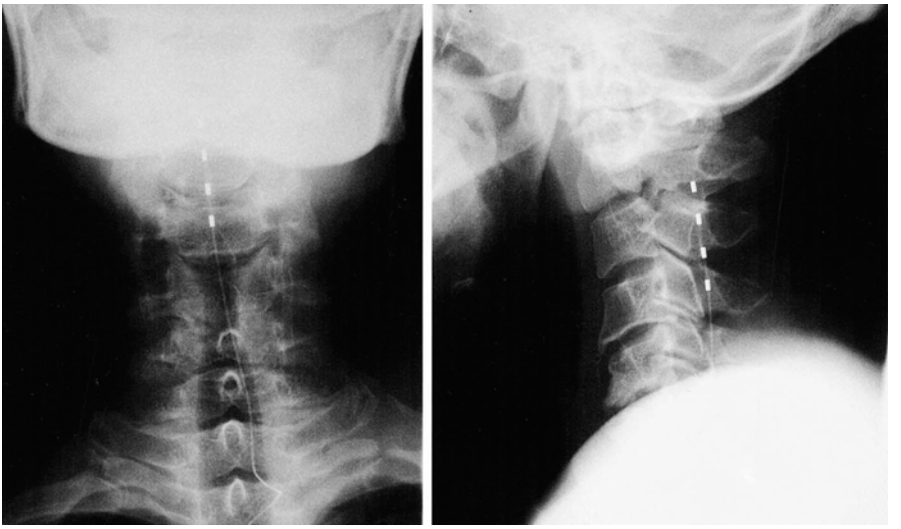

FIG. 2.4. The electrode was inserted through the epidural needle and advanced to the appropriate position. The tip of the electrode was usually placed on the C2 or C3 segment. The epidural needle was then removed and the electrode was fixed with adhesive tape to the skin

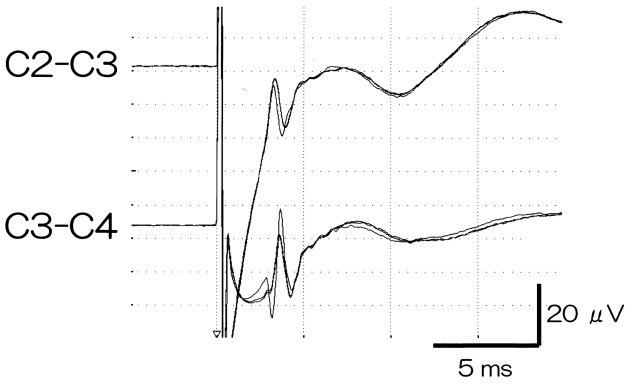

Fig. 2.5. Normal responses from the epidural space of the spinal cord with transcranial electrical stimulation

and caudal to the tumor). Differential recordings were obtained between two recording surfaces on each catheter-type electrode. After initial positioning of the catheter-type electrode, high impedance, or the presence of an unacceptable stimulus artifact indicated poor electrical contact of the recording surfaces, and repositioning of the electrode was necessary.

Recording from the catheter-type electrode rostral to the tumor served as a control measurement of the approaching signal. Recordings caudal to the lesion allowed monitoring of the functional integrity of the tract traversing the tumor site. In the case of high cervical spinal cord pathology, a lack of space sometimes precluded placement of a rostral control electrode.

All recordings and impedance measurements were obtained using the signal processor Neuropack 2200 (MEB-2208; Nihon Kohden, Tokyo, Japan). Data were recorded in 20–40-ms epochs with filter settings of 10 Hz to 2 kHz (Fig. 2.5).

2.1.4.2 From Muscle: TCE-Evoked Electromyogram (EMG)

Transcranial electrically evoked muscle potentials were usually obtained from an intramuscular needle or surface electrode pairs recording both abductor pollicis brevis (APB) and tibialis anterior (TA) muscles. Recordings were sometimes also obtained from both first dorsal interosseous and abductor hallucis muscle. Multichannel evoked EMG was typically performed with a pair of stainless steel needle-type electrodes placed subcutaneously, approximately 2–4 cm apart, positioned over the target muscle.

Evoked EMG monitoring from APB with TES was always performed, regardless of the site of a spinal lesion. For surgical procedures in the spinal cord inferior to the T1 level, monitoring of the evoked EMG from APB was used to confirm proper stimulating condition and anesthesia compatibility. An additional factor that helped determine which muscles were monitored was if nerve roots might be at risk for mechanical irritation by the surgical procedure. Filtering of EMG signals was

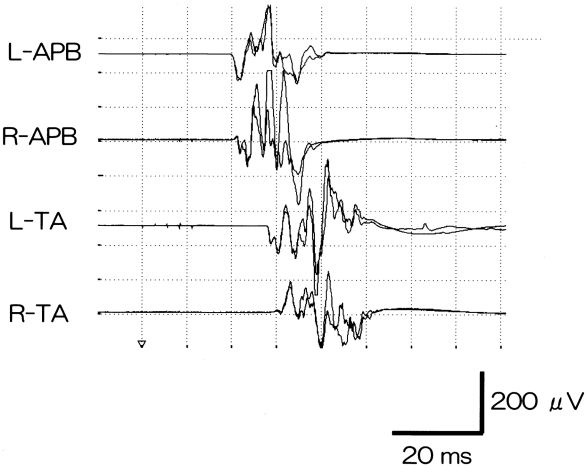

FIG. 2.6. Normal responses from muscles with transcranial electrical stimulation. *L*, left; *R*, right; *APB*, abductor pollicis brevis; *TA*, tibialis anterior

typically 20 Hz to 1.5 kHz, and gain was adjusted from 50 to 1000 μV/division (Fig. 2.6).

2.1.5 Discussion

TES-MEP (motor evoked potentials) monitoring has been becoming popular as intraoperative monitoring for the last several years, aiming at avoiding postoperative motor deficits. In particular, repetitive TES is a rather effective method to activate motor pathways and record stable response from muscles. Also, potentials recorded from the spinal epidural space after TES are used to predict impairment of motor pathway. However, parts still exist in its origin and conducting pathways that remain unclear.

On the other hand, in experimental animals and humans it has repeatedly been demonstrated that a corticospinal direct (D) response after direct stimulation of the motor cortex can be recorded from the spinal cord or the spinal epidural space (Katayama et al., 1988; Patton and Amassian, 1954; Yamamoto et al., 1990). It was confirmed that the corticospinal D response is recorded only when the motor cortex is stimulated. Thus, recordings of the corticospinal D response during intracranial surgery in humans would be of value for reducing neurological complications resulting from unnecessary damage to the CST (Katayama et al., 1988a,b; Tsubokawa et al., 1987; Yamamoto et al., 2004).

Several characteristics of human motor evoked potentials with direct stimulation are consistent with the idea that TES in humans can activate the motor cortex selectively, and produce spinal, as well as muscle, responses corresponding to the D response observed in classic animal experiments. However, it has become increasingly clear that such stimulation procedures may activate multiple neural pathways, and that they can produce responses that resemble but are totally different from the D

response. We previously demonstrated that TES with current delivery across the skull overlying the motor cortex caused noncorticospinal tract-mediated spinal cord responses (Yamamoto et al., 1990, 1991). These responses were characterized by the following: (1) the conduction velocity of the initial wave of the responses to TES was much faster than the conduction velocity of the initial wave of the response to direct motor cortex stimulation; (2) there was a lower threshold at more caudal points of stimulation; (3) the initial wave caused by TES was eliminated by ablation of the cerebellum and ablation with lesions within the ventromedial part of the spinal cord in animal experiments using cats; (4) the initial wave of the response to TES remained after ablation of the primary motor cortex and intercollicullar transaction, in animal experiments. These findings suggested that the generators of these responses include pathways originating in the brainstem or cerebellum and running through the ventromedial part of the spinal cord. The possibility that the D wave generally is difficult to produce selectively by TES is high.

Therefore, when spinal cord responses are recorded with TES, we cannot establish precisely which of the cortical, subcortical, brainstem, or even spinal cord structures are being activated to generate the recorded signals. Rothwell et al. (1994) mentioned that TES at high intensities can access the CST at the pyramidal decussation; and, at threshold intensities used to stimulate the scalp of the conscious human, TES can activate the CST neurons at or near the cell body in the primary motor cortex. However, it is very difficult to regulate the stimulation parameters at such a threshold intensity level during an entire operative course. For the reasons described above, signals from the spinal cord with TES are not always reliable practically as a monitoring procedure for the CST during surgery. As such, this technique is not an appropriate predictor of postoperative motor deficit. It can be recommended that, when transcranial stimulation is used for intraoperative neurophysiological monitoring during spinal cord surgery, recording should be performed from muscles in the extremities. Therefore, we advocate that muscle recording with TES is an appropriate monitoring measure during spinal cord surgery. In addition, it is not suitable for monitoring during intracranial and cervicomedullary surgery even though recordings are obtained from muscles.

2.2 TCE-Evoked SCPs in Animals and Human

Yoichi Katayama and Takamitsu Yamamoto

2.2.1 Introduction

Motor evoked spinal cord potentials occurring in response to direct stimulation of the motor cortex (motor-evoked SCPs), which have been employed for the intraoperative monitoring of motor functions in intracranial lesions in humans (Katayama et al., 1988; Tsubokawa et al., 1995; Yamamoto et al., 2004), can be an indicator of the function of the descending tracts within the spinal cord. While recordings of motor-evoked SCPs involve invasive procedures for the stimulation, it has been claimed that motor-evoked SCPs can be recorded by transcranial brain stimulation through the intact skull in humans (Levy et al., 1984a; Morota et al., 1997) as well as cats (Levy et

al., 1984b). This transcranial electrically evoked spinal cord potential TCE-evoked SCP appears to be a potentially useful indicator of the descending tracts within the spinal cord; however, the problems arising from the current spread caused by high-voltage electrical stimulation have not yet been resolved.

2.2.2 Experimental Studies

Thirty cats were initially anesthetized with ketamine (10 mg/kg). Anesthesia was subsequently maintained by periodic administration of various doses of Nembutal (5–40 mg/kg, i.v.). The electroencephalographic pattern recorded from stainless steel screws implanted in the skull was used to assure that each cat was adequately anesthetized throughout the recording session. A laminectomy that exposed the dorsal surface of the dura of the cervical (C2–3) and thoracic spinal (Th12) segments was performed in order to insert the epidural recording electrode. In 15 animals, a craniotomy that exposed the dura overlying the right frontoparietal cortices was carried out. The animals were paralyzed and artificially ventilated during the recording session.

SCPs evoked by direct and transcranial electrical stimulations of the motor cortex were recorded with a flexible wire electrode inserted at varying lengths into the dorsal epidural space from the exposed edge of the laminectomized area. For the recording of motor-evoked SCPs, the motor cortex (anterior sigmoid gyrus) and other cortical areas were stimulated throughout the exposed overlying dura with bipolar silver ball electrodes (interpolar distance, 2.5 mm) by means of a monophasic square pulse of 0.2 ms duration delivered at frequencies of 2 Hz except where otherwise stated. For the recording of TCE-evoked SCPs, stimulation was applied with stainless steel needles inserted into various areas of the scalp overlying the intact skull. The skull was not penetrated by the needles. Alternating square pulses were applied to a pair of needles inserted into symmetrical areas of the scalp (interpolar distance, 20 mm). Pulses of 0.5 ms were delivered at frequencies of 2 Hz. The intensity of stimulation was adjusted to the supramaximal levels for the investigated potentials. Signals from each of the recording electrodes were fed into an amplifier with a bandpass of 0.5 Hz to 6 KHz and led into a signal averaging processor.

SCPs by direct motor cortex electrical stimulation (anterior sigmoid gyrus) recorded at the dorsal aspect of the midline of the C2–C3 segments revealed an initial negative wave (N1) followed by polyphasic waves. N1 was often preceded by a positive wave (P1), which overlapped with N1. While P1 and N1 were resistant to pentobarbital sodium, the following polyphasic waves disappeared in deep pentobarbital sodium anesthesia (Fig. 2.7a). The threshold for N1 was as low as 480 μA in the anterior sigmoid gyrus. While identical responses were evoked by stimulation applied to the posterior sigmoid gyrus and orbital cortex with a stronger intensity, stimulation of other cortical areas was not capable of evoking responses with a latency as short as that of N1 recorded with motor cortex stimulation (Fig. 2.7b). N1 followed repetitive stimulations of more than 500 Hz (Fig. 2.7c). Although, as the recording electrodes were moved caudally, P1 and N1 became decreased in amplitude and prolonged in latency progressively, P1 and N1 were clearly traced down to T10 (Fig. 2.8). The conduction velocity calculated from differences in latency between several recording sites was 50–60 m/s for N1 (Fig. 2.9a). P1 and N1, and the following polyphasic waves, were all abolished by intercollicular transection (Fig. 2.9b).

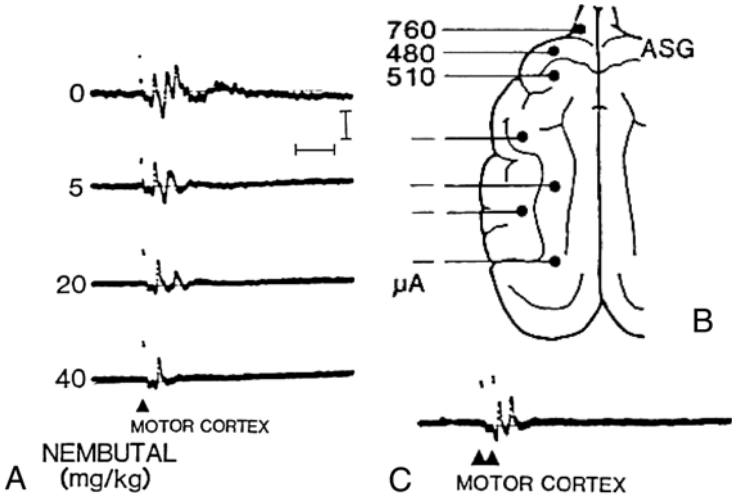

Fig. 2.7A–C. Representative examples of motor-evoked spinal cord potentials (motor-evoked SCPs) occurring in response to direct stimulation of the motor cortex. **A** Effects of administration of progressive doses of pentobarbital sodium (i.v.). **B** Threshold of motor-evoked SCPs for stimulation of various cortical areas. The threshold was lowest in the motor cortex, i.e., anterior sigmoid gyrus (*ASG*). **C** Motor-evoked SCPs in response to double pulse stimulation of the ASG at 667 Hz recorded in the preparation shown in **A** with administration of 40 mg/kg pentobarbital sodium. Calibrations: time scale, 5 ms; amplitude, 5 μV

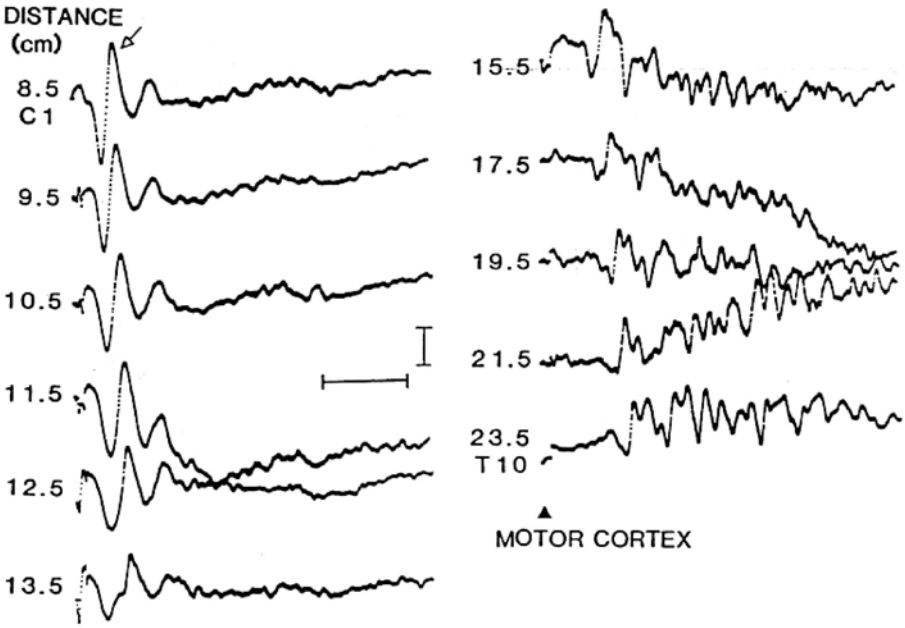

Fig. 2.8. Motor-evoked SCPs recorded at various levels of the spinal cord between C1 and T10. The distances between the stimulation and recording electrodes are shown on the left. N1 of motor-evoked SCPs is indicated by the *arrow*. Calibrations: time scale, 5 ms; amplitude, 2 μV for distances ranging from 8.5 to 13.5 cm and 1 μV for distances ranging from 15.5 to 23.5 cm

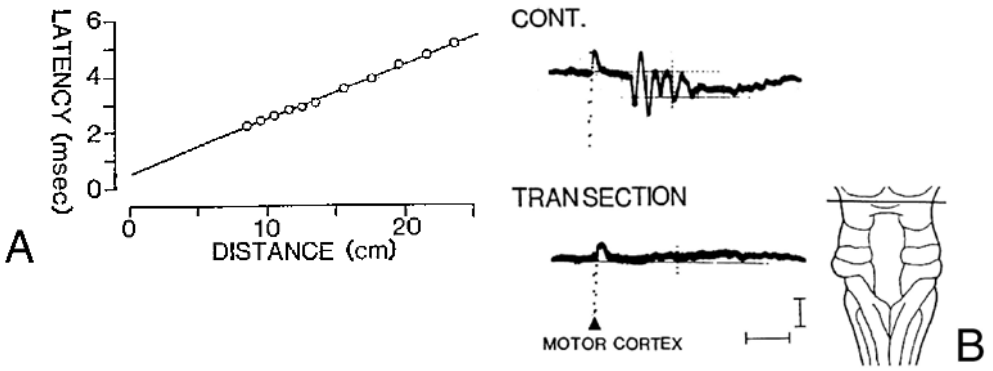

FIG. 2.9. **A** Regression line between the peak latency of N1 of SCP by direct motor cortex stimulation and the stimulation-recording distance. The conduction velocity as indicated by the regression coefficient was 55.4 m/s. **B** Effects of intercollicular transection on SCP by direct motor cortex stimulation. Calibrations: time scale, 5 ms; amplitude, 2 μV

TCE-evoked SCP recorded at the C2–C3 segments contained large shock artifacts. For this reason, recordings of the TCE-evoked SCP at the C2–C3 segments were abandoned. TCE-evoked SCP recorded from the dorsal aspect of the T9–T10 segments consisted of an initial negative wave (N1) followed by two other negative waves (N2 and N3) (Fig. 2.10a). N1 was often preceded by a positive deflection (P1), which covaried with N1.

N1 was evoked by stimulation with a pair of needles placed upon the skin overlying the caudal edge of the skull with a lowest threshold of 7 mA. As the stimulation site was moved onto a more rostral or caudal region, the threshold increased. The latency of N1 was not changed by moving the stimulation sites from the anterior to the posterior scalp areas. In the region of the scalp overlying the motor cortex, the threshold was as high as 30 mA (Fig. 2.10b). N1 but not N2 and N3 followed repetitive stimulations of more than 500 Hz (Fig. 2.10c). The direct- and TCE-evoked SCPs at different thoracic levels were recorded in several preparations. Although N1, N2, or N3 of the TCE-evoked SCP became prolonged in latency as the recording site was moved caudally, none of N1, N2 or N3 of the TCE-evoked SCP covaried in latency and amplitude with N1 of the SCP by direct motor cortex stimulation (Fig. 2.11). The conduction velocity calculated from recordings at several different thoracic segments was 65–80 m/s for N1 (Fig. 2.12a). We found that intercollicular as well as bulbar transection at various levels did not abolish the N1 evoked by stimulation of the region of the scalp overlying the motor cortex. In fact, the amplitude of N1 was even enhanced after brain stem transection. When the transection level was moved down to the C2 segment, N1 disappeared. In contrast, N2 and N3 were abolished following intercollicular transection (Fig. 2.12b).

2.2.3 Comparison Between Direct- and TCE-evoked SCPs

It has been reported by Levy et al. (1984a,b) that a transcranial current applied between electrodes placed at the skull overlying the motor cortex and the hard palate in cats can activate the motor cortex and evoke spinal cord responses identical to the pyramidal D response. However, they did not provide direct evidence that the motor cortex was

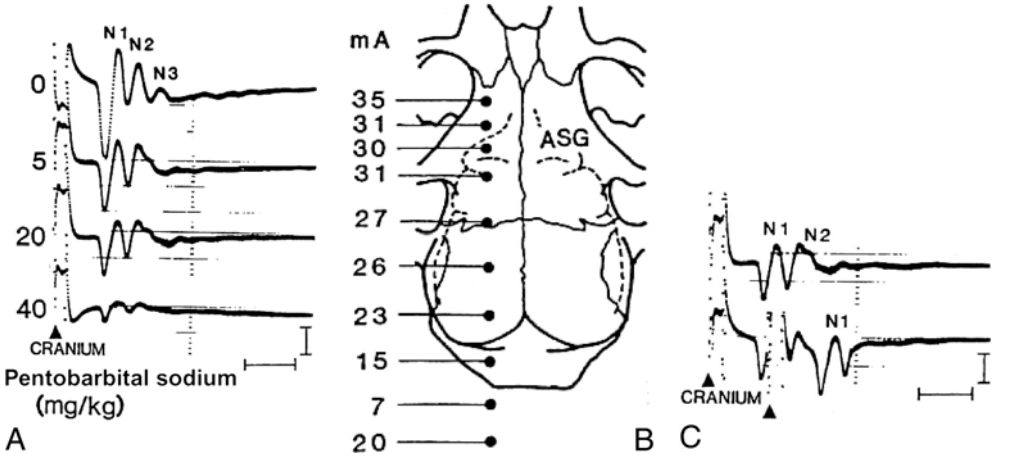

Fig. 2.10A–C. Representative examples of transcranial electrically evoked spinal cord potentials (TCE-evoked SCPs). **A** Effects of administration of progressive doses of pentobarbital sodium (i.v.). Three negative waves (N1, N2, and N3) were all influenced by pentobarbital sodium. **B** Thresholds of TCE-evoked SCPs for stimulation of various scalp areas. Stimuli were applied to a pair of needles placed symmetrically. Only stimulation sites on the left side are illustrated. The threshold was not lowest in the scalp areas overlying the motor cortex, i.e., anterior sigmoid gyrus (*ASG*). **C** Effects of double pulse stimulation of the scalp. *Upper trace*, control; *lower trace*, double pulse stimulation at 450 Hz. Calibrations; time scale, 2 ms; amplitude, 1 μV

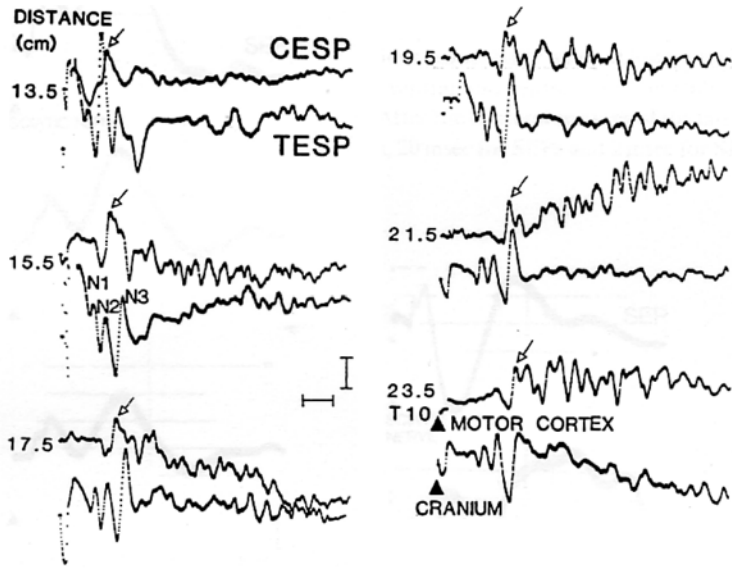

Fig. 2.11. Motor-evoked SCPs and TCE-evoked SCP recorded at various levels of the thoracic spinal cord. The distances between the stimulation and recording electrodes are shown on the *left*. *Upper traces*, motor-evoked SCPs; *lower traces*, TCE-evoked SCPs. N1 of each trace of motor-evoked SCPs is indicated by an *arrow*. None of N1, N2, and N3 of TCE-evoked SCPs covaried with N1 of motor-evoked SCPs in their latency or amplitude. Calibrations; time scale, 2 ms; amplitude, 2 μV for the distance of 13.5 cm and 1 μV for the remaining traces

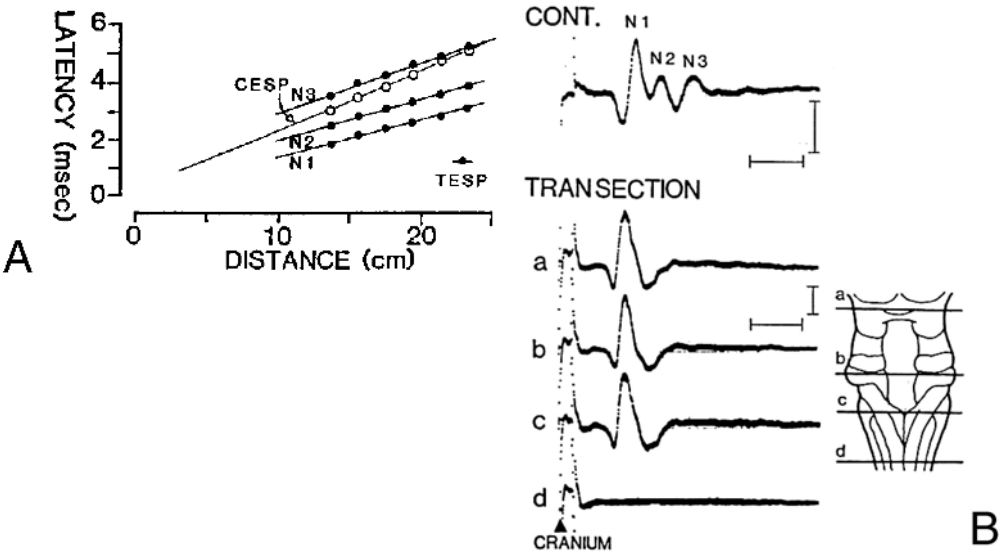

FIG. 2.12. **A** Regression lines between the peak latencies of N1, N2, and N3 of TCE-evoked SCP (*TESP*), and the stimulation-recording distances. None of the regression lines for N1, N2, or N3 matched the regression line for motor-evoked SCPs (*CESP*) obtained in the same preparation. **B** Effects of transection at various levels of the brainstem and the spinal cord on TCE-evoked SCP. N2 and N3 disappeared after intercollicular transection (indicated by *a*). N1 disappeared only after transection at the rostral cervical spinal cord (indicated by *d*)

actually stimulated by this technique. Furthermore, the site that can evoke the spinal cord response with the lowest threshold has not yet been systematically explored. Our research has provided several lines of evidence to indicate that TCE-evoked SCP were not evoked by activation of the motor cortex (Katayama et al., 1986).

First, the site which evoked TCE-evoked SCP with the lowest threshold was demonstrated to be located within the posterior scalp areas rather than within the areas overlying the motor cortex. This finding suggested that TCE-evoked SCP might not be attributable to activation of the motor cortex. The latency of TCE-evoked SCP was not changed by moving the stimulation sites from the anterior to the posterior scalp areas. Thus, the TCE-evoked SCP recorded by stimulation of the anterior scalp areas and those recorded by stimulation of the posterior scalp areas may be responses evoked by activation of the same neural structures. Second, TCE-evoked SCP were demonstrated to be recorded even after brain stem transection at the medulla oblongata. TCE-evoked SCP disappeared only after transection at the rostral cervical segment. This observation indicates that TCE-evoked SCP are evoked by activation of neural structures located within the vicinity of the cervicomedullary junction. Third, TCE-evoked SCP exhibited physiological characteristics inconsistent with the idea that TCE-evoked SCP were mediated via the pyramidal tracts. The conduction velocity calculated for N1 of TCE-evoked SCP was 65–80 m/s. This value is in agreement with the conduction velocity previously reported for spinal cord potentials evoked by transcranial stimulation, but is at variance with the conduction velocity for the pyramidal tract mentioned above.

In other animal experiments and clinical applications, much research has supported the notion that TCE-evoked SCP may activate corticospinal fibers deep within the brain (Burke et al., 1990; Edgley et al., 1990; Hess et al., 1986; Rothwell et al., 1994). In the anesthetized monkey, Edgley et al. (1990) made direct recordings from the pyramidal tract, and reported that TCE-evoked SCP can activate fibers at the pyramidal decussation. We also emphasize that motor-evoked SCPs and TCE-evoked SCP display a number of differences in their physiological properties.

2.3 TCE-Evoked Potentials from Muscle and TCE-Evoked SCPs

Takamitsu Yamamoto and Yoichi Katayama

2.3.1 Introduction

It has been demonstrated that motor evoked potentials elicited by direct stimulation of the motor cortex can be recorded from the spinal epidural space (Katayama et al., 1988; Yamamoto et al., 1991) or appropriate muscles (Cedzich et al., 1996; Kombos et al., 2001; Taniguchi et al., 1996), and noninvasive transcranial electrical stimulation of the human brain to evoke motor responses is now widely used in clinical practice (Deletis et al., 2001; Morota et al., 1997). However, it has also been reported that transcranial electrical stimulation of the motor cortex at high intensities can access corticospinal neurons at the pyramidal decussation, and that corticospinal neurons can be activated at or near the cerebral cortex with a threshold level stimulation intensity (Rothwell et al., 1984). We clinically recorded motor evoked spinal cord potentials in response to direct stimulation of the motor cortex from a spinal epidural electrode (motor-evoked SCPs), and compared them with transcranially evoked spinal cord potentials recorded from the spinal epidural space (TCE-evoked SCP). Furthermore, the clinical features of compound muscle action potentials (Cedzich et al., 1996; Deletis et al., 2001; Kombos et al., 2001; Taniguchi et al., 1996) in response to direct motor cortex or transcranial stimulation were investigated.

2.3.2 Methods

For the recording of TCE-evoked SCP and CMAP-T, transcranial electrical stimulation was performed with a Digitimer D185 stimulator (Digitimer, UK), and a "corkscrew type" stimulating electrode was placed over the cranium at C3/C4 (10–20 International EEG System). Single stimuli of 200–960 V, duration 50–100 μs, separated by a minimum of 3 s, were employed. For the recording of motor-evoked SCPs, a flexible four-channel, platinum wire electrode (Quad; Medtronic) was inserted into the epidural space of the cervical vertebrae. The motor cortex was directly stimulated with a multicontact plate electrode (Unique Medical, Komae, Japan). This device has four contact points consisting of plate electrodes of 5 mm in diameter and spaced 5 mm apart. The stimuli were applied as monophasic square wave pulses of 0.2–0.5 ms duration delivered at 2 Hz. Signals from the electrodes were fed into an amplifier, with a bandpass range of 5 Hz to 5 kHz for TCE-evoked SCP and motor-evoked SCPs, and averaged for 16 sweeps using Synax 2100 (NEC, Tokyo, Japan). For the recording of

direct- and TCE-evoked electromyogram, five pulses at a frequency of 500 Hz and a pulse duration of 0.05 ms were employed and recorded with a bandpass range of 10 Hz to 2 kHz. The study was approved by the Committee for Clinical Trials and Research in Humans of our university and by the Japanese Ministry of Health and Welfare as part of an advanced medical care program.

2.3.3 Results

2.3.3.1 Comparison Between Direct- and TCE-evoked SCPs

Direct- and TCE-evoked SCPs were recorded in the same subjects and employing the same electrodes which were inserted into the cervical epidural space. TCE-evoked SCPs was recorded before the craniotomy, and SCPs by direct electrical stimulation of the motor cortex was recorded after the craniotomy. These recordings were carried out under general anesthesia and with muscle relaxant. There were many points of difference between direct- and TCE-evoked SCPs, as follows: (1) SCPs by direct electrical stimulation of the motor cortex can be evoked with a lower stimulation intensity compared to TCE-evoked SCPs; (2) the first negative potential (N1) evoked by a high stimulation intensity, which corresponded to about 50 mA for SCPs by direct electrical stimulation of the motor cortex and 960 V for TCE-evoked SCPs, was 10 μV in SCPs by direct electrical stimulation of the motor cortex and 50 μV in TCE-evoked SCPs; (3) the latency of the peak of N1 was faster in TCE-evoked SCPs than in SCPs by direct electrical stimulation of the motor cortex, and (4) the conduction velocity of TCE-evoked SCPs was faster than that of SCPs by direct electrical stimulation of the motor cortex (Fig. 2.13).

Regression lines between the peak latency of N1 and recording distances from the C2 vertebra indicated that SCPs by direct electrical stimulation of the motor cortex has its origin at 145 mm rostral to the C2 level and TCE-evoked SCPs at 50 mm rostral to the C2 level (Fig. 2.14).

2.3.3.2 Stimulation Intensity and TCE-evoked SCPs

The threshold of TCE-evoked SCPs was from 240 to 480 V. The amplitude of N1 increased with increasing stimulation intensity; however, no new N1 wave appeared at a short latency. Only late components with a low amplitude appeared following N1 with a stimulation intensity of over 720 V (Fig. 2.15).

2.3.3.3 Features of TCE-evoked Electromyogram

TCE-evoked electromyogram were recorded under continuous infusion of propofol and alfentanil without muscle relaxant. Nitrous oxide and inhalational anesthetics were not used during the TCE-evoked electromyogram recording. For the recording, a pair of subdermal needle electrodes was used. TCE-evoked electromyogram from the bilateral thenar and anterior tibial muscles were elicited with a short train of electrical stimuli applied either transcranially or by stimulation of the exposed motor cortex. For transcranial stimulation, C3 was selected for anode stimulation and C4 for cathode stimulation. With increasing stimulation intensity, the TCE-evoked electromyogram of the thenar on the side contralateral side to the transcranial anode stimulation was recorded first. Second, the TCE-evoked electromyogram of the anterior tibial muscle on the side contralateral to the transcranial anode stimulation was recorded. Third, the TCE-evoked electromyogram of the thenar ipsilateral to the

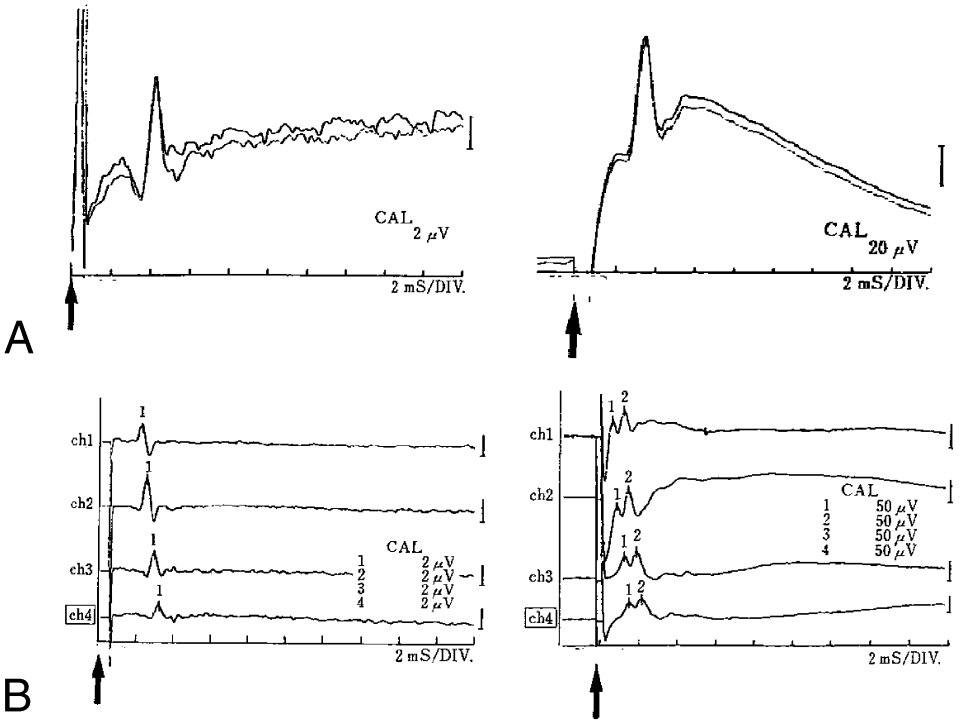

FIG. 2.13. Spinal cord potentials (SCPs) occurring in response to direct stimulation of the motor cortex and recorded from a spinal epidural electrode (*left*) and transcranially evoked spinal cord potentials recorded from the spinal epidural space (TCE-evoked SCPs) (*right*) recorded in the same subjects and using the same electrodes that were inserted into the cervical epidural space. The amplitude of the first negative potential (N1) evoked by a high stimulation intensity, which corresponded to about 50 mA (duration, 0.2 ms) for SCPs by direct electric stimulation of the motor cortex and 960 V (duration, 0.1 ms) for TCE-evoked SCPs. The amplitude of TCE-evoked SCPs was much larger than that of SCPs by direct electric stimulation of the motor cortex. Calibrations: time scales, 2 ms/division; amplitude, 2 μV (left) and 20 μV (right). **B** SCPs by direct electric stimulation of the motor cortex (*left*) and TCE-evoked SCPs (*right*) recorded in the same subjects and using the same four-channel wire electrode placed within the cervical epidural space. This wire electrode has four contact points measuring 1.5 mm in length and spaced 1.5 mm apart. Ch 1 is recorded from the most rostral contact point, and Ch 4 is recorded from the most caudal point. The latency of the peak of N1 was faster in TCE-evoked SCPs than in SCPs by direct electric stimulation of the motor cortex. The conduction velocity was 75 m/s in TCE-evoked SCPs and 65 m/s in SCPs by direct electric stimulation of the motor cortex

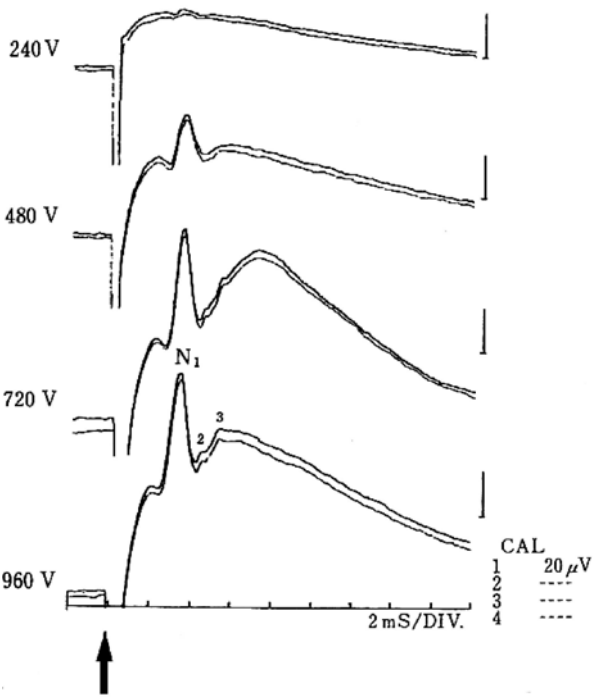

Fig. 2.14. Effect of changes of stimulation intensity on TCE-evoked SCPs. The threshold of TCE-evoked SCPs was 240 V, and the amplitude of N1 increased with increasing stimulation intensity. Late components with a low amplitude appeared following N1 with a stimulation intensity of over 720 V

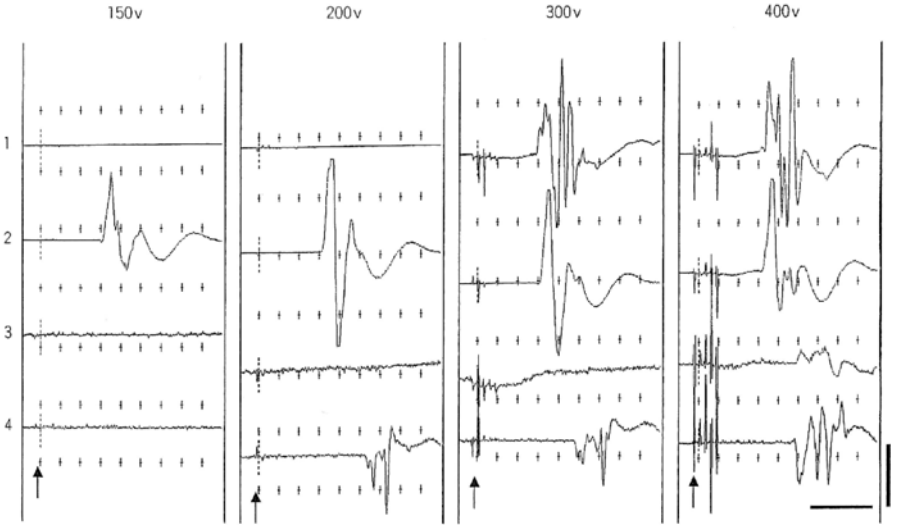

Fig. 2.15. Transcranial compound muscle action potentials (TCE-evoked electromyogram) when placing the stimulating electrodes at C3 (anode) and C4 (cathode). With increasing stimulation intensity, the TCE-evoked electromyogram of the right thenar was recorded first. Second, the TCE-evoked electromyogram of the right anterior tibial muscle was recorded. Third, the TCE-evoked electromyogram of the left thenar was recorded, and finally the TCE-evoked electromyogram of the left anterior tibial muscle was recorded

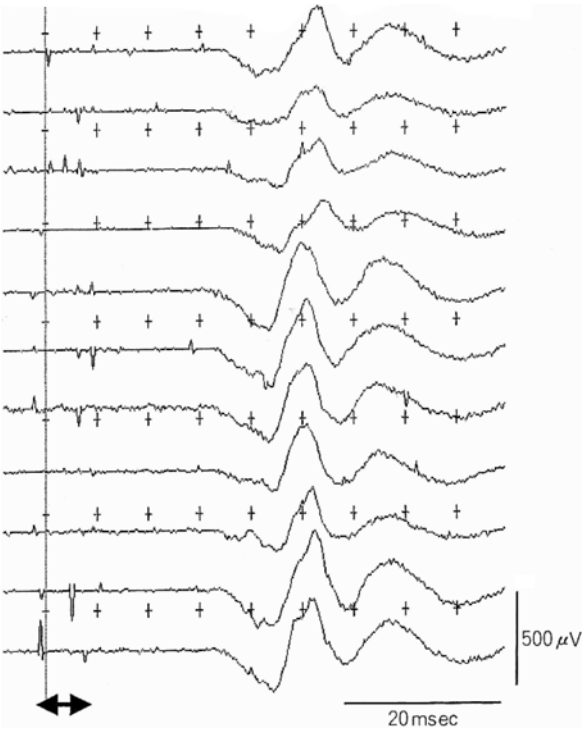

Fig. 2.16. CMAP-T when placing the stimulating electrodes at C3 (anode) and C4 (cathode) with 5 train stimulation at 400 V. Averaging is not necessary. However, the amplitude and the latency are slightly different at each recording

transcranial stimulation was recorded, and finally the TCE-evoked electromyogram of the ipsilateral anterior tibial muscle was recorded (Fig. 2.16).

In contrast to direct- and TCE-evoked SCPs, summation and averaging are not necessary for TCE-evoked electromyogram. However, the amplitude and the latency are slightly different at each recording. It is necessary therefore to check several continuous recordings for clinical use.

2.3.4 Discussion

SCPs by direct electric stimulation of the motor cortex consists of an initial D wave and a later sequence of volleys termed I-waves (Amassian et al., 1987; Patton and Amassian, 1954). The D wave reflects impulses arising from direct activation of the axons of corticospinal tract (CST) neurons, whereas the I waves reflect impulses arising from indirect activation of the CST neurons via synaptic activity, and the D wave is recorded only when the primary motor cortex is stimulated (Amassian et al., 1987; Katayama et al., 1988; Patton and Amassian, 1954; Yamamoto et al., 1991). The mean conduction velocity of the D wave was 62.1 ± 3.5 m/s. We have reported that a 30%–40% decrease in the D-wave amplitude is critical for causing persistent motor disturbance which can be detected by the Muscle Maneuver Test (MMT), and that less than a 30% decrease may indicate postoperative preservation of motor function

including transient motor disturbance with subsequent complete recovery as evaluated by the MMT (Yamamoto et al., 1991). We found many points at difference between direct- and TCE-evoked SCPs, and concluded that the first negative wave (N1) of TCE-evoked SCP is evoked by stimulation of the brainstem. In animal experiments, Edgley et al. (1990) have demonstrated that transcranial electrical stimulation over the motor cortex can activate fibers deep within the cranium, at the pyramidal decussation. In the clinical setting, Rothwell et al. (1994) used different placements of the stimulating electrode, and located the anode electrode at the vertex and the cathode on one side, 7 cm lateral to the vertex. They reported that transcranial electrical stimulation of the motor cortex at high intensities can access corticospinal neurons at the pyramidal decussation, and that stimulation of the brainstem and the spinal cord preferentially accesses corticospinal axons. They also noted that a threshold level stimulation intensity has the possibility of activating corticospinal neurons at or near the cerebral cortex; however, the threshold level stimulation intensity yields an unreliable response and is not suitable for intraoperative monitoring. Despite the fact that the origin of TCE-evoked SCP differs from that of SCPs by direct electric stimulation of the motor cortex, the importance of monitoring TCE-evoked SCP during spinal cord operation has been emphasized (Deletis et al., 2001), and it has been reported that a decline of more than 50% in the N1 amplitude of TCE-evoked SCP should serve as a serious warning sign (Morota et al., 1997).

Monitoring of TCE-evoked electromyogram in response to direct motor cortex stimulation or transcranial electrical stimulation is also a useful procedure. Kombos et al. (2001) monitored the TCE-evoked electromyogram occurring after direct stimulation of the motor cortex, and indicated that a spontaneous shift in latency of greater than 15% or a sudden reduction in amplitude of the potential of greater than 80% represented a warning criterion. However, the criteria for warning of irreversible motor disturbance with TCE-evoked electromyogram clearly differ in different reports (Morota et al., 1997; Pechstein et al., 1996), and disappearance of TCE-evoked electromyogram or a 50% decrease in TCE-evoked electromyogram can be regarded as a warning criterion. Care thus needs to be exercised concerning the depth of anesthesia, use of muscle relaxant, and changes in the excitability of α-motoneurons.

2.4 Effects of Intravenous and Inhalational Anesthetics

S. Denda and Koki Shimoji

2.4.1 Introduction

Somatosensory evoked potentials (SEP) from the scalp have often been used for detection of spinal cord injuries during surgery, but false-negative cases have been reported on motor functions postoperatively (Ginsburg et al., 1985; Lesser et al., 1986). Evoked spinal cord potentials (SCPs) in response to peripheral nerve or spinal cord stimulation have come into clinical use for monitoring spinal cord injury during spine, spinal cord or aortic surgeries since methods of spinal cord stimulation (Shimoji et al., 1971a) or recording SCPs from the epidural space in humans were developed (Shimoji et al., 1971b).

Since the technique of transcranial electric or magnetic stimulation of motor cortex was developed (Barker and Jalinous, 1985; Merton and Morton, 1980), this method has been tested for detection of motor tract injuries during surgeries (Boyd et al., 1986; Levy et al., 1987). It was reported that the magnetic motor evoked potential was more sensitive than electrical stimulation in the monitoring of motor function (Lee et al., 1995). Although transcranial magnetic stimulation has an advantage of painlessness even during awake state, there are also drawbacks in terms of monitoring during surgery such as difficulty of fixation of the coil at the same site for a long time and variability of its responses; effects of anesthetics on motor evoked spinal cord potentials are not well understood. Hicks et al. (1992) showed that the greatest depressant effect was on the I wave recorded from the human epidural space which is produced by higher threshold and has a longer latency, suggesting synaptic activation of corticospinal neurons in its origin.

2.4.2 Methods for Recording TCE-Evoked SCPs

Transcranial electric stimulation (TCE) was delivered to the motor area via stainless steel electroencephalographic disc electrodes with a diameter of 15 mm fixed to the scalp at the vertex and 5 cm lateral and 1 cm anterior after anesthesia was induced with ketamine (1 mg/kg, i.v.). Constant voltage stimuli at 0.5 Hz with time constant of 100 μs through a stimulator designed for TCES (Digitimer D180A; Digitimer) are usually used. Before surgery, one or two epidural catheter electrodes (Unique Medical) for recording TCE-evoked SCPs were introduced percutaneously into the posterior epidural space at the T1 to T12 levels, based on the methods of epidural block (Shimoji et al., 1971a,b). The effects of stimulus intensity were tested at 1.1–5.0 times threshold strength for the initial component (C1) (see Fig. 2.17), and effects of isoflurane were studied at the stimulus intensity of 2.0 times threshold strength for C1. End-tidal concentration of isoflurane (0.5%, 1.0%, 1.5%) was kept at least for 5 min. TCE-evoked SCPs were recorded using an averager, Neuropack IV or Neuropack (Nihon Kohden, Tokyo, Japan) with bandpass filter setting between 5 and 3 kHz, and 20 responses were summated with an analysis time of 30 ms (Denda et al., 1998).

Figure 2.17a demonstrates an example of TCE-evoked SCPs with the stimulus intensities of 1.1–5.0 times threshold strength (T) for the initial component (C1). The C1 appeared first at 10%–35% of maximal output (1200 V). The increase in the stimulus intensity was associated with the significant decrease in the onset latencies of C1 (Fig. 2.17b). Interpeak latencies between C1 and the later components (C2–C6) remained unchanged even with the increase in the stimulus intensity. Approximate conduction velocity of C1α, C1β, and C1γ calculated by the distances between the stimulating and recording electrodes at 5.0T were 100.4 ± 8.4 m/s (mean ± SD) (range, 86–111 m/s), 81.1 ± 6.7 m/s (mean ± SD) (range, 70–89 m/s), and 69.8 ± 7.3 m/s (mean ± SD) (range, 59–73 m/s), respectively. The amplitudes of C1, C2, C3, C4, C5, and C6 at 2.0T were 20.7 ± 16.0, 4.6 ± 2.5, 9.4 ± 9.4, 8.9 ± 8.8, 10.9 ± 11.0, and 6.4 ± 5.2 μV, respectively. The amplitude of C1 gradually increased from 1.1T to 2.0T and then decreased above 2.0T with waveform changes (widening with three peaks) (Fig. 2.17). The amplitudes of C2 tended to show similar changes to those of C1, although the changes were not significant. The amplitudes of C3 to C6 tended to increase with the increases in the stimulus intensity but not significantly.

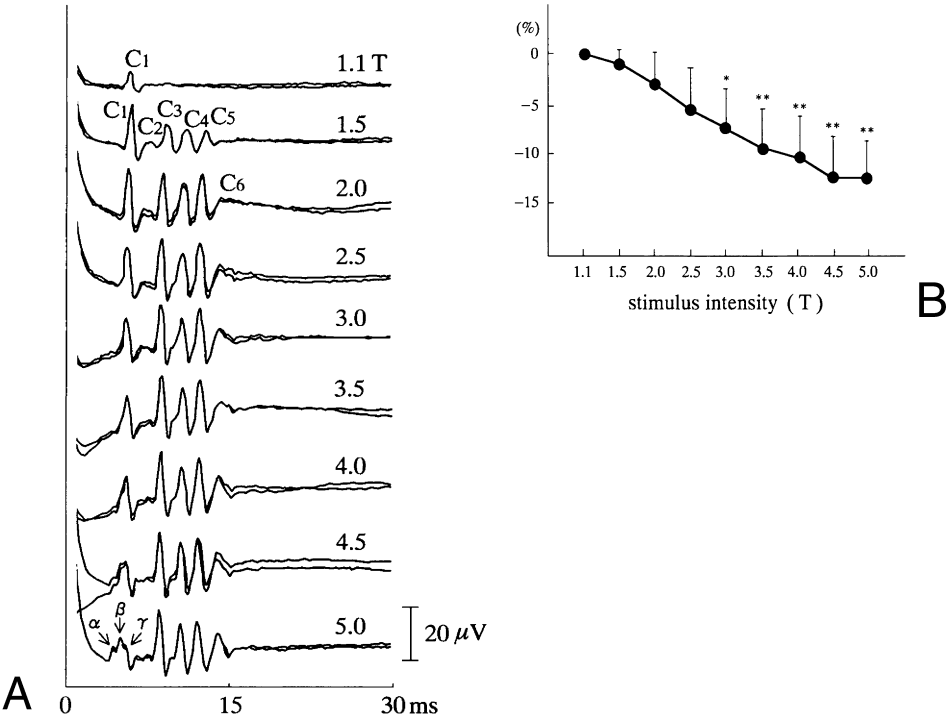

FIG. 2.17. The effect of graded stimulation on the transcranial electrically evoked spinal cord potential (TCE-evoked SCP). **A** The specimen records of spinal cord potential (SCP), recorded from the posterior epidural space at the T8 vertebral level in a patient (male, 67 years, disc herniation), in response to increasing stimulus intensities of transcranial electric stimulation (TCES) during fentanyl (4 μg/kg i.v.) and ketamine (2 mg/kg i.v.) anesthesia under complete muscle relaxation (vecuronium 0.15 mg/kg i.v.). *T* indicates the threshold stimulus intensity for C1. Each trace represents summated response ($n = 20$). Two traces are superimposed at each stimulus intensity. Note that the C1 component decreases in amplitude with widening of the duration, eventually to form the three peaks (α, β, and γ). **B** The changes (mean ± standard deviation) in the onset latency of C1 with the increase in the stimulus intensity of TCES. *Asterisks* show significant differences from the value at 1.1 times the threshold strength (*T*). Upward deflection represents positivity (*$P < 0.05$, **$P < 0.001$). (Denda et al., unpublished data)

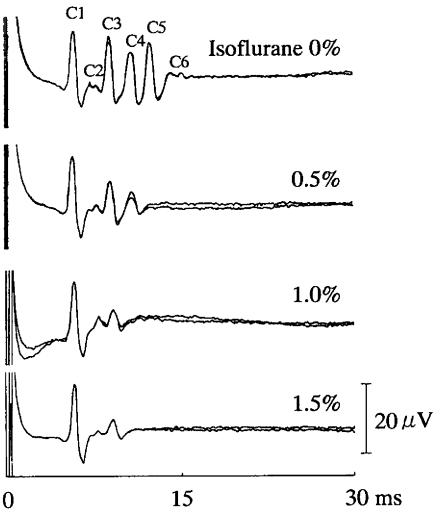

FIG. 2.18. An example of changes in the waveforms of the TCE-evoked SCPs with isoflurane at 0.5%, 1.0%, and 1.5% end-tidal concentration. Note that the C1/2 component does not significantly change in amplitude with 1.5% isoflurane, while components C3–C6 are vulnerable to the anesthetic with stronger suppression on later components. Two traces ($n = 20$) are superimposed. Deflections at the start of each trace (0) denote the stimulus artifacts. Upward deflection represented positivity. (Denda et al., unpublished data)

2.4.3 The Effects of Inhalation Anesthetics

Figure 2.18 demonstrates specimen traces of TCE-evoked SCPs during isoflurane anesthesia. The peak latencies of all components did not significantly change after isoflurane. The amplitudes of C3–C6 decreased in order of later components with increasing concentrations of the anesthetic, while the amplitudes of C1/C2 did not significantly change during isoflurane anesthesia.

Thus, the present study has demonstrated that TCE-evoked SCPs, recorded from the posterior epidural space in humans, are composed of at least six spike-like potentials. It also suggests that these are two components in the TCE-evoked SCP: the one, produced by direct activation of corticospinal neurons or axons (similar to the "D waves" recorded from the muscle) and the other, the following waves by transynaptic activation of corticospinal neurons (I waves) (Boyd et al., 1986; Levy et al., 1987). D waves of the SCP are found to be the lowest in threshold and shortest in latency, whereas I waves are higher in threshold and longer in latency (Amassian et al., 1987). By increase in the stimulus intensities applied directly on the motor cortex, the latency of the D wave decreased with its waveform to produce the three components, suggesting that these components of the D wave are subcortically generated nonsynaptic activities with three different conduction velocities (Burke et al., 1990). Two mechanisms for formation of subcomponents of the C1 can be assumed as follows. First, the motor neurons producing the C1 component are composed of three different fiber-diameter populations, of which median-sized neurons are dominant in number and closer to the cortical surface. The second, wider spread of the electrical current by intense stimulation evokes both the smaller motor neurons and larger motor neurons or fibers lying deeper in the brain to produce shorter latency spikes, which inhibit the activation of median-sized motor neurons.

The present results that the latencies and amplitudes of C1/C2 component did not significantly change even during 1.5% end-tidal concentration of the anesthetic also support the thesis that C1/C2 components are activated nonsynaptically. The later components (C3–C6) are thought to be postsynaptically activated components of corticospinal neurons, since these components are vulnerable to this inhalation anesthetic. Isoflurane is reported to cause marked attenuation of the muscle responses evoked by direct or transcranial electrical stimulation of the motor cortex in rats or humans (Calancie et al., 1991; Deletis et al., 1993; Haghighi et al., 1990; Haghighi, 1998; Kalkman et al., 1991). It was shown (Haghighi, 1998; Ubags et al., 1998) that the isoflurane at 1 MAC (1.2%) completely abolished the cortical and brainstem motor evoked electromyograms (EMGs) within minutes, while the motor evoked EMGs elicited by direct stimulation of cervical spinal roots remained unchanged in rat. This result suggests that isoflurane inhibits the neurotransmission of the cortical interneuron and the relay from first- to second-order motoneurons without significant effect on neuromuscular junctions. In regard to the TCE-evoked SCPs in humans, Hicks et al. (1992) also showed that there were only minor changes in the D wave with the administration of isoflurane but the greatest depressant effect on I waves occurred at an end-tidal concentration of 0.5% isoflurane. The present study showed that the amplitudes of C1/C2 by TCE-evoked SCPs did not significantly change, whereas those of C3–C6 became suppressed dose-dependently with the increase in isoflurane concentration. Thus, the behaviors of C1/C2 of SCPs recorded from the posterior epidural space in humans by TCES coincide with the D waves of the SCP reported by the previous investigators, while C3–C6 in the present study are similar to the behaviors of the I waves.

The tests were carried out under background anesthesia with ketamine in the present study. There should be some significant additional effects of ketamine on the actions of the inhalational anesthetic. Nevertheless, TCES could hardly be carried out in a wakeful state, since it causes pain. On the other hand, TCES produces a reproducible constant evoked potential, which seems advantageous for quantification of the values of changes in the potentials during surgical monitoring.

The effects of other inhalation anesthetics such as halothane and sevoflurane are similar to those of isoflurane (Denda et al., 1998).

Section D
Case Studies (Clinical Applications)

Chapter 1
Monitoring by SCPs During Surgical Operations

1.1 Spine Surgery: Scoliosis Surgery

Hitoshi Fujioka and Koki Shimoji

Neurological deficits after spinal cord or spine surgery pose a serious problem. There have been many attempts to monitor spinal cord function during spine or spinal cord surgery by using somatosensory evoked potentials (SEP) recorded from the scalp (Grundy and Villani, 1988; Levy et al., 1984). Unfortunately these potentials are susceptible to the effects of anesthetic agents and vary during the course of anesthesia and surgery (McPherson et al., 1985; McPherson and Ducker, 1988; Clark and Rosner, 1973; Samra et al., 1987; McPherson and Levitt, 1991).

Another method of intraoperative assessment of cord function is the "wake-up" test (Vauzelle et al., 1973). However, this provides only an assessment of motor function at a particular moment and not moment-to-moment monitoring of cord function and it may be very unpleasant for the patients.

Intraoperative monitoring of spinal cord function using spinal cord potentials (SCP) recorded with epidural catheter electrodes is thought to be reliable, as epidurally recorded ascending conducted SCP (ascending SCP) remain constant and are almost unaffected by anesthetic agents (Macon et al., 1982; Tamaki et al., 1981, 1984; Tsuyama et al., 1978). In order to prevent spinal cord damage caused by manipulation of the spinal cord or spine, we have been monitoring spinal cord function during surgery using epidural recording (Shimoji et al., 1971), which permits simple and safe recording of stable ascending SCPs.

A survey of changes in the conducted SCP is presented in order to define the critical values of changes in amplitude and latency caused by surgical manipulation of the spine during scoliosis surgery in relation to postoperative neurological sequelae (Fujioka et al., 1994; Spanish Society of Clinical Neurophysiology, 2004).

For monitoring spinal cord functions during corrective surgery for scoliosis, we have recorded the ascending SCPs percutaneously from the posterior epidural space at the C5–7 levels in response to epidural stimulation of the cauda equina in 134 patients. The ascending SCP consists of three spike-like components (C1, C2, and C3)

followed by slow components, as demonstrated in the previous section. The epidurally recorded ascending SCPs were not affected by anesthetic agents, providing that stability of anesthesia is maintained during surgery. There were no significant differential effects of spinal distractions on each of the three spike potentials. There were no postoperative neurological abnormalities in patients whose ascending SCP showed no changes, amplitude increases, or amplitude decreases of less than 50% or latency increases (>0.2 ms) during spinal manipulations (no false negatives, but some false positives) (Table 1.1). Five patients who suffered postoperative neurological damage exhibited more than 50% changes in amplitude of the ascending SCP during surgery. All these neurological sequelae occurred in the first 80 patients. In the last 54 patients, in whom the distraction forces on the spine were controlled rapidly by observation of the amplitude changes in ascending SCP (Fig. 1.1), there were no postoperative neurological abnormalities, except for one patient in whom an accidental spinal cord injury was produced by a hook. The results suggest that the traction force on the spine must be reduced immediately when the amplitudes of the ascending SCP decrease by more than 50% of control values with or without latency increases. The results also indicate that the surgical traction compresses the spinal vessels leading to spinal ischemia rather than mechanical damage to the spinal tissues (Fig. 1.2) (Fujioka et al., 1994), which reveals that therapeutic aids should be focused intensively on vascular support (Arai et al., 2004).

Table 1.1. Relationships between changes in the ascending SCP and postoperative neurological findings in patients with scoliosis

C1 component changes	*n*	Duration of changes in SCP			Postop. neurological findings	
		Transient (<20 min)	Prolonged (<2–4 h)	No recovery	No change	Disturbed
No change	81				81	0
Amplitude						
Increase (>10%)	13	4	0	9	13	0
Decrease (<50%)	14	11	3	0	14	0
Decrease (>50%)						
Without latency change	12	8	1	3[a]	10	2
With latency increase (>0.2 ms)	4	3	0	1	3	1
Latency increase only (>0.2 ms)	4	0	4	0	4	0
Abolishment	6	4	1[b]	1	4	2
Total	134				129	5

[a] One patient in whom displacement of the epidural electrode was noticed at the end of operation is also included.

[b] Partial recovery (Fujioka et al., 1994).

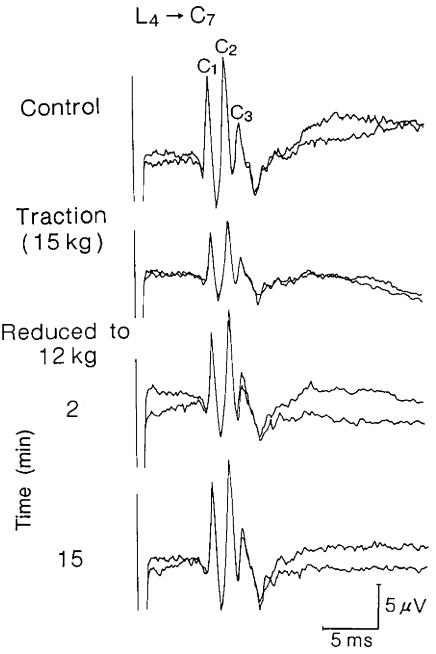

FIG. 1.1. An example of control of traction force by monitoring ascending spinal cord potentials (SCP) during spine surgery. The ascending SCP elicited by epidural stimulation of the cauda equina (*L4*) was recorded from the posterior epidural space at the cervical enlargement (*C7*) in a 26-year-old female patient with idiopathic scoliosis. The amplitude of the polyphasic spikes was reduced suddenly (amplitudes of C1, C2, C3 components decreased to 47%, 47.5%, 49% of control values, respectively) by traction of the spine with 15 kg. These changes in the ascending SCP recovered within 15 min after reduction of the traction force to 12 kg. (From Fujioka et al., 1992)

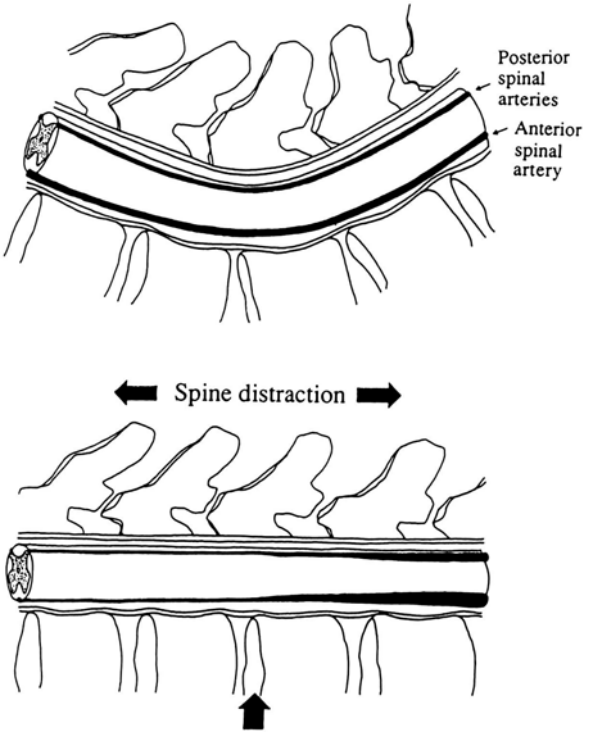

FIG. 1.2. The mechanism of spinal cord damage by surgical manipulations of spines, showing that ischemia of the spinal cord tissues caused by surgical compression on the spinal arteries rather than mechanical trauma leads to spinal cord damage. Normal blood flow is maintained in both the anterior and posterior arteries before surgical manipulations (*upper illustration*) in a patient with scoliosis. Surgical manipulation such as spine traction or compression may cause the disturbance of blood flow, leading to ischemia of the spinal cord

1.2 Spinal Cord Surgery

1.2.1 Dorsal Root Entry Zone Lesion (DREZL)

Tomohiro Yamakura and Koki Shimoji

The dorsal root entry zone lesion (DREZL), introduced by Sindou (1972) and extensively applied by Nashold et al. (1976; Nashold and Ostdahl, 1979), has been successfully carried out by many clinicians especially for control of deafferentation pain syndromes. However, the DREZL procedures sometimes cause sensory deficits as well as motor

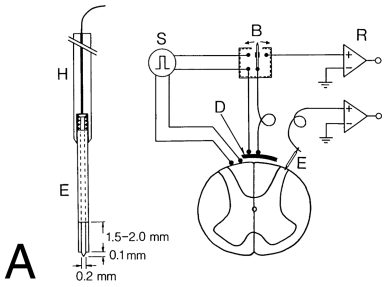

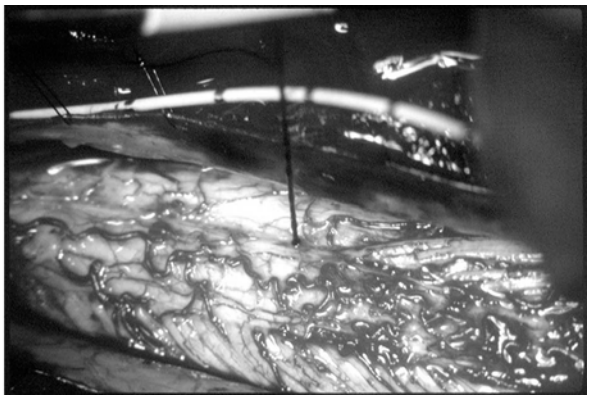

Fig. 1.3A,B. Methods of recording the somatosensory evoked SCPs during dorsal root entry zone lesion (DREZL) operation. **A** Schematic presentation of the coagulation electrode (*E*) with a holder (*H*), and arrangements for stimulation (*S*) and recording (*R*) during dorsal root entry zone lesion (DREZL) for pain relief. Stimulation was applied to the spinal cord from the epidural space by the catheter electrode and/or directly by Ag/AgCl ball-tip electrodes that were fixed to the cord surface with the floating method. Recording was made by a similar electrode as used for coagulation but with a 0.1-mm uncoated tip, inserted into the DREZ approximately 0.1 mm in depth, and with the epidural catheter electrode. A switch box (*B*) was used alternately for stimulation and recording from the epidural space. *D*, dura mater. **B** Photograph showing the coagulation electrode inserted into the DREZ for both surgical coagulation and recording the SCPs. Note that there are no dorsal rootlets in the area where the electrode is inserted, whereas normal dorsal rootlets originating from the DREZ are demonstrated in the caudal area of the ipsilateral side and all areas of the contralateral side (same patient in Fig. 1.4). (From Fujioka et al., 1992)

weakness (Ishijima et al., 1985; Jeanmonod and Sindou, 1991). Our studies on the DREZL (Ishijima et al., 1985; Kumagai et al., 1992) also indicate that although the operation yields a dramatic pain-relieving effect, there are several problems after surgery such as the decrease in its effectiveness during the follow-up, sensory deficits, and motor weakness. Recently, several measures have been tried successfully for repair of the injured spinal cord using embryonic stem cell transplantation (McDonald et al., 2004) or neural precursors (Kocsis et al., 2004) in experimental animals; we still need detailed studies for application of these techniques to the human spinal cord.

We therefore applied the monitoring of the spinal cord potentials (SCPs) during DREZLs: first, to see whether DREZLs are harmful to ortho- and antidromic conduction in the spinal cord; second, to study the influences of DREZLs on the SCPs activated by segmental, ascending, and descending volleys; and third, to compare the waveforms of SCPs recorded directly from the dorsal root entry zone (DREZ) with those recorded from the posterior epidural space which have been extensively studied for a long time in our laboratory.

The SCPs have been recorded from the DREZ and posterior epidural space in patients before, during, and after DREZL under general anesthesia (Fig. 1.3A,B). The SCPs from the DREZ activated by segmental, ascending, and descending volleys were basically the same in fundamental waveform as those recorded from the posterior

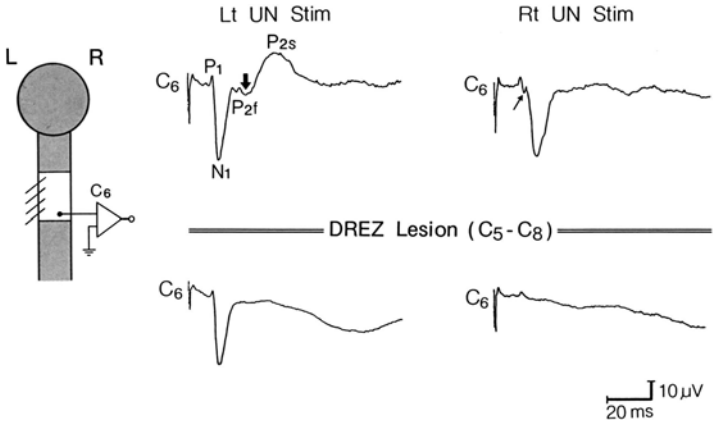

Fig. 1.4. Segmentally evoked SCP recorded from the dorsal root entry zone (*DREZ*) (C6 level) in response to left (*Lt*) (intact side) and right (*Rt*) (avulsed side) ulnar nerve (C7, C8, T1) stimulations at the wrist in a patient (74 years, male) with partial brachial plexus avulsion (C5, C6, C7) before and after DREZL, during neuroleptanesthesia. The roots C8–T1 were intact in this patient (see Fig. 1.3B). Before DREZL (*upper sweeps*), the segmental SCP consists of the P1, N1, and P2 (*P2f* and *P2s*) components responding to left ulnar nerve stimulation, while that evoked by right ulnar nerve stimulation gives clearly the P1 and N1 with delayed peak latency but hardly the P2 wave. Note the absence of the N1 and the negative-going phase of the P1 produced by right ulnar nerve stimulation, and the decrease in the amplitudes of the N1 and P2 components evoked by left ulnar nerve stimulation after DREZL (*lower traces*). Deflections at the start of each sweep represent the stimulus artifact. A *large arrow* denotes a negative dip, which separates the P2 into the first (*P2f*) and second (*P2s*) components. A *small arrow* shows the negative-going phase of the P1. Upward deflection indicates positivity in this and Fig. 1.5. Schema on the *left* illustrates the position of the recording electrode. (From Fujioka et al., 1992)

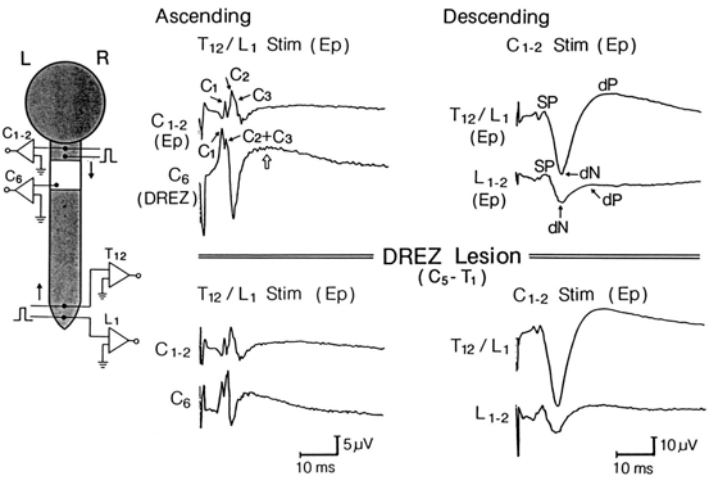

FIG. 1.5. The SCPs evoked by ascending and descending volleys along the cord before (*upper sweeps*) and after (*lower sweeps*) DREZL in a patient (47 years, female) with left complete brachial plexus avulsion. Ascending volleys were applied from the posterior epidural space at the T12 (rostral electrode) and L1 (caudal electrode) vertebral levels, while descending volleys were applied to the C1/2 level epidurally (*Ep*). Recording was also carried out with the same electrodes that were used for stimulation, as arranged in the left side of this figure during neuroleptanesthesia. Note that the slower component (*open arrow*) of the SCP evoked by ascending volleys, recorded from the DREZ, was decreased without changes in the spike-like potentials (*C1*, *C2*, *C3*) following DREZL. Note also that slow components (*dN* and *dP*) of the SCPs, recorded at the T12 vertebral level from the posterior epidural space, evoked by descending volleys at the C1/2 level from the posterior epidural space were increased in amplitude without change in the initial spike potential (*SP*) amplitude following DREZL. *Ep* and *DREZ* denote recordings from the epidural space and DREZ, respectively. *SP*, *dN*, and *dP* represent, respectively, spike potentials, slow negative, and positive potentials evoked by descending volleys. Schema on the *left* illustrates the position of the stimulating and recording electrodes. *Shaded areas* indicate the epidural space. (From Fujioka et al., 1992)

epidural space. The segmentally activated slow negative (N1) wave, reflecting synchronized activity of dorsal horn neurons, and positive (P2) wave, thought to indicate primary afferent depolarization, were affected by DREZL in all four subjects tested, even by contralateral stimulation, suggesting that these components of the segmental SCPs in humans partly reflect the activity of contralateral dorsal horn neurons (Fig. 1.4). The spike-like potentials activated by ascending volleys were not affected by DREZL, while the subsequent slow components were decreased at the lesioned level (Fig. 1.5). This may indicate that ascending spinal cord tracts are not affected by the operation, and suggests that the origin of the slow components following the three spike potentials by ascending volleys lies at least in part in the segmental dorsal horn. The slow negative and positive components, recorded at a rostral segment from DREZ, in response to the descending volleys, were augmented after DREZL, suggesting that activation of ascending or descending inhibition through a feedback loop via supraspinal structures might occur at least transiently following DREZL (Fig. 1.5). All

components of the SCPs activated by descending volleys were decreased or disappeared in recordings from the lesioned level, as expected. Thus, intraoperative recording of the SCPs during DREZL might also be beneficial for monitoring spinal cord injury, and also for studying human spinal cord function (Nashold et al., 1985; Prestor et al., 1989; Fujioka et al., 1992).

1.2.2 Spinal Cord Tumor

Chikashi Fukaya and Yoichi Katayama

1.2.2.1 Introduction

There is now evidence indicating that complete surgical excision is the best therapeutic approach for the majority of spinal cord tumors. Radical excision is always associated with the risk of inflicting a greater neurological deficit. Mechanisms of spinal cord injury during a surgical procedure include ischemia and compression, which may be detected by somatosensory evoked potential (SEP) monitoring at reversible stage. However, motor deficits can occur without an SEP change. Several kinds of motor-evoked potential (MEP) monitoring have been developed, aiming to avoid intraoperative impairment of motor function. These monitoring procedures could promote more timely motor compromise detection and intervention.

We summarize our clinical experience with monitoring of muscle-evoked potentials by transcranial electrical brain stimulation and SEP, in patients who underwent spinal cord tumor resection. These case studies provide an assessment of neurophysiological monitoring using multimodality-evoked potentials during spinal cord surgery.

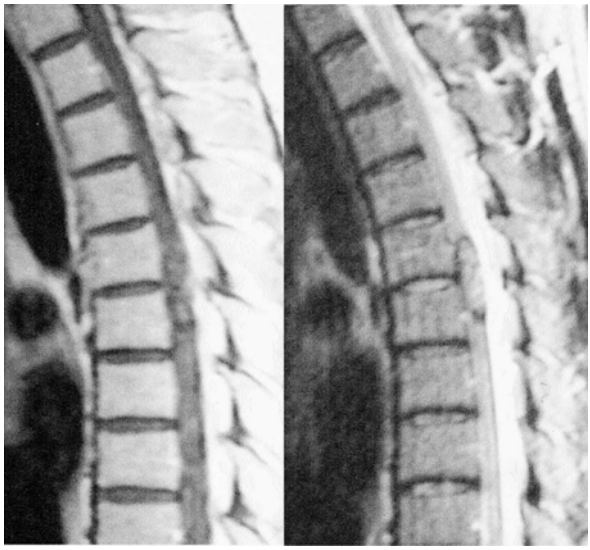

Fig. 1.6. Magnetic resonance (MR) imaging revealed expansion of a tumor in the mid-thoracic region, including the right Th 5–6 nerve root area. *Left*, T1-weighted image; *right*, T2-weighted image

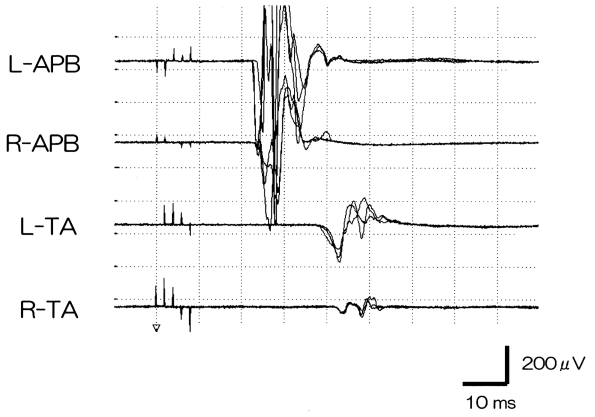

FIG. 1.7. TCE-evoked electromyogram by electrical brain stimulation monitoring was successful with total intravenous anesthesia (TIVA) from the beginning of surgery. Clear responses from the muscles evoked during soft-tissue dissection were observed. *APB*, abductor pollicis brevis; *TA*, tibialis anterior

1.2.2.2 Case 1

1.2.2.2.1 History and Presentation

A 38-year-old right-handed man complained of mild motor weakness of both legs, and nervous system examination showed diminished tactile sense and vibratory sensation; the knee and ankle reflexes were exaggerated bilaterally, and the Babinski reflex was elicited bilaterally, but was more pronounced on the right. MR imaging revealed expansion of a tumor in the mid-thoracic region, including the right Th 5–6 nerve root area (Fig. 1.6). The patient was referred to our hospital for an aggressive attempt at complete or near complete resection of the tumor.

1.2.2.2.2 Multimodality-Evoked Spinal Cord Potential Monitoring

Propofol and fentanyl were used to induce anesthesia. After endotracheal intubation, the patient was anesthetized with a constant intravenous infusion of propofol and fentanyl. Neuromuscular blockade was omitted after intubation. Infusion of propofol and fentanyl was used to maintain anesthesia. Then thoracic laminoplasty and tumor resection were performed.

Recording and stimulation used a Neuropack 2200 (MEB-2208; Nihon Kohden, Tokyo, Japan) and a Digitimer D185 (Digitimer, Welwyn Garden City, UK). Somatosensory evoked potential-involved bilateral median nerve and anterior tibial nerve were recorded using standard methods. Responses recorded from muscles with transcranial electrical stimulation (TCES) were obtained from intramuscular needle pairs recording both abductor pollicis brevis (APB) and tibialis anterior (TA) muscles. Transcranial electrical stimulation was performed with a constant voltage of 50–100-μs duration rectangular pulses through two corkscrew-design electrodes fixed on scalp sites overlying the bilateral motor cortices. Transcranial electrical stimulation began with three pulses at 2-ms interstimulus intervals (ISI). Five pulses produced more consistent responses, and so were used for monitoring. Details of the technique for TCES and recording from muscle and spinal epidural space were mentioned in Chapter 5, in Section A.

1.2.2.2.3 Intraoperative Findings of Monitoring

Somatosensory evoked potentials with bilateral anterior tibial nerve stimulation were already unclear prior to surgery. TCE-evoked electromyogram monitoring was suc-

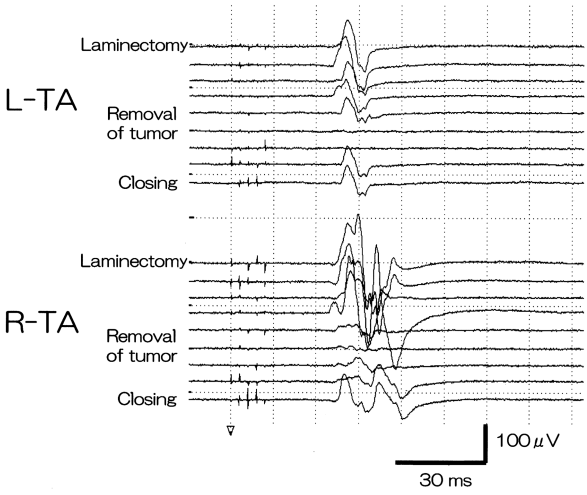

FIG. 1.8. During the tumor resection, responses from bilateral tibialis anterior muscles were significantly decreased. However, these changes recovered immediately after temporal interpretation of the surgical manipulation. *TA*, tibialis anterior

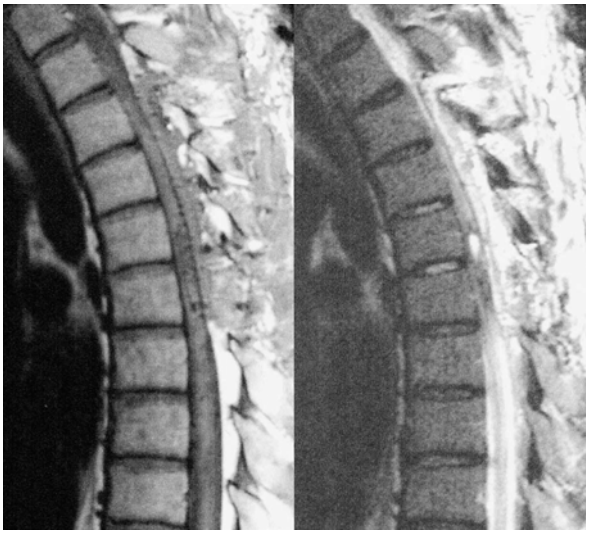

FIG. 1.9. Total removal was confirmed by postoperative MR images. *Left*, T1-weighted image; *right*, T2-weighted image

cessful with total intravenous anesthesia (TIVA) from the beginning of surgery. Figure 1.7 shows responses evoked during soft-tissue dissection to expose the cervical laminae. The initial stimulus voltage required for clear arm and leg responses were monitored after left anodal stimulation, and then vice versa. During the tumor resection, responses from bilateral TA were significantly decreased. However, these changes recovered immediately after temporal interpretation of the surgical manipulation (Fig. 1.8). Then tumor resection was continued in the other direction, with meticulous microsurgical manipulation. After such a procedure, essentially the threshold intensities for TCE-evoked electromyogram in all four limbs were not elevated significantly. The final amplitudes of muscle responses were almost the same as in the initial condition.

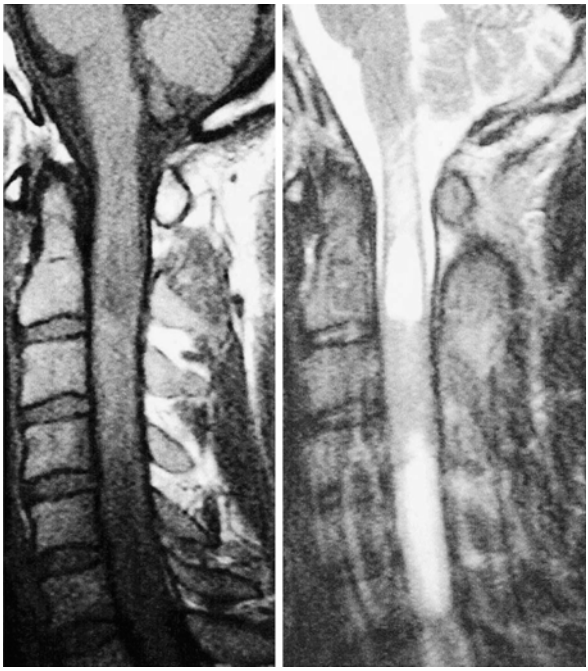

Fig. 1.10. The tumor was observed in sagittal MR imaging to be an extensive mass along the inside of the spinal cord from C2–4, accompanying upper and lower side sphyngomyelia in C2 and C4–6. *Left*, T1-weighted image; *right*, T2-weighted image

1.2.2.2.4 Postoperative Course

After extubation, the patient's neurological findings were evaluated. Motor function on the left side seemed approximately normal. Right lower-extremity strength was 4/5 in manual muscle testing. These neurological findings on motor function were not much different from the preoperative neurological motor functions. Pain-temperature sensation was reduced in the left lower extremity, and vibration-proprioception sense and touch sensation were reduced in both lower extremities, but these degrees were almost the same as in the preoperative condition. One week after surgery, these neurological deficits in the lower extremities had improved sufficiently to allow ambulation with a walker, and the patient's activity of daily life was unaffected. Total removal was confirmed by postoperative magnetic resonance images (Fig. 1.9). The pathologic diagnosis was a cavernous angioma.

1.2.2.3 Case 2

1.2.2.3.1 History and Presentation

This patient was a 36-year-old right-handed man, in whom occasional episodes of paresthesia in a right C6–8 distribution were the only symptoms. The original tumor was observed to be an extensive mass along the inside of the spinal cord from C2–4 accompanying by upper and lower side syringomyelia in C2 and C4–6 (Fig. 1.10).

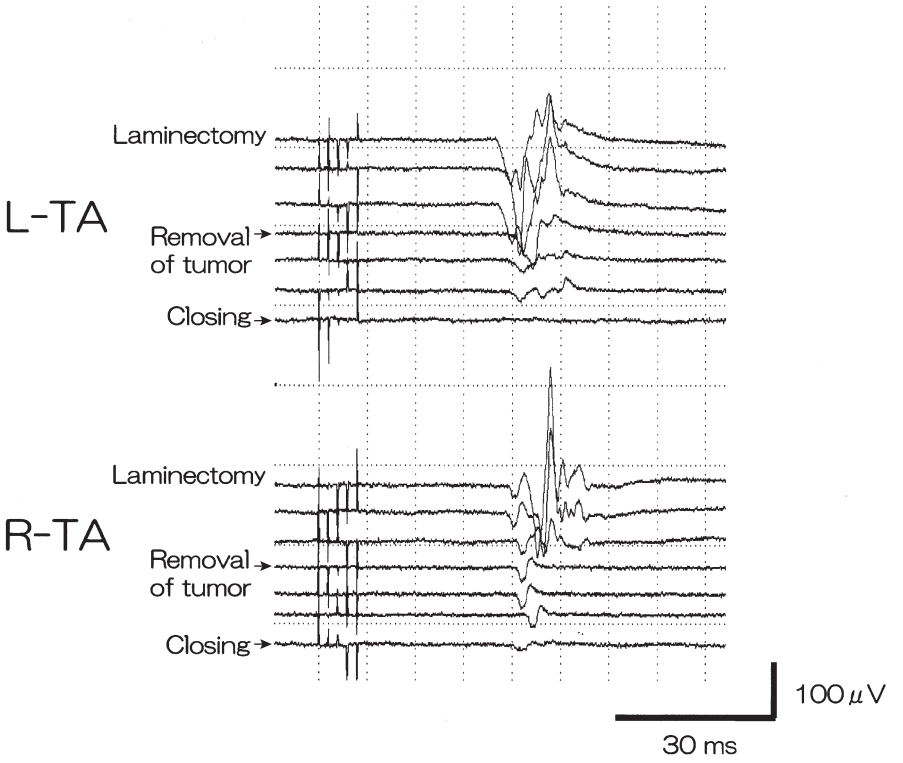

Fig. 1.11. Transcranial stimulation with 600 V and five stimulus train on C3–4 (anode–cathode) and C4–3 (anode–cathode) elicited clear responses from bilateral abductor pollicis brevis and tibialis anterior (*TA*). Several hours later, during tumor resection, changes in responses were evident, as shown in this figure. Because of the complete absence of response in the right APB (data not shown) and bilateral TA muscles during resection of tumor, we predicted a severe motor deficit in the right upper and bilateral lower extremities

1.2.2.3.2 Multimodality-Evoked Spinal Cord Potential Monitoring

Recording methods for the SEP and TCE-evoked electromyogram were almost the same as in Case 1.

1.2.2.3.3 Intraoperative Findings of Monitoring

Somatosensory evoked potentials with right median nerve stimulation were already unclear prior to surgery; however, those produced by left median and bilateral anterior tibial nerve stimulations were evident. These SEP responses were decreased and became unclear after incision of the dorsal side of the spinal cord and the start of tumor resection. Stimulation with 600 V and five stimulus trains on C3–4 (anode–cathode) and C4–3 (anode–cathode) elicited clear responses from bilateral APB and TA before incision of spinal cord. Several hours later, however, during tumor resection, changes in such motor responses were evident, as shown in Fig. 1.11. Also,

threshold intensities for TCE-evoked electromyogram in all four limbs were elevated during these operative procedures. Because of the complete absence of response in the right APB (data not shown) and TA muscles to the final stimulus pattern, we predicted a severe motor deficit in the right upper and bilateral lower extremities.

Based on these findings, a decision was made to limit the extent of tumor resection, and we held the tumor resection to subtotal removal. At the end stages of this resection, the 800-V, five-pulse stimulus train was no longer adequate for evoking responses in the patient's TA muscle bilaterally.

1.2.2.3.4 Postoperative Course

The pathological diagnosis was a cellular ependymoma, and subtotal resection was confirmed by MR images. Neurological evaluation was conducted 3 days after surgery.

Pain-temperature sensation and vibration-proprioception sense were markedly reduced in both lower extremities. Touch sensation was also reduced in both lower extremities than preoperatively. Similar, but much milder, sensory disturbance was also noted in both upper limbs and the trunk. Muscle strength of each extremity was ranked based on the manual muscle testing. Right wrist extensor and the right triceps muscles were each 3/5, and right wrist flexors were 3/5. Left upper extremity muscles were grossly intact. Right TA muscle was 2/5, and left was 3/5. Bilateral quadriceps muscles were almost 3/5. Thus far, he had hardly walked and was just starting rehabilitation.

1.2.2.4 Discussion

Somatosensory evoked potentials assess the functional integrity of afferent pathways and reflect activity primarily in the posterior columns. Neither the anterior spinal cord nor motor pathways, specifically, are monitored using SEPs. Jones et al. (2003) reported two cases of quadriparesis following anterior cervical discectomy with normal perioperative SEPs. Electrical activation of the motor cortex or brainstem can be performed transcranially in several ways. EEG scalp electrodes (Merton and Morton, 1980; Boyd et al., 1986) or electrode plates placed adjacent to the scalp and hard palate (Levy, 1987) can be used to stimulate the motor cortex. Zentner (1989) presented the results of monitoring descending pathways with single pulse TCE-evoked electromyogram in 50 patients during the spinal surgery. According to his report, there were false-positive results in approximately 20%, and no false-negative findings. He described that TCE-evoked electromyogram monitoring during spinal surgery is a sensitive method for early detection of impending neurological complications. He also mentioned that major problems were the influence of anesthesia and the definition of acceptable limits for changes in amplitudes. Other researchers also suggested that false-negative recordings are rare using TCE-evoked electromyogram, but false positives may be common (Levy, 1987; Jones et al., 1996).

To avoid such frequent false-positive results, repetitive TCES was developed in the mid-1990s (Pechstein et al., 1996a). Comparison of single with repetitive TCES to activate the corticospinal tract suggested that repetitive stimulation caused more responses than single stimulation, and it was confirmed that use of repetitive stimulation is a rather effective method to activate the corticospinal tract during spinal cord surgery (Haghighi and Gaines, 2003; Pechstein et al., 1996b).

Recently, McDonald (2002) reviewed safety and complications of transcranial TCE-evoked electromyogram monitoring, based on comparison with other experimental brain stimulation methods and clinical experience. According to his report, there have been remarkably few adverse events; these included seizure induction, tongue laceration, and cardiac arrhythmia. His conclusion suggested that with appropriate precautions in expert hands the well-established benefits of TCE-evoked electromyogram monitoring decidedly outweigh the associated risks. This conclusion was also confirmed in 33 scoliosis surgeries in neurologically normal patients (MacDonald et al., 2003).

On the other hand, appropriate critical points to detect operative injury of neural tissue in this monitoring technique have been investigated. Calancie et al. (2001) evaluated whether changes in the minimum stimulus intensity (threshold level) required to elicit a response from a given muscle predict motor status postoperatively, and they mentioned that monitoring of the intraoperative threshold-level has proven to be a accurate technique to prevent or minimize inadvertent motor deficits during spinal surgery.

Morota et al. (1997) recorded the traveling waves of the spinal cord, through catheter-type electrodes placed in epidural space, in 32 consecutive patients with intramedullary spinal cord tumors. From their results, it was suggested that decline of more than 50% in amplitude during tumor removal should serve as a serious warning sign to the surgeon. However, owing to some reports that compared TCES with direct cortical stimulation (Katayama et al., 1991, 1993), non-corticospinal tract-mediated spinal cord responses are induced readily from epidural space by TCES. When spinal cord responses are recorded with transcranial stimulation, it cannot be established precisely which structures are being activated to produce the recorded signals (Yamamoto et al., 1991). As such, care must be taken to understand the meaning of a potential recorded from spinal epidural space with TCES.

1.3 Spinal Cord Hypothermia During Aortic Surgery

Tatsuhiko Kano and Seiji Watanabe

The peak latencies of the 1st and 2nd waves of conducting SCP were gradually prolonged and the durations were widened, as the body temperature decreased. The amplitudes of the 1st and 2nd waves showed a biphasic change in the course of cooling. The amplitude gradually increased until around 30°C and then turned to decline below the baseline level, during which supramaximal electric stimulation was delivered (Kondo et al., 1996). The sequences of the biphasic change in amplitude are shown as a superimposed form in Fig. 1.12. The conducting SCP could be available as an intraoperative monitoring of spinal function even under deep hypothermia with

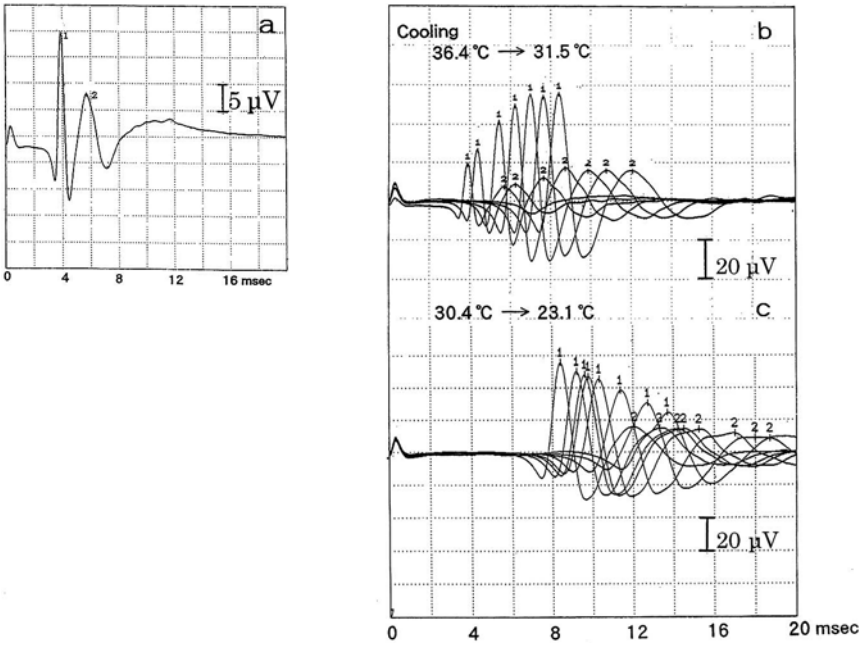

Fig. 1.12a–c. Effects of hypothermia on the conducting spinal cord potentials (SCPs) in a 56-year-old patient undergoing thoracoabdominal aortic surgery. The conducting SCP was recorded from the epidural space at the T12/L1 vertebral level in response to supramaximal electrical stimulation applied epidurally at the C6/C7 vertebral level. The levels of the epidural electrodes were confirmed preoperatively by X-ray examination. Blood cooling was initiated by using cardiopulmonary bypass under intravenous anesthesia with fentanyl and midazolam. Subsequent serial changes of the 1st and 2nd waves of the conducting SCPs were superimposed. **a** before cooling; **b** during the cooling process from a rectal temperature of 36.4° to 31.5°C; **c** during the cooling process from a rectal temperature of 30.4° to 23.1°C. Note that the peak latencies of the 1st and 2nd waves of conducting SCPs were gradually prolonged and the durations were widened with the reduction of body temperature. The amplitudes of the 1st and 2nd waves showed a biphasic change in the course of cooling. The amplitude gradually increased until around 30°C and then declined below the baseline level (from Kondo et al., 1996)

extracorporeal circulation. When blood temperature reached near 10°C, the 1st wave was divided in two components. The divided 1a and 1b waves were congregated to the 1st wave with rewarming (Kondo et al., 1996) (Fig. 1.13). In an animal experiment with surface cooling to 24°C and rewarming using a water mattress, the latency difference (ms) of the 1st wave of conducting SCP from the precooling baseline indicated negative correlation with esophageal temperature (°C) ($\gamma = 0.88$ on cooling, $\gamma = 0.80$ on rewarming) (Kano et al., 1994). The conducting SCP elicited with the supramaximal electrical stimulation was confirmed to show temporary augmentation in amplitude before an eventual decrease under cooling. Local spinal cord blood flow (SCBF) and arterial blood pressure gradually decreased as the body temperature decreased. These tended to return to the pre-cooling baselines after the initiation of rewarming. Within the esophageal temperature range of 38° to 24°C, a positive correlation was observed between the esophageal temperature (°C) and local spinal cord blood flow (SCBF) ($\gamma = 0.79$ on cooling, $\gamma = 0.83$ on rewarming).

The segmental SCP recorded from the epidural space at the lumbosacral enlargement level in response to posterior tibial nerve stimulation at the popliteal fossa was not useful for spinal function monitoring in a case of surgery even under mild hypothermia. The segmental SCP easily fell into a false negative response under hypothermia.

1.3.1 Discussion

Changes in the human compound nerve action potential (NAP) during physiological temperature decrease occur by the following mechanism; NAP of a single myelinated

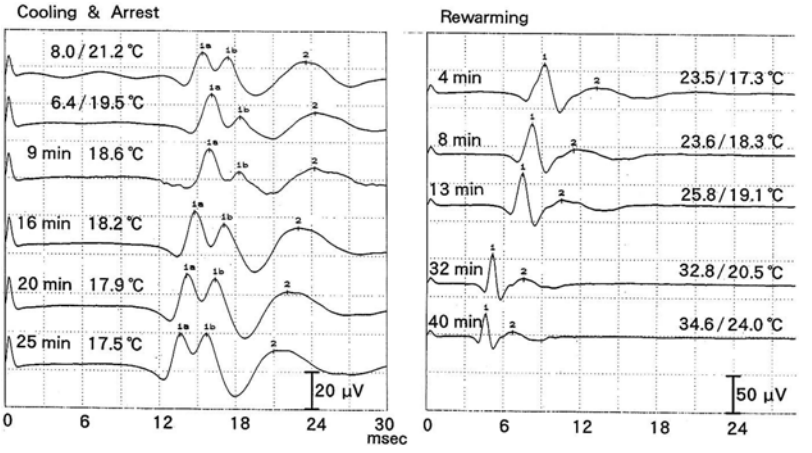

Fig. 1.13. Effects of deep hypothermia, circulatory arrest, and rewarming on the conducting SCPs in the same patient as in Fig. 1.12. *min* (left), time after circulatory arrest; *min* (right), time after the restart of cardiopulmnary bypass (rewarming); *lines*, blood temperature being sent from the cardiopulmonary circuit/rectal temperature; *1*, 1st wave of the conducting SCP, *2*, 2nd wave of the conducting SCP. Note that when the blood temperature reached near 10°C, the 1st wave was divided clearly into two components. The divided 1a and 1b waves were coalesced to the 1st wave with rewarming (from Kondo et al., 1996)

nerve fiber is only mildly increased in amplitude but considerably increased in duration, the summed effect on the compound NAP from a nerve trunk being an increase in both amplitude and duration (Bolton et al., 1981). Thus, amplitude augmentation under mild hypothermia would be explained by temporal summation[1] of the NAP constituting the conducting SCP. The dividing of the 1st wave of the conducting SCP under deep hypothermia indicates that the conducting SCP represents the conduction of several descending and ascending spinal tracts. Kida et al. observed in cats that systemic cooling caused an increase in latency, duration and amplitude of the conducting SCP as the body temperature decreased, and the conducting SCP was little affected by local cooling of the stimulating site (Kida et al., 1994). The authors suggested that the configuration changes in the conducting SCP under hypothermia were not due to changes of the stimulus threshold, but due to the interactions of individual spike potentials. The biphasic response in amplitude with cooling was also observed in motor evoked potentials evoked by transcranial electric stimulation (Meylaerts et al., 1999).

The segmental SCP seems to be inferior to the conducting SCP in reliability for spinal function monitoring under hypothermia. The probable reason is that temporal dispersion is enhanced under hypothermia in the course of conduction of the compound NAP along the peripheral nerve stimulated. Similarly, the distance between the stimulation and recording sites is longer in the recording of the segmental SCP than in that of the conducting SCP. And the temperature reduction in the peripheral nerve of the extremities might be more severe that in the spinal cord surrounded by the cerebrospinal fluid under hypothermia.

In summary, the conducting SCP was so sensitive to the changes in body temperature that the amplitude, latency, and duration were easily altered with cooling and subsequent rewarming. Body temperature monitoring is indispensable for the interpretation of changes in the SCP configuration, especially in surgery under hypothermia. The segmental SCP involving the long peripheral nerves would not be a proper choice for spinal function monitoring under hypothermia.

---

[1] Synchronization of an individual NAP consisting the compound NAP would be impaired under hypothermia, because the hypothermic influence is different depending on the size or function of the nerve fibers. If the prolongation of duration is remarkable as compared with the delay of peak latency in the individual NAP, the amplitude of compound NAP would be enhanced and the duration would be widened. The peak latency of each NAP of the compound NAP is dispersed during the long conduction on the nerve tissue, resulting in reduced amplitude and widened duration of the compound NAP. Development of temporal summation or dispersion under the circumstance of hypothermia would be dependent on the degree of hypothermia, the characteristics of the nerve fibers, the distance between the stimulation and recording sites and so on.)

1.4 Spinal Cord Ischemia During Aortic Surgery

1.4.1 Somatosensory Evoked SCPs

Tatsuhiko Kano and Hideki Harada

The SCP has been monitored during surgery to prevent postoperative paraplegia in patients undergoing repair of descending thoracic or thoracoabdominal aortic aneurysm. The segmental SCP subsequently flattened in 3 of 4 patients after aortic cross-clamping, in whom neurological deficits were not observed at all in the postoperative period (Kano et al., 1995). Figure 1.14 is shows the sequential changes of the segmental SCP. Thus, we have often met such false negative cases in spinal function monitoring by the segmental SCP.

The conducting SCP during aortic cross-clamping rapidly decreased in amplitude with prolongation of latency in 5 of 7 patients under the initiation of femoro-femoral venoarterial partial bypass (F-F bypass). The conducting SCP eventually disappeared following temporary amplitude augmentation after aortic cross-clamping in 1 of the

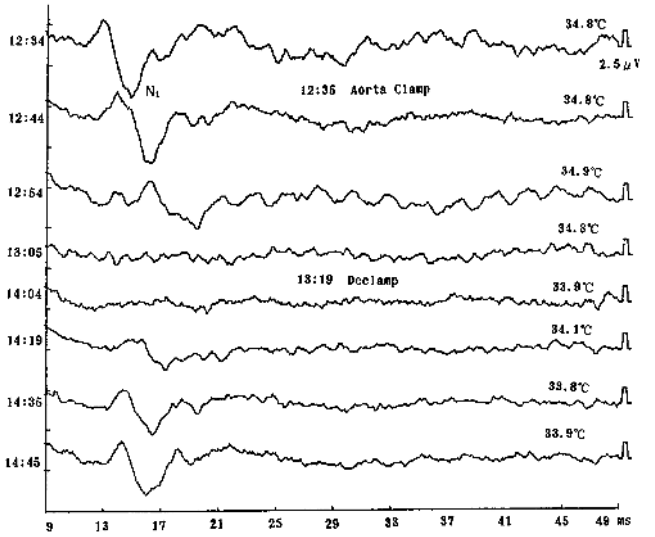

Fig. 1.14. Effects of ischemia by aortic cross-clamping on the segmental SCPs in a 71-year-old man undergoing abdominal aortic surgery. The segmental SCP was recorded from the epidural space at the T12/L1 vertebral level in response to the supramaximal electrical stimulation of the posterior tibial nerve at the popliteal fossa. Anesthesia was maintained mainly by intravenous fentanyl and midazolam, supplemented by intermittent inhalation of less than 0.8% isoflurane, as needed. Sequential changes of the segmental SCP before, during, and after aortic cross-clamping are shown and the changes in esophageal temperature are indicated on the *right side*. The N1 wave of the segmental SCP disappeared 30 min (13:05) after the cross-clamp (12:35) and reappeared 53 min (14:12) after declamp (13:19) with no neurological sequelae. The esophageal temperature was kept between 35.3° and 36.7°C throughout the surgery. Note the false positive response of the segmental SCPs (from Kano et al., 1995)

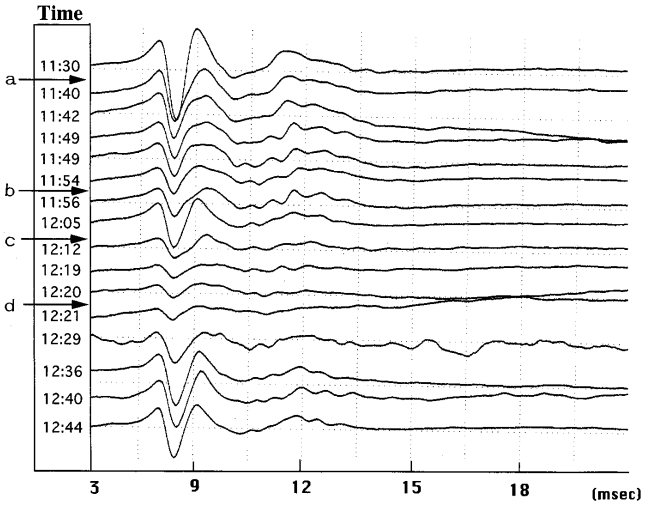

FIG. 1.15. Effects of ischemia by aortic cross-clamping on the conducting SCPs in a 43-year-old man undergoing thoracic aortic surgery. The conducting SCP was recorded from the epidural space at the T12/L1 vertebral level in response to supramaximal electrical stimulation applied epidurally at the C7/T1 vertebral level. The longitudinal levels of the epidural electrodes were confirmed preoperatively with anteroposterior X-rays. Anesthesia was maintained mainly by intravenous fentanyl and propofol, supplemented by intermittent inhalation of less than 1% sevoflurane, as needed. Serial changes of the conducting SCPs before, during, and after repeated aortic cross-clampings are shown. The proximal clamp was placed between the left subclavian artery and the left carotid artery, and the distal clamp at the T6 vertebral level under the initiation of cardiopulmonary bypass via the femoral vein and artery (F-F bypass). The distal clamp was revised according to the changes in SCPs; *a* and *c* indicate that the distal clamp was placed at the T6 vertebral level, and *b* and *d* at the T4 level. The esophageal temperature was kept between 35.3° and 36.7°C throughout the surgery. Note that the amplitude reduction of the conducting SCP suggesting impending spinal ischemia showed a tendency to return to the baseline by moving the distal clamp cephalad from the T6 vertebral level to the T4 under the F-F bypass. This episode was repeated twice. The patient was free from any neurological disorders postoperatively (from Harada et al., 1998)

5 patients. In that patient the conducting SCP reappeared immediately after declamping. The times of aortic cross-clamping and of the SCP disappearance were 63 and 53 min, respectively. The esophageal temperature during that time was in the range of 34.0–35.1°C. The patient had no neurological sequelae (Kano et al., 1995). The conducting SCP decreased in amplitude without latency prolongation after aortic cross-clamping in another case study, in which the distal clamp was moved from the T6 vertebral level to the T4 under F-F bypass. The reduced amplitude then returned to the baseline amplitude. This episode was repeated twice. The patient was free from any neurological disorders postoperatively (Harada et al., 1998) (Fig. 1.15).

1.4.1.1 Discussion

Epidural electrodes used to be introduced on the day before surgery to avoid development of an epidural hematoma. However, patients complained of sleep impairment

due to the epidural catheter electrodes on the back. Currently the epidural electrodes for SCP monitoring are introduced before induction of anesthesia on the day of surgery and at least 1 h before heparinization, and are removed on the next day after confirming an activated coagulation time of less than 150 s.

The segmental SCP is useful as a sensitive indicator of spinal cord ischemia under general anesthesia with mild hypothermia. However, the segmental SCP is too susceptible to anesthesia and also to moderate or profound hypothermia. Therefore it is hard to say in clinical situations that the segmental SCP is superior to the conducting SCP in reliability. Besides, the segmental SCP, involving two nervous elements, the spinal cord and the peripheral nerve, would not be favorable in specificity of detecting spinal ischemia, especially under hypothermia. Temporal dispersion could easily occur rather than temporal augmentation in monitoring of the segmental SCP, including the long conduction in the peripheral nerve. However, the period tolerable for reduction or abolition of the conducting SCP, in which spinal function is reversible without postoperative neurological symptoms, is not still clear.

Discrimination between ischemia and hypothermia is extremely important. Amplitude reduction without latency prolongation can be considered as a sign of spinal ischemia, as shown in Fig. 1.15. Amplitude reduction with latency prolongation in the conducting SCP is a common characteristic in spinal ischemia and hypothermia, which is caused by temporal dispersion of the afferent volley and conduction block (Seyal and Mull, 2002). Furthermore, temporary amplitude augmentation prior to subsequent reduction is also seen in spinal ischemia as well as hypothermia, although it is rare in ischemia. This amplitude augmentation phenomenon was never observed in postsynaptic components. It was shown in an animal study that there was a close relationship between amplitude augmentation and stimulation strength; the weaker the stimulation, the larger the rate of augmentation, suggesting a subliminal fringe[2] and increased excitability of nerve fibers under ischemia (Iizuka and Kurokawa, 1982). Even when the delivered electrical stimulation was supramaximal, the amplitude augmentation developed. Monitoring of the body temperature is crucial for the judgment of ischemia or hypothermia. We have developed a thin thermocouple wire probe for cerebrospinal fluid (CSF) temperature monitoring. This was mounted on the tip of a CSF drainage catheter (Mishima et al., 1999).

In summary, the conducting SCP is closely observed for 15 min after aortic cross-clamping before dividing the aortic aneurysm in the graft replacement surgery. If an amplitude reduction of more than 50% of baseline is found following the test clamp, we advise the surgeons to release the clamp temporarily or to make another bypass route between the aorta and the artery nourishing the spinal cord. In our hospital the conducting SCP has been used for intraoperative monitoring in combination with motor evoked potentials produced by transcranial electrical stimulation, to detect ischemia.

---

[2] NAP develops when the resting membrane potential is depolarized by stimulation and is raised to a critical level. The conducting SCP is considered as a kind of compound NAP. If the stimulation is not strong enough to excite all the nerve fibers constituting the spinal tracts (submaximal stimulation), the amplitude of the compound NAP will be increased by ischemic depolarization of the resting membrane potentials or by the application of stronger electrical stimulation.

1.4.2 TCE-Evoked Electromyograms During Thoracoabdominal Aortic Surgery

Satoru Fukuda and Hai-long Dong

For protection from spinal cord ischemia, it is important to understand the surgical procedures for thoraco abdominal aortic aneurysm (TAAA) in conjunction with somatosensory evoked potential (SSEP) and evoked electromyogram (evoked EMG). In most institutes, (1) deep hypothermic cardiopulmonary bypass (CPB) with circulatory arrest (Kouchoukos et al., 2001, 2002) or (2) left heart bypass (or femoral vein–femoral artery bypass: F-F bypass) with distal aortic perfusion and cerebrospinal fluid (CSF) drainage (Coselli et al., 2002; Safi et al., 1997a,b, 2003) is undertaken for operations on TAAA. In both techniques, hypothermia is used for protection from spinal cord ischemia during surgery. In the former technique, CPB is established immediately after the chest is opened, and the patient is cooled to 12°–15°C at nasopharyngeal temperatures and 15°–19°C at bladder temperatures until electroencephalographic (EEG) silence is achieved (Kouchoukos et al., 2001, 2002). Therefore, in this technique EEG and evoked monitoring cannot be used, because the amplitudes of EEG, SSEP, and evoked EMG are almost abolished at this temperature. In contrast, in the latter technique the systemic moderate hypothermia is used at 32°–34°C at core temperature (rectum). The evoked monitoring is available at this temperature. The CSF drainage and distal aortic perfusion are important adjuncts for the spinal cord ischemia, which is detectable in evoked monitoring.

In operations with left heart bypass with distal aortic perfusion, the heparin-coated circuit consists of an outflow cannula in the left atrium (or left inferior pulmonary vein), an inflow cannula in the femoral artery or distal aorta, and a centrifugal pump (Fig. 1.16). This method decreases the use of heparin (1 mg/kg: active coagulation time: 250–300 s) due to the heparin-coated circuit, and stabilizes the hemodynamics with decreasing preload of the left ventricle. As no blood reservoir is incorporated in this closed circuit, cell-saving allows direct reinfusion of unwashed blood from the reservoir during massive bleeding. If a heat exchanger is not incorporated into this circuit, excessive hypothermia might occur. The hemodynamic instability due to massive bleeding and excessive hypothermia might influence the evoked potentials. In contrast, the F-F bypass tends to lead to bleeding due to complete heparinization (3 mg/kg), but hemodynamic stabilization is easily obtainable with this bypass, in which a blood reservoir is incorporated. A double-lumen endobronchial tube is positioned for selective right lung ventilation and left lung deflation to obtain a good operative field. Therefore, it is necessary for the patient to have a right lung respiratory reserve to maintain oxygenation during one-lung ventilation.

After exposing the proximal thoracic aorta and dissecting at the hilum of the left lung in patients with type I and II TAAA, the operator proceeds cephalad, exposing the phrenic, vagus, and left recurrent nerves. The thoracic aorta is clamped sequentially, beginning distal or proximal to the left subclavian artery and at the mid-descending thoracic aorta between T4 and T7 (Safi et al., 2003). After clamping, the dissected aorta between the clamping sites is excised, and the proximal anastomosis with an artificial graft is begun. At this point, distal aortic perfusion from the left heart bypass provides arterial flow to the viscera, kidneys, lower extremities, and lower

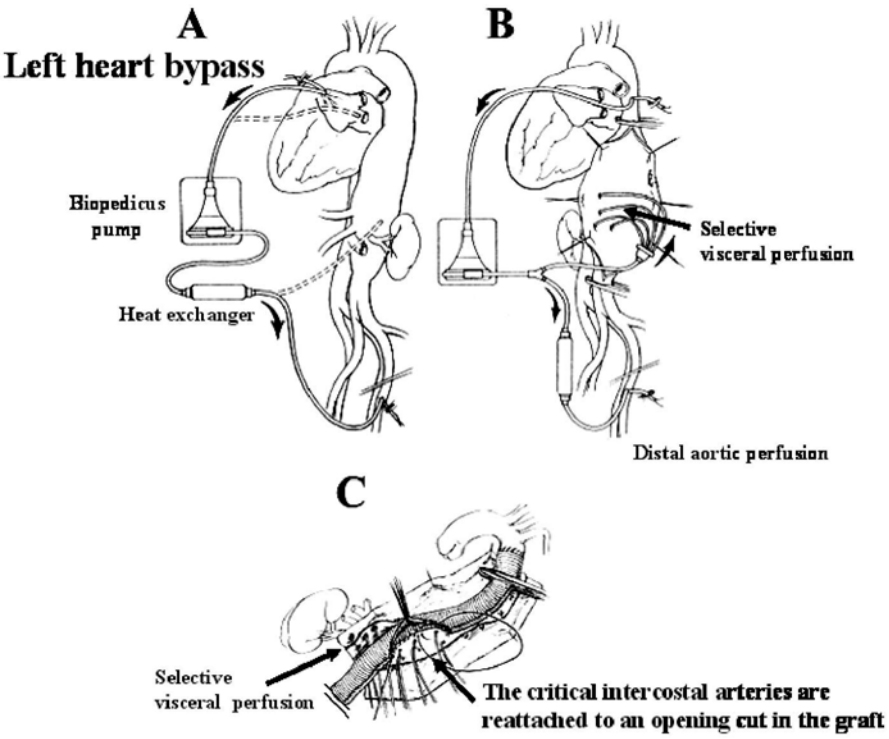

FIG. 1.16A–C. Surgical procedures in thoracoabdominal aortic aneurysm (TAAA) operations. **A** For left heart bypass with distal aortic perfusion, the heparin-coated circuit is used with centrifugal pump and heat exchanger. As no blood reservoir is incorporated in this closed circuit, surgical teams sometimes use femoral vein–femoral artery (F-F) bypass to compensate for massive bleeding and to obtain hemodynamic stabilization. (From Safi et al., 1998, with permission). **B** After opening the chest, the thoracic aorta is clamped sequentially, beginning distal or proximal to the left subclavian artery and the mid-descending thoracic aorta between T4 and T7. After completion of the proximal anastomosis, the mid-descending aortic clamp is moved distally to the infrarenal aorta. At this point, the responses to evoked EMG sometimes decrease to less than 25% of the baseline. In the event of an abnormal response being observed, the operator immediately has to reattach the critical intercostal arteries and lumbar arteries to an opening cut in the artificial graft or to the artificial graft by a short interposition bypass graft. (From Safi et al., 1998, with permission). **C** After clamping the aorta and cutting the aneurysm open, the visceral organs are perfused with cold oxygenated blood from the bypass circuit through balloon perfusion catheters into these arteries. During these procedures, keeping the pressure of the distal aorta at 60–70 mmHg is very important for the protection against spinal cord ischemia, because patients with aneurysms such as types II and III have collaterals from lumbar and/or pelvic circulation. If myogenic MEP responses appear abnormal, the anesthesiologist must check the systemic arterial pressure, the pressure in the distal aorta or aortic clamp, and so on. (From Svensson and Crawford, 1997, with permission)

intercostals and lumbar arteries (Fig. 1.16A) (Safi et al., 1998). After completion of the proximal anastomosis, the mid-descending aortic clamp is moved distally to the infrarenal aorta and the aneurysm is then opened longitudinally posterior to the left renal artery, to accommodate intercostals and visceral reattachment (Coselli, 2004). (Fig. 1.16C) At this point if the TCE-evoked electromyogram amplitude decreases less than 25% of baseline, which the anesthesiologists consider an indication of critical spinal cord ischemia, and the operators prompt spinal cord revascularization. Reattachment of patent, lower intercostal arteries (T8 to T12) is performed routinely except in cases of occluded arteries and heavily calcified or atheromatous aorta, when it is technically not feasible (Estrera et al., 2001). Thus, during operations for TAAA, monitoring of myogenic TCE-evoked electromyogram is an effective technique to detect spinal cord ischemia within several minutes. This modality may also help to identify segmental arteries that need to be reattached (de Haan et al., 1997) A typical decrease in the response of myogenic TCE-evoked electromyogram is shown in Fig. 1.17. After clamping the aorta, myogenic TCE-evoked electromyogram suddenly discreased.

For extensive aneurysms, sequential clamping is used. In some institutions, this distal aortic clamp forceps is moved to a subsequent clamp site (usually three vertebral segments) on the descending thoracic aorta, and as many intercostal arteries as can be found within these segments are reconstructed. Measurements of SSEP and TCE-evoked electromyogram are carried out and evaluated at every stage of reimplantation. Preserved segmental arteries were reimplanted when TCE-evoked electromyogram amplitude decreased to below 25% of baseline or when SSEP amplitude decreased to below 50% of baseline (Kuniyoshi et al., 2003). If the reattachments of the lower intercostal arteries are finished and abnormalities in SSEP and TCE-evoked electromyogram measurements are not observed, the proximal clamping forceps is

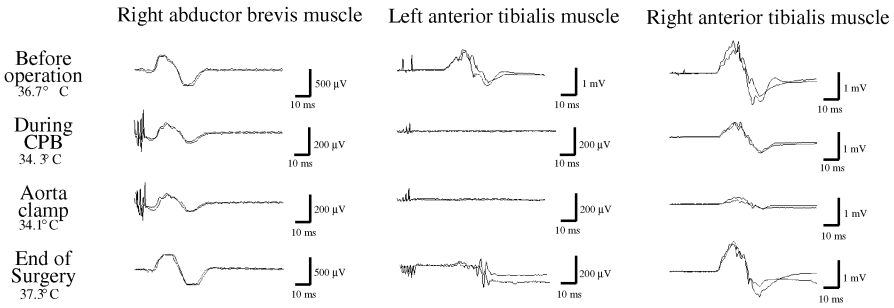

Fig. 1.17. TCE-evoked electromyogram monitoring in a 73-year-old male patient with Crawford type II aneurysm. The response in the abductor brevis muscle to transcranial electrical stimulation (TCES) was regarded as a control. After insertion of the cannula for distal aortic perfusion in F-F bypass, the responses of left tibialis anterior muscle to TCE-evoked electromyogram disappeared due to leg ischemia. It took a long time to restore these responses. After aortic clamp, the responses to right TCE-evoked electromyogram were extremely decreased, and the operator promptly attached the critical intercostal arteries and lumbar arteries to an opening cut in the artificial graft. Thereafter, the responses to TCE-evoked electromyogram recovered

released and the intercostal arteries are reperfused. The intercostal arteries (T8 to T12) and lumbar arteries (L1, L2) responsible for preserving the blood supply to the spinal cord often branch off the aorta near the diaphragm. The critical intercostal arteries and lumbar arteries are reattached to an opening cut in the artificial graft (Fig. 1.16B) (Safi et al., 1998) or by a short interposition bypass graft. During these procedures, the celiac, superior mesenteric, and renal arteries are selectively delivered (300–600 ml/min) with cold oxygenated blood from the bypass circuit through balloon perfusion catheters into these arteries (Estrera et al., 2001; Safi et al., 1998; Svensson and Crawford, 1997) (Fig. 1.16B,C). The temperature of the left kidney is kept below 20°C. To prevent excessive hypothermia due to the cold visceral perfusion, core body temperature is kept 32°C and 33°C by warming the lower extremities using a heat exchanger in the circuit. During these procedures, the TCE-evoked electromyogram measurement is important for detecting spinal cord ischemia. Sakamoto et al. (2003) reported that a reduction of core temperature to 28°C did not influence TCE-evoked electromyogram amplitudes as long as a train of multiple pulses. If the TCE-evoked electromyogram in the muscles in the lower extremities appear abnormal and those in the upper extremities are without change, spinal ischemia should be considered. Once the visceral anastomosis is completed, the operator moves the descending thoracic clamp down on the graft and restores the flow to the viscera. A clamp is placed above the iliac bifurcation on the left common iliac artery and the distal aortic graft anastomosis can be performed (Safi et al., 2003). Rewarming is begun until the nasopharyngeal temperature reaches 36°C.

Distal aortic perfusion is important to protect the spinal cord from ischemia. This adjunct (Fig. 1.16A,B) (Safi et al., 1998) is perfused from the femoral artery. Therefore, the amplitudes of SSEP and TCE-evoked electromyogram are often attenuated or abolished because of ischemia in the lower extremities on the side of inserting the cannula, as shown in Fig. 1.17. As the perfusion pressure in spinal cord flow decreases to below 60 mmHg, the flow to the spinal cord decreases (Griffiths et al., 1978). Therefore, it is necessary to keep the distal aortic perfusion pressure at 60–70 mmHg to protect against spinal cord ischemia. In fact, it is reported that loss of TCE-evoked electromyogram could be attributed to low distal blood pressure (DBP) and an increase of distal bypass flow, which in turn raised DBP to above 60 mmHg, restoring TCE-evoked electromyogram (Dong et al., 2002). As mentioned above, blood supply to the spinal cord depends upon a highly variable collateral system and sometimes comes from the lumbar arteries or pelvic circulation (Jacobs et al., 2002a,b). If an abnormality of SSEP and TCE-evoked electromyogram is observed, the anesthesiologists have to pay attention to the distal aortic perfusion pressure as well as the operative procedures.

CSF drainage is another important adjunct for prevention of spinal cord ischemia (Coselli et al., 2002; Safi et al., 2003). The 14-F CSF drainage catheter is kept in place between the L3 and L4 intervertebral space on the preoperative day. The CSF pressure is maintained below 10 mmHg during the operation and for 3 days postoperatively (Safi et al., 2003). The high CSF pressure decreases the perfusion pressure of the spinal cord, hence the occurrence of the abnormality in SSEP and TCE-evoked electromyogram monitoring.

In summary, good cooperation of surgeons and anesthesiologists greatly contributes to the prevention of spinal cord ischemia during TAAA operation.

1.5 Cardiovascular Surgery

1.5.1 Somatosensory Evoked SCPs

Toshikazu Takada and Koki Shimoji

Although new approaches to the therapy of spinal cord injury has been tried extensively (Dobkin and Havton, 2004), the most serious complications of aortic surgery are still noticed in ischemic spinal cord and/or brain dysfunctions caused by an aortic clamp or emboli (Lake, 1984; Kunihara et al., 2004). As neurological signs and symptoms of ischemic lesions by aortic clamping are masked during anesthesia, an alternative measure should be undertaken for monitoring the brain and spinal cord functions. Although several neurophysiological techniques have been successfully used to detect early signs of CNS dysfunction due to carotid surgery, there are some difficulties in monitoring CNS functions in aortic surgery. First, it is hard to define the anticipated sites of ischemia preoperatively, since there are considerable anatomical variations of arterial outflows to the spinal cord (Carpenter and Sutin, 1983; Uezu et al., 2003) (Fig. 1.18A,B). Second, although the skin surface recording of spinal cord potentials (SCP) has been attempted, it is often hard to reproduce the potentials and also takes a considerable amount of time to average the response.

Therefore, a new method of monitoring spinal cord and brain functions should be developed for use during aortic surgery. Multimodal and/or multispatial recordings of evoked potentials, using a specially designed epidural catheter electrode or pharyngeal (esophageal) electrode, might be of value for this purpose (Maruyama et al., 1988).

To detect brain and spinal cord ischemia produced by aortic cross-clamping, the somatosensory evoked potentials from the skull and spinal epidural space and, if needed, auditory brainstem responses, should be recorded simultaneously and sequentially in patients during aortic surgery.

All evoked potentials are prolonged linearly in latency and vary in amplitude as the body temperature decreases. Systemic ischemia caused by total circulatory arrest produces an abrupt latency prolongation and amplitude decrease in all modality responses. Local ischemia by aortic clamping demonstrates unparalleled changes in evoked potentials, which makes it possible to detect the site of ischemia (Fig. 1.19).

By aortic clamping, the spinal cord as well as peripheral nerves below the level may suffer ischemic injuries. Multispatial recordings and/or stimulations would yield more information for monitoring spinal cord functions during aortic surgery. For instance, clamping of the abdominal aorta may induce both spinal and peripheral nerve ischemia. In such a case not only tibial nerve stimulation at the popliteal space and SCP recording at the level of T12/L1 of the posterior epidural space but also spinal cord stimulation at the T12/L1 level and SEP recording from the scalp may lead to a more accurate estimate of the ischemic region (Fig. 1.20).

When anticoagulants are used or there are contraindications in the patients for placement of epidural catheter electrodes, posterior pharyngeal or upper esophageal recording of the spinal cord potential using the surface electrodes attached to the

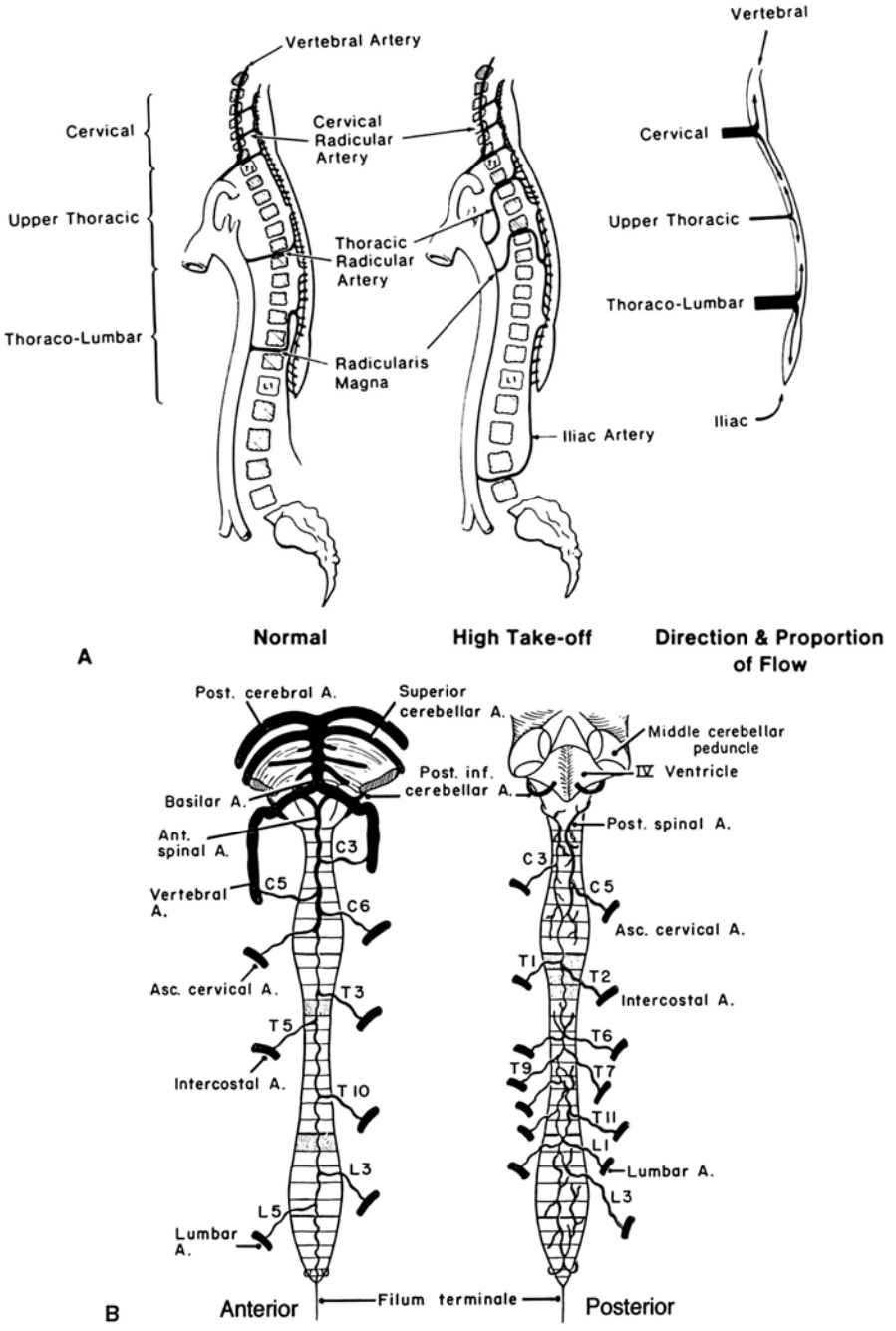

FIG. 1.18. Variability of the take-off level of the blood supply from the aorta to the human spinal cord (**A**) and potentially vulnerable segments (*stippled*) of the spinal cord to ischemia (**B**). *Letters and numbers* indicate important radicular arteries (**B**) (After Crock and Yoshizawa, 1977; Lo et al., 2002; Biglioli et al., 2004)

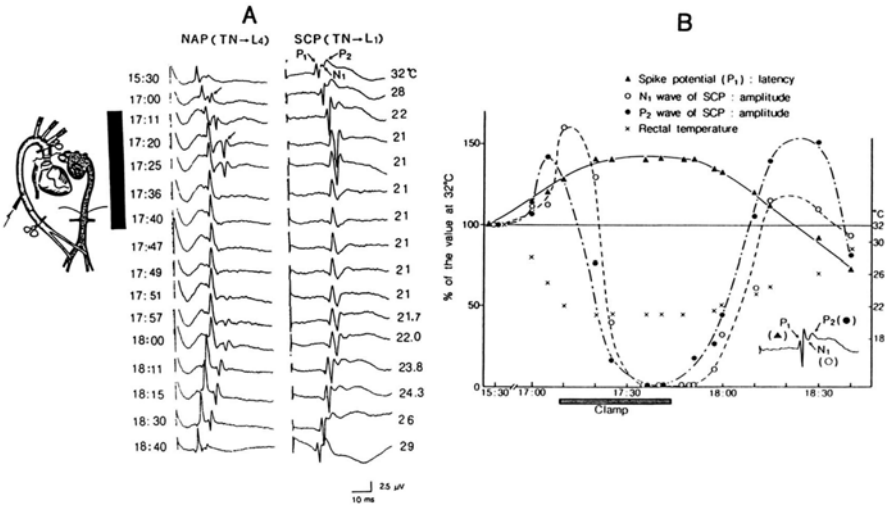

FIG. 1.19A,B. Simultaneous recording of nerve action potential (*NAP*) recorded from the posterior epidural space (PES) at L4 vertebral level and segmental spinal cord potential (*SCP*) recorded from the PES at L1 vertebral level during arch replacement operation in a patient with a dissecting aneurysm under nitrous oxide–fentanyl anesthesia. **A** Specimen records of NAP recorded from the posterior epidural space at the L4 level (the cauda equina) in response to tibial nerve (*TN*) stimulation at the popliteal space with an illustration of operation (clamping time is shown by a *large black bar*). Both the NAP and spike potential (*P1*) of the SCP were prolonged in latency and increased in amplitude by the decrease in body temperature. After the arch-replacement was performed, clamping (shown by a *vertical bar*) was carried out on the artificial vessel for manipulation of the aneurysm, as shown in the schematic drawing. By use of this clamp, latencies of both the NAP and P1 were prolonged with increases in their amplitudes. The N1 and P1 waves of the segmental SCP disappeared after a transient facilitation and reappeared gradually after declamping. The spike potentials marked by *arrows* in the NAP traces seem to indicate the reflex potentials. **B** Graphical representation of the sequential changes in the P1 latency and both the N1 and P2 amplitudes with rectal temperature. During the clamp, rectal temperature decreased but remained at 21°C, and the P1 latency showed an increase, while the amplitudes of the N1 and P2 waves rapidly decreased after transient facilitation by the clamp (Maruyama et al., 1988)

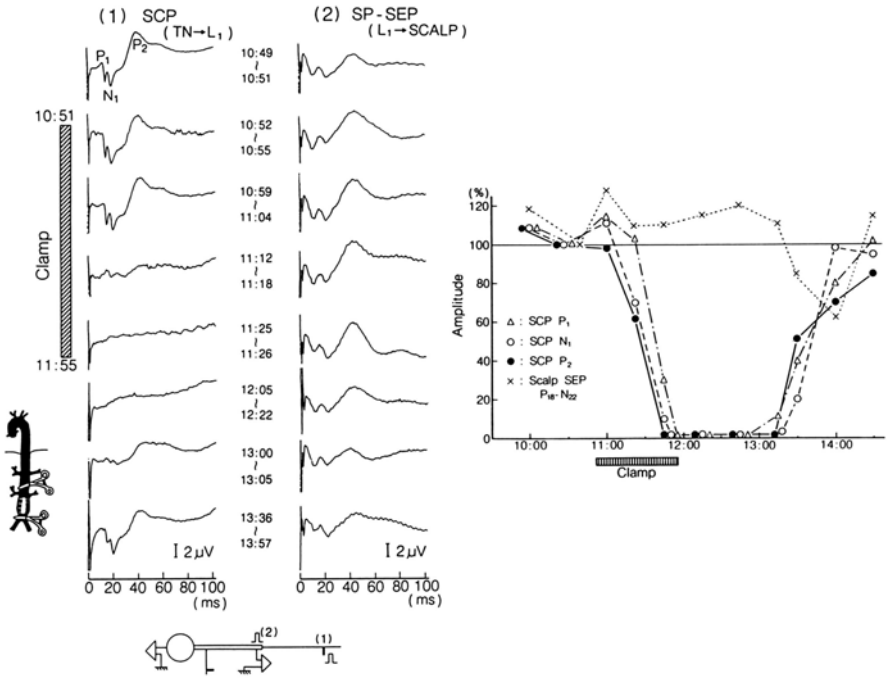

Fig. 1.20. The effect of ischemia caused by cross-clamp of the abdominal aorta on the segmental spinal cord potential (*SCP*) and the somatosensory evoked potential (*SEP*) from the scalp in response to spinal cord stimulation. *Left* Specimen records of the segmental SCPs from the posterior epidural space at the L1 vertebral level in a patient who underwent a Y-graft replacement under nitrous oxide–fentanyl anesthesia. *Right* Graphic presentation of the sequential changes in each component of the SCPs. Note that the SCPs in response to tibial nerve stimulation (*TN* → *L1*) disappeared completely without any substantial changes in the scalp SEP (*L1* → *SCALP*) in response to epidural stimulation of the cord during cross-clamping of the abdominal artery. This indicates that ischemia is present in the peripheral nerves but not in the spinal cord. Graphic representation of amplitude changes in each component of the SCP and SEP by cross-clamping of the abdominal aorta (*shaded bar*). *TN* → *L1*, tibial nerve stimulation at the popliteal fossa and SCP recording from the posterior epidural space at the L1 level; *L1* → *SCALP*, epidural stimulation of the spinal cord at the L1 level and SEP recording from the contralateral somatosensory area of the scalp. Note that all components of the SCP disappeared by cross-clamping of the aorta, whereas the SEP in response to spinal cord stimulation at the level of L1 remains substantially unchanged. *Left* and *bottom* insertions show cross-clamp of the abdominal aorta and sites of recordings and stimulations, respectively (Maruyama et al., 1988)

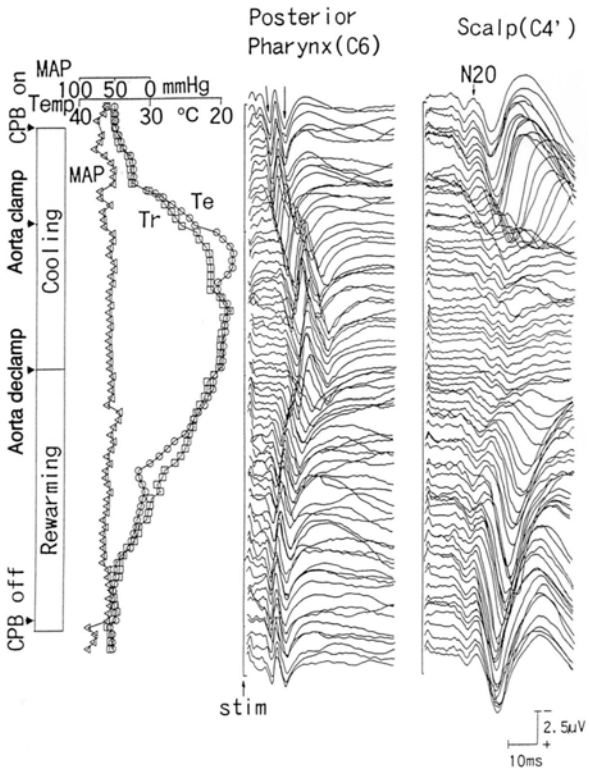

FIG. 1.21. Sequential sampling of continuous recording of both the ascending SCP and scalp SEP during aortic clamping and declamping in a patient with abdominal aneurysm who underwent artificial graft replacement under nitrous oxide–fentanyl anesthesia. The ascending SCP was recorded from the posterior pharynx with an electrode attached to the endotracheal tube; the SEP was recorded from the somatosensory area (*C4'*). Electrical stimulation was applied to the left tibial nerve at the popliteal fossa. Note that P9 and P13, corresponding to the C1 and C2 components of the spinal cord potential recorded from the posterior epidural space, increased in amplitude with prolongation of their latencies by cross-clamping of the aorta during cooling, while all components of the scalp SEP disappeared. Then, all components of both SCP and SEP showed full recovery by declamping of the aorta during rewarming. *MAP*, mean arterial pressure; *Tr*, rectal temperature; *Te*, esophageal temperature; *CPB*, cardiopulmonary bypass. *Vertical lines* at the start of the records denote the stimulation (*stim*) time period. Upward deflection indicates negativity in this recording. (Unpublished data, Takada et al.)

intratracheal tube may be useful for spinal cord as well as brain function monitoring (Fig. 1.21) (Takada et al., unpublished data).

Thus, recording of multimodal and multispatial evoked potentials along the sensory tract might provide a more accurate monitoring of an ischemic lesion and its site in the spinal cord and the brain during aortic and other surgeries (Lyon et al., 2004; Murkin, 2004).

1.5.2 Motor Evoked Potential

Satoru Fukuda and Hai-long Dong

1.5.2.1 Introduction

The operations for thoracoabdominal and descending TAAA are the most invasive surgical procedures despite significant reductions in morbidity and mortality rates by virtue of the development of recent anesthesia and surgical techniques. However, the mortality rate reported in the recent literature is still from 4.8% to 17.8% (Cina et al., 2002; Coselli et al., 2000, 2002; Jacobs et al., 2002b; Kouchoukos et al., 2002; Rectenwald et al., 2002; Safi et al., 2003). In addition to a significant risk of mortality, postoperative complications include various organ disorders such as renal failure, pneumonia, bleeding and paraplegia or paraparesis in the lower extremities.

The recent incidence of postoperative paraplegia in deep hypothermic cardiopulmonary bypass with circulatory arrest technique or left heart bypass (or femoral vein–femoral artery bypass: F-F bypass) with distal aortic perfusion and cerebrospinal fluid (CSF) drainage technique described below has improved even more to be between 2.8% and 4.6% (Coselli et al., 2000, 2002; Jacobs et al., 2002b; Kouchoukos et al., 2002; Safi et al., 2003) in comparison with that in the past "cross-clamp and go" technique (16%) (Svensson et al., 1993). This improvement of the incidence of postoperative paraplegia or paresis largely depends on the progress in the monitoring during operation as well as the preoperative identification of the Adamkiewicz artery, hypothermia during operations, avoidance of hyperglycemia and the advanced operative techniques and its adjuncts.

The postoperative motor dysfunctions include immediate and delayed paraplegia (Safi et al., 1997a,b). The prognoses of these disorders are different between two types of paraplegia (Safi et al., 1997a,b). The immediate type is often found during an emergency from anesthesia. The prognosis of this type is worse and leads to the early death (Azizzadeh et al., 2000; Safi et al., 1997a,b; Svensson et al., 1993). In contrast, in the delayed type, paraplegia can be recovered by CSF drainage, maintenance of blood pressure and normal oxygen supply (Gravereaux et al., 2001; Hill et al., 1994; Hollier et al., 1992; Safi et al., 1997a,b). Preoperative renal dysfunction, acute dissection, and type II thoracoabdominal aortic aneurysm (Fig. 1.22) are significant predictors of delayed neurologic deficit (Estrera et al., 2003).

1.5.2.2 Abnormal Blood Supply to the Spinal Cord in Patients with Descending Aortic and Thoracoabdominal Aneurysm

A branch of the intercostal arteries enters the spinal canal along with the spinal nerve, and divides into the anterior radicular artery and the posterior radicular artery as shown in Fig. 1.23 (Gotoh, 1993). The left and right anterior radicular artery are fused to the anterior spinal artery on the ventral part of the spinal cord. On the dorsal part of the spinal cord, two left and right posterior spinal arteries run and fuse with the posterior radicular artery. The largest anterior radicular artery is called the Adamkiewicz artery, which is important for the supply of the blood to the motor

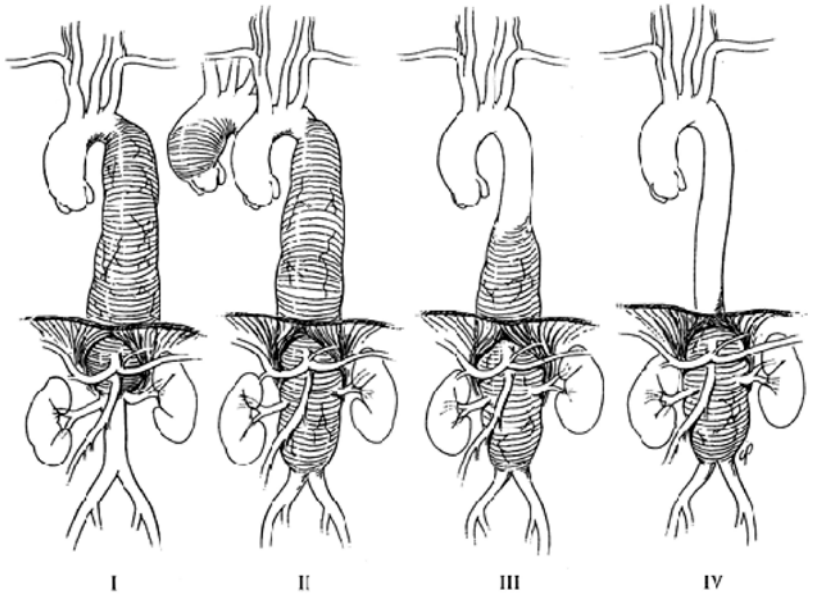

FIG. 1.22. Crawford classification. According to Crawford, the thoracoabdominal aneurysm is classified into four types. Among them, Types II and III are often supplied by other arterial systems such as lumbar and pelvic circulation. Type II is a predictor of delayed neurologic deficit. (From Coselli and LeMaire, 1999, with permission)

neurons. According to the arteriographic examination by Kieffer et al. (2002), the Adamkiewicz artery was successfully found in 419 patients (86.0%) and arose from a left intercostal or lumbar artery in 323 patients (77.1%), and from between T8 and L1 levels in 361 patients (86.2%) among 480 subjects. However, the blood supply to the anterior spinal arteries is complicated so that the patency and preservation of the anterior spinal arteries during TAAA surgery does not necessarily prevent spinal cord ischemia. Jacobs et al. (2002a) performed the prospective documentation of patent segmental arteries during TAAA repair and the assessment of their functional contribution to the spinal cord blood supply in 184 patients, evaluated by myogenic motor evoked potential (MEP) or TCE-evoked electromyogram (EMG). In eight of 68 type I cases, no segmental arteries were seen between the fifth thoracic vertebrae (T5) and the first lumbar vertebrae (L1) and MEP levels remained adequate because of distal aortic perfusion. In 18 of 91 type II cases, the aortic segment T5 to L1 did not contain patent arteries, and in six of these patients, the segment L1 to L5 did not have lumbar arteries either. In the latter patients, MEP levels depended on the pelvic circulation provided with the left heart bypass graft. In the other 12 of 91 type II cases, only the lumbar arteries were patent between L3 and L5. In seven of 25 type III cases, the MEP levels also depended on lumbar arteries L3 to L5. In three of 25 cases, no segmental arteries were available, and MEP recovered after the reperfusion of the pelvic circulation. These findings indicate that in patients with TAAA, especially in Type II

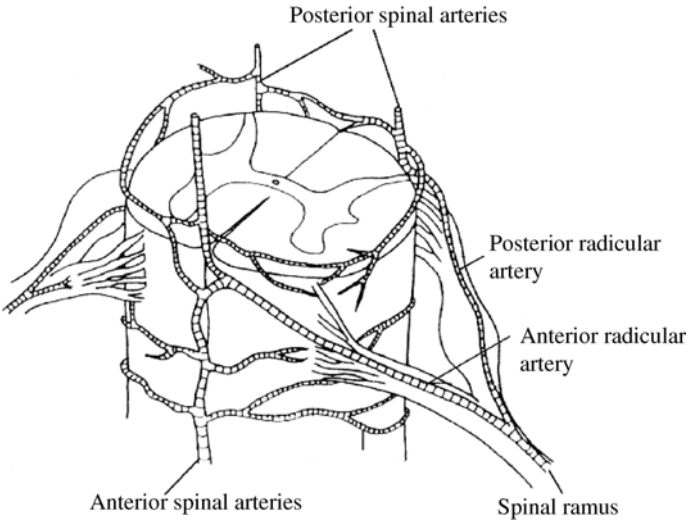

Fig. 1.23. Spinal cord blood supply in a normal patient. The anterior spinal artery supplies two thirds of the ventral spinal cord including motor neurons, whereas two posterior arteries supply one third of the dorsal part of the spinal cord. In normal patients, the Adamkiewicz artery mainly provides blood supply to the anterior horn in the spinal cord. Therefore, it is important to identify the Adamkiewicz artery using magnetic resonance angiography or multidetector row computed tomography preoperatively. (From Gotoh, 1993, with permission)

and III, blood supply to the spinal cord depends upon a highly variable collateral system (Jacobs et al., 2002b).

1.5.2.2.1 Monitoring During TAAA Surgery

MEP versus somatosensory evoked potential (SSEP) from the scalp. In patients with TAAA, the evoked potentials on Cz–FPz from the scalp are recorded in response to posterior tibial nerve stimulation. As mentioned above, the abnormality of the SSEP is defined as 50% decrease in amplitude and/or more than 1 ms prolongation in latency. Both the amplitude and latency of SSEP are influenced by anesthetics and hypothermia during operation. SSEP after stimulation of the posterior tibial nerve or common peroneal nerve shows function of sensory information in the posterior horn and column, which has a blood supply from the posterior spinal arteries. On the other hand, the anterior horn receives a blood supply from the anterior spinal artery as shown in Fig. 1.23. Thus, SSEP is not suitable for monitoring of motor dysfunction during TAAA operation (Dong et al., 2002; Meylaerts et al., 1999). Crawford et al. (1988) showed that for detection of motor dysfunction the incidence of false-negative SSEP response was 13% and false-positive response was 67%. In the other study, it took 7–30 min to detect abnormality in SSEP after spinal cord ischemia (de Haan et al., 1998). Dong et al. (2002) reported that a total of 16 patients among 56 TAAA patients (28.6%) showed evidence of spinal cord ischemia in myogenic MEP responses, only 4 of whom had delayed congruent SSEP changes. SSEP changes appeared 3–12 min after loss of myogenic MEP. This may be due to the fact that the

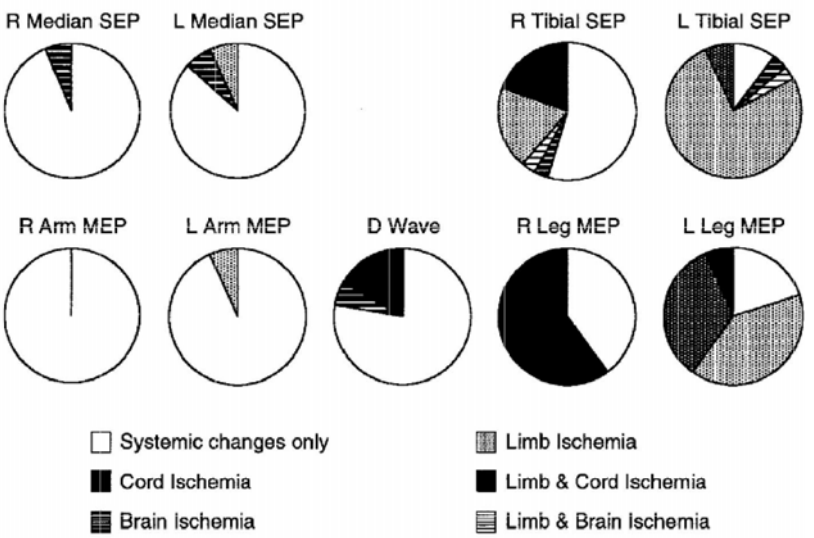

FIG. 1.24. Causes of the evoked potential changes. The abnormal somatosensory evoked potential (SSEP) responses reflect mainly systemic alterations in addition to brain and spinal cord ischemia and lower extremity ischemia due to cannulation for cardiopulmonary bypass (CPB). The left femoral artery is usually used for cannulation for CPB. Therefore, left leg ischemia often occurs, and thus responses of left leg SSEP and myogenic motor evoked potential (*MEP*) disappear (see Fig. 1.17). Myogenic MEP is more susceptible to spinal cord ischemia than spinal MEP. (From MacDonald and Janusz, 2002, with permission)

metabolic rate in posterior horn cells is lower than that in anterior horn cells in spinal cord (Marcus et al., 1977). Further, the high vulnerability of the anterior horn cells to ischemia is demonstrated in magnetic resonance imaging (MRI) (Mawad et al., 1990). Therefore, monitoring of SSEP of itself may not be a reliable method to detect spinal cord ischemia during TAAA operation.

Although the sensitivity of SSEP monitoring is less sensitive for motor dysfunction caused by spinal cord ischemia, the measurement of SSEPs provide detection of systemic alterations and cerebral or limb ischemia as shown in Fig. 1.24 (MacDonald and Janusz, 2002). Therefore, simultaneous MEP and SSEP measurements are important for monitoring spinal cord ischemia during TAAA operations.

TCE-Evoked Electromyogram (MEP). Cerebral cortex stimulation techniques include transcranial electrical stimulation (TCES) and transcranial magnetic simulation (TCMS). Magnetic stimulation may elicit primarily I waves (Burke and Hicks, 1998), because it is essentially electrical brain stimulation, though the delivery of electromagnetic energy to the head is via a magnetic field rather than by directly conducted electrical current. The I waves provoked by magnetic stimulation are greatly suppressed by anesthetics. Therefore, at present the TCMS technique may not be suitable for intraoperative MEP monitoring during TAAA operation (Legatt, 2002).

MEP responses can be recorded from the lower lumbar spinal cord (spinal MEPs), peripheral nerve (nerve MEPs), or from muscles (myogenic MEPs) as shown in Fig. 1.25 (de Haan et al., 1998).

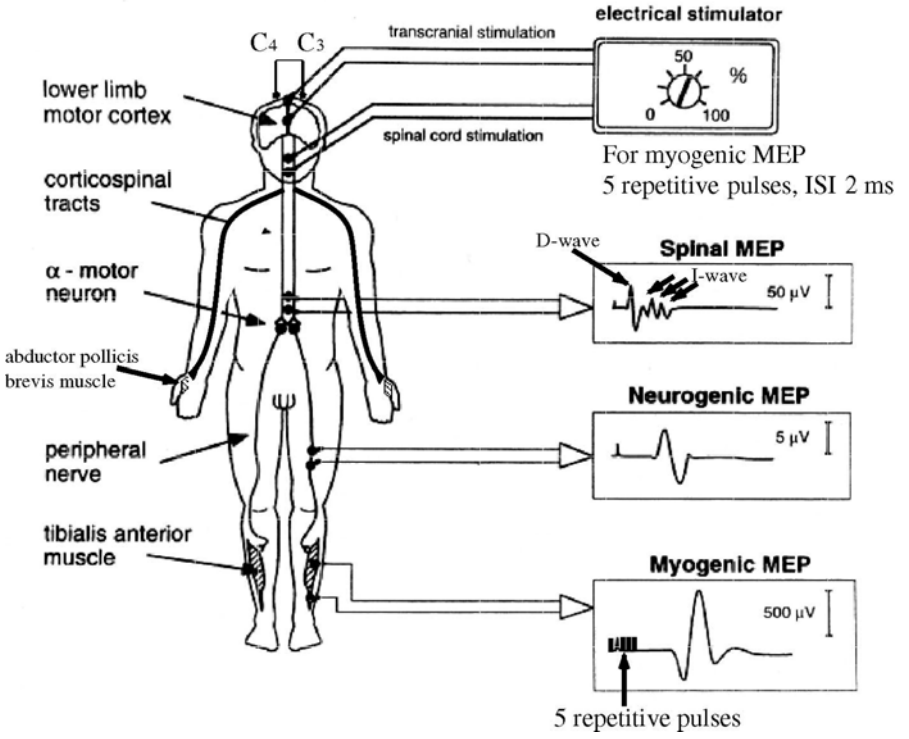

Fig. 1.25. Schematic motor evoked potential (*MEP*) monitoring. Usually, transcranial electrical stimulation (TCES) is performed through the electrodes placed at C3–C4 (International 10–20 system) on the scalp (interstimulus interval: 2 ms and 5–6 repetitive stimulations). MEP responses can be measured at lumbar spinal cord (spinal MEPs), peripheral nerve (neurogenic MEPs), and muscles (myogenic MEPs). Among these, myogenic MEP is the most reliable method to detect spinal cord ischemia using 5–6 repetitive stimulations. During myogenic MEP monitoring, the muscle T1 response in train-of-four monitoring should be kept 45%–55% of baseline (From de Haan et al., 1997, with permission)

Spinal MEP. As shown in the previous section, TCES typically produces a D wave followed by I waves recorded from the posterior epidural space of the lower lumbar spinal cord. The D wave reflects direct activation of the pyramidal cell axons that leave the cortex and interneurons. The I waves are generated by activation of cortical interneurons, with subsequent transynaptic activation of the cortical pyramidal neurons that contribute to the corticospinal tract (Amassian et al., 1987). In experimental animals, the D wave persists when the stimulating electrode is advanced through the cortex into the underlying white matter, since the axons of the corticospinal tract are still being stimulated, while the I waves are lost when the electrode is placed too far from the cortex to stimulate the cortical interneurons.

Temporary inactivation of the cortical circuitry or ablation of the cortex will also eliminate the I waves, which are dependent on cortical synaptic function (Paton and Amassian, 1960).

Spinal motor-evoked potentials (MEPs) are not influenced by neuromuscular blocking agents and anesthetic agents, and relatively stable responses are obtained from run to run without the need for a multipulse stimulator used in TCE-evoked electromyogram (EMG) as described below. However, this monitoring reflects only conduction in the corticospinal tracts, and the loss of D-wave reflections is more likely to occur at a time when permanent damage has ocurred in the spinal cord (Legatt, 2004). In addition, spinal monitoring of D waves may fail to detect unilateral damage to the motor pathways (Burke and Hicks, 1998; MacDonald, 2002), and the D-wave amplitude decreases toward lower lumbar epidural space as shown in Fig. 1.26 (MacDonald and Janusz, 2002).

In several animal experiments, the abnormal spinal MEPs appeared 11–24 min after spinal cord ischemia. de Haan et al. (1996) reported that the responses were detected from the lumbar epidural space in spinal MEP and from the soleus muscle in TCE-evoked electromyogram (EMG), and the effect of aortic occlusion was assessed in nine rabbits. The peak-to-peak amplitude of the direct D wave recorded from the epidural space gradually decreased during aortic occlusion in eight animals and increased in one. The median (10th to 90th percentiles) time to a 50% reduction in amplitude was 11.3 (3–22) min. In contrast, TCE-evoked electromyogram (EMG) disappeared within 2 min after the start of occlusion in all animals. Furthermore, in dog spinal cord experiments the observed time between onset of spinal ischemia and appearance of abnormal responses were 21 ± 7 and 24 ± 4 min, respectively (Elmore et al., 1991; Reuter et al., 1992). The time to detect the abnormal responses in spinal MEPs is too long to allow prompt interventions, when spinal cord ischemia may happen during TAAA operations.

Peripheral Nerve Action Potentials. To avoid the use of TCES and the paralyzed muscles with muscle relaxants and anesthetics, which attenuate or abolish the TCE-evoked electromyogram (EMG), a technique of rostral spinal cord stimulation and

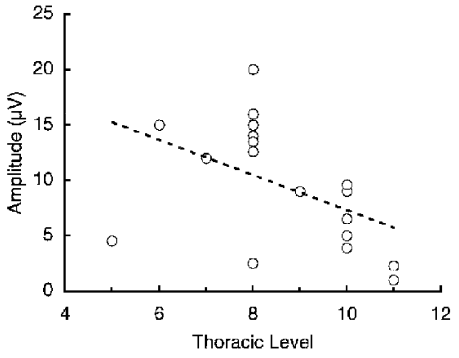

FIG. 1.26. D-wave amplitude decreases toward lower thoracic levels during spinal MEP monitoring. The blood supply to spinal cord is usually supplied from the Adamkiewicz artery derived from T8–L1. In type II and III aneurysms, collateral circulation such as lumbar and/or pelvic circulation is developed. Therefore, the D wave should be recorded at the lumbar level. However, the amplitude gradually decreases toward lower levels. This is also the problem in monitoring spinal cord ischemia using spinal MEP. (From MacDonald and Janusz, 2002, with permission)

recording from peripheral nerves was proposed (Owen et al., 1988). The large afferent somatosensory fibers conducting within the peripheral nerves continue to the dorsal columns without synapse, and it has been demonstrated that neurogenic motor evoked potentials reflect mainly the retrograde conduction within the somatosensory fibers (Toleikis et al., 2000). In fact, in two patients during spinal deformity corrective surgery the anterior spinal cord injury preserved SSEP and neurogenic MEPs postoperatively (Minahan et al., 2001), whereas paraplegia was identified immediately upon recovery from anesthesia. Therefore, spinal neurogenic MEP seems to be not suitable for the monitoring of motor dysfunction in the spinal cord.

TCE-evoked electromyogram (EMG). TCE-evoked electromyogram (EMG) elicited by single pulse stimulation has been shown to be greatly depressed with volatile anesthetics like nitrous oxide (Zentner and Ebner, 1989), isoflurane (Kalkman et al., 1991), and sevoflurane (Kawaguchi et al., 1998) as well as intravenous anesthetic agents such as barbiturate (Taniguchi et al., 1993), propofol (Kalkman et al., 1992; Taniguchi et al., 1993), and midazolam (Kalkman et al., 1992; Schonle et al., 1989). Etomidate exerted the least depressive action on TCE-evoked electromyogram (EMG) among the above intravenous anesthetic agents (Kalkman et al., 1992; Taniguchi et al., 1993). In contrast, ketamine (Ghaly et al., 2001) and opioids (Kalkman et al., 1992; Thees et al., 1999) do not influence the TCE-evoked electromyogram (EMG).

To overcome these depressant actions by anesthetics during measurements of TCE-evoked electromyogram (EMG), TCES using trains of five or six pulses (interstimulus interval, 2 ms) was recently developed (Multipulse D-185, Digitimer Ltd, Welwyn Garden City, UK). This is because temporal summation of the excitatory postsynaptic potentials amplifies TCE-evoked electromyogram (EMG) and reduces variability. Kalkman et al. (1995) reported that application of paired TCES increases amplitudes and reproducibility of TCE-evoked electromyogram (EMG) during anesthetic-induced depression of the motor system. The effect may represent temporal summation of stimulation, which means that the first stimulus lowers the excitation threshold of the cortical and spinal motor neurons, thereby facilitating the initiation of neuronal discharge by the second stimulus. Each time a neuronal terminal depolarizes, sodium channels open for a period of 1–2 ms. After closure of the channels, the resulting excitatory postsynaptic potential decreases over the next 10–15 ms. A second opening of the same channels within this period will result in an augmentation (temporal summation) of the excitatory postsynaptic potential. The more rapid the rate of repetitive depolarization, the greater is the postsynaptic potential that develops. The counterpart of temporal summation is spatial summation, which is the summation of excitatory postsynaptic potentials from several synaptic terminals converging on the motor neuron. If paired TCES increases the number of cortical motor neuron firings, the spatial summation may occur at the spinal level (Guyton, 1991).

Following are the usual procedures for monitoring TCE-evoked electromyogram (EMG) (TCE-evoked EMG) during TAAA operations. The electrodes are placed at Cz–Fz or C3–C4 (International 10–20 system) on the scalp. The electrodes placed at C3–C4 are used for obtaining compound muscle action potentials (CMAP), EMG, from both the biceps brachii muscle or abductor pollicis brevis muscle in upper and tibialis anterior muscle or abductor hallucis muscle in lower extremities, and those at Cz–Fz are used only for EMG from the muscles in lower extremities, as shown in Fig.

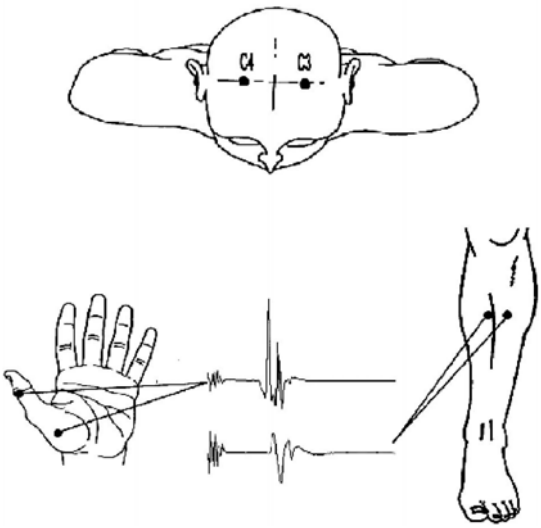

Fig. 1.27. Transcranial electrical stimulation (TCES) sites on the scalp and recording sites for the muscles in upper and lower extremities. Usually, C3–C4 is used for TCES. In upper extremities, biceps brachii or abductor pollicis brevis muscle is used to obtain compound muscle action potentials (CMAP) as a control. In lower extremities, tibialis anterior muscle or abductor hallucis muscle is used for recording CMAP. (From Deletis et al., 2001, with permission)

1.27 (Deletis et al., 2001). Usually, the electrodes are placed at C3–C4, since the EMG in the upper extremities is regarded as a control. Trains of five or six with interstimulus interval at 2 ms are usually used. As the EMG induced by TCES is large in amplitude, averaging techniques as used in SSEP are not necessary. The EMG is influenced by anesthetics and muscle relaxants. For anesthesia during TAAA operation, propofol and opioids (fentanyl or remifentanyl) with or without ketamine are usually used. Although propofol greatly attenuates EMG, this effect may be overcome by high-frequency repetitive stimulation. As a component of total intravenous agents (TIVA), propofol combined with opioids has produced acceptable conditions for TCE-evoked electromyogram (EMG) (TCE-evoked EMG) (Calancie et al., 1998; Pechstein et al., 1998).

Recently, Kakinohana et al. (2003) reported that during the immediate reflow following a noninjurious interval of spinal ischemia, intrathecal morphine potentiates transient spastic paraplegia in rats and a patient with TAAA. Reversal by naloxone suggests that this effect results from an opioid receptor (μ receptor)-mediated potentiation of a transient block of inhibitory neurons caused by spinal ischemia. There is a selective degeneration of small- and medium-sized interneurons typically localized between laminae V and VII (Taira and Marsala, 1996), in which the inhibitory interneurons as well as facilitating interneurons exist (Ghez and Krakauer, 2000). In spastic paraplegia, excitatory tonic activity in the spinal motor neurons might predominate as the result of a decrease in inhibition mediated by inhibitory interneurons. This finding suggests a caution that opioids might aggravate such interneuronal

damage. Therefore, if the TCE-evoked EMG decreases to raise suspicion of spinal cord ischemia following aortic clamp and does not show recovery, the anesthetic agents should be changed to another inhalant (isoflurane) or ketamine anesthesia for fear of aggravating the possible interneuronal damage due to opioids in spinal cord.

For monitoring TCE-evoked EMG, it is necessary to keep the effect of muscle relaxants constant. Using continuous intravenous muscle relaxants, the T1 response of train of four should be kept at 45%–55% of baseline to obtain stable TCE-evoked EMG responses (van Dongen et al., 1999).

However, TCE-evoked EMG monitoring cannot always predict neurologic outcome after spinal cord ischemia in rats and humans (Kakinohana et al., 2005). In this study, complete spastic paraplegic occurred after spinal cord ischemia despite the preservation of TCE-evoked EMG.

The abnormal responses in TCE-evoked EMG is usually defined as 25% of control (Jacobs et al., 2002a; Lips et al., 2002). If the TCE-evoked EMG both in the upper and lower extremities show abnormal, systemic factors like anesthesia depth, doses of muscle relaxants, cerebral ischemia, or systemic hypotension should be considered.

Chapter 2
Diagnosis by Spinal Cord Potentials of Spinal Diseases

Hiroyuki Shimizu and Koki Shimoji

Morphological diagnosis of spinal diseases has recently been improved by the development of computed tomography (CT), magnetic resonance imaging (MRI), and several types of endoscope. On the other hand, functional diagnosis of the spinal diseases has continued to be made through clinical signs and EEG/evoked potentials from the scalp. Recent application of spinal cord potentials to the functional diagnosis of spinal cord diseases has shown great promise for the objective characterization of their pathophysiology (Yamada et al., 2004).

Not only somatosensory evoked spinal cord potentials (SCPs) but also motor evoked SCPs may provide more accurate functional diagnosis of the diseases. Noninvasive surface recording may suffice for such needs in some cases. However, when more detailed measures of the potentials are needed, recording from the spinal epidural space that is close to the cord separated only by the dura may be recommended. For instance, the potentials from the skin surface are so small and difficult for spatial discrimination that it is difficult to analyze the segmental functions and slow components with these potential changes (Fig. 2.1). As described previously, if an obstacle lies between the recording electrodes and lesions of the cord, recorded potentials may lead to misjudgment of the potentials.

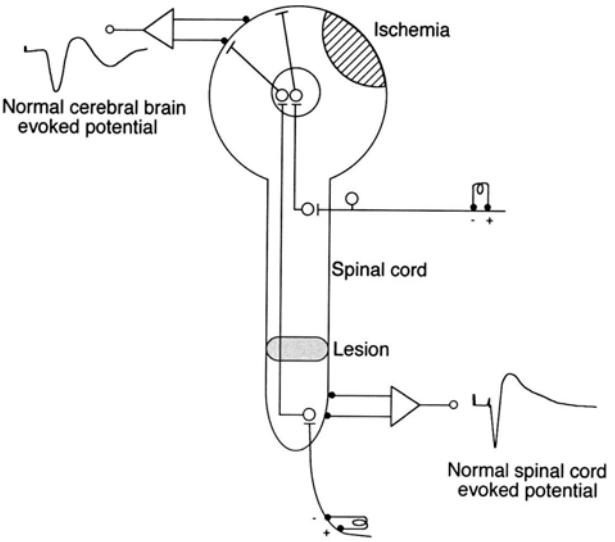

Fig. 2.1. Schematic presentation of detectable and undetectable areas of ischemia or lesion by diseases or during surgery by a specific recording arrangement of somatosensory evoked potentials. When ischemia or lesion exists in the spinal cord above the level of the spinal cord potential (SCP) recording (T12/L1 level) in response to tibial nerve stimulation, the segmental SCP may remain unchanged. Simultaneous recording from the scalp may or may not detect ischemia when ischemia exists in the region outside the receptive area. The scalp somatosensory evoked potential may also remain unchanged in response to median nerve stimulation even when ischemia/lesion exists in the contralateral area of the brain or below the level of the cervical cord. Thus, when ischemia is present in the brain ipsilateral to the stimulation, evoked potentials may not reveal any abnormalities under this stimulation and recording arrangement. Bilateral and/or multispatial stimulation and recording arrangements are needed in such cases for accurate monitoring of spinal cord as well as brain ischemia/lesion

2.1 Spinal Cord Potentials in Patients with ALS

Shimizu et al. (1979a,b) reported that the slow potentials (negative and positive potentials) evoked by descending volleys could not be demonstrated in any of the six patients who all showed typical signs of amyotrophic lateral sclerosis (ALS) (muscle weakness, muscular atrophy, fasciculation, hyper-reflexia) (Fig. 2.2). There were, however, no significant changes in conduction velocities of ascending and descending impulses along the cord in these patients. The mechanisms for absence of the slow potentials evoked by descending volleys in patients with ALS, in which the pyramidal tract is affected, remains to be answered.

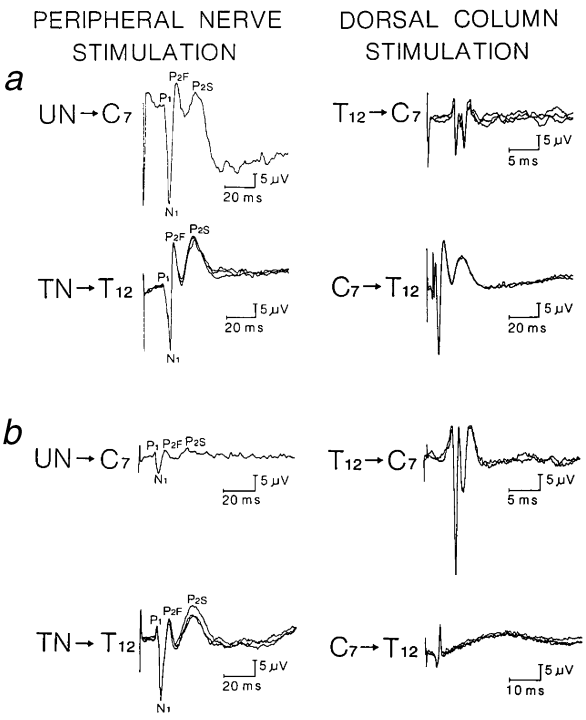

FIG. 2.2. Segmental spinal cord potentials (SCPs) (*left*), and conducting and descending SCPs (*right*) in a normal subject (**a**) and a patient with amyotrophic lateral sclerosis (ALS) (47 years, male) (**b**). *UN → C7*, ulnar nerve stimulation and recording from the posterior epidural space at the C7 vertebral level (segmental SCPs); *TN → T12*, tibial nerve stimulation and recording from the T12 vertebral level (segmental SCP); *T12 → C7*, spinal cord stimulation from the posterior epidural space at the T12 vertebral level and recording from the posterior epidural space at the C7 vertebral level (conductive SCP); *C7 → T12*, spinal cord stimulation from the epidural space at the C7 vertebral level and recording from the posterior epidural space at the T12 vertebral level (descending SCP). Note that there are no slow components following the single spike potential in the descending SCP in the patient with ALS (From Shimizu et al., 1979a,b)

2.2 Spinal Cord Potentials in Patients with Tabes Dorsalis

Neurosyphilis is sometimes found in the 3rd or 4th stage of syphilis infection, and shows good recovery when it is properly treated (Jacquemin et al., 2003). Figure 2.3a shows histological sections of the spinal cord of a patient suffering from neurosyphilis (69 years, male). He complained of paraparesis and an intractable stabbing pain in his back, which was relieved by strong mechanical tapping of the back skin or transcutaneous electrical stimulation. Histology demonstrated degenerations of the dorsal column and superficial layers of the dorsal horn. The SCPs in this patient several months before his death showed no significant potential configurations that could be discriminated from the background activity, recorded from the posterior epidural

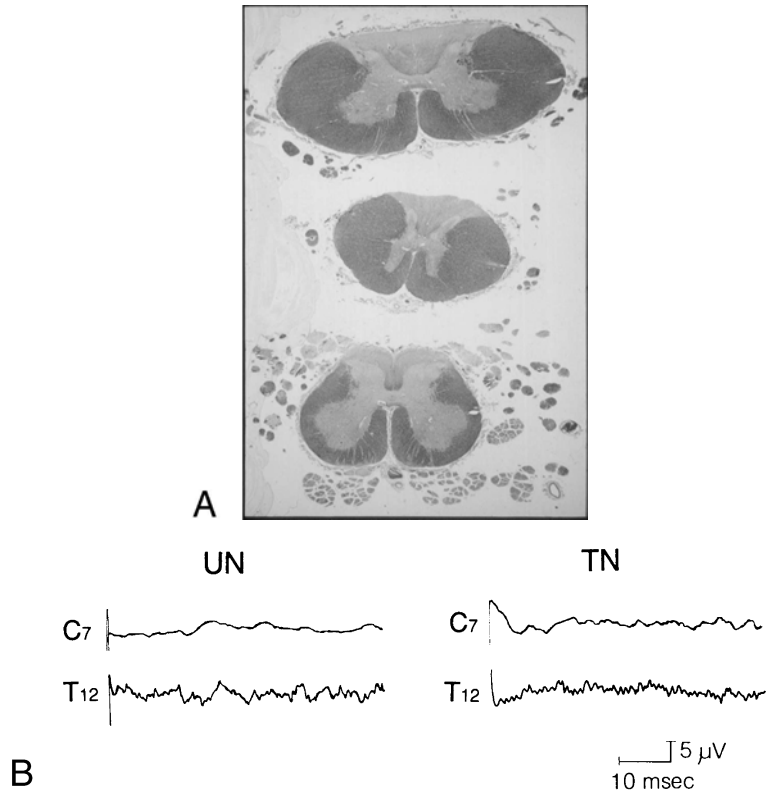

Fig. 2.3A,B. Spinal cord potentials in a patient with tabes dorsalis. **A** Cross section of the spinal cord in a patient (69 years, male) with tabes dorsalis following his death. Note that the dorsal column of the spinal cord and dorsal root entry zone are completely degenerated in the cervical, thoracic, and lumbar cord. **B** Spinal cord potentials in the same patient. Ulnar nerve (*UN*) stimulation at the elbow produced no significant potentials in the posterior epidural space either at the C7 or T12 vertebral level. Tibial nerve (*TN*) stimulation at the popliteal space also did not produce any appreciable potential changes in the posterior epidural space either at the C7 or T12 vertebral space ($n = 25$). (Shimizu et al., unpublished data)

space both at the cervical and lumbar levels (Fig. 2.3b). The SCP findings also indicate that the segmental SCPs are produced by volleys in large peripheral nerve fibers, since the disease mainly involves the symptoms and signs caused by degeneration of large nerve fibers.

2.3 Spinal Cord Potentials in Patients with Spinal Tumors

Motor paresis with segmental pain and dysesthesia in a patient disclosed an intraspinal malignant astrocytoma by CT scan and MRI. Nerve conduction along the cord after electrical stimulation of the cauda equina was completely blocked (Fig. 2.4).

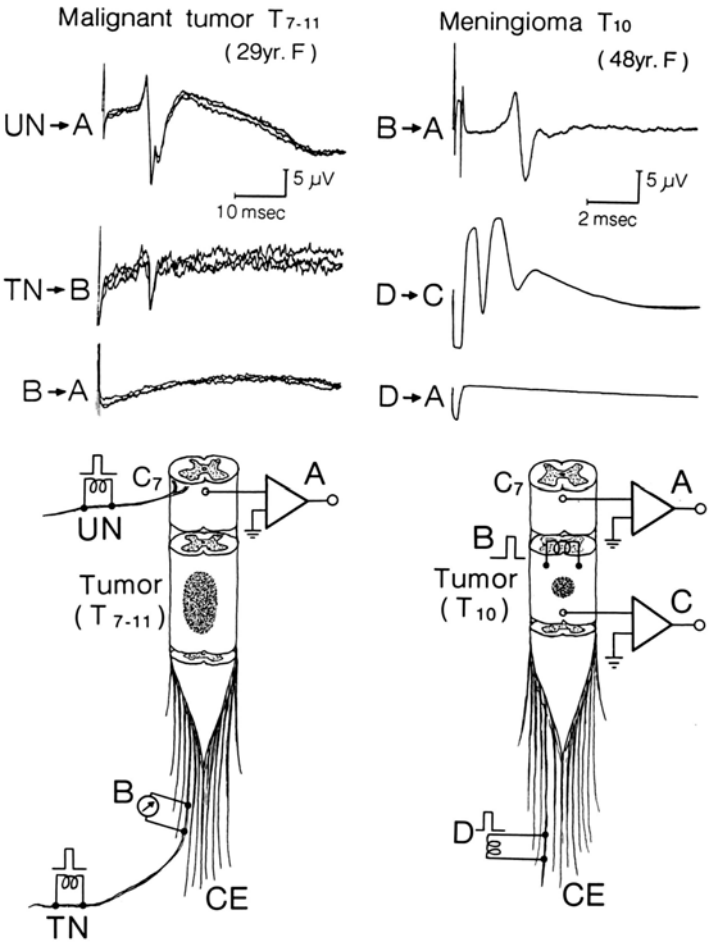

Fig. 2.4. Spinal cord potentials in a patient with a spinal cord tumor recorded before surgery. *Left traces* The SCPs in a patient (29 years, female) with a malignant tumor of the spinal cord that occupied the T7–T11 levels. Ulnar nerve stimulation produced normal segmental SCP at the level of C7 ($UN \rightarrow A$). Tibial nerve stimulation provoked also the nerve action potential at the cauda equina ($TN \rightarrow B$), while cauda equina stimulation did not produce any potential change at the level of C7 ($B \rightarrow A$). *Right traces* The SCPs in a patient (48 years, female) with meningioma at the T10 level. Spinal cord stimulation at the level of T9 with 2-times threshold strength produced a single spike potential ($B \rightarrow A$). A strong (5-times threshold strength) cauda equina stimulation from the epidural space at the level of L4 vertebral level produced polyphasic spike potentials at T11 just below the level of the meningioma ($D \rightarrow C$), but not at the vertebral level of C7 ($D \rightarrow A$). All recordings and stimulations are made from the posterior epidural space except tibial nerve stimulation. *Bottom* Schematic illustrations show the simulating and recording electrode levels. *CE*, cauda equina. (Shimizu et al., unpublished data)

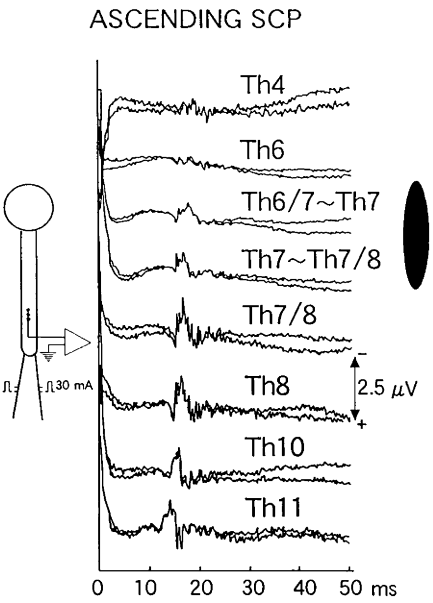

Fig. 2.5. Ascending spinal cord potentials (*SCP*) in a patient with a spinal subarachnoid cyst located at the T7–T8 level. Recording was made by an electrode attached to the tip of a fine epidural fiberscope, which was moving backward step by step from the 4th thoracic level (*Th4*) along the cord through the posterior epidural space. A stimulating catheter electrode was inserted into the epidural space at the level of the L5/S (illustrated in the *left insert*). Note that the ascending SCPs are suppressed above the cyst and at the region occupied by the cyst, and then suddenly increase below the level of the cyst. The fiberscope also identified the cyst by subarachnoid observation before surgical removal. (Unpublished data, Shimoji et al.)

Another patient with a meningioma complained of light paraparesis and deep sense disturbance in the legs. Neurophysiological tests in this patient also showed that the conductive SCP was completely lost (Fig. 2.4). Thus, the neurophysiological findings in the patients with spinal tumors seem to be more sensitive than clinical signs and symptoms. On the other hand, although the size of the spinal cord became almost one third of the unaffected area, the electrophysiological test demonstrated fairly well maintained conduction along the cord (Fig. 2.5). The mechanism of the differences between these diseases in neurophysiological tests found in the conduction along the cord may arise from different speeds of the pathological changes in the spinal cord. Thus, some discrepancies between clinical signs and electrophysiological findings frequently exist just as do those between clinical signs and histologies, and need to be further studied.

References

Section A: Chapter 1

Al-Chaer ED, Lawand NB, Westlund KN, Willis WD. Visceral nociceptive input into the ventral posterolateral nucleus of the thalamus: a new function for the dorsal column pathway. J Neurophysiol 1996a;76:2661–74.

Al-Chaer ED, Lawand NB, Westlund KN, Willis WD. Pelvic visceral input into the nucleus gracilis is largely mediated by the postsynaptic dorsal column pathway. J Neurophysiol 1996b;76:2675–90.

Al-Chaer ED, Westlund KN, Willis WD. Nucleus gracilis: an integrator for visceral and somatic information. J Neurophysiol 1997;78:521–7.

Al-Chaer ED, Feng Y, Willis WD. Comparative study of viscerosomatic input onto postsynaptic dorsal column and spinothalamic tract neurons in the primate. J Neurophysiol 1999;82: 1876–82.

Angaut-Petit D. The dorsal column system: II. Functional properties and bulbar relay of the postsynaptic fibres of the cat's fasciculus gracilis. Exp Brain Res 1975;22:471–93.

Apkarian AV, Hodge CJ. Primate spinothalamic pathways. III. Thalamic terminations of the dorsolateral and ventral spinothalamic pathways. J Comp Neurol 1989;288:493–511.

Apkarian AV, Shi T. Squirrel monkey lateral thalamus. I. Somatic nociresponsive neurons and their relation to spinothalamic terminals. J Neurosci 1994;14:6779–95.

Berne RM, Levy MN. Principles of physiology. 3rd ed. St. Louis: Mosby; 2000.

Bernard JF, Besson JM. The spino(trigemino)pontoamygdaloid pathway: electrophysiological evidence for an involvement in pain processes. J Neurophysiol 1990;63:473–90.

Boivie J. An anatomical reinvestigation of the termination of the spinothalamic tract in the monkey. J Comp Neurol 1979;186:343–70.

Brown AG. Cutaneous afferent fibre collaterals in the dorsal columns of the cat. Exp Brain Res 1968;5:293–305.

Brown AG. Organization of the spinal cord: the anatomy and physiology of identified neurones. Berlin: Springer; 1981.

Brown PB, Fuchs JL. Somatotopic representation of hindlimb skin in cat dorsal horn. J Neurophysiol 1975;38:1–9.

Burgess PR, Clark FJ. Dorsal column projection of fibres from the cat knee joint. J Physiol 1969;203:301–15.

Burstein R, Giesler GJ. Retrograde labeling of neurons in spinal cord that project directly to nucleus accumbens or the septal nuclei in the rat. Brain Res 1989;497:149–54.

Burstein R, Potrebic S. Retrograde labeling of neurons in the spinal cord that project directly to the amygdala or the orbital cortex in the rat. J Comp Neurol 1993;335:469–85.

Burstein R, Cliffer KD, Giesler GJ. Direct somatosensory projections from the spinal cord to the hypothalamus and telencephalon. J Neurosci 1987;7:4159–64.

Burstein R, Cliffer KD, Giesler GJ. Cells of origin of the spinohypothalamic tract in the rat. J Comp Neurol 1990;291:329–44.
Carlton SM, Westlund KN, Zhang D, Sorkin LS, Willis WD. Calcitonin gene-related peptide containing primary afferents synapse on primate spinothalamic tract cells. Neurosci Lett 1990;109:76–81.
Carlton SM, Westlund KN, Zhang D, Willis WD. GABA-immunoreactive terminals synapse on primate spinothalamic tract cells. J Comp, Neurol 1992;322:528–37.
Carpenter MB, Sutin J. Human neuroanatomy. 8th ed. Baltimore: Williams and Wilkins; 1983.
Cliffer KD, Burstein R, Giesler GJ. Distributions of spinothalamic, spinohypothalamic and spinotelencephalic fibers revealed by anterograde tracing of PHA-L in rats. J Neurosci 1991;11:852–68.
Cliffer KD, Hasegawa T, Willis WD. Responses of neurons in the gracile nucleus of cats to innocuous and noxious stimuli: Basic characterization and antidromic activation from the thalamus. J Neurophysiol 1992;68:818–32.
Coulter JD, Jones EG. Differential distribution of cortico-spinal projections from individual cytoarchitectonic fields in the monkey. Brain Res 1977;129:335–40.
Creutzfeldt OD. Cortex cerebri: performance, structural and functional organization of the cortex. Oxford: Oxford University Press; 1995.
Crosby EC, Humphrey T, Lauer EW. Correlative anatomy of the nervous system. New York: MacMillan; 1962.
De Groat WC. Anatomy of the central neural pathways controlling the lower urinary tract. Eur Urol 1998;34(Suppl 1):2–5.
Ferrington DG, Downie JW, Willis WD. Primate nucleus gracilis neurons: Responses to innocuous and noxious stimuli. J Neurophysiol 1988;59:886–907.
Gingold SI, Greenspan JD, Apkarian AV. Anatomic evidence of nociceptive inputs to primary somatosensory cortex: relationship between spinothalamic terminals and thalamocortical cells in squirrel monkeys. J Comp Neurol 1991;308:467–90.
Grant G, Boivie J, Silfvenius H. Course and termination of fibres from the nucleus z of the medulla oblongata. An experimental light microscopical study in the cat. Brain Res 1973;55:55–70.
Guan Y, Guo W, Zou SP, Dubner R, Ren K. Inflammation-induced upregulation of AMPA receptor subunit expression in brain stem pain modulatory circuitry. Pain 2003;104:401–13.
Haber LH, Martin RF, Chatt AB, Willis WD. Effects of stimulation in nucleus reticularis gigantocellularis on the activity of spinothalamic tract neurons in the monkey. Brain Res 1978;153:163–8.
Hirshberg RM, Al-Chaer ED, Lawand NB, Westlund KN, Willis WD. Is there a pathway in the posterior funiculus that signals visceral pain? Pain 1996;67:291–305.
Holstege G. The somatic motor system. In: Holstege G, Bandler R, Saper CB, editors. The emotional motor system. Progress in brain research vol. 107. Amsterdam: Elsevier; 1996. p. 9–26.
Hylden JLK, Hayashi H, Bennett GJ, Dubner R. Spinal lamina I neurons projecting to the parabrachial area in the cat midbrain. Brain Res 1985;336:195–8.
Jones EG. The thalamus. New York: Plenum; 1985.
Kevetter GA, Willis WD. Spinothalamic cells in the rat lumbar cord with collaterals to the medullary reticular formation. Brain Res 1982;238:181–5.
Kuypers HGJM. Anatomy of the descending pathways. In: Brooks VB, editor. Handbook of physiology. Section 1. The nervous system. vol. 2, Motor control, Part 1. Bethesda: American Physiological Society; 1981; pp. 597–666.
Light AR, Perl ER. Spinal termination of functionally identified primary afferent neurons with slowly conducting myelinated fibers. J Comp Neurol 1979;186:133–50.
Lissauer H. Beitrag zum Faserverkauf im Hinterhorn des menschlichen Ruckenmark und zum Verhalten desselben bei Tabes dorsalis. Arch Psychiat Nervenkrankh 1886;17:377–438.
Mehler WR. The anatomy of the so-called "pain tract" in man: an analysis of the course and distribution of the ascending fibers of the fasciculus anterolateralis. In: French JD, Porter RW, editors. Basic research in paraplegia. Springfield: Charles C. Thomas; 1962. p. 26–55.

Mehler WR, Feferman ME, Nauta WJH. Ascending axon degeneration following anterolatreral cordotomy. An experimental study in the monkey. Brain 1960;83:718–51.
Mettler FA. Neuroanatomy. St. Louis: Mosby; 1948.
Nadelhaft I, Roppolo J, Morgan C, DeGroat WC. Parasympathetic preganglionic neurons and visceral primary afferents in monkey sacral spinal cord revealed following application of horseradish peroxidase to pelvic nerve. J Comp Neurol 1983;216:36–52.
Nagy GG, Al-Ayyan M, Andrew D, Fukaya M, Watanabe M, Todd AJ. Widespread expression of the AMPA receptor GluR2 subunit at glutamatergic synapses in the rat spinal cord and phosphorylation of GluR1 in response to noxious stimulation revealed with an antigen-unmasking method. J Neurosci 2004;24:5766–77.
Nauta HJW, Soukup VM, Fabian RH, Lin JT, Grady JJ, Williams CGA, Campbell GA, Westlund KN, Willis WD. Punctate mid-line myelotomy for the relief of visceral cancer pain. J Neurosurg (Spine 1) 2000;92:125–30.
Nolte J. The human brain. An introduction to its functional anatomy. 5th ed. St. Louis: Mosby; 2002.
Oguro K, Kobayashi J, Aiba H, Kobayashi S, Hojo H. Electrographic study of brainstem reflex myoclonus. Electromyogr Clin Neurophysiol 1997;37:99–106.
Patterson JT, Head PA, McNeill DL, Chumg K, Coggeshall RE. Ascending unmyelinated primary afferent fibers in the dorsal funiculus. J Comp Neurol 1989;290:384–90.
Patterson JT, Coggeshall RE, Lee WT, Chung K. Long ascending unmyelinated afferent axons in the rat dorsal column: Immunohistochemical localizations. Neurosci Lett 1990;108:6–10.
Paxinos G, Mai JK. The human nervous system. Amsterdam: Elsevier; 2004.
Petit D, Burgess PR. Dorsal column projection of receptors in cat hairy skin supplied by myelinated fibers. J Neurophysiol 1968;31:849–55.
Phillips CG, Porter R. Corticospinal neurons: their role in movement. New York: Academic Press; 1977.
Pompeiano O, Brodal A. Spino-vestibular fibers in the cat. An experimental study. J Comp Neurol 1957;108:353–82.
Rexed B. The cytoarchitectonic organization of the spinal cord in the cat. J Comp Neurol 1952;96:415–66.
Rexed B. A cytoarchitectonic atlas of the spinal cord in the cat. J Comp Neurol 1954;100:297–380.
Romanes GJ. Cunningham's textbook of anatomy. 12th ed. Oxford: Oxford University Press; 1981.
Sadjapour K, Brodal A. The vestibular nuclei in man: A morphological study in the light of experimental findings in the cat. J Hirnforsch 1968;10:299–319.
Schaible HG, Neugebauer V, Cervero F, Schmidt RF. Changes in tonic descending inhibition of spinal neurons with articular input during the development of acute arthritis in the cat. J Neurophysiol 1991;66:1021–32.
Scheibel ME, Scheibel AB. Terminal axon patterns in cat spinal cord. II. The dorsal horn. Brain Res 1968;9:32–58.
Schoenen J, Faull RL. Spinal cord; cyto- and chemoarchitecture. In: Paxinos G, Mai JK, editors. The human nervous system. 2nd ed. Amsterdam: Elsevier; 2004. p. 190–232.
Spike RC, Puskar Z, Andrew D, Todd AJ. A quantitative and morphological study of projection neurons in lamina I of the rat lumbar spinal cord. Eur J Neurosci 2003;18:2433–48.
Sugiura Y, Lee CL, Perl ER. Central projections of identified, unmyelinated (C) afferent fibers innervating mammalian skin. Science 1986;234:358–61.
Sugiura Y, Terui N, Hosoya Y. Difference in distribution of central terminals between visceral and somatic unmyelinated (C) primary afferent fibers. J Neurophysiol 1989;62:834–40.
Sun H, Ren K, Zhing CM, Ossipov MH, Malan TP, Lai J, Porreca F. Nerve injury-induced tactile allodynia is mediated via ascending spinal dorsal column projections. Pain 2001;90:105–11.
Todd AJ. Anatomy of primary afferents and projection neurons in the rat spinal dorsal horn with particular emphasis on substance P and the neurokinin 1 receptor. Exp Physiol 2002;87:245–9.
Uddenberg N. Functional organization of long, second-order afferents in the dorsal funiculus. Exp Brain Res 1968;4:377–82.

Wei F, Dubner R, Ren K. Nucleus reticularis gigantocellularis and nucleus raphe magnus in the brain stem exert opposite effects on behavioral hyperalgesia and spinal Fos protein expression after peripheral inflammation. Pain 1999;80:127–41.
Westlund KN, Carlton SM, Zhang D, Willis WD. Glutamate-immunoreactive terminals synapse on primate spinothalamic tract cells. J Comp Neurol 1992;322:519–27.
Whitsel BL, Petrucelli LM, Sapiro G. Modality representation in the lumbar and cervical fasciculus gracilis of squirrel monkeys. Brain Res 1969;15:67–78.
Wiberg M, Westman J, Blomqvist A. Somatosensory projection to the mesencephalon: an anatomical study in the monkey. J Comp Neurol 1987;264:92–117.
Willis WD. Long-term potentiation in spinothalamic neurons. Brain Res Rev 2002; 40:202–14.
Willis WD. Thalamo-cortical system of nociception in animals. In: Chen J, Chen ACN, Han JS, Willis WD, editors. Experimental pathological pain: from molecules to brain functions. Beijing: Science Press; 2003. p. 165–96.
Willis WD. Physiology and anatomy of the spinal cord pain system. Merskey H, Loeser JD, Dubner R, editors. Paths of Pain. Seattle: IASP Press; 2005. p. 85–100.
Willis WD, Coggeshall RE. Sensory mechanisms of the spinal cord. 3rd ed. New York: Kluwer Academic/Plenum Publishers; 2004.
Willis WD, Grossman RG. Medical neurobiology, 3rd ed. St. Louis: The C.V. Mosby Company; 1981.
Willis WD, Westlund KN. Neuroanatomy of the pain system and of the pathways that modulate pain. J Clin Neurophysiol 1997;14;2–31.
Wilson VJ, Melville Jones G. Mammalian vestibular physiology. New York: Plenum; 1979.
Ye Z, Westlund KN. Ultrastructural localization of glutamate receptors subunits (NMDAR1, AMPA GluR1 and GluR2/3) and spinothalamic tract cells. NeuroReport 1996;7:2581–5.
Ye Z, Wimalawansa SJ, Westlund KN. Receptor for calcitonin gene-related peptide: localization in the dorsal and ventral spinal cord. Neuroscience 1999;92:1389–97.
Yezierski RP, Gerhart KD, Schrock BJ, Willis WD. A further examination of effects of cortical stimulation in primate spinothalamic tract cells. J Neurophysiol 1983;49:424–41.

Section A: Chapter 2

Alvarez-Leefmans FJ, Leon-Olea M, Mendoza-Sotelo J, Alvarez FJ, Anton B, Garduno R. Immunolocalization of the Na(+)-K(+)-2Cl(−) cotransporter in peripheral nervous tissue of vertebrates. Neuroscience 2001;104(2):569–82.
Andrew D, Craig AD. Spinothalamic lamina I neurones selectively responsive to cutaneous warming in cats. J Physiol 2001;537:489–95.
Apkarian AV, Hodge CJ. Primate spinothalamic pathways. I. A quantitative study of the cells of origin of the spinothalamic pathway. J Comp Neurol 1989;288:447–73.
Beall JE, Applebaum AE, Foreman RD, Willis WD. Spinal cord potentials evoked by cutaneous afferents in the monkey. J Neurophysiol 1977;40:199–211.
Chung JM, Kenshalo DR, Gerhart KD, Willis WD. Excitation of primate spinothalamic neurons by cutaneous C-fiber volleys. J Neurophysiol 1979;42:1354–69.
Craig AD, Krout K, Andrew D. Quantitative response characteristics of thermoreceptive and nociceptive lamina I spinothalamic neurons in the cat. J Neurophysiol 2001;86:1459–80.
Dostrovsky JO, Craig AD. Cooling specific spinothalamic neurons in the monkey. J Neurophysiol 1996;76:3656–65.
Dougherty PM, Sluka KA, Sorkin LS, Westlund KN, Willis WD. Neural changes in acute arthritis in monkeys: I. Parallel enhancement of responses of spinothalamic tract neurons to mechanical stimulation and excitatory amino acids. Brain Res Rev 1992;17:1–13.
Eccles JC. The physiology of synapses. New York: Springer; 1964.
Eccles JC, Kostyuk PG, Schmidt RF. Central pathways responsible for depolarization of primary afferent fibres. J Physiol 1962;161:237–57.

Eccles JC, Schmidt RF, Willis WD. Pharmacological studies on presynaptic inhibition. J Physiol 1963a;168:500–30.
Eccles JC, Schmidt RF, Willis WD. The location and the mode of action of the presynaptic inhibitory pathways on to group Ia afferent fibers from muscle. J Neurophysiol 1963b;26:506–22.
Ferrington DG, Sorkin LS, Willis WD. Responses of spinothalamic tract cells in the superficial dorsal horn of the primate lumbar spinal cord. J Physiol 1987;388:681–703.
Foreman RD, Schmidt RF, Willis WD. Effects of mechanical and chemical stimulation of fine muscle afferents upon primate spinothalamic tract cells. J Physiol 1979;286:215–31.
Foreman RD, Blair RW, Weber RN. Viscerosomatic convergence onto T2–T4 spinoreticular, spinoreticular-spinothalamic, and spinothalamic tract neurons in the cat. Exp Neurol 1984;85:597–619.
Giesler GJ, Yezierski RP, Gerhart KD, Willis WD. Spinothalamic tract neurons that project to medial and/or lateral thalamic nuclei: Evidence for a physiological novel population of spinal cord neurons. J Neurophysiol 1981;46:1285–308.
Maixner W, Dubner R, Bushnell MC, Kenshalo DR, Oliveras JL. Wide-dynamic-range dorsal horn neurons participate in the encoding process by which monkeys perceive the intensity of noxious heat stimuli. Brain Res 1986;374:385–8.
Mendell LM. Physiological properties of unmyelinated fiber projections to the spinal cord. Exp Neurol 1966;16:316–32.
Milne RJ, Foreman RD, Giesler GJ, Willis WD. Convergence of cutaneous and pelvic visceral nociceptive input onto primate spinothalamic neurons. Pain 1981;11:163–83.
Owens CM, Zhang D, Willis WD. Changes in the response states of primate spinothalamic tract cells caused by mechanical damage of the skin or activation of descending controls. J Neurophysiol 1992;67:1509–27.
Surmeier DJ, Honda CN, Willis WD. Responses of primate spinothalamic neurons to noxious thermal stimulation of glabrous and hairy skin. J Neurophysiol 1986;56:328–50.
Willis WD. Evoked spinal cord potentials in the cat and monkey: use in the analysis of spinal cord function. In: Homma S, Tamaki T, editors; Shimoji K, Kurokawa T, co-editors. Fundamentals and clinical application of spinal cord monitoring. Tokyo: Saikon; 1984. p. 3–19.
Willis WD. Neural mechanisms of pain discrimination. In: Lund JS, editor. Sensory processing in the mammalian brain. Oxford: Oxford University Press; 1989. p. 130–43.
Willis WD. Dorsal root potentials and dorsal root reflexes: a double-edged sword. Exp Brain Res 1999;124:395–421.
Willis WD, Coggeshall RE. Sensory mechanisms of the spinal cord. 3rd ed. New York: Kluwer Academic/Plenum; 2004.
Willis WD, Trevino DL, Coulter JD, Maunz RA. Responses of primate spinothalamic tract neurons to natural stimulation of hindlimb. J Neurophysiol 1974;37:358–72.
Willis WD, Kenshalo DR, Leonard RB. The cells of origin of the primate spinothalamic tract. J Comp Neurol 1979;188:543–74.
Willis WD, Zhang X, Honda CN, Giesler GJ. Projections from the marginal zone and deep dorsal horn to the ventrobasal nuclei of the primate thalamus. Pain 2001;92:267–76.
Zhang D, Owens CM, Willis WD. Short-latency excitatory postsynaptic potentials are evoked in primate spinothalamic tract neurons by corticospinal tract volleys. Pain 1991;45:197–201.

Section A: Chapter 3

Alvarez-Leefmans FJ, Gamiño SM, Giraldez F, Nogierón, I. Intracellular chloride regulation in amphibian dorsal root ganglion neurons studied with ion-selective microelectrodes. J Physiol 1988;406:225–46.
Besson JM, Chaouch A. Peripheral and spinal mechanisms of nociception. Physiol Rev 1987;67:67–186.

Broman J, Adahl F. Evidence for vesicular storage of glutamate in primary afferent terminals. NeuroReport 1994;5:1801–4.
Chung K, Lee WT, Carlton SM. The effects of dorsal rhizotomy and spinal cord isolation on calcitonin gene-related peptide-containing terminals in the rat lumbar dorsal horn. Neurosci Lett 1988;90:27–32.
Conn PJ, Pin JP. Pharmacology and functions of metabotropic glutamate receptors. Annu Rev Pharmacol Toxicol 1997;37:205–37.
Curtis DR, Phillis JW, Watkins JC. Chemical excitation of spinal neurons. Nature 1959;183:611–12.
De Biasi S, Rustioni A. Glutamate and substance P coexist in primary afferent terminals in the superficial laminae of spinal cord. Proc Natl Acad Sci USA 1988;85:7820–4.
Dingledine R, Borges K, Bowie D, Traynelis SF. The glutamate receptor ion channels. Pharmacol Rev 1999;51:7–61.
Dougherty PM, Willis WD. Enhancement of spinothalamic neuron responses to chemical and mechanical stimulation following combined iontophoretic application of N-methyl-D-aspartic acid and substance P. Pain 1991;47:85–93.
Dougherty PM, Palecek J, Paleckova V, Sorkin LS, Willis WD. The role of NMDA and non-NMDA excitatory amino acid receptors in the excitation of primate spinothalamic tract neurons by mechanical, chemical, thermal, and electrical stimuli. J Neurosci 1992;12:3025–41.
Eccles JC. The physiology of synapses. New York: Springer; 1964.
Hollman M, Heinemann S. Cloned glutamate receptors. Annu Rev Neurosci 1994;17: 31–108.
Hori Y, Lee KH, Chung JM, Endo K, Willis WD. The effects of small doses of barbiturate on the activity of primate nociceptive tract cells. Brain Res 1984;307:9–15.
Hunt SP, Kelly JS, Emson PC. The electron-microscopic localization of methionin-enkephalin within the superficial layers (I and II) of the spinal cord. Neuroscience 1980;5:1871–90.
Kandel ER, Schwatrz JH, Jessell TM, editors. Principles of neural science. 4th ed. New York: McGraw-Hill; 2000. p. 240–8.
Lin Q, Peng YB, Willis WD. Role of GABA receptor subtypes in inhibition of primate spinothalamic tract neurons: difference between spinal and periaqueductal gray inhibition. J Neurophysiol 1996;75:109–23.
Miller BA, Woolf CJ. Glutamate-mediated slow synaptic currents in neonatal rat deep dorsal horn neurons in vitro. J Neurophysiol 1996;76:1465–76.
Näsström J, Schneider SP, Perl ER. Differential L-glutamate responsiveness among superficial dorsal horn neurons. J Neurophysiol 1994;72:2956–65.
Nicoll RA, Schenker C, Leeman SE. Substance P as a transmitter candidate. Annu Rev Neurosci 1980;3:227–68.
Ruda MA, Iadarola MJ, Cohen LV, Young WS. In situ hybridization histochemistry and immunocytochemistry reveal an increase in spinal dynorphin biosynthesis in a rat model of peripheral inflammation and hyperalgesia. Proc Natl Acad Sci USA 1988;85:622–6.
Salter MW, De Koninck Y, Henry, JL. Physiological roles for adenosine and ATP in synaptic transmission in the spinal dorsal horn. Prog Neurobiol 1993;41:125–56.
Sawynok, J, Sweeney, MI. The role of purines in nociception. Neuroscience 1989;32:557–69.
Schoepp DD. Unveiling the functions of presynaptic metabotropic glutamate receptors in the central nervous system. J Pharmacol Exp Ther 2001;299:12–20.
Wiesenfeld-Hallin Z, Hökfelt T, Lundberg JM, Firssmann WG, Reunecke M, Tschopp FA, Fischer JA. Immunoreactive calcitonin gene-related peptide and substance P coexist in sensory neurons in the spinal cord and interact in spinal behavioral responses of the rat. Neurosci Lett 1984;52:199–204.
Willcockson WS, Chung JM, Hori Y, Lee KH, Willis WD. Effects of iontophoretically released amino acids and amines on primate spinothalamic tract cells. J Neurosci 1984;4:732–40.
Willcockson WS, Kim J, Shin HK, Chung JM, Willis WD. Actions of opioids on primate spinothalamic tract neurons. J Neurosci 1986;6:2509–20.

Willis WD. Control of nociceptive transmission in the spinal cord. In: Ottoson D, editor. Progress in sensory physiology, vol. 3. Berlin: Springer; 1982.
Willis WD. Anatomy and physiology of descending control of nociceptive responses of dorsal horn neurons: comprehensive review. In: Fields HL, Besson JM, editors. Progress in brain research, vol. 75. Amsterdam: Elsevier; 1988. p. 1–29.
Willis WD. Dorsal root potentials and dorsal root reflexes: a double-edged sword. Exp Brain Res 1999;124:395–421.
Willis WD, Coggeshall RE. Sensory mechanisms of the spinal cord. 3rd ed. New York: Kluwer Academic/Plenum; 2004.
Wu SY, Dun SL, Wright MT, Chang JK, Dun NJ. Endomorphin-like immunoreactivity in the rat dorsal horn and inhibition of substantia gelatinosa neurons in vitro. Neuroscience 1999;89:317–21.
Yoshimura M, Jessell TM. Amino acid-mediated EPSPs at primary afferent synapses with substantia gelatinosa neurons in the rat spinal cord. J Physiol 1990;430:315–35.
Zadina JE, Hackler L, Ge LJ, Kastin AJ. A potent and selective endogenous agonist for the mu-opiate receptor. Nature 1997;386:499–502.

Section A: Chapter 4

Andres-Trelles F, Cowan CM, Simmonds MA. The negative potential wave evoked in cuneate nucleus by stimulation of afferent pathways: its origins and susceptibility to inhibition. J Physiol (Lond) 1976;258:173–86.
Armett CJ, Gray JAB, Palmer JF. A group of neurones in the dorsal horn associated with cutaneous mechanoreceptors. J Physiol (Lond) 1961;156:611–22.
Austin GM, McCouch GP. Presynaptic component of intermediary cord potential. J Neurophysiol 1955;18:441–51.
Barron DH, Matthews BHC. The interpretation of potential changes in the spinal cord. J Physiol (Lond) 1938;92:276–321.
Beall JE, Applebaum AE, Foreman RD, Willis WD. Spinal cord potentials evoked by cutaneous afferents in the monkey. J Neurophysiol 1977;40:199–211.
Bernhard CG. The spinal cord potentials in leads from the cord dorsum in relation to peripheral source of afferent stimulation. Acta Physiol Scand 1953;29(Suppl)106:1–29.
Campbell B. The distribution of potential fields within the spinal cord. Anat Rec 1945;91:77–88.
Carpenter DO, Rudomín P. The organization of primary afferent depolarization in the isolated spinal cord of the frog. J Physiol (Lond) 1973;229:471–93.
Christensen BN, Perl ER. Spinal neurons specifically excited by noxious or thermal stimuli: marginal zone of the dorsal horn. J Neurophysiol 1970;33:293–307.
Eccles JC, Malcolm JL. Dorsal root potentials of the spinal cord. J Neurophysiol 1946;9:139–60.
Eccles JC, Kostyuk PG, Schmidt RF. Central pathway responsible for depolarization of primary afferent fibers. J Physiol (Lond) 1962a;161:237–57.
Eccles JC, Kostyuk PG, Schmidt RF. Presynaptic inhibition of the central actions of flexor reflex afferents. J Physiol (Lond) 1962b;161:258–81.
Eccles JC, Magni F, Willis WD. Depolarization of central terminals of Group I afferent fibres from muscle. J Physiol (Lond) 1962c;160:62–93.
Eccles JC, Schmidt RF, Willis WD. Depolarization of the central terminals of cutaneous afferent fibers. J Neurophysiol 1963a;26:646–61.
Fernandez de Molina A, Gray JAB. Activity in the dorsal spinal grey matter after stimulation of cutaneous nerves. J Physiol (Lond) 1957;137:126–40.
Fitzgerald M, Wall PD. The laminar organization of dorsal horn cells responding to peripheral C fiber stimulation. Exp Brain Res 1980;41:36–44.
Gasser HS, Graham HT. Potentials produced in the spinal cord by stimulation of dorsal roots. Am J Physiol 1933;103:303–20.

Hayatsu K, Tomita M, Fujihara H, Baba H, Yamakura T, Taga K, Shimoji K. The placement of the epidural catheter at the predicted site by electrical stimulation test. Anesth Analg. 2001;93:1035–9.

Howland B, Lettvin JY, McCulloch WS, Pitts W, Wall PD. Reflex inhibition by dorsal root interaction. J Neurophysiol 1955;18:1–17.

Hughes J, Gasser HS. Some properties of the spinal cord potentials evoked by a single afferent volley. Am J Physiol 1934a;108:295–306.

Hughes J, Gasser HS. The response of the spinal cord to two afferent volleys. Am J Physiol 1934b;108:307–21.

Kano T, Shimoji K. Influence of anesthesia on intraoperative monitoring of SCEPs. In: Dimitrijevic MR, Halter JA, editors. Atlas of human spinal cord evoked potentials. Boston: Butterworth-Heinemann; 1995. p. 97–106.

Koketsu K. Intracellular slow potential of dorsal root fibers. Am J Physiol 1956a;184:338–44.

Koketsu K. Intracellular potential changes of primary afferent nerve fibers in spinal cord of cats. J Neurophysiol 1956b;19:375–92.

Lindblom UF, Ottoson JO. Localization of the structure generating the negative cord dorsum potential evoked by stimulation of low threshold cutaneous fibers. Acta Physiol Scand 1953a;29(Suppl 106):180–90.

Lindblom UF, Ottoson JO. Effects of spinal sections on the spinal cord potentials elicited by stimulation of low threshold cutaneous fibers. Acta Physiol Scand 1953b;29(Suppl)106:191–208.

Lloyd DPC. Electrotonus in dorsal nerve roots. Cold Spring Harbor Symp Quant Biol 1952;17:203–19.

Lupa K, Niechaj A. Bilateral dorsal root potentials in the lower sacral spinal cord. Pfluegers Arch 1977;369:187–92.

Magladery JW, Porter WE, Park AM, Teasdall RD. Electrophysiological studies of nerve reflex activity in normal man. IV. The two-neurone reflex and identification of certain action potentials from spinal roots and cord. Bull Johns Hopkins Hosp 1951;88:499–519.

Mendell L. Properties and distribution of peripherally evoked presynaptic hyperpolarization in cat lumbar spinal cord. J Physiol (Lond) 1972;226:769–92.

Rudomín P, Leonard RB, Willis WD. Primary afferent depolarization and inhibitory interactions in spinal cord of the stingray, *Dasyatis sabina*. J Neurophysiol 1978;41:126–37.

Schmidt RF. Presynaptic inhibition in the vertebrate central nervous system. Ergeb Physiol Biol Chem Exp Pharmakol 1971;63:20–101.

Shimoji K, Higashi H, Kano T. Epidural recording of spinal electrogram in man. Electroencephalogr clin Neurophysiol 1971;30:236–9.

Shimoji K, Higashi H, Kano T, Asai S, Morioka T. Electrical management of intractable pain. Jpn J Anesthesiol 1971;20:444–7.

Shimoji K, Kano T, Higashi H, Morioka T, Henschel EO. Evoked spinal electrograms recorded from epidural space in man. J Appl Physiol 1972;33:468–71.

Shimoji K, Ito Y, Ohama K, Sawa T, Ikezono E. Presynaptic inhibition in man during anesthesia and sleep. Anesthesiology 1975;43:388–91.

Shimoji K, Matsuki M, Ito Y, Masuko K, Maruyama M, Iwane T, Aida S. Interactions of human cord dorsum potential. J Appl Physiol 1976;40:79–84.

Shimoji K, Matsuki M, Shimizu H. Wave-form characteristics and spatial distribution of evoked spinal electrogram in man. J Neurosurg 1977;46:304–13.

Shimoji K, Shimizu H, Maruyama Y. Origin of somatosensory evoked responses recorded from the cervical skin surface. J Neurosurg 1978;48:980–4.

Shimoji K, Shimizu H, Maruyama Y, Matsuki M. Dorsal column stimulation in man: facilitation of primary afferent depolarization. Anesth Analg 1982;61:410–13.

Shimoji K, Shimizu H, Maruyama Y, Fujioka H. Human spinal cord potentials produced by ascending and descending volleys. In: Homma S, Tamaki T, editors. Fundamentals and clinical application of spinal cord monitoring. Tokyo: Saikon; 1984. p. 45–59.

Wall PD. Excitability changes in afferent fibre terminations and their relation to slow potentials. J Physiol (Lond) 1958;142:1–21.

Yates BJ, Thompson FJ, Mickle JP Origin and properties of spinal cord field potentials. Neurosurgery 1982;11:439–45.

Section B: Chapter 1

Andersen P, Eccles JC, Sears TA. Presynaptic inhibitory action of cerebral cortex on the spinal cord. Nature 1962;194:740–1.

Andersen P, Eccles JC, Sears TA. Cortically evoked depolarization of primary afferent fibers in the spinal cord. J Neurophysiol 1964;27:63–77.

Andres-Trelles F, Cowan CM, Simmonds MA. The negative potential wave evoked in cuneate nucleus by stimulation of afferent pathways: its origins and susceptibility to inhibition. J Physiol (Lond) 1976;258:173–86.

Austin GM, McCouch GP. Presynaptic component of intermediary cord potential. J Neurophysiol 1955;18:441–51.

Baba H, Yoshimura M, Nishi S, Shimoji K. Synaptic responses of substantia gelatinosa neurones to dorsal column stimulation in rat spinal cord in vitro. J Physiol (Lond) 1994;478(Pt 1):87–99.

Beall JE, Applebaum AE, Foreman RD, Willis WD. Spinal cord potentials evoked by cutaneous afferents in the monkey. J Neurophysiol 1977;40:199–211.

Benoist JM, Besson JM, Conseiller C, Le Bars D. Action of bicuculline on presynaptic inhibition of various origins in the cat's spinal cord. Brain Res 1972;43:672–6.

Benoist JM, Besson JM, Boissier JR, Le Bars D. Modifications of presynaptic inhibition or various origins by local application of convulsant drugs on cat's spinal cord. Brain Res 1974;71:172–7.

Bernhard CG. The spinal cord potentials in leads from the cord dorsum in relation to peripheral source of afferent stimulation. Acta Physiol Scand 1953;29(Suppl)106:1–29.

Bernhard CG, Koll W. On the effect of strychnine, asphyxia, and dial on the spinal cord potentials. Acta Physiol Scand 1953;29(Suppl 106):30–41.

Bernhard CG, Widen L. On origin of negative and positive spinal cord potentials evoked by stimulation of low threshold cutaneous fibers. Acta Physiol Scand 1953;29(Suppl 106):42–54.

Campbell B. The distribution of potential fields within the spinal cord. Anat Rec 1945;91:77–88.

Carpenter DO, Rudomín P. The organization of primary afferent depolarization in the isolated spinal cord of the frog. J Physiol (Lond) 1973;229:471–93.

Carpenter D, Engberg I, Lundberg A. Presynaptic inhibition in the lumbar cord evoked from the brain stem. Experientia 1962;18:450–1.

Carpenter D, Lundbeg A, Norrsell U. Primary afferent depolarization evoked from the sensorimotor cortex. Acta Physiol Scand 1963;59:126–42.

Christensen BN, Perl ER. Spinal neurons specifically excited by noxious or thermal stimuli: marginal zone of the dorsal horn. J Neurophysiol 1970;33:293–307.

Coombs JS, Curtis DR, Landgren S. Spinal cord potentials generated by impulses in muscle and cutaneous afferent fibres. J Neurophysiol 1956;19:452–67.

Eccles JC, Krnjevic K. Potential changes recorded inside primary afferent fibers within the spinal cord. J Physiol (Lond) 1959;149:250–73.

Eccles JC, Sherrington CS. Reflex summation in the ipsilateral spinal flexion reflex. J Physiol (Lond) 1930;69:1–27.

Eccles JC, Kostyuk PG, Schmidt RF. Central pathway responsible for depolarization of primary afferent fibers. J Physiol (Lond) 1962a;161:237–57.

Eccles JC, Kostyuk PG, Schmidt RF. Presynaptic inhibition of the central actions of flexor reflex afferents. J Physiol (Lond) 1962b;161:258–81.

Eccles JC, Magni F, Willis WD. Depolarization of central terminals of Group I afferent fibres from muscle. J Physiol (Lond) 1962c;160:62–93.

Eccles JC, Schmidt RF, Willis WD. Depolarization of the central terminals of cutaneous afferent fibers. J Neurophysiol 1963a;26:646–61.

Eccles JC, Schmidt RF, Willis WD. The mode of operation of the synaptic mechanism producing presynaptic inhibition. J Neurophysiol 1963b;26:532–8.
Fernandez de Molina A, Gray JAB. Activity in the dorsal spinal grey matter after stimulation of cutaneous nerves. J Physiol (Lond) 1957;137:126–40.
Ferner H. Eduard Pernkopf Altas der Topographischem und Angewandten Anatomie des Menschen. Munich: Urban und Schwarzenberg; 1963.
Fitzgerald M, Wall PD. The laminar organization of dorsal horn cells responding to peripheral C fiber stimulation. Exp Brain Res 1980;41:36–44.
Gasser HS, Graham HT. Potentials produced in the spinal cord by stimulation of dorsal roots. Am J Physiol 1933;103:303–20.
Gregor M, Zimmermann M. Dorsal root potentials produced by afferent volleys in cutaneous Group III fibers. J Physiol (Lond) 1973;232:413–25.
Hughes J, Gasser HS. Some properties of the spinal cord potentials evoked by a single afferent volley. Am J Physiol 1934a;108:295–306.
Koketsu K. Intracellular slow potential of dorsal root fibers. Am J Physiol 1956a;184:338–44.
Koketsu K. Intracellular potential changes of primary afferent nerve fibers in spinal cord of cats. J Neurophysiol 1956b;19:375–92.
Lindblom UF, Ottoson JO. Localization of the structure generating the negative cord dorsum potential evoked by stimulation of low threshold cutaneous fibers. Acta Physiol Scand 1953;29(Suppl 106):180–90.
Maruyama Y, Shimoji K, Shimizu H, Kuribayashi H, Fujioka H. Human spinal cord potentials evoked by different sources of stimulation and conduction velocities along the cord. J Neurophysiol 1982;48:1098–107.
Réthelyi M, Szentágothai J. The large synaptic complexes of the substantia gelatinosa. Exp Brain Res 1969;7:258–74.
Schmidt RF. Control of the access of afferent activity to somatosensory pathways. In: Iggo A, editor. Handbook of sensory physiology, vol. II, somatosensory system. Heidelberg: Springer; 1973. p. 151–206.
Shimoji K, Kano T, Higashi H, Morioka T, Henschel EO. Evoked spinal electrograms recorded from epidural space in man. J Appl Physiol 1972;33:468–71.
Shimoji K, Ito Y, Ohama K, Sawa T, Ikezono E. Presynaptic inhibition in man during anesthesia and sleep. Anesthesiology 1975;43:388–91.
Shimoji K, Matsuki M, Ito Y, Masuko K, Maruyama M, Iwane T, Aida S. Interactions of human cord dorsum potential. J Appl Physiol 1976;40:79–84.
Shimoji K, Matsuki M, Shimizu H. Wave-form characteristics and spatial distribution of evoked spinal electrogram in man. J Neurosurg 1977;46:304–13.
Shimoji K, Shimizu H, Maruyama Y. Origin of somatosensory evoked responses recorded from the cervical skin surface. J Neurosurg 1978;48:980–4.
Shimoji K, Maruyama Y, Shimizu H, Fujioka H, Taga K. Spinal cord monitoring—a review of current techniques and knowledge. In: Schramm J, Jones SJ, editors. Spinal cord monitoring. Heidelberg: Springer; 1985. p. 16–28.
Takada T, Denda S, Baba H, Fujioka H, Yamakura T, Fujihara H, Taga K, Fukuda S, Shimoji K. Somatosensory evoked potentials recorded from the posterior pharynx to stimulation of the median nerve and cauda equina. Electroencephalogr Clin Neurophysiol 1996;100:493–9.
Tang AH. Dorsal root potentials in the chloralose-anesthetized cat. Exp Neurol 1969;25:393–400.
Wall PD. Excitability changes in afferent fibre terminations and their relation to slow potentials. J Physiol (Lond) 1958;142:1–21.
Wall PD. The origin of a spinal-cord slow potential. J Physiol (Lond) 1962;164:508–26.
Willis WD, Coggeshall RE. Sensory mechanisms of the spinal cord. New York: Plenum; 2004.
Willis WD, Weis MA, Skinner RD, Bryan RN. Differential distribution of spinal cord field potentials. Exp Brain Res 1973;17:169–76.
Yoshimura M, Jessell TM. Amino-acid mediated EPSPs at primary afferent synapses with substantia gelatinosa neurones in rat spinal cord. J Physiol (Lond) 1990;430:315–35.

Section B: Chapter 2

Barron DH, Matthews BHC. The interpretation of potential changes in the spinal cord. J Physiol (Lond) 1938;92:276–321.
Bernhard CG. The spinal cord potentials in leads from the cord dorsum in relation to peripheral source of afferent stimulation. Acta Physiol Scand 1953;29(Suppl)106:1–29.
Cracco RQ. Spinal evoked response: peripheral nerve stimulation in man. Electroencephalogr Clin Neurophysiol 1973;35:379–86.
Delbeke J, McComas AJ, Kopec SJ. Analysis of evoked lumbosacral potentials in man. J Neurol Neurosurg Phychiatry 1978;41:293–302.
Dorfman LJ. Indirect estimation of spinal cord conduction velocity in man. Electroencephalogr Clin Neurophysiol 1977;42:26–34.
Dorfman LJ, Bosley TM, Cummins FL. Electrophysiological localization of central somatosensory lesions in patients with multiple sclerosis. Electroencephalogr Clin Neurophysiol 1978;44:742–53.
Ertekin C. Evoked electrospinogram in spinal cord and peripheral nerve disorders. Acta Neurol Scand 1978;57:329–44.
Glees P, Soler J. Fiber content of the posterior column and synaptic connections of the nucleus gracilis. Z Zellforsch Mikrosk Anat 1951;36:381–400.
Happel LT, LeBlanc HJ, Kline DG. Spinal cord potentials evoked by peripheral nerve stimulation. Electroencephalogr Clin Neurophysiol 1975;38:349–54.
Lloyd DPC, McIntyre AK. Dorsal column conduction of group I muscle afferent impulese and their relay through Clarke's column. J Neurophysiol 1950;13:39–54.
Lupa K, Niechaj A. Bilateral dorsal root potentials in the lower sacral spinal cord. Pfluegers Arch 1977;369:187–92.
Maruyama Y, Shimoji K, Shimizu H, Kuribayashi H, Fujioka H. Human spinal cord potentials evoked by different sources of stimulation and conduction velocities along the cord. J Neurophysiol 1982;48:1098–107.
Rustioni A. Non-primary afferents to the nucleus gracilis from the lumbar cord of the cat. Brain Res 1972;51:81–95.
Sarnowski RJ, Cracco RQ, Vogel HB, Mount F. Spinal evoked response in the cat. J Neurosurg 1975;43:326–36.
Shimoji K, Higashi H, Kano T. Epidural recording of spinal electrogram in man. Electroencephalogr Clin Neurophysiol 1971;30:236–9.
Shimoji K, Kano T, Higashi H, Morioka T, Henschel EO. Evoked spinal electrograms recorded from epidural space in man. J Appl Physiol 1972;33:468–71.
Trevino DL, Maunz RA, Bryan RN, Willis WD. Location of cells of origin of the spinothalamic tract in the lumbar enlargement of the cat. Exp Neurol 1972;34:64–77.

Section B: Chapter 3

Abdelmoumene M, Besson JM, Aleonard P. Cortical areas exerting presynaptic inhibitory action on the spinal cord in cat and monkey. Brain Res 1970;20:327–9.
Andersen P, Eccles JC, Sears TA. Presynaptic inhibitory action of cerebral cortex on the spinal cord. Nature 1962;194:740–1.
Austin GM, McCouch GP. Presynaptic component of intermediary cord potential. J Neurophysiol 1955;18:441–51.
Barnes CD, Fung SJ, Adams WL. Inhibitory effects of substantia nigra on impulse transmission from nociceptors. Pain 1979;6:207–15.
Basbaum AI, Clanton CH, Fields HL. Opiate and stimulus-produced analgesia: functional anatomy of a medullospinal pathway. Proc Natl Acad Sci USA 1976;73:4685–8.

Beall JE, Applebaum AE, Foreman RD, Willis WD. Spinal cord potentials evoked by cutaneous afferents in the monkey. J Neurophysiol 1977;40:199–211.
Bernhard CG, Widen L. On origin of negative and positive spinal cord potentials evoked by stimulation of low threshold cutaneous fibers. Acta Physiol Scand 1953;29(Suppl 106):42–54.
Besson JM, Rivot JP. Spinal interneurones involved in presynaptic controls of supraspinal origin. J Physiol (Lond) 1973;230:235–54.
Cervero F, Molony V, Iggo A. Supraspinal linkage of substantia gelatinosa neurones: effects of descending impulses. Brain Res 1980;175:351–5.
Chan SHH. Negative potentials evoked by nucleus reticularis gigantocellularis in the spinal trigeminal tract of the cat. Exp Neurol 1980;68:249–57.
Chan SHH, Barnes CD. A presynaptic mechanism evoked from brain stem reticular formation in the lumbar cord and its temporal significance. Brain Res 1972;45:101–14.
Dubuisson D, Wall PD. Descending influences on receptive fields and activity of single units recorded in laminae 1, 2 and 3 of cat spinal cord. Brain Res 1980;199:283–98.
Eccles JC. The physiology of synapses. New York: Academic Press; 1964. p. 220–38.
Eccles JC, Kostyuk PG, Schmidt RF. Central pathway responsible for depolarization of primary afferent fibers. J Physiol (Lond) 1962;161:237–57.
Engberg I, Lundberg A, Ryall RW. Reticulospinal inhibition of transmission in reflex pathways. J Physiol (Lond) 1968a;194:201–23.
Engberg I, Lundberg A, Ryall RW. Reticulospinal inhibition of interneurones. J Physiol (Lond) 1968b;194:225–36.
Fields HL, Basbaum AI. Brainstem control of spinal pain-transmission neurons. Ann Rev Physiol 1978;40:217–48.
Fields HL, Basbaum AI, Clanton CH, Anderson SD. Nucleus raphe magnus inhibition of spinal cord dorsal horn neurons. Brain Res 1977;126:441–53.
Foreman RD, Beall JE, Applebaum AE, Coulter JD, Wills WD. Effects of dorsal column stimulation on primate spinothalamic tract neurons. J Neurophysiol 1976;39:534–46.
Handwerker HO, Iggo A, Zimmermann M. Segmental and supraspinal actions on dorsal horn neurons responding to noxious and non-noxious skin stimuli. Pain 1975;1:147–65.
Hodge CJ Jr, Apkarian AV, Stevens R, Vogelsang G, Wisnicki HJ. Locus coeruleus modulation of dorsal horn unit responses to cutaneous stimulation. Brain Res 1981;204:415–20.
Hongo T, Jankowska E, Lundberg A. Convergence of excitatory and inhibitory action on interneurones in the lumbosacral cord. Exp Brain Res 1966;1:335–58.
Knelsley LW, Biber MP, Lavail JH. A study of origin of brain stem projections to monkey spinal cord using the retrograde transport method. Exp Neurol 1978;60:116–39.
Kostyuk PG, Vasilenko DA. Spinal interneurons. Ann Rev Physiol. 1979;41:115–26.
Kuypers HGJM, Maisky VA. Retrograde axonal transport of horseradish peroxidase from spinal cord to brain stem cell groups in the cat. Neurosci Lett 1975;1:9–14.
Lindblom UF, Ottoson JO. Effects of spinal sections on the spinal cord potentials elicited by stimulation of low threshold cutaneous fibers. Acta Physiol Scand 1953;29(Suppl)106:191–208.
Lloyd DPC. Electrotonus in dorsal nerve roots. Cold Spring Harbor Symp Quant Biol 1952;17:203–19.
Lundberg A. Supraspinal control of transmission in reflex paths to motoneurons and primary afferents. In: Eccles JC, Schade JP, editors. Progress in brain research, vol. 12. Amsterdam: Elsevier; 1964. p. 197–219.
Lundberg A, Norrsell U, Voorhoeve P. Pyramidal effects on lumbosacral inter-neurones activated by somatic afferents. Acta Physiol Scand 1962;56:220–9.
Martin RF, Haber LH, Willis WD. Primary afferent depolarization of identified cutaneous fibers following stimulation in medial brain stem. J Neurophysiol 1979;42:779–90.
Maruyama Y, Shimoji K, Shimizu H, Kuribayashi H, Fujioka H. Human spinal cord potentials evoked by different sources of stimulation and conduction velocities along the cord. J Neurophysiol 1982;48:1098–107.

Menétrey D, Chaouch A, Besson JM. Location and properties of dorsal horn neurons at origin of spinoreticular tract in lumbar enlargement of the rat. J Neurophysiol 1980;44:862–77.
Motamedi F, York DH. Effects of a nigral descending pathway on cervical spinal cord afferent fibers and interneurons. Exp Neurol 1980;68:258–69.
Proudfit HK, Anderson EG. New long latency bulbospinal evoked potentials blocked by serotonin antagonist. Brain Res 1974;65:542–6.
Rudomín P, Leonard RB, Willis WD. Primary afferent depolarization and inhibitory interactions in spinal cord of the stingray, *Dasyatis sabina*. J Neurophysiol 1978;41:126–37.
Schmidt RF. Presynaptic inhibition in the vertebrate central nervous system. Ergeb Physiol Biol Chem Exp Pharmakol 1971;63:20–101.
Shimizu H, Shimoji K, Maruyama Y, Sato Y, Harayama H, Tsubaki T. Slow cord dorsum potentials elicited by descending volleys in man. J Neurol Neurosurg Psychiatry 1979a;2:242–6.
Shimizu H, Shimoji K, Maruyama Y, Sato Y, Kuribayashi H. Interaction between human evoked electrospinograms elicited by segmental and descending volleys. Experimentia 1979b;35: 1199–200.
Shimizu H, Shimoji K, Maruyama Y, Matsuki M, Kuribayashi H, Fujioka H. Human spinal cord potentials produced in lumbo-sacral enlargement by descending volleys. J Neurophysiol 1982;48:1108–20.
Shimoji K, Kano T. Evoked electrospinogram: interpretation origin and effects of anesthetics. In: Mori K, editor. Effect of anesthesia on the central nervous system. Boston: Little Brown; 1975. p. 171–89.
Shimoji K, Kitamura H, Ikezono E, Shimizu H, Okamoto K, Iwakura Y. Spinal hypalgesia and analgesia by low-frequency electrical stimulation in the epidural space. Anesthesiology 1974;41:91–4.
Shimoji K, Ito Y, Ohama K, Sawa T, Ikezono E. Presynaptic inhibition in man during anesthesia and sleep. Anesthesiology 1975;43:388–91.
Shimoji K, Matsuki M, Ito Y, Masuko K, Maruyama M, Iwane T, Aida S. Interactions of human cord dorsum potential. J Appl Physiol 1976;40:79–84.
Shimoji K, Matsuki M, Shimizu H. Wave-form characteristics and spatial distribution of evoked spinal electrogram in man. J Neurosurg 1977;46:304–13.
Shimoji K, Shimizu H, Maruyama Y, Matsuki M. Dorsal column stimulation in man: facilitation of primary afferent depolarization. Anesth Analg 1982;61:410–3.
Skinner RD, Willis WD. Spinal cord potentials produced by ventral cord volleys in the cat. Exp Neurol 1970;27:318–33.
Tang AH. Dorsal root potentials in the chloralose-anesthetized cat. Exp Neurol 1969;25:393–400.
Tobita T, Okamoto M, Shimizu M, Yamakura T, Fujihara T, Shimoji K, Baba H. The effects of isoflurane on conditioned inhibition by dorsal column stimulation. Anesth Analg 2003;97: 436–41.
Tomita M, Shimoji K, Denda S, Tobita T, Uchiyama S, Baba H. Spinal tracts producing slow components of spinal cord potentials evoked by descending volleys in man. Electroencephalogr Clin Neurophysiol 1996;100:68–73.
Wall PD. The laminar organization of dorsal horn and effects of descending impulse. J Physiol (Lond) 1967;188:403–23.
Willis WD, Coggeshall RE. Sensory mechanisms of the spinal cord. New York, Plenum; 2004.

Section B: Chapter 4

Andersen P, Eccles JC, Sears TA. Presynaptic inhibitory action of cerebral cortex on the spinal cord. Nature 1962;194:740–1.
Basbaum AI, Ralston DD, Ralston HJ III. Bulbospinal projections in the primate: a light and electron microscopic study of a pain modulating system. J Comp Neurol 1986;250:311–23.

Besson JM, Rivot JP. Heterosegmental, heterosensory and cortical inhibitory effects on dorsal interneurones in the cat's spinal cord. Electroencephalogr Clin Neurophysiol 1972;33:195–206.

Besson JM, Guilbaud G, Le Bars D. Descending inhibitory influences exerted by the brain stem upon the activities of dorsal horn lamina V cells induced by intra-arterial injection of bradykinin into the limb. J Physiol (Lond) 1975;248:725–39.

Carpenter D, Engberg I, Lundberg A. Primary afferent depolarization evoked from the brain stem and the cerebellum. Arch Ital Biol 1966;104:73–85.

Denda S, Shimoji K, Tomita M, Baba H, Yamakura T, Masaki H, Endoh H, Fukuda, S. Central nuclei and spinal pathways in feedback inhibitory spinal cord potentials in ketamine-anaesthetized rats. Br J Anaesth 1996;76:258–65.

Fung SJ, Barnes CD. Locus coeruleus control of spinal cord activity. In: Barnes CD, editor. Brainstem control of spinal cord function. Orlando: Academic Press; 1984. p. 215–55.

Gebhart GF. Descending modulation of pain (Review). Neurosci Biobehav Rev 2004;27:729–37.

Mokha SS, McMillan JA, Iggo A. Pathways mediating descending control of spinal nociceptive transmission from the nuclei locus coeruleus (LC) and raphe magnus (NRM) in the cat. Exp Brain Res 1986;61:597–606.

Morton CR, Maisch B, Zimmermann M. Diffuse noxious inhibitory controls of lumbar spinal neurons involve a supraspinal loop in the cat. Brain Res 1987;410:347–52.

Rudomín P, Solodkin M, Jiménez I. Synaptic potentials of primary afferent fibers and motoneurons evoked by single intermediate nucleus interneurons in the cat spinal cord. J Neurophysiol 1987;57:1288–313.

Saadé NE, Tabet MS, Banna NR, Atweh SF, Jabbur SJ. Inhibition of nociceptive evoked activity in spinal neurons through a dorsal column-brain stem-spinal loop. Brain Res 1985;339:115–8.

Shimizu H, Shimoji K, Maruyama Y, Matsuki M, Kuribayashi H, Fujioka H. Human spinal cord potentials produced in lumbo-sacral enlargement by descending volleys. J Neurophysiol 1982;48:1108–20.

Shimoji K, Ito Y, Ohama K, Sawa T, Ikezono E. Presynaptic inhibition in man during anesthesia and sleep. Anesthesiology 1975;43:388–91.

Shimoji K, Matsuki M, Ito Y, Masuko K, Maruyama M, Iwane T, Aida S. Interactions of human cord dorsum potential. J Appl Physiol 1976;40:79–84.

Shimoji K, Matsuki M, Shimizu H. Wave-form characteristics and spatial distribution of evoked spinal electrogram in man. J Neurosurg 1977;46:304–13.

Shimoji K. Human spinal cord potentials (SCPs). Ascending recording variations—an update. In: Ducker TB, Brown RH, editors. Neurophysiology and standards of spinal cord monitoring. New York: Springer; 1986a. p. 19–28.

Shimoji K, Fujioka H, Maruyama Y, Hokari T, Takada T. Spinal cord potentials (SCPs) produced by descending volleys in the rat. In: Ducker TB, Brown RH, editors. Neurophysiology and standards of spinal cord monitoring, New York: Springer; 1986b. p. 73–81.

Shimoji K, Fujioka H, Maruyama Y, Shimizu H, Hokari T, Takada T. Spinal cord potentials (SCPs) produced by descending volleys in man. In: Ducker TB, Brown RH, editors. Neurophysiology and standards of spinal cord monitoring. New York: Springer; 1986c. p. 114–21.

Shimoji K, Fujiwara N, Fukuda S, Denda S, Takada T, Maruyama Y. Effects of isoflurane on spinal inhibitory potentials. Anesthesiology 1990;72:851–7.

Shimoji K, Sato Y, Denda S, Takada T, Fukuda S, Hokari T. Slow positive dorsal cord potentials activated by heterosegmental stimuli. Electroencephalogr Clin Neurophysiol 1992a;85:72–80.

Shimoji K, Fujiwara N, Denda S, Tomita M, Toyama M, Fukuda S. Effects of pentobarbital on heterosegmentally activated dorsal root depolarization in the rat: investigation by sucrose-gap technique in vivo. Anesthesiology 1992b;76:958–66.

Shimoji K, Tomita M, Tobita T, Baba H, Takada T, Fukuda S, Aida S, Fujiwara N. Erb's point stimulation produces slow positive potentials in human lumbar spinal cord. J Clin Neurophysiol 1994;11:365–74.

Sirkin DW, Feng AS. Autoradiographic study of descending pathways from the pontine reticular formation and the mesencephalic trigeminal nucleus in the rat. J Comp Neurol 1987;256:483–93.
Villanueva L, Peschanski M, Calvino B, Le Bars D. Ascending pathways in the spinal cord involved in triggering of diffuse noxious inhibitory controls in the rat. J Neurophysiol 1986;55:34–55.
Willis WD Jr. The raphe-spinal system. In: Barnes CD, editor. Brainstem control of spinal cord function. Orlando: Academic Press; 1984. p. 141–214.
Wolters JG, de Boer-Van Huizen R, Ten Donkelaar HJ, Leenen L. Collateralization of descending pathways from the brain-stem to the spinal cord in a lizard, varanus exanthematicus. J Comp Neurol 1986;251:317–33.

Section B: Chapter 5

Kaieda R, Maekawa T, Takeshita H, Maruyama Y, Shimizu H, Shimoji K. Effects of diazepam on evoked electrogram in man. Anesth Analg 1981;61:410–3.
Kano T, Shimoji K. The effects of ketamine and neuroleptanalgesia on the evoked electrospinogram and electromyogram in man. Anesthesiology 1974;40:241–6.
Kano T, Hashiguchi A. Effects of electrical current application on the evoked spinal cord potentials in dogs. Shimoji K, Kurokawa T, Tamaki T, Willis Jr WD, editors. Spinal cord monitoring and electrodiagnosis. Berlin: Springer; 1991. p. 13–9.
Kano T, Higashi H, Shimoji K, Morioka T. The patterns of evoked spinal electrogram in man. Rinshou Seiri (Japanese Clinical Physiology) 1971;1:559–66.
Kano T, Morioka T, Shimizu H. Effect of doxapram hydrochloride on electric potentials evoked from the somatosensory and the motor systems of man under thiamylal anesthesia. In: Homma S, Tamaki T, editors. Fundamental and clinical application of spinal cord monitoring. Tokyo: Saikon; 1984. p. 307–15.
Kano T, Harada H, Mishima Y, Niiyama S. Effects of anesthesia and hypothermia on the evoked spinal cord potentials. Rinshou Nouha (Jpn J Clin Encephal) 1998;40:20–4.
Maruyama Y, Shimoji K, Shimizu H, Sato Y, Kuribayashi H, Kaieda. Effects of morphine on human spinal cord and peripheral nervous activities. Pain 1980;8:63–73.
Mishima Y, Niiyama S, Kano T. CSF temperature monitoring under deep hypothermia with extracorporeal circulation. In: Kano T (ed), Proc of 3rd Jap SNACC. Shinkou, Kurume; 1999. p. 4648.
Shimizu H, Shimoji K, Maruyama Y, Matsuki M, Kuribayashi H, Fujioka H. Human spinal cord potentials produced in lumbosacral enlargement by descending volleys. J Neurophysiol 1982;48:1108–20.
Shimoji K, Kano T. Evoked spinal electrogram in a quadriplegic patient. Electroencephalogr Clin Neurophysiol 1973;35:659–62.
Shimoji K, Kano T, Higashi H, Morioka T, Henshel EO. Evoked spinal electrograms recorded from epidural space in man. J Appl Physiol 1972;33:468–71.
Shimoji K, Kano T, Nakashima H, Shimizu H. The effects of thiamylal sodium on electrical activities of the central and peripheral nervous systems in man. Anesthesiology 1974;40:234–40.
Shimoji K, Shimizu H, Maruyama Y, Matsuki M, Kuribayashi H, Fujioka H. Dorsal column stimulation in man: Facilitation of primary afferent depolarization. Anesth Analg 1982;61:410–3.
Shimoji K, Maruyama Y, Shimizu H, Fujioka H, Urano S. The effects of anesthetics on somatosensory evoked potentials from the brain and spinal cord in man. In: Gomez QJ, Egay LM, Cruz-Odi MF, editors. Anaesthesia—safety for all. Amsterdam: Elsevier Science; 1984. p. 159–64.
Shimoji K, Matsuki M, Shimizu H, Maruyama Y. The effects of epidural lidocaine on spinal cord and peripheral nervous activities in man. In: Wust HJ, Darcystantion-Hicks M, editors. Verlag fur Medizin. Heidelberg: Dr Ewald Fisher; 1987. p. 138–48.

Tabo E, Ohkuma Y, Shimizu I, Nagaro T, Arai T. Changes in human evoked spinal potentials (ESP) by epidural lidocaine. Masui (Jap J Anesth) 1993;42:1484–7.

Section C: Chapter 1

Amassian VE, Eberle L, Maccabee PJ, Cracco RQ. Modelling magnetic coil excitation of human cerebral cortex with a peripheral nerve immersed in a brain-shaped volume conductor: the significance of fiber bending in excitation. Electroencephalogr Clin Neurophysiol 1992;85:291–301.

Barker AT, Jalinous R. Non-invasive magnetic stimulation of human motor cortex. Lancet 1985;1:1106–7.

Ben-David B, Haller G, Taylor P. Anterior spinal fusion complicated by paraplegia: a case report of a false-negative somatosensory-evoked potential. Spine 1987;12:536–9.

Burke D, Hicks RG, Stephen JPH. Corticospinal volleys evoked by anodal and cathodal stimulation of the human motor cortex. J Physiol (Lond) 1990;425:283–99.

Burke D, Hicks RG, Gandevia SC, Stephen J, Woodforth I, Crawford M. Direct comparison of corticospinal volleys in human subjects to transcranial magnetic and electrical stimulation. J Physiology (Lond) 1993;470:383–93.

Calancie B, Klose KJ, Baier S, Green BA. Isoflurane-induced attenuation of motor evoked potentials caused by electrical motor cortex stimulation during surgery. J Neurosurg 1991;74:897–904.

Edgeley SA, Eyre JA, Lemon RN, Miller S. Excitation of the corticospinal tract by electromagnetic and electrical stimulation of the scalp in the macaque monkey. J Physiol (Lond) 1990;425:301–20.

Fujiki M, Isono M, Hori S, Ueno S. Corticospinal direct response to transcranial magnetic stimulation in humans. Electroencephalogr Clin Neurophysiol 1996;101:48–57.

Ghez C. Cortical control of voluntary movement. In: Kandel ER, Schwartz JH, editors. Principals of neural science. Elsevier North Holland; 1981. p. 323–57.

Ginsburg HH, Shetter AG, Raudzens PA. Postoperative paraplegia with preserved intraoperative somatosensory evoked potentials. J Neurosurg 1985;63:296–300.

Grundy BL, Villani RM. Evoked potentials: intraoperative and ICE monitoring. New York: Springer; 1988.

Haghighi SS, Green KD, Oro JJ, Drake RK, Kracke GR. Depressive effect of isoflurane anesthesia on motor evoked potentials. Neurosurgery 1990;26:993–7.

Herdmann J, Lumenta CB, Huse KO. Magnetic stimulation for monitoring of motor pathways in spinal procedures. Spine 1993;18:551–9.

Hicks R, Burke D, Stephen J, Woodforth I, Crawford M. Corticospinal volleys evoked by electrical stimulation of human motor cortex after withdrawal of volatile anaesthetics. J Physiol (Lond) 1992;456:393–404.

Huang YZ, Edwards MJ, Bhatia KP, Rothwell JC. One-Hz repetitive transcranial magnetic stimulation of the premotor cortex alters reciprocal inhibition in DYT1 dystonia. Mov Disord 2004;19:54–9.

Iida H, Dohi S, Tanahashi T, Watanabe Y, Takenaka M. Spinal conduction block by intrathecal ketamine in dogs. Anesth Analg 1997;85:106–10.

Kalkman CJ, Drummond JC, Ribberink AA. Low concentrations of isoflurane abolish motor evoked responses to transcranial electrical stimulation during nitrous oxide/opioid anesthesia in humans. Anesth Analg 1991;73:410–5.

Kalkman CJ, Drummond JC, Ribberink AA, Patel PM, Sano T, Bickford RG. Effects of propofol, etomidate, midazolam, and fentanyl on motor evoked responses to transcranial electrical or magnetic stimulation in humans. Anesthesiology 1992;76:502–9.

Kalkman CJ, Drummond JC, Patel PM, Sano T, Chesnut RM. Effects of droperidol, pentobarbital, and ketamine on myogenic transcranial magnetic motor-evoked responses in humans. Neurosurgery 1994;35:1066–70.

Kalkman CJ, Ubags LH, Been HD, Swaan A, Drummond JC. Improved amplitude of myogenic motor evoked responses after paired transcranial electrical stimulation during sufentanil/nitrous oxide anesthesia. Anesthesiology 1995;83:270–6.

Katayama Y, Tsubokawa T, Maejima S, Hirayama T, Yamamoto T. Corticospinal direct response in humans: identification of the motor cortex during intracranial surgery under general anaesthesia. J Neurol Neurosurg Psychiatry 1988;51:50–9.

Kawaguchi M, Furuya H. Intraoperative spinal cord monitoring of motor function with myogenic motor evoked potentials: a consideration in anesthesia. J Anesth 2004;18:1828.

Kawaguchi M, Sakamoto T, Shimizu K, Ohnishi H, Karasawa J. Effect of thiopentone on motor evoked potentials induced by transcranial magnetic stimulation in humans. Br J Anaesth 1993;71:849–53.

Kawaguchi M, Sakamoto T, Ohnishi H, Shimizu K, Karasawa J, Furuya H. Intraoperative myogenic motor evoked potentials induced by direct electrical stimulation of the exposed motor cortex under isoflurane and sevoflurane. Anesth Analg 1996a;82:593–9.

Kawaguchi M, Shimizu K, Furuya H, Sakamoto T, Ohnishi H, Karasawa J. Effect of isoflurane on motor-evoked potentials induced by direct electrical stimulation of the exposed motor cortex with single, double, and triple stimuli in rat. Anesthesiology 1996b;85:1176–83.

Kitagawa H, Møller AR. Conduction pathways and generators of magnetic evoked spinal cord potentials: a study in monkeys. Electroencephalogr Clin Neurophysiol 1994;93:57–67.

McPherson RW, Ducker TB. Augmentation of somatosensory evoked potentials waves in patients with cervical spinal stenosis. In: Ducker TB, Brown RH, editors. Neurophysiology and standards of spinal cord monitoring. Berlin: Springer; 1988. p. 168–76.

Merton PA, Morton HB. Stimulation of the cerebral cortex in the intact subject. Nature (Lond) 1980;285:227.

Rothwell JC, Day BL, Amassian VE. Near threshold electrical and magnetic transcranial stimuli activate overlapping sets of cortical neurones in humans. J Physiol (Lond) 1992;452:109P.

Shimoji K, Higashi H, Kano T. Epidural recording of spinal electrogram in man. Electroencephalogr Clin Neurophysiol 1971;30:236–9.

Shimoji K, Kano T, Higashi H, Morioka T, Henschel EO. Evoked spinal electrograms recorded from epidural space in man. J Appl Physiol 1972;33:468–71.

Shimoji K, Matsuki M, Masuko K, Maruyama M, Iwane T, Aida S. Interactions of human cord dorsum potential. J Appl Physiol 1976;40:79–84.

Stone JL, Ghaly RF, Levy WJ, Kartha R, Krinsky L, Roccaforte P. A comparative analysis of enflurane anesthesia on primate motor and somatosensory evoked potentials. Electroencephalogr Clin Neurophysiol 1992;84:180–7.

Taniguchi M, Cedzich C, Schramm J. Modification of cortical stimulation for motor evoked potentials under general anesthesia: Technical description. Neurosurgery 1993;32: 219–26.

Thompson PD, Day BL, Crockard HA, Calder I, Murry NMF, Rothwell JC, Marsden CD. Intraoperative recording of motor tract potentials at the cervico-medullary junction following scalp electrical and magnetic stimulation of the motor cortex. J Neurol Neurosurg Psychiatry 1991;54:618–23

Tobita T, Denda S, Takada T, Endoh H, Baba H, Yamakura T, Fukuda S, Shimoji K. Effects of fentanyl on spinal cord potentials and electromyogram evoked by transcranial magnetic stimulation in man. In: Hashimoto I, Kakigi R, editors. Recent advances in human neurophysiology. Amsterdam: Excerpta Medica; 1998. p. 1034–7.

Zentner J, Kiss I, Ebner A. Influence of anesthetics—nitrous oxide in particular—on electromyographic response evoked by transcranial electrical stimulation of the cortex. Neurosurgery 1989;24:253–6.

Zentner J, Albrecht T, Heuser D. Influence of halothane, enflurane, and isoflurane on motor evoked potentials. Neurosurgery 1992;31:298–305.

Section C: Chapter 2

2.1

Agnew WF, McCreery DB. Considerations for safety in the sue of extracranial stimulation for motor evoked potentials. Neurosurgery 1987;20:143–7.

Boyd SG, De Silva LVK. EEG and serum prolactin studies in relation to transcutaneous stimulation of central motor pathways. J Neurol 1986;49:954–6.

Cohen LG, Hallett M. Non-invasive electrical stimulation of the brain does not cause short-term changes in the electroencephalogram. In: Rossini PM, Marsden CD, editors. Non-invasive stimulation of brain and spinal cord. New York: Alan R. Liss; 1988. p. 159–61.

Katayama Y, Tsubokawa T, Sugitani S, et al. Assessment of spinal cord injury with multimodality evoked spinal cord potentials Part 1. Localization of lesions in experimental spinal cord injury. Neuro-Orthopedics 1986;1:130–41.

Katayama Y, Tsubokawa T, Maejima S, et al. Corticospinal direct response to stimulation of exposed motor cortex in humans. In: Ducker TB, Brown RH, editors. Neurophysiology and standards of spinal cord monitoring. Berlin New York: Springer; 1988a. p. 100–5.

Katayama Y, Tsubokawa T, Maejima S, et al. Corticospinal direct response in humans: identification of the motor cortex during intracranial surgery under general anaesthesia. J Neurol Neurosurg Psychiatry 1988b;51:50–9.

Patton HD, Amassian VE. Single and multiple-unit analysis of cortical stage of pyramidal tract activation. J Neurophysiol 1954;17:345–63.

Rothwell J, Burke D, Hicks R, et al. Transcranial electrical stimulation of the motor cortex in man: further evidence for the site of activation. J Physiol 1994;481:243–50.

Tsubokawa T, Katayama Y, Maejima S, et al. Assessment of spinal cord injury with multimodality evoked spinal cord potentials Part 2. Correlation with neurological outcome in clinical spinal cord injury. Neuro-Orthopedics 1987;3:82–9.

Yamamoto T, Xing JA, Katayama Y, et al. Spinal cord responses to feline transcranial brain stimulation: evidence for involvement of cerebellar pathways. J Neurotrauma 1990;7:247–56.

Yamamoto T, Katayama Y, Tsubokawa T, et al. Experimental study of the origin of transcranially evoked descending spinal cord potentials. In: Shimoji K, Kurokawa T, Tamaki T, Willis WD, editors. Spinal cord monitoring and electrodiagnosis. Berlin: Spinger; 1991. p. 36–42.

Yamamoto T, Katayama Y, Nagaoka T, et al. Intraoperative monitoring of the corticospinal motor evoked potential (D-wave): clinical index for postoperative motor function and functional recovery. Neurol Med Chir (Tokyo) 2004;44:170–80.

2.2

Burke D, Hicks R, Stephen JPH. Corticospinal volleys evoked by anodal and cathodal stimulation of the human motor cortex. J Physiol 1990;425:283–9.

Edgley SA, Eyre JA, Lemon RN, Miller S. Excitation of the corticospinal tract by electromagnetic and electrical stimulation of the scalp in the macaque monkey. J Physiol 1990;425: 301–20.

Hess CW, Mills KR, Murray NMF. Percutaneous stimulation of the human brain: A comparison of electrical and magnetic stimuli. J Physiol 1986;378:35P.

Katayama Y, Tsubokawa T, Sugitani M, Maejima S, Hirayama T, Yamamoto T. Assessment of spinal cord injury with multimodality evoked spinal cord potentials. Part 1. Localization of lesions in experimental spinal cord injury. Neuro-Orthopedics 1986;1:130–41.

Katayama Y, Tsubokawa T, Maejima S, Hirayama T, Yamamoto T. Corticospinal direct response in humans: Identification of the motor cortex during intracranial surgery under general anesthesia. J Neurol Neurosurg Psychiatry 1988;51:50–9.

Levy WJ, McCaffrey M, York DH, Tanzer F. Motor evoked potentials from transcranial stimulation of the motor cortex in humans. Neurosurgery 1984a;15:287–302.

Levy WJ, McCaffrey M, York DH, Tanzer F. Motor evoked potentials from transcranial stimulation of the motor cortex in cats. Neurosurgery 1984b;15:214–27.
Morota N, Deletis V, Constantini S, Kofler M, Cochen H, Epstein FJ. The role of motor evoked potentials (MEPs) during surgery of intramedullary spinal cord tumors. Neurosurgery 1997;41:1327–36.
Rothwell J, Burke D, Hicks R, Stephen J, Woodforth I, Crawford M. Transcranial electrical stimulation of the motor cortex in man: Further evidence for the site of activation. 1994;481:243–50.
Tsubokawa T, Katayama Y, Yamamoto T. Intraoperative monitoring of corticospinal and spinospinal MEPs. In: Dimitrijevic MR, Halter JA, editors. Atlas of human spinal cord evoked potentials. Boston: Butterworth-Heinemann; 1995. p. 85–96.
Yamamoto T, Katayama Y, Nagaoka T, Kobayashi K, Fukaya C. Intraoperative monitoring of the corticospinal motor evoked potential (D-wave): Clinical index for postoperative motor function and functional recovery. Neurol Med Chir (Tokyo) 2004;44:170–80.

2.3

Amassian VE, Stewart M, Quirk GJ, Rosenthal JL: Physiological basis of motor effects of transient stimulus to cerebral cortex. Neurosurgery 1987;20:74–93.
Deletis V, Isgum V, Amassian V: Neurophysiological mechanisms underlying motor evoked potentials (MEP's) elicited by a train of electrical stimuli. Part 2. Relationship between epidurally and muscle recorded MEPs in man. Clin Neurophysiol 2001;112:445–2.
Edgley BSA, Eyre JA, Lemon RN, Miller S: Excitation of the corticospinal tract by electromagnetic and electrical stimulation of the scalp in the macaque monkey. J Physiol 1990;425:301–20.
Cedzich C, Taniguchi M, Schafer S, Schramm J: Somatosensory evoked potential phase reversal and direct motor cortex stimulation during surgery in and around the central region. Neurosurgery 1996;38:962–70.
Katayama Y, Tsubokawa T, Maejima S, Hirayama T, Yamamoto T: Corticospinal direct response in humans: Identification of the motor cortex during intracranial surgery under general anaesthesia. J Neurol Neurosurg Psychiatry 1988;51:50–9.
Kombos T, Suess O, Ciklatekerlio O, Brock M: Monitoring of intraoperative motor evoked potentials to increase the safety of surgery in and around the motor cortex. J Neurosurg 2001;95:608–14.
Morota N, Deletis V, Constsntini S, Kofler M, Cohen H, Epstein FJ: The role of motor evoked potentials during surgery for intramedullary spinal cord tumors. Neurosurgery 1997;41:1327–36.
Patton HD, Amassian VE: Single- and multiple-unit analysis of cortical stage of pyramidal tract activation. J Neurophysiol 1954;17:345–63.
Pechstein U, Cedzich C, Nadstawek J, Schramm J: Transcranial high-frequency repetitive electrical stimulation for recording myogenic motor evoked potentials with the patient under general anesthesia. Neurosurgery 1996;39:335–43.
Rothwell J, Burke D, Hicks R, Stephen J, Woodforth I, Crawford M: Transcranial electrical stimulation of the motor cortex in man: Further evidence for the site of activation. J Physiol 1994;481:243–50.
Taniguchi M, Cedzich C, Schram J: Modification of cortical stimulation for motor evoked potentials under general anesthesia: Technical description. Neurosurgery 1996;38:962–70.
Yamamoto T, Katayama Y, Nagaoka T, Kobayashi K, Fukaya C: Intraoperative monitoring of the corticospinal motor evoked potential (D-wave): Clinical index for postoperative motor function and functional recovery. Neurol Med Chir (Tokyo) 1991;31:401–5.

2.4

Amassian VE, Stewart M, Quirk GJ, Rosenthal JL: Physiological basis of motor effects of a transient stimulus to cerebral cortex. Neurosurgery 1987;20:74–93.
Barker AT, Jalinous R: Non-invasive magnetic stimulation of human motor cortex. Lancet 1985;1:1106–7.
Boyd SG, Rothwell JC, Cowan JMA: A method of monitoring function in corticospinal pathways during scoliosis surgery with a note on motor conduction velocities. J Neurol Neurosurg Psychiatry 1986;49:251–7.
Burke D, Hicks RG, Stephen JPH: Corticospinal volleys evoked by anodal and cathodal stimulation of the human motor cortex. J Physiol (London) 1990;425:283–99.
Calancie B, Klose KJ, Baier S, Green BA: Isoflurane-induced attenuation of motor evoked potentials caused by electrical motor cortex stimulation during surgery. J Neurosurg 1991;74:897–904.
Deletis V, Kiprovski K, Morota N: The influence of halothane, enflurane, and isoflurane on motor evoked potentials. Neurosurgery 1993;33:173–4.
Denda S, Tomita M, Tobita T, Taga T, Fukuda S, Shimoji K: Effects of isoflurane on the spinal cored potentials by transcranial electric stimulation. In: Hashimoto I, Kakigi R, editors. Recent advances in human neurophysiology. Amsterdam: Elsevier; 1998;1022–6.
Ginsburg HH, Shetter AG, Raudzeus PA: Postoperative paraplegia with preserved intraoperative somatosensory evoked potentials. J Neurosurg 1985;63:296–300.
Haghighi SS, Green KD, Oro JJ, Drake RK, Kracke GR: Depressive effect of isoflurane anesthesia on motor evoked potentials. Neurosurgery 1990;26:993–7.
Haghighi SS: Influence of isoflurane anesthesia on motor evoked potentials elicited by transcortical, brainstem, and spinal root stimulation. Neurol Res 1998;20:555–8.
Hicks RG, Woodforth IJ, Crawford MR, Stephen JPH, Burke DJ: Some effects of isoflurane on I waves of the motor evoked potential. Br J Anaesth 1992;69:130–6.
Kalkman CJ, Drummond JC, Ribberink AA: Low concentrations of isoflurane abolish motor evoked responses to transcranial electrical stimulation during nitrous oxide/opioid anesthesia in humans. Neurosurg Anesthesia 1991;73:410–5.
Lee WY, Hou WY, Yang LH, Lin SM: Intraoperative monitoring of motor function by magnetic motor evoked potentials. Neurosurgery 1995;36:493–500.
Lesser RP, Raudzens PA, Luders H, Nuwer MR, Goldie WD, Morris III HH, Dinner DS, Klem G, Hahn JF, Shetter AG, Ginsburg HH, Gurd AR: Postoperative neurological deficits may occur despite unchanged intraoperative somatosensory evoked potentials. Ann Neurol 1986;19:22–5.
Levy WJ: Clinical experience with motor and cerebellar evoked potential monitoring. Neurosurgery 1987;20:169–82.
Merton PA, Morton HB: Stimulation of the cerebral cortex in the intact subject. Nature (Lond) 1980; 285, 227.
Shimoji K, Higashi H, Kano T, Asai S, Morioka T: Electrical management of intractable pain. Jpn J Anesthesiol 1971a;20:444–7.
Shimoji K, Higashi H, Kano T: Epidural recording of spinal electrogram in man. Electroencephalogr Clin Neurophysiol 1971b;30:236–9.
Ubags LH, Kalkmanose CJ, Been HD: Influence of isoflurane on myogenic motor evoked potentials to single and multiple transcranial stimuli during nitrous oxide/opioid anesthesia. Neurosurgery 1998;43:90–5.

Section D: Chapter 1

Amassian VE, Stewart M, Quick GJ, Rosenthal JL. Physiological basis of motor effects of a transient stimulus to cerebral cortex. Neurosurgery 1987;20:74–93.

Arai M, Goto T, Seichi A, Nakamura K. Effects of antithrombin three on spinal cord-evoked potentials and functional recovery after spinal cord injury in rats. Spine 2004;29:405–12.

Azizzadeh A, Huynh TT, Miller CC 3rd, Safi HJ. Reversal of twice-delayed neurologic deficits with cerebrospinal fluid drainage after thoracoabdominal aneurysm repair: a case report and plea for a national database collection. J Vasc Surg 2000;31:592–8.

Bolton CF, Sawa GM, Carter K. The effects of temperature on human compound action potentials. J Neurol Neurosurg Psychiatry 1981;44:407–13.

Boyd SG, Rothwell JC, Cowan JM, et al. A method of monitoring function in corticospinal pathways during scoliosis surgery with a note on motor conduction velocities. J Neurol Neurosurg Psychiatry 1986;49:251–7.

Burke D, Hicks RG. Surgical monitoring of motor pathways. J Clin Neurophysiol 1998;15:194–205.

Calancie B, Harris W, Brindle GF, et al. Threshold-level repetitive transcranial electrical stimulation for intraoperative monitoring of central motor conduction. J Neurosurg Spine 2001;95:161–8.

Calancie B, Harris W, Broton JG, Alexeeva N, Green BA. "Threshold-level" multipulse transcranial electrical stimulation of motor cortex for intraoperative monitoring of spinal motor tracts: description of method and comparison to somatosensory evoked potential monitoring. J Neurosurg 1998;88:457–70.

Carpenter MB, Sutin J. Human neuroanatomy. 8th ed. Baltimore: Williams & Wilkins; 1983. p. 707–41.

Cina CS, Lagana A, Bruin G, Ricci C, Doobay B, Tittley J, Clase CM. Thoracoabdominal aortic aneurysm repair: a prospective cohort study of 121 cases. Ann Vasc Surg 2002;16:631–8.

Clark DL, Rosner BS. Neurophysiological effects of general anesthetics. I. The electroencephalogram and sensory evoked responses in man. Anesthesiology 1973;38:564–82.

Coselli JS. Thoracic aortic aneurysms. In: Ascher E, editor. Vascular surgery. Massachusetts: Blackwell; 2004. p. 663–86.

Coselli JS, LeMaire SA. Surgical techniques. Thoracoabdominal aorta. Cardiol Clin 1999;17:751–65.

Coselli JS, LeMaire SA, Miller CC 3rd, Schmittling ZC, Koksoy C, Pagan J, Curling PE. Mortality and paraplegia after thoracoabdominal aortic aneurysm repair: a risk factor analysis. Ann Thorac Surg 2000;69:409–14.

Coselli JS, Lemaire SA, Koksoy C, Schmittling ZC, Curling PE. Cerebrospinal fluid drainage reduces paraplegia after thoracoabdominal aortic aneurysm repair: results of a randomized clinical trial. J Vasc Surg 2002;35:631–9.

Crawford ES, Mizrahi EM, Hess KR, Coselli JS, Safi HJ, Patel VM. The impact of distal aortic perfusion and somatosensory evoked potential monitoring on prevention of paraplegia after aortic aneurysm operation. J Thorac Cardiovasc Surg 1988;95:357–67.

Crock HV, Yoshizawa H. The blood supply of the vertebral column and spinal cord in man. New York: Springer; 1977.

de Haan P, Kalkman CJ, Ubags LH, Jacobs MJ, Drummond JC. A comparison of the sensitivity of epidural and myogenic transcranial motor-evoked responses in the detection of acute spinal cord ischemia in the rabbit. Anesth Analg 1996;83:1022–7.

de Haan P, Kalkman CJ, de Mol BA, Ubags LH, Veldman DJ, Jacobs MJ. Efficacy of transcranial motor-evoked myogenic potentials to detect spinal cord ischemia during operations for thoracoabdominal aneurysms. J Thorac Cardiovasc Surg 1997;113:87–100; discussion 100–1.

de Haan P, Kalkman CJ, Jacobs MJ. Spinal cord monitoring with myogenic motor evoked potentials: early detection of spinal cord ischemia as an integral part of spinal cord protective strategies during thoracoabdominal aneurysm surgery. Semin Thorac Cardiovasc Surg 1998;10:19–24.

Deletis V, Rodi Z, Amassian VE. Neurophysiological mechanisms underlying motor evoked potentials in anesthetized humans. Part 2. Relationship between epidurally and muscle recorded MEPs in man. Clin Neurophysiol 2001;112:445–52.

Dobkin BH, Havton LA. Basic advances and new avenues in therapy of spinal cord injury. Annu Rev Med 2004,55:255–82.
Dong CC, MacDonald DB, Janusz MT. Intraoperative spinal cord monitoring during descending thoracic and thoracoabdominal aneurysm surgery. Ann Thorac Surg 2002;74:S1873–6.
Elmore JR, Gloviczki P, Harper CM, Pairolero PC, Murray MJ, Bourchier RG, Bower TC, Daube JR. Failure of motor evoked potentials to predict neurologic outcome in experimental thoracic aortic occlusion. J Vasc Surg 1991;14:131–9.
Estrera AL, Miller CC 3rd, Huynh TT, Porat E, Safi HJ. Neurologic outcome after thoracic and thoracoabdominal aortic aneurysm repair. Ann Thorac Surg 2001;72:1225–30; discussion 1230–21.
Estrera AL, Miller CC 3rd, Huynh TT, Azizzadeh A, Porat EE, Vinnerkvist A, Ignacio C, Sheinbaum R, Safi HJ. Preoperative and operative predictors of delayed neurologic deficit following repair of thoracoabdominal aortic aneurysm. J Thorac Cardiovasc Surg 2003;126:1288–94.
Fujioka H, Shimoji K, Tomita M, Denda S, Hokari T, Yohyama M. Effects of dorsal root entry zone lesion on spinal cord potentials evoked by segmental, ascending and descending volleys. Acta Neurochir (Wien) 1992;117:135–42.
Fujioka H, Shimoji K, Tomita M, Denda S, Takada T, Homma T, Uchiyama S, Takahashi H, Tobita T, Baba H. Spinal cord potential recordings from the extradural space during scoliosis surgery. Br J Anaesth 1994;73:350–6.
Ghaly RF, Ham JH, Lee JJ. High-dose ketamine hydrochloride maintains somatosensory and magnetic motor evoked potentials in primates. Neurol Res 2001;23:881–6.
Ghez C, Krakauer J. The organization of movement. In: Kandel E, Schwartz J, Jessell T, editors. Principles of neural science. New York: McGraw-Hill; 2000. p. 653–73.
Gotoh N. Anatomy in spinal vessels. Spine Spinal Cord 1993;6:35–9.
Gravereaux EC, Faries PL, Burks JA, Latessa V, Spielvogel D, Hollier LH, Marin ML. Risk of spinal cord ischemia after endograft repair of thoracic aortic aneurysms. J Vasc Surg 2001;34:997–1003.
Griffiths IR, Pitts LH, Crawford RA, Trench JG. Spinal cord compression and blood flow. I. The effect of raised cerebrospinal fluid pressure on spinal cord blood flow. Neurology 1978;28:1145–51.
Grundy BL, Villani RM. Evoked potentials: intraoperative and ICE Monitoring. Berlin New York: Springer; 1988.
Guyton AC. Organisation of the nervous system: basic functions of synapses and transmitter substances. In: Textbook of medical physiology. Philadelphia: Saunders; 1991. p. 478–94.
Haghighi SS, Gaines RW. Repetitive vs. single transcranial electrical stimulation for intraoperative monitoring of motor conduction in spine surgery. Mol Med 2003;100:262–5.
Harada H, Kaneko S, Kano T, Tayama K, Akashi H, Aoyagi S. Safety management of a patient undergoing thoracic aortic surgery by spinal evoked potential monitoring. Ann Thorac Cardiovasc Surg 1998;4:37–40.
Hill AB, Kalman PG, Johnston KW, Vosu HA. Reversal of delayed-onset paraplegia after thoracic aortic surgery with cerebrospinal fluid drainage. J Vasc Surg 1994;20:315–7.
Hollier LH, Money SR, Naslund TC, Proctor CD, Sr., Buhrman WC, Marino RJ, Harmon DE, Kazmier FJ. Risk of spinal cord dysfunction in patients undergoing thoracoabdominal aortic replacement. Am J Surg 1992;164:210–3; discussion 213–4.
Iizuka T, Kurokawa T. Transient augmentation of the evoked spinal cord and peripheral nerve action potentials through ischemia. Jap J Orthoped 1982;56:163–70.
Ishijima B, Shimizu H, Takahashi H, Yasue S, Shimizu H, Shimoji K. Dorsal root entry zone-tomy and trigeminal spinal nucleotomy for deafferented pain with the consideration of the pain modulation mechanisms in the dorsal horn. Neurosurgeons 1985;4:1–12.
Jacobs MJ, de Mol BA, Elenbaas T, Mess WH, Kalkman CJ, Schurink GW, Mochtar B. Spinal cord blood supply in patients with thoracoabdominal aortic aneurysms. J Vasc Surg 2002a;35:30–7.

Jacobs MJ, Elenbaas TW, Schurink GW, Mess WH, Mochtar B. Assessment of spinal cord integrity during thoracoabdominal aortic aneurysm repair. Ann Thorac Surg 2002b;74:S1864–66.

Jeanmonod D, Sindou M. Somatosensory function following dorsal root entry zone lesions in patients with neurogenic pain or spasticity. J Neurosurg 1991;74:916–32.

Jones SJ, Harrison R, Koh KF, et al. Motor evoked potential monitoring during spinal surgery: responses of distal limb muscles to transcranial cortical stimulation with pulse trains. Electroencephalogr Clin Neurophysiol 1996;100:375–83.

Jones SJ, Buonamassa S, Crockard HA. Two cases of quadriparesis following anterior cervical discectomy, with normal perioperative somatosensory evoked potentials. J Neurol Neurosurg Psychiatry 2003;74:273–6.

Kakinohana M, Marsala M, Carter C, Davison JK, Yaksh TL. Neuraxial morphine may trigger transient motor dysfunction after a noninjurious interval of spinal cord ischemia: a clinical and experimental study. Anesthesiology 2003;98:862–70.

Kakinohana M, Kawabata T, Miyata Y, Sugahara K. Myogenic transcranial motor evoked potentials monitoring cannot always predict neurologic outcome after spinal cord ischemia in rats. J Thorac Cardiovasc Surg 2005;129:46–52.

Kalkman CJ, Drummond JC, Ribberink AA. Low concentrations of isoflurane abolish motor evoked responses to transcranial electrical stimulation during nitrous oxide/opioid anesthesia in humans. Anesth Analg 1991;73:410–5.

Kalkman CJ, Drummond JC, Ribberink AA, Patel PM, Sano T, Bickford RG. Effects of propofol, etomidate, midazolam, and fentanyl on motor evoked responses to transcranial electrical or magnetic stimulation in humans. Anesthesiology 1992;76:502–9.

Kalkman CJ, Ubags LH, Been HD, Swaan A, Drummond JC. Improved amplitude of myogenic motor evoked responses after paired transcranial electrical stimulation during sufentanil/nitrous oxide anesthesia. Anesthesiology 1995;83:270–6.

Kano T, Sadanaga M, Sakamoto M, Higashi K, Matsumoto M. Effects of systemic cooling and rewarming on the evoked spinal cord potentials and local spinal cord blood flow in dogs. Anesth Analg 1994;78:897–904.

Kano T, Sadanaga M, Matsumoto M, Ikuta Y, Sakaguchi H, Gotoh H, Miyauchi Y. Spinal function monitoring by evoked spinal cord potentials in aortic aneurysm surgery. J Anesth 1995;9:44–51.

Katayama Y, Tsubokawa T, Hirayama T, et al. Embolization of intramedullary spinal arteriovenous malformation fed by the anterior spinal artery with monitoring of the corticospinal motor evoked potential–case report. Neurol Med Chir. (Tokyo) 1991;31: 401–5.

Katayama Y, Tsubokawa T, Yamamoto T, et al. Changes in the corticospinal MEP (D-wave) during microsurgical removal of intramedullary spinal cord tumors: experience in 16 cases. In: Jones SJ, Boyd S, Hetree M, Smith NJ, editors. Handbook of spinal cord monitoring. London: Kluwer Academic; 1993. p. 321–6.

Kawaguchi M, Inoue S, Kakimoto M, Kitaguchi K, Furuya H, Morimoto T, Sakaki T. The effect of sevoflurane on myogenic motor-evoked potentials induced by single and paired transcranial electrical stimulation of the motor cortex during nitrous oxide/ketamine/fentanyl anesthesia. J Neurosurg Anesthesiol 1998;10:131–6.

Kida Y, Takano H, Kitagawa H, Tsuji H. Effects of systemic cooling on conductive spinal evoked potentials. Spine 1994;19:341–5.

Kieffer E, Fukui S, Chiras J, Koskas F, Bahnini A, Cormier E. Spinal cord arteriography: a safe adjunct before descending thoracic or thoracoabdominal aortic aneurysmectomy. J Vasc Surg 2002;35:262–8.

Kocsis JD, Akiyama Y, Radtke C. Neural precursors as a cell sources to repair the demyelinated spinal cord. J Neurotrauma 2004;21:441–9.

Kondo K, Harada H, Kaneko S, Tayama K, Kano T. Intraoperative monitoring of the conductive evoked spinal cord potentials under deep hypothermia. J Electrodiag Spinal Cord 1996;18:160–2.

Kouchoukos NT, Masetti P, Rokkas CK, Murphy SF, Blackstone EH. Safety and efficacy of hypothermic cardiopulmonary bypass and circulatory arrest for operations on the descending thoracic and thoracoabdominal aorta. Ann Thorac Surg 2001;72:699–707; discussion 707–698.

Kouchoukos NT, Masetti P, Rokkas CK, Murphy SF. Hypothermic cardiopulmonary bypass and circulatory arrest for operations on the descending thoracic and thoracoabdominal aorta. Ann Thorac Surg 2002;74:S1885–7; discussion S1892–88.

Kumagai Y, Shimoji K, Honma T, Uchiyama S, Ishijima B, Hokari T, Fujioka H, Fukuda S, Ohama E Problems related to dorsal root entry zone lesions. Acta Neurochir 1992;117:135–42.

Kunihara T, Shiiya N, Yasuda K. Strategy for spinal cord protection during thoracoabdominal aortic surgery. Kyobu Geka 2004;57:319–24.

Kuniyoshi Y, Koja K, Miyagi K, Shimoji M, Uezu T, Arakaki K, Yamashiro S, Mabuni K, Senaha S, Nakasone Y. Prevention of postoperative paraplegia during thoracoabdominal aortic surgery. Ann Thorac Surg 2003;76:1477–84.

Lake CL. Cardiovascular anesthesia. New York: Springer; 1984. p. 383–409.

Legatt AD. Current practice of motor evoked potential monitoring: results of a survey. J Clin Neurophysiol 2002;19:454–60.

Legatt A. Motor evoked potential monitoring. Am J END Technol 2004;44:223–43.

Levy WJ, Grundy BL, Smith NT. Monitoring the electroencephalogram and evoked potentials during anesthesia. In: Saidman LJ, Smith NT, editors. Monitoring in anesthesia. Boston: Butterworth; 1984. p. 227–67.

Levy WJ Jr. Clinical experience with motor and cerebellar evoked potential monitoring. Neurosurgery 1987;20:169–82.

Lips J, de Haan P, de Jager SW, Vanicky I, Jacobs MJ, Kalkman CJ. The role of transcranial motor evoked potentials in predicting neurologic and histopathologic outcome after experimental spinal cord ischemia. Anesthesiology 2002;97:183–91.

Lyon R, Lieberman JA, Grabovac MT, Hu S. Strategies for managing decreased motor evoked potential signals while distracting the spine during correction of scoliosis. J Neurosurg Anesthesiol 2004;16:167–70.

MacDonald DB. Current practice of motor evoked potential monitoring: Results of a survey. J Clin Neurophysiol 2002;19:454–60.

MacDonald DB. Safety of intraoperative transcranial electrical stimulation motor evoked potential monitoring. J Clin Neurophysiol 2002;19:416–29.

MacDonald DB, Janusz M. An approach to intraoperative neurophysiologic monitoring of thoracoabdominal aneurysm surgery. J Clin Neurophysiol 2002;19:43–54.

MacDonald DB, Al Zayed Z, Khoudeir I, et al. Monitoring scoliosis surgery with combined multiple pulse transcranial electric motor and cortical somatosensory-evoked potentials from the lower and upper extremities. Spine 2003;28:194–203.

Macon JB, Poletti CE, Seet WH, Ojemann RG, Zervas NT. Conducted somatosensory evoked potentials during spinal surgery. Part 2: Clinical applications. J Neurosurg 1982;57:354–9.

Marcus ML, Heistad DD, Ehrhardt JC, Abboud FM. Regulation of total and regional spinal cord blood flow. Circ Res 1977;41:128–34.

Maruyama Y, Shimoji K, Fujioka H, Takada T, Endoh H. Brain and spinal cord monitoring by multispatial and multimodal evoked potentials during aortic surgery. In: Ducker TB, Brown RH, editors. Neurophysiology and standards of spinal cord monitoring. New York: Springer; 1988. p. 177–87.

Mawad ME, Rivera V, Crawford S, Ramirez A, Breitbach W. Spinal cord ischemia after resection of thoracoabdominal aortic aneurysms: MR findings in 24 patients. Am J Neuroradiol 1990;11:987–91.

McDonald JW, Becker D, Holekamp TF, Howard M, Liu S, Lu A, Platik MM, Qu Y, Stewart T, Vadivelu S. Repair of the injured spinal cord and the potential of embryonic stem cell transplantation. J Neurotrauma 2004;21:383–93.

McPherson RW, Levitt RC. Etomidate augmentation of scalp recorded somatosensory waves: time course, reproducibility, and dose effect. In: Shimoji K, Kurokawa T, Tamaki T, Willis

WD Jr, editors. Spinal cord monitoring and electrodiagnosis. Berlin: Springer; 1991. p. 163–70.

McPherson RW, Mahla M, Johnson R, Traystman RJ. Effects of enflurane, isoflurane, and nitrous oxide on somatosensory evoked potentials during fentanyl anesthesia. Anesthesiology 1985;62:626–33.

Merton PA, Morton HB. Stimulation of the cerebral cortex in the intact human subject. Nature 1980;285:227.

Meylaerts SA, de Haan P, Kalkman CJ, Lips J, De Mol BA, Jacobs MJ. The influence of regional spinal cord hypothermia on transcranial myogenic motor-evoked potential monitoring and the efficacy of spinal cord ischemia detection. J Thorac Cardiovasc Surg 1999;118:1038–45.

Meylaerts SA, Jacobs MJ, van Iterson V, de Haan P, Kalkman CJ. Comparison of transcranial motor evoked potentials and somatosensory evoked potentials during thoracoabdominal aortic aneurysm repair. Ann Surg 1999;230:742–9.

Minahan RE, Sepkuty JP, Lesser RP, Sponseller PD, Kostuik JP. Anterior spinal cord injury with preserved neurogenic 'motor' evoked potentials. Clin Neurophysiol 2001;112:1442–50.

Mishima Y, Niiyama S, Kano T. CSF temperature monitoring under deep hypothermia with extracorporeal circulation. In: Kano T, editor. Proceedings of 3rd Japanese SNACC. Kurume: Shinkou; 1999. p. 46–8.

Morota N, Deletis V, Constantini S, et al. The role of motor evoked potentials during surgery for intramedullary spinal cord tumors. Neurosurgery 1997;41:1327–36.

Murkin JM. Perioperative multimodality neuromonitoring: an overview. Semin Cardiothorac Vasc Anesth 2004;8:167–171.

Nashold BS Jr, Ostdahl RH. Dorsal root entry zone lesions for pain relief. J Neurosurg 1979;51:59–69.

Nashold BS Jr, Urban B, Zorub DS. Phantom relief by focal destruction of substantia gelatinosa of Rolando. In: Bonica JJ, Albe-Fessard D, editors. Advances in pain research and therapy, vol. 1. New York: Raven; 1976. p. 959–63.

Nashold BS Jr, Ovelmen-Levitt J, Sharpe R, Higgins AC. Intraoperative evoked potentials recorded in man directly from dorsal roots and spinal cord. J Neurosurg 1985;62:680–93.

Owen JH, Laschinger J, Bridwell K, Shimon S, Nielsen C, Dunlap J, Kain C. Sensitivity and specificity of somatosensory and neurogenic-motor evoked potentials in animals and humans. Spine 1988;13:1111–8.

Paton HD, Amassian VE. The pyramidal tract: its excitation and functions. In: Handbook of physiology: neurophysiology. Washington: Physiological Society; 1960. p. 837–61.

Pechstein U, Cedzich C, Nadstawek J, et al. Transcranial high-frequency repetitive electrical stimulation for recording myogenic motor evoked potentials with the patient under general anesthesia. Neurosurgery 1996a;39:335–43.

Pechstein U, Cedzich C, Nadstawek J, et al. Transcranial high-frequency repetitive electrical stimulation for recording myogenic motor evoked potentials with the patient under general anesthesia. Neurosurgery 1996b;39:335–43.

Pechstein U, Nadstawek J, Zentner J, Schramm J. Isoflurane plus nitrous oxide versus propofol for recording of motor evoked potentials after high frequency repetitive electrical stimulation. Electroencephalogr Clin Neurophysiol 1998;108:175–81.

Prestor B, Zgur T, Dolenc VV. Subpial spinal evoked potentials in patients undergoing junctional dorsal root entry zone coagulation for pain relief. Acta Neurochir (Wien) 1989;101:56–62.

Rectenwald JE, Huber TS, Martin TD, Ozaki CK, Devidas M, Welborn MB, Seeger JM. Functional outcome after thoracoabdominal aortic aneurysm repair. J Vasc Surg 2002;35:640–7.

Reuter DG, Tacker WA, Jr., Badylak SF, Voorhees WD 3rd, Konrad PE. Correlation of motor-evoked potential response to ischemic spinal cord damage. J Thorac Cardiovasc Surg 1992;104:262–72.

Safi HJ, Campbell MP, Miller CC 3rd, Iliopoulos DC, Khoynezhad A, Letsou GV, Asimacopoulos PJ. Cerebral spinal fluid drainage and distal aortic perfusion decrease the incidence of neu-

rological deficit: the results of 343 descending and thoracoabdominal aortic aneurysm repairs. Eur J Vasc Endovasc Surg 1997a;14:118–24.
Safi HJ, Miller CC 3rd, Azizzadeh A, Iliopoulos DC. Observations on delayed neurologic deficit after thoracoabdominal aortic aneurysm repair. J Vasc Surg 1997b;26:616–22.
Safi HJ, Campbell MP, Ferreira ML, Azizzadeh A, Miller CC. Spinal cord protection in descending thoracic and thoracoabdominal aortic aneurysm repair. Semin Thorac Cardiovasc Surg 1998;10:41–4.
Safi HJ, Miller CC 3rd, Huynh TT, Estrera AL, Porat EE, Winnerkvist AN, Allen BS, Hassoun HT, Moore FA. Distal aortic perfusion and cerebrospinal fluid drainage for thoracoabdominal and descending thoracic aortic repair: ten years of organ protection. Ann Surg 2003;238:372–80.
Sakamoto T, Kawaguchi M, Kakimoto M, Inoue S, Takahashi M, Furuya H. The effect of hypothermia on myogenic motor-evoked potentials to electrical stimulation with a single pulse and a train of pulses under propofol/ketamine/fentanyl anesthesia in rabbits. Anesth Analg 2003;96:1692–7.
Samra SK, Vanderzant CW, Domer PA, Sackellares JC. Differential effects of isoflurane on human median nerve somatosensory evoked potentials. Anesthesiology 1987;66:29–35.
Schonle PW, Isenberg C, Crozier TA, Dressler D, Machetanz J, Conrad B. Changes of transcranially evoked motor responses in man by midazolam, a short acting benzodiazepine. Neurosci Lett 1989;101:321–4.
Seyal M, Mull B. Mechanisms of signal change during intraoperative somatosensory evoked potential monitoring of the spinal cord. J Clin Neurophysiol 2002;19:409–15.
Shimoji K, Higashi H, Kano T. Epidural recording of spinal electrogram in man. Electroencephalogr Clin Neuropohysiol 1971;30:236–9.
Sindou M. Etude de la jonction radiculomédullaire postérieure. La radicellotomie postérieure sélective dans la chirurgie de la douleur. Lyon: Medical Thesis; 1972.
Spanish Society of Clinical Neurophysiology. A practical guide to carrying out neurophysiological monitoring in spine surgery. Rev Neurol 2004;38:879–85.
Svensson LG, Crawford ES. Techniques for dissection involving the distal aorta. In: Svensson LG, Crawford ES, editors. Cardiovascular and vascular disease of the aorta. Philadelphia: Saunders; 1997. p. 359–70.
Svensson LG, Crawford ES, Hess KR, Coselli JS, Safi HJ. Experience with 1509 patients undergoing thoracoabdominal aortic operations. J Vasc Surg 1993;17:357–68; discussion 368–70.
Taira Y, Marsala M. Effect of proximal arterial perfusion pressure on function, spinal cord blood flow, and histopathologic changes after increasing intervals of aortic occlusion in the rat. Stroke 1996;27:1850–8.
Tamaki T, Tsuji H, Inoue S, Kobayashi M. The prevention of iatrogenic spinal cord injury utilizing the evoked spinal cord potentials. Int Orthop 1981;4:313–17.
Tamaki T, Noguchi T, Takano H, Tsuji H, Nakagawa T, Imai K, Inoue S. Spinal cord monitoring as a clinical utilization of the spinal evoked potentials. Clin Orthop 1984;184:58–64.
Taniguchi M, Nadstawek J, Langenbach U, Bremer F, Schramm J. Effects of four intravenous anesthetic agents on motor evoked potentials elicited by magnetic transcranial stimulation. Neurosurgery 1993;33:407–15; discussion 415.
Thees C, Scheufler KM, Nadstawek J, Pechstein U, Hanisch M, Juntke R, Zentner J, Hoeft A. Influence of fentanyl, alfentanil, and sufentanil on motor evoked potentials. J Neurosurg Anesthesiol 1999;11:112–8.
Toleikis JR, Skelly JP, Carlvin AO, Burkus JK. Spinally elicited peripheral nerve responses are sensory rather than motor. Clin Neurophysiol 2000;111:736–42.
Tsuyama N, Tsuzuki N, Kurokawa T, Imai T. Clinical application of spinal cord action potential measurement. Int Orthop 1978;2:39–46.
Uezu T, Koja K, Kuniyoshi Y, Miyagi K, Shimoji M, Arakaki K, Yamashiro S, Mabuni K, Senaha S. Blood distribution to the anterior spinal artery from each segment of intercostals and lumbar arteries. J Cardiovasc Surg 2003;44:637–45.

van Dongen EP, ter Beek HT, Schepens MA, Morshuis WJ, Langemeijer HJ, de Boer A, Boezeman EH. Within-patient variability of myogenic motor-evoked potentials to multipulse transcranial electrical stimulation during two levels of partial neuromuscular blockade in aortic surgery. Anesth Analg 1999;88:22–7.

Vauzelle C, Stagnara P, Jouvinroux P. Functional monitoring of spinal cord activity during spinal surgery. Clin Orthop 1973;93:173–8.

Yamamoto T, Katayama Y, Tsubokawa T, et al. Experimental study of the origin of transcranially evoked descending spinal cord potentials. In: Shimoji K, Kurokawa T, Tamaki T, Willis WD, editors. Spinal cord monitoring and electrodiagnosis. Berlin: Springer; 1991. p. 36–42.

Zentner J. Noninvasive motor evoked potential monitoring during neurosurgical operations on the spinal cord. Neurosurgery 1989;24:709–12.

Zentner J, Ebner A. Nitrous oxide suppresses the electromyographic response evoked by electrical stimulation of the motor cortex. Neurosurgery 1989;24:60–2.

Section D: Chapter 2

Jacquemin GL, Proulx P, Gilbert DA, Albeart G, Morcos R. Functional recovery from paraplegia caused by syphilitic meningomyeliltis. J Spinal Cord Med 2003;25:133–7.

Shimizu H, Shimoji K, Maruyama Y, Sato Y, Harayama H, Tsubaki T. Slow cord dorsum potentials elicited by descending volleys in man. J Neurol Neurosurg Psychiatry 1979a;2:242–6.

Shimizu H, Shimoji K, Maruyama Y, Sato Y, Kuribayashi H. Interaction between human evoked electrospinograms elicited by segmental and descending volleys. Experimentia 1979b;35:1199–200.

Yamada T, Yeh M, Kimura J. Fundamental principles of somatosensory evoked potentials. Phys Med Rehabil Clin North Am 2004;15:19–42.

Index